Dottorato in Architettura
Dottorato in Diritto ed Economia
Dottorato in Ingegneria Civile, Ambientale e Industriale
Dottorato in Ingegneria dell'Informazione
Dottorato in Scienze Agrarie, Alimentari e Forestali

Direttore della Scuola di Dottorato
prof. Paolo Fuschi

Collegio dei docenti
Dottorato di Ricerca in Scienze Agrarie, Alimentari e Forestali
XXXVII ciclo

Leonardo Schena

Abenavoli Maria Rosa
Barreca Francesco
Di Fazio Salvatore
Giuffrè Angelo Maria
Gulisano Giovanni
Li Destri Giulia
Lombardi Fabio
Modica Giuseppe
Monti Michele
Muscolo Adele Maria
Palmeri Vincenzo
Panuccio Maria Rosaria
Piscopo Amalia Rosa Maria
Poiana Marco
Porto Paolo
Proto Andrea Rosario
Schena Leonardo
Sicari Vincenzo
Spampinato Giovanni
Strano Alfio
Sunseri Francesco
Zema Demetrio Antonio
Zimbalatti Giuseppe
Zimbone Santo Marcello

On the cover the cover features a 3D-rendered DNA double helix, symbolizing genetics and molecular biology. Beneath it, a sequence of nucleotide bases highlights the theme of genetic coding and nucleotide sequences. This cover was created using Canva. The image used is licensed under Canva's terms of use.

I would like to express my deep gratitude to Professor Cacciola for her attentive guidance throughout this journey. I am especially thankful for the work ethic and methodology she instilled in me, which I will carry in the future. Her support and advice have been crucial to both my professional and personal growth.
I would also like to extend my sincere thanks to Professors Li Destri and Pane, as well as Dr. Santilli, for the opportunities they have given me over the years and for their valuable contributions to my development.
A special thank you goes to Dr. David E. L. Cooke and the entire Cell and Molecular Sciences group at the James Hutton Institute. Working with you has been an enriching and rewarding experience.
I am deeply grateful to Rossana, Federico, Francesco, Cristian, and Mario from the Molecular Plant Pathology Laboratory at Di3A for their unwavering support during my doctoral studies.
I would also like to thank my fiancée, Aurora, for her constant and unwavering support throughout this journey.
Finally, a heartfelt thank you to my friends and family, especially my mother, father, and siblings. Your support has been indispensable to me.

Dr. Sebastiano Conti Taguali obtained his Master's degree in Agricultural Sciences and Technologies (LM-69) in October 2021 from the Department of Agriculture, Food, and Environment (Di3A) at the University of Catania, graduating with a score of 110/110 cum laude and receiving special mention for his academic career. His research activities focus on: I. The characterization and monitoring of emerging phytopathogenic fungi and oomycetes; II. The study of the influence of environmental and ecological factors on the geographical distribution of fungal and oomycete populations; III. Transcriptomic analysis in plant-pathogen-antagonist and plant-pathogen-biostimulant systems to identify natural and sustainable defense strategies; IV. The evaluation of the efficacy and application of eco-friendly formulations for the control of pre- and post-harvest diseases; V. The analysis of mycotoxins in plant matrices.

Dottorato di Ricerca
Scienze Agrarie Alimentari e Forestali

SCUOLA DI DOTTORATO
Università Mediterranea di Reggio Calabria

DIPARTIMENTO DI AGRARIA

DOTTORATO DI RICERCA
Scienze Agrarie, Alimentari e Forestali

S.S.D. AGRI-05/B
XXXVII CICLO

OMICS SCIENCES IN PLANT DISEASE: NEW APPROACHES FOR UNDERSTANDING AND MANAGING PLANT-MICROBE INTERACTIONS UNDER CHANGING ENVIRONMENTAL CONDITIONS

Dottorando
Sebastiano Conti Taguali [redacted]

Tutor
prof.ssa Maria Giulia Li Destri Nicosia [redacted]

Co-tutor
prof.ssa Santa Olga Cacciola [redacted]

dott.ssa Elena Santilli [redacted]

Coordinatore del Dottorato
prof. Leonardo Schena [redacted]

Dipartimento di Agraria

INDEX

Abstract 1

Sommario 2

1. General Introduction 3

References 8

2. Genome sequencing and assembly of *Phytophthora oleae*, isolate VK10A, causative agent of rot of olive drupes 12

References 19

3. Exploring the impact of various treatments on gene expression in olive (*Olea europaea* L.) drupes infected by *Phytophthora oleae*: Insights from RNA sequencing-based transcriptome analysis 23

3.1 Abstract 23

3.2 Introduction 24

3.3 Materials and methods 26

3.3.1 Microorganisms and plant material 26

3.3.2 Preparation of *P. oleae*-inoculum 26

3.3.3 Preparation of *T. atroviride*-culture filtrate 26

3.3.4 Preparation of *C. oleophila* cell suspension 27

3.3.5 Evaluating the effectiveness of *C. oleophila* and *Trichoderma*-culture filtrate in controlling rots of drupes by *P. oleae* 27

3.3.6. Assessing the experimental assay to study the transcriptome of olive drupes and *P. oleae* in the system olive drupe-*P. oleae*-*C. oleophila*/*T. atroviride*-culture filtrate 28

3.3.7 RNA isolation from infected olive drupes and cDNA synthesis for RT-PCR 28

3.3.8 Quantitative Real Time-PCR (RT-qPCR) analysis of gene expression 28

3.3.9 Total RNA preparation and Illumina mRNA sequencing 29

3.3.10 *De novo* mRNA analysis 30

3.3.11 RNAseq data analysis 30

3.3.12 LC-MS identification of proteins in protein filtrate 31

3.4 Results 31

3.4.1 Evaluating the effectiveness of *C. oleophila* strain O and *T. atroviride*-culture filtrate in controlling the rot of olive drupes incited by *P. oleae* 31

3.4.2 Differential RNA analysis at 72 hours post inoculation with *P. oleae* 33

3.4.2.1 Comparison 1: intact olive drupes (treatment ID1) vs. wounded drupes treated with sterile distilled water (treatment ID2) 33

3.4.2.2 Comparison 2: *Phytophthora oleae*-inoculated wounded drupes (treatment ID3) vs. sterile distilled water-treated wounded drupes (treatment ID2) 37

3.4.2.3 Comparison 3: wounded olive drupes pre-treated with *C. oleophila* and inoculated with *P. oleae* (treatment ID5) vs. wounded olive drupes inoculated with *P. oleae* (treatment ID3). 45

3.4.2.4 Comparison 4: wounded olive drupes pre-treated with *Trichoderma atroviride*-culture filtrate and inoculated with *Phytophthora oleae* (treatment ID4) versus wounded drupes inoculated with *P. oleae* (treatment ID3). 48

3.4.2.5 Comparison 5: overall differential mRNA expression of olive genes 53

3.4.2.6. Comparison 6: wounded olive drupes pre-treated with *C. oleophila* cell suspension (treatment ID7) versus wounded drupes pre-treated with sterile distilled water (treatment ID2) 57

3.4.2.7 Comparison 7: wounded olive drupes pre-treated with *T. atroviride*-culture filtrate (treatment ID6) versus wounded drupes pre-treated with sterile distilled water (treatment ID2) 57

3.4.2.8. Comparison 8: *P. oleae* differentially expressed genes during olive fruit infection (treatment ID3) as compared to its in vitro growth in several culture media 58

3.4.2.9 Comparison 9: differentially expressed genes of *P. oleae* during olive drupe infection (treatment ID3) as compared to olive drupe inoculated with *P. oleae* and pre-treated with either *C. oleophila* (treatment ID5) or *T. atroviride*-culture filtrate (treatment ID4) 66

3.4.2.10 RT-qPCR validation of selected genes of *Olea europaea* and *Phytophthora oleae*. 71

3.5 Discussion 77

3.6 Conclusion 83

3.7 References 84

4. Physiological and biochemical responses of olive fruit to *Colletotrichum* infection: A metabolomic Insight _____ 102

4.1 Abstract 102

4.2 Introduction 103

4.3 Material and methods 105

4.3.1 Plant material and experimental design 105

4.3.2 Fungal isolates and inoculum 107

4.3.3 Determination of photosynthetic pigments content 107

4.3.4 Determination of lipid peroxidation 108
4.3.5 Hydrogen peroxide analysis 108
4.3.6 Total carbohydrate assay 109
4.3.7 Statistical analysis 109
4.4 Results 110
4.4.3 Pathogenicity assays 110
4.4.4 Photosynthetic pigment analysis 111
4.4.5 MDA and H_2O_2 analysis 113
4.4.7 Heatmap and PCA analysis of metabolic profiles 117
4.5 Discussion 121
4.6 References 126
5. Environmental and agronomic factors shaping rhizosphere microbial communities in organically and conventionally managed citrus orchards: An omics approach 131
5.1 Abstract 131
5.2 Introduction 132
5.3 Material and methods 134
5.3.1 sampling sites 134
5.3.1.1 Features of sampling sites 139
5.3.2 Collection of soil samples 139
5.3.3 Determination of physicochemical soil 140
5.3.4 Soil microbiome analyses 141
5.3.4.1 Environmental DNA (eDNA) extraction and Illumina libraries preparation 141
5.3.4.2 Bioinformatic processing for taxonomical classifications 141
5.3.4.3 Computation of microbiome indexes and network properties 142
5.3.4.4 Statistical analyses 142
5.4 Results 143
5.4.1 Physicochemical properties of soils 143
5.4.2 Variability of core microbiome in soil of organically and conventionally managed citrus orchards 146
5.4.2.1 Microbiome structure (prokaryotic and fungal phyla) 146
5.4.2.2 Microbiome structure (prokaryiotic and fungal genera) 147

5.4.2.3 Variability of microbiome structure in relation to seasonality and farming system 149
5.4.2.4 Microbiome structure (prokaryotic and fungal species) 151
5.4.3 Modelling of microbiome indexes and microbiome network indicators 151
5.4.3.1 Farming system and network properties: co-exclusion and co-occurrence 151
5.4.3.2 Influence of management on α-diversity, Chao1 and Shannon indexes 151
5.4.3.3 BeCrop® indexes, with focus on management 152
5.4.3.3 BeCrop® indexes with focus on management vs. seasonality 153
5.4.4 Effects of environmental and management factors on microbial community array 153
5.5 Discussion 159
5.6 Conclusion 165
5.7 References 167
6. Is climate change impacting *Phytophthora* diversity in organically and conventionally managed citrus orchards in Sicily? Insights from metabarcoding and baiting 179
6.1 Abstract 179
6.2. Introduction 180
6.3 Material and methods 183
6.3.1 Citrus orchards 183
6.3.2 Collection of rhizosphere soil samples and establishment of sub-samples for metabarcoding and baiting processing 189
6.3.3 Baiting processing, isolation procedure and molecular identification 189
6.3.4. Sample processing for metabarcoding analyses 190
6.3.4.1 Environmental DNA (eDNA). Extraction from rhizosphere soil samples and PCR amplification 190
6.3.4.2 Screening for the eligibility of eDNA samples to *Phytophthora*-metabarcoding processing 190
6.3.4.3 PCR amplifications 191
6.3.4.3.1 ITS-1 region barcode 191
6.3.4.3.2 *Rps10* gene barcode 191
6.3.4.4 Illumina sequencing library preparation and sequencing 192
6.3.4.5 Bioinformatics analyses 192
6.3.4.6 Statistical analyses 193

6.4 Results 194
6.4.1 *Phytophthora* species isolated by baiting 194
6.4.2 *Phytophthora* taxa identified by metabarcoding 194
6.4.2.1 Preliminary screening for checking suitability of eDNA samples to *Phytophthora*-metabarcoding processing 194
6.4.2.2 *Phytophthora* taxa identified by metabarcoding of the ITS-1 region 195
6.4.2.3 *Phytophthora* taxa identified by metabarcoding of the *rps10* gene 199
6.4.3 *Phytophthora*-positive rhizosphere soil samples recorded - comparison of outcomes from baiting and metabarcoding of ITS-1 and *rps10* gene 202
6.4.5 . Known *Phytophthora* taxa recorded per citrus-producing area - comparison of outcomes from baiting, metabarcoding of ITS-1 region and *rps10* gene 204
6.4.6 Influence of environmental factors on the overall occurrence of *Phytophthora* taxa 205
6.5 Discussion 209
6.6 Conclusions 215
6.7 References 217
7. Conclusions and Future Perspectives 225
7.1 References 228

Abstract

Plant diseases caused by fungi and oomycetes pose significant threats to global agriculture, leading to considerable economic losses and jeopardizing food security, particularly in the Mediterranean region. This thesis investigates the role of omics sciences—genomics, transcriptomics, metabolomics, and metagenomics—in addressing these challenges by enhancing the understanding of plant-pathogen interactions within the context of climate change.

Focusing on major fungal pathogens affecting olive and citrus crops, the research explores various aspects of plant-microbe interactions to develop rational, innovative, and environmentally friendly disease management strategies. Specific objectives include elucidating the genomic features of the recently emerged olive pathogen, *Phytophthora oleae*; evaluating the influence of biocontrol agents on the transcriptome of infected olive drupes; analyzing the metabolomic profiles of different olive cultivars under *Colletotrichum* infection; and assessing the impact of organic versus conventional management practices on microbial communities in citrus orchards.

Key findings demonstrate the significant potential of omics approaches in providing critical insights into the mechanisms of pathogenicity and plant resistance. Genome sequencing of *Phytophthora oleae* reveals essential pathogenicity mechanisms, while RNA sequencing highlights the influence of biocontrol agents such as *Candida oleophila* and *Trichoderma atroviride* on gene expression in olive drupes. Metabolomic analysis identifies physiological markers associated with resistance in olive cultivars, and the investigation into soil microbial diversity emphasizes the importance of sustainable management practices in maintaining microbial health and resilience.

The integration of these findings contributes to a comprehensive understanding of the molecular interactions between plants, pathogens, and microbial communities in the holobionte perspective. While challenges remain in the practical application of these insights, this research paves the way for the development of actionable strategies to reduce dependence on chemical inputs and promote sustainable agriculture in the Mediterranean region. Future directions include optimizing biocontrol agent formulations, exploring soil microbiome interactions, developing early diagnostic tools based on metabolomic markers, and creating predictive models to adapt to climate change impacts on pathogen dynamics.

Sommario

Le malattie delle piante causate da funghi e oomiceti rappresentano una grave minaccia per l'agricoltura globale, causando notevoli perdite economiche e compromettendo la sicurezza alimentare, in particolare nella regione Mediterranea. Questa tesi intende essere un esempio di come le scienze omiche—genomica, trascrittomica, metabolomica e metagenomica—possono avere un ruolo fondamentale nella gestione di queste sfide, migliorando la comprensione delle interazioni pianta-patogeno nel contesto del cambiamento climatico. Avendo per oggetto patogeni fungini di interesse per l'olivicoltura e l'agrumicoltura , la ricerca esplora vari aspetti delle interazioni pianta-patogeno per sviluppare strategie razionali, innovative e sostenibili di gestione delle malattie. Gli obiettivi specifici includono lo studio delle caratteristiche genomiche di *Phytophthora oleae*, un patogeno emergente dell'olivo, la valutazione dell'influenza degli agenti di biocontrollo sul trascrittoma delle drupe di olivo infette, l'analisi dei profili metabolomici di diverse cultivar di olivo infette da *Colletotrichum* e la valutazione dell'impatto delle pratiche di gestione in regime di agricoltura biologica rispetto a quelle convenzionali sulle comunità microbiche negli agrumeti. I risultati più salienti dimostrano il potenziale degli approcci omici nel fornire informazioni critiche sui meccanismi di patogenicità e resistenza nelle interazioni patogeno-pianta ospite. Il sequenziamento genomico di *Phytophthora oleae* rivela meccanismi di patogenicità essenziali, mentre il sequenziamento dell'RNA evidenzia l'influenza di agenti di biocontrollo come *Candida oleophila* e *Trichoderma atroviride* sull'espressione genica nelle drupe dell'olivo. L'analisi metabolomica identifica marcatori biochimici associati alla resistenza nelle cultivar di olivo, e l'indagine sulla diversità del microbioma del suolo sottolinea l'importanza delle pratiche di gestione sostenibili nel mantenimento della salute e della resilienza degli agroecosistemi.Nel loro insieme questi risultati contribuiscono a una visione olistica delle interazioni molecolari tra piante, patogeni e comunità microbiche. Sebbene l'applicazione pratica di queste intuizioni rimanga ancora una sfida da affrontare, questa ricerca pone le basi per lo sviluppo di strategie concrete per ridurre la dipendenza da prodotti chimici di sintesi che hanno elevato impatto ambientale e promuovere un'agricoltura sostenibile nella regione Mediterranea. Le prospettive future della ricerca sono le seguenti: l'ottimizzazione delle formulazioni degli agenti di biocontrollo, l'approfondimento dello studio delle interazioni e della dinamica del microbioma del suolo, lo sviluppo di strumenti diagnostici precoci basati su marcatori metabolomici e la creazione di modelli predittivi per contrastare gli effetti del cambiamento climatico sull'epidemiologia dei patogeni.

1. General Introduction

Plant diseases caused by fungi and oomycetes pose significant threats to global agriculture, leading to substantial economic losses and compromising food security. The challenge of managing these diseases is further exacerbated by global climate change, which can influence pathogen virulence and their distribution (Lahlali et al., 2024; Singh et al., 2023). The widespread use of synthetic chemical pesticides in agriculture has become increasingly unsustainable due to their persistence and potential for bioaccumulation, leading to contamination of soil and water ecosystems (Zhou et al., 2024). These contaminants alter the balance of microbial communities, harm non-target species, and contribute to the emergence of resistant pathogen strains (Karpouzas et al., 2014; Stanley and Preetha, 2016). Additionally, the persistence of pesticide residues in the environment poses significant risks to human health, as these chemicals can reach water supplies and accumulate in the food chain (Ahouangninou et al., 2012; Syafrudin et al., 2021). To address these challenges, the European Parliament and the Council of the European Union have introduced the Sustainable Use of pesticides Regulation (SUR), which replaces Directive 2009/128/EC. This regulation aims to reduce the use and risk of chemical pesticides by 50% across the EU by 2030, as part of the Farm to Fork Strategy and the European Green Deal. Member States are required to establish their own targets and implement strategies that include Integrated Pest Management (IPM) and alternative methods to minimize reliance on chemical pesticides. In the current regulatory and environmental context, omics sciences are emerging as powerful technological tools that provide innovative solutions for understanding and managing plant-microbe interactions. These disciplines, which include transcriptomics, metabolomics, and metagenomics, enable comprehensive analyses of biological systems, providing deep insights into the genetic, molecular, and community-level interactions between plants and pathogens. By elucidating the mechanisms of pathogen virulence, host resistance, the role of microbial communities in plant health, the ecology and epdemiology of pathogens and the effects of management practices on microbial communities in agroecosystems, these advanced methodologies provide knowledge that can concur to the development of eco-friendly and sustainable disease management strategies.

The Mediterranean region is renowned for cultivation of olive and citrus that are crops essential to the region's agricultural economy and deeply rooted in its cultural heritage. These crops thrive in the Mediterranean climate, characterized by hot, dry summers and

mild rainy winters. However, they are increasingly facing significant challenges due to climate change and emergent and re-emergent plant pathogens (Cacciola and Gullino, 2019) .

Olive tree is one of the most significant perennial crops in the Mediterranean region. With a cultivation area of about 9 million hectares, its cultivation in the Mediterranean is mainly concentrated in Spain, Tunisia, Italy, Morocco, Turkey, and Greece (FAOSTAT, 2021). Globally, olive oil production reaches around 3.5 million tons annually, with more than 90% coming from the Mediterranean region. Spain is the leading producer, accounting for roughly 45% of global olive oil output, followed by Italy at 10%, Greece at 7%, and Portugal at 6% (IOC, 2022)(IOC, 2022). In the last decades, there has been a shift towards more intensive olive farming systems to meet global demand, characterized by the use of high-yielding cultivars and advanced management practices (Azenzem et al., 2024). This intensification, while boosting production, has also increased the susceptibility of olive groves to waterlogged conditions and certain soil-borne pathogens, thereby introducing new challenges to maintain olive productivity (Azenzem et al., 2024; Cacciola et al., 2011).

Similarly, citrus cultivation holds a prominent place in Mediterranean agriculture, contributing significantly to both local economies and global markets (Ciriminna and Angellotti, 2024). Citrus species, including sweet oranges (*Citrus* x *sinensis* L.), rank among the most important fruit crops worldwide due to their economic value and high demand for fresh fruit and juice production. In 2019, global citrus production reached 143.76 million tonnes in 2019, with a total cultivated area of approximately 8.5 million hectares (FAO, 2021). The leading producers include China, Brazil, and the United States (Spreen et al., 2020). The Mediterranean region plays a crucial role in citrus cultivation due to its favorable climate. Primary producers in this area include Spain, Italy, Turkey, and Greece (FAO, 2021). Spain leads the European market with a production of about 6 million tonnes of citrus in 2019, followed by Italy with approximately 2.86 million tonnes in the same year (FAO, 2021). Like olives, citrus crops are increasingly vulnerable to the effects of climate change and the emergence or re-emergence of plant diseases. The spread of fungal and oomycete pathogens has become a significant challenge, often causing diseases leading to substantial yield losses. These diseases include mal secco disease of lemon, caused by *Plenodomus tracheiphilus*, as well as a range of rots caused by *Phytophthora* species (Cacciola and Magnano di San Lio, 2008; Migheli et al., 2009). These challenges require the adoption of sustainable management practices to preserve the health of citrus groves and maintain their productivity amidst changing environmental conditions.

In this thesis, we have employed advanced omics approaches to generate knowledge that contributes to the development of rational strategies for managing fungal and oomycete diseases in olive and citrus orchards.

These approaches encompass genomics, metagenomics, transcriptomics, and metabolomics, each providing a unique lens through which to explore the complex interactions between plants and pathogens.

Genomics provides a comprehensive representation of the genetic architecture of both plants and pathogens, offering key insights into how genes contribute to plant immunity, pathogenicity, and other factors that affect disease dynamics (Crandall et al., 2020; Xu and Wang, 2019). With the development of high-throughput sequencing technologies, it is now possible to sequence entire genomes with greater accuracy and speed. Next-generation sequencing (NGS) methods, such as Illumina, have transformed genomic studies by enabling large-scale data generation, though these technologies often result in shorter reads and incomplete draft genomes (Xu and Wang, 2019). In contrast, third-generation platforms, like PacBio and Oxford Nanopore, allow for long-read sequencing that captures complete genome sequences (Wang et al., 2021). In the study of plant disease ecology and health, microbial genomics can be divided into two main categories. The first category focuses on structural genomics, which involves mapping and assigning genes to individual chromosomes, thereby creating a physical map of the entire genome (Crandall et al., 2020). The second category involves functional genomics, which integrates genomic data with transcriptomic and proteomic information to provide a comprehensive understanding of gene functions and interactions (Barone et al., 2008).

Metagenomics, an extension of genomic studies, focuses on analyzing DNA obtained directly from environmental samples. By extracting and sequencing DNA from environmental samples such as soil, water, or plant tissues, it is possible to analyze complex microbial communities without the need to isolate and cultivate microorganisms (Crandall et al., 2020). This approach enables the identification of both taxonomic diversity and gene functions within microbial populations, which is essential for understanding mechanisms of microbe-microbe and host-microbe interactions and their implications for soil and plant health (Larkin, 2015; Segata et al., 2013). Metagenomics thus represents a powerful tool for deepening the understanding of plant and soil microbiome diversity and functions, offering novel insights for improving plant and soil health (Crandall et al., 2020).

Transcriptomics, a powerful branch of functional genomics, has revolutionized the study of gene expression by enabling the investigation of the complex molecular mechanisms underlying various biological processes, including development and stress responses (Rich-Griffin et al., 2020; Vishwanath et al., 2024). It involves the comprehensive analysis of the entire set of RNA molecules, collectively known as the transcriptome, expressed in a specific tissue or organism. By studying gene expression patterns at a global level, transcriptomics provides valuable insights into the dynamic and coordinated regulation of gene activity. This knowledge not only enhances our understanding of biological systems, but also paves the way for innovations in disease resistance and crop improvement (Nejat et al., 2018). In the context of host-microbe interactions, transcriptomics reveals the gene expression dynamics during these interactions, offering a dynamic view of how hosts adjust their gene activity in response to pathogenic attacks. This approach has provided critical information on the regulatory pathways activated during infection, including those involving signaling molecules that are central to host defense responses (Livaja et al., 2008; Mukherjee, 2022). Using RNA sequencing (RNA-seq), transcriptomics allows for the tracking of gene expression changes over time and across tissues, highlighting how specific genes are regulated in response to microbial presence (Sriden and Charoensawan, 2022). This approach helps in understanding the mechanisms of host defense and uncovers the strategies employed by pathogens to suppress host immunity (Livaja et al., 2008).

Metabolomics is centered on the identification and quantification of metabolites and chemical footprints of cellular processes across different biological species. In plants, metabolism is itself a complex process involving numerous mechanisms within primary and specialized pathways, all of which support to promote plant growth and development. The metabolome, which refers to the complete set of metabolites within an organism, can be analyzed to reveal genetic or environmental variations. This approach is crucial for investigating gene-environment interactions, characterizing mutants, phenotyping, identifying biomarkers, and facilitating drug discovery (Razzaq et al., 2019). Metabolomics has become essential for understanding metabolic networks involved in stress tolerance in plants. While traditional methods primarily relied on morphological observations to differentiate between susceptible and resistant plants or between diseased and healthy conditions, modern molecular analyses now include identifying defense responses, such as analyzing defense-related molecules like reactive oxygen species (ROS) (Castro-Moretti et al., 2020). The integration of advanced analytical tools, such as liquid chromatography–mass spectrometry (LC-MS), gas

chromatography–mass spectrometry (GC-MS), and nuclear magnetic resonance (NMR), has revolutionized metabolic profiling, enabling a more precise analysis of complex biochemical pathways (Chang et al., 2019; Cuperlovic-Culf et al., 2019; Razzaq et al., 2019; Zhou et al., 2019). Metabolites serve multiple functions during plant–pathogen interactions, including defense against pathogen invasion, signal transduction, enzyme regulation, cell-to-cell communication, and antimicrobial activity (Castro-Moretti et al., 2020; Vinayavekhin and Saghatelian, 2010). Understanding the dynamics of these chemical compounds and their roles is essential for deciphering the complex interactions between plants and pathogens. Metabolomics offers critical insights into these interactions by analyzing key metabolites under various physiological conditions, thereby playing a pivotal role in elucidating plant defense mechanisms (Castro-Moretti et al., 2020). Recent advances in multi-omic sciences in Plant Pathology have furthered the understanding of the structure and functions of plant-associated microbes, and the holobiome and pathobiome paradigms have emerged as more evolved and comprehensive concepts compared with the conventional one of pathosystem (Bass et al., 2019; Lyu et al., 2021; Mannaa and Seo, 2021; Vandenkoornhuyse et al., 2015) .

By focusing on major diseases of citrus and olive in the Mediterranean region, this thesis aims to enhance our understanding of plant-pathogen interactions within the context of climate change, ultimately contributing to the development of rationale, innovative and environmentally friendly solutions for disease management.

The specific objectives of this thesis are listed below.

i. To achieve a comprehensive genomic understanding of *Phytophthora oleae*, a recently emerged olive pathogen, through genome sequencing and assembly, providing insights into its pathogenicity mechanisms.

ii. To investigate the impact of biocontrol agents, including *Candida oleoph*ila and *Trichoderma atroviride*, on the transcriptome of olive drupes infected by *P. oleae*, using RNA sequencing. This objective aims to uncover the molecular basis of the plant's defense response and evaluate the efficacy of biocontrol treatments in mitigating disease severity.

iii. To explore the metabolome of different olive cultivars under infections by *Colletotrichum* species responsible for olive anthracnose, focusing on the analysis of key metabolites such as malondialdehyde (MDA), chlorophyll a (CHL-A), chlorophyll b (CHL-B), total carotenoids, and hydrogen peroxide (H_2O_2), in order

to identify physiological and biochemical markers associated with resistance or susceptibility to the pathogens.

iv. To evaluate the influence of organic and conventional management practices on rhizosphere microbial communities in Sicilian citrus orchards, to examine the composition of the core microbiome and seasonal changes in bacterial and fungal communities, to analyze microbial interactions, and to assess species richness and diversity using alpha diversity indices. This research also aimed at unveiling microbial processes involved in nutrient cycling through BeCrop® indexes, focusing on processes such as carbon and nitrogen cyclings. Finally, this line of research was aimed at evaluating the impact of environmental and agronomic factors, including soil type, rootstock, and irrigation practices, on microbial communities.

v. To investigate the diversity of *Phytophthora* communities in citrus orchards of Eastern Sicily using an integrated approach that combines leaf-baiting with metabarcoding, targeting both the ITS-1 region and the *rps10* gene. Conducted after a period of severe drought, the study aimed to assess potential changes in *Phytophthora* communities, as well as the influences of management practices (conventional vs. organic), rootstock, soil physicochemical characteristics, tillage frequency and depth, plant health status (healthy vs. unhealthy), and geographic area of production.

References

Ahouangninou, C., Martin, T., Edorh, P., Bio-Bangana, S., Samuel, O., St-Laurent, L., et al. (2012) Characterization of health and environmental risks of pesticide use in market-gardening in the rural city of Tori-Bossito in Benin, West Africa. *Journal of Environmental Protection*, 03, 241–248. https://doi.org/10.4236/jep.2012.33030.

Azenzem, R., Koussa, T. & Alfeddy, M.N. (2024) Root and crown rot caused by oomycetes: an emerging threat to olive trees. *Tropical Plant Pathology*, 49, 331–345.

Barone, A., Chiusano, M.L., Ercolano, M.R., Giuliano, G., Grandillo, S. & Frusciante, L. (2008) Structural and functional genomics of tomato. *International Journal of Plant Genomics*, 2008, 820274. https://doi.org/10.1155/2008/820274.

Bass, D., Stentiford, G.D., Wang, H.C., Koskella, B. & Tyler, C.R. (2019) The Pathobiome in Animal and Plant Diseases. *Trends in Ecology and Evolution*, 34, 996–1008.

https://doi.org/10.1016/j.tree.2019.07.012.

Cacciola, S.O., Faedda, R., Pane, A. & Scarito, G. (2011) Root and crown rot of olive trees caused by *Phytophtora* spp. *Olive Diseases and Disorders*, 661, 305–327.

Cacciola, S.O. & Gullino, M.L. (2019) Emerging and re-emerging fungus and oomycete soil-borne plant diseases in Italy. *Phytopathologia Mediterranea*, 58, 451–472. https://doi.org/10.14601/Phyto-10756.

Cacciola, S.O. & Magnano di San Lio, G. (2008) Management Of Citrus Diseases Caused By *Phytophthora* Spp. Integrated Management of Diseases Caused by Fungi, Phytoplasma and Bacteria. Springer, pp. 61–82.

Castro-Moretti, F.R., Gentzel, I.N., Mackey, D. & Alonso, A.P. (2020) Metabolomics as an emerging tool for the study of plant–pathogen interactions. *Metabolites*, 10, 52. https://doi.org/10.3390/metab010020052.

Chang, J., Cheong, B.E., Natera, S. & Roessner, U. (2019) Morphological and metabolic responses to salt stress of rice (*Oryza sativa* L.) cultivars which differ in salinity tolerance. *Plant Physiology and Biochemistry*, 144, 427–435. https://doi.org/10.1016/j.plaphy.2019.10.017.

Ciriminna, R. & Angellotti, G. (2024) early bioeconomy era : a case study. 356–364. https://doi.org/10.1002/bbb.2588.

Crandall, S.G., Gold, K.M., Jiménez-Gasco, M. del M., Camila, Filgueiras, C. & Willett, D.S. (2020) A multi-omics approach to solving problems in plant disease ecology. *PLoS ONE*, 15, 1–23. https://doi.org/10.1371/journal.pone.0237975.

Cuperlovic-Culf, M., Vaughan, M.M., Vermillion, K., Surendra, A., Teresi, J. & McCormick, S.P. (2019) Effects of Atmospheric CO2 Level on the Metabolic Response of Resistant and Susceptible Wheat to Fusarium graminearum Infection. *Molecular Plant-Microbe Interactions*, 32, 379–391. https://doi.org/10.1094/MPMI-06-18-0161-R.

FAO (2021) *Citrus Fruit Statistical Compendium*. Rome, Italy. Available online: https://www.fao.org/publications/card/fr/c/CB6492EN/.

FAOSTAT (2021) Food and agriculture organization of the United Nations Statistical Dataset. Statistical Division, FAO: Rome. https://www.fao.org/faostat/en/#data/QCL

IOC (2022) The World of Olive Oil (IOC). https://www.internationaloliveoil.org/the-world-of-olive-oil/

Karpouzas, D.G., Kandeler, E., Bru, D., Friedel, I., Auer, Y., Kramer, S., et al. (2014) A tiered assessment approach based on standardized methods to estimate the impact of

nicosulfuron on the abundance and function of the soil microbial community. *Soil Biology and Biochemistry*, 75, 282–291. https://doi.org/10.1016/j.soilbio.2014.04.022.

Lahlali, R., Taoussi, M., Laasli, S.E., Gachara, G., Ezzouggari, R., Belabess, Z., et al. (2024) Effects of climate change on plant pathogens and host-pathogen interactions. *Crop and Environment*, 3, 159–170. https://doi.org/10.1016/J.CROPE.2024.05.003.

Larkin, R.P. (2015) Soil Health Paradigms and Implications for Disease Management∗. *Annual Review of Phytopathology*, 53, 199–221. https://doi.org/10.1146/annurev-phyto-080614-120357.

Livaja, M., Zeidler, D., Rad, U. von & Durner, J. (2008) Transcriptional responses of A*rabidopsis thaliana* to the bacteria-derived PAMPs harpin and lipopolysaccharide. *Immunobiology*, 213, 161–171. https://doi.org/10.1016/j.imbio.2007.10.004.

Lyu, D., Zajonc, J., Pagé, A., Tanney, C.A.S., Shah, A., Monjezi, N., et al. (2021) Plant holobiont theory: The phytomicrobiome plays a central role in evolution and success. *Microorganisms*, 9, 675. https://doi.org/10.3390/microorganisms9040675.

Mannaa, M. & Seo, Y.S. (2021) Plants under the attack of allies: Moving towards the plant pathobiome paradigm. *Plants*, 10, 125. https://doi.org/10.3390/plants10010125.

Migheli, Q., Cacciola, S.O., Balmas, V., Pane, A., Ezra, D. & San Lio, G.M. Di (2009) Mal secco disease caused by *phoma tracheiphila*: A potential threat to lemon production worldwide. *Plant Disease*, 93, 852–867. https://doi.org/10.1094/PDIS-93-9-0852.

Mukherjee, A. (2022) What do we know from the transcriptomic studies investigating the interactions between plants and plant growth-promoting bacteria? *Frontiers in Plant Science*, 13.

Nejat, N., Ramalingam, A. & Mantri, N. (2018) Advances in transcriptomics of plants. *Advances in Biochemical Engineering/Biotechnology*. https://doi.org/10.1007/10_2017_52.

Razzaq, A., Sadia, B., Raza, A., Hameed, M.K. & Saleem, F. (2019) Metabolomics: A way forward for crop improvement. *Metabolites*, 9, 303. https://doi.org/10.3390/metab09120303.

Rich-Griffin, C., Stechemesser, A., Finch, J., Lucas, E., Ott, S. & Schäfer, P. (2020) Single-cell transcriptomics: A high-resolution avenue for plant functional genomics. *Trends in Plant Science*, 25, 186–197. https://doi.org/10.1016/j.tplants.2019.10.008.

Segata, N., Börnigen, D., Morgan, X.C. & Huttenhower, C. (2013) PhyloPhlAn is a new method for improved phylogenetic and taxonomic placement of microbes. *Nature Communications*, 4, 1–11. https://doi.org/10.1038/ncomms3304.

Singh, B.K., Delgado-Baquerizo, M., Egidi, E., Guirado, E., Leach, J.E., Liu, H., et al. (2023)

Microbiology nature reviews microbiology Climate change impacts on plant pathogens, food security and paths forward. *Nature Reviews Microbiology*, 21, 640–656.

Spreen, T.H., Gao, Z., Fernandes, W. & Zansler, M.L. (2020) Global economics and marketing of citrus products. *The Genus Citrus*, 471–493. https://doi.org/10.1016/B978-0-12-812163-4.00023-1.

Sriden, N. & Charoensawan, V. (2022) Large-scale comparative transcriptomic analysis of temperature-responsive genes in *Arabidopsis thaliana*. *Plant Molecular Biology*, 110, 425–443. https://doi.org/10.1007/s11103-021-01223-y.

Stanley, J. & Preetha, G. (2016) Pesticide Toxicity to Microorganisms: Exposure, Toxicity and Risk Assessment Methodologies. Pesticide Toxicity to Non-target Organisms. pp. 351–410.

Syafrudin, M., Kristanti, R.A., Yuniarto, A., Hadibarata, T., Rhee, J., Al-Onazi, W.A., et al. (2021) Pesticides in drinking water-a review. *International Journal of Environmental Research and Public Health*, 18, 468. https://doi.org/10.3390/ijerph18020468.

Vandenkoornhuyse, P., Quaiser, A., Duhamel, M., Van, A. Le & Dufresne, A. (2015) The importance of the microbiome of the plant holobiont. *New Phytologist*, 206, 1196–1206. https://doi.org/10.1111/nph.13312.

Vinayavekhin, N. & Saghatelian, A. (2010) Untargeted metabolomics. In current protocols in Molecular Biology; John Wiley & Sons, Inc.: Hoboken, NJ, USA,. pp. 1–24.

Vishwanath, P.P., Bidaramali, V., Lata, S. & Yadav, R.K. (2024) Transcriptomics: illuminating the molecular landscape of vegetable crops: a review. *Journal of Plant Biochemistry and Biotechnology*. https://doi.org/10.1007/s13562-023-00871-z.

Wang, Yunhao, Zhao, Y., Bollas, A., Wang, Yuru & Au, K.F. (2021) Nanopore sequencing technology, bioinformatics and applications. *Nature Biotechnology*, 39, 1348–1365. https://doi.org/10.1038/s41587-021-01108-x.

Xu, J. & Wang, N. (2019) Where are we going with genomics in plant pathogenic bacteria? *Genomics*, 111, 729–736. https://doi.org/10.1016/j.ygeno.2018.04.011.

Zhou, S., Zhang, Y.K., Kremling, K.A., Ding, Y., Bennett, J.S., Bae, J.S., et al. (2019) Ethylene signaling regulates natural variation in the abundance of antifungal acetylated diferuloylsucroses and *Fusarium graminearu*m resistance in maize seedling roots. *New Phytologist*, 221, 2096–2111. https://doi.org/10.1111/nph.15520.

Zhou, W., Li, M. & Achal, V. (2024) A comprehensive review on environmental and human health impacts of chemical pesticide usage. *Emerging Contaminants*, 11, 100410. https://doi.org/10.1016/J.EMCON.2024.100410.

2. Genome sequencing and assembly of *Phytophthora oleae*, isolate VK10A, causative agent of rot of olive drupes

Sebastiano Conti Taguali[1,2], Mario Riolo[1], Federico La Spada[1], Santa Olga Cacciola[1*], Giuseppe Dionisio[3*]

[1] Catania University, Department of Agriculture, Food and Environment (UNICT, Di3A), Via S. Sofia 100, 95123 Catania (Italy).

[2] Mediterranea University of Reggio Calabria, Department of Agricultural Science, Località Feo di Vito, 89122 Reggio di Calabria (Italy).

[3] Aarhus University, Department of Agroecology, section of Crop Biotechnology and Genetics, Forsoegsvej 1, 4200 Slagelse (Denmark)

* Corresponding authors: giuseppe.dionisio@agro.au.dk; olga.cacciola@unict.it

The genus *Phytophthora*, often referred to as "plant destroyers," is a taxon of oomycetes including several species well known for causing devastating plant diseases (Davison, 1998). The genus *Phytophthora* is rapidly expanding (Brasier et al., 2022) and, despite the discordance between molecular phylogeny and morphology-based taxonomy, it is well-recognized and organized in multiple phylogenetic clades encompassing more than 223 taxa (Abad et al., 2023).

The genus includes many economically important species that affect a wide range of plant hosts, including vegetables, fruit and nut trees, forest trees, and nursery crops. *Phytophthora oleae* is a newly identified species within the *Phytophthora* genus (NCBI:txid2107226), known for causing significant diseases in plants, particularly in olives. This pathogen has been isolated from rhizosphere soil an roots of olive trees with root rots as well as from rotten drupes. *Phytophthora oleae* affects wild and cultivated olive trees in Mediterranean regions, notably in Italy and Spain (Ruano-Rosa et al., 2018; González et al., 2019). In Spain, *P. oleae* has been identified as a pathogen causing severe decline in wild olive (*Olea europaea* var. *sylvestris*) forests, which are of high ecological value and serve as a key genetic source for olive improvement programs (González et al., 2019). The pathogen was consistently isolated from the rootlets of symptomatic wild olives in a protected forest, alongside other *Phytophthora* species, such as *P. cryptogea*

and *P. megasperma* (González et al., 2019). The identification of *P. oleae* was confirmed through morphological analysis and genetic sequencing of the ITS regions and cox1 sequences (González et al., 2019) (https://idtools.org/phytophthora/index.cfm?entityID=5133&packageID=1131). Notably, *P. oleae* exhibits a maximum growth at a relatively low temperature of 19.9°C on carrot agar medium, distinguishing it from other *Phytophthora* species affecting olives (González et al., 2019). The pathogenicity of *P. oleae* was confirmed on healthy wild olive seedlings, indicating its potential threat not only to wild olive populations, but also to cultivated olive orchards, especially considering the climate change scenario and rainfall patterns in southern Spain (González et al., 2019).

In southern Italy, *P. oleae* has been associated with rot of mature olive drupes in two local cultivars of olive (Ruano-Rosa et al., 2018; Brasier et al., 2022), indicating its role in determining significant damages to olive production. The identification of *P. oleae* as a pathogen of both fruit and roots underscores its versatility and the potential of this species to jeopardize the olive cultivation in the Mediterranean.

In this study, *P. oleae* VK10A has been isolated from a rotten olive drupe collected from a wild olive (*Olea europaea* var. *sylvestris*) tree belonging to the "Complesso Speleologico Villasmundo S. Alfio Nature Reserve (NR)" (Melilli, Siracusa, Italy; DATUM WGS 84, 37°13'17.2"N 15°06'22.3"E). Species identity of the isolate VK10A was confirmed through amplification, sequencing, and BLAST analysis of the Internal Transcriber Spacer regions of the ribosomal DNA. Results showed that the ITS sequence of the isolate VK10A had a 100% identity with of the *P. oleae* isolate P02a (CBS7670, GenBank accession KY982934.1), paratype of the *P. oleae type* isolate P01a (ex-type: CBS7669), belonging to clade 2d (Ruano-Rosa et al., 2018; Jung et al., 2024). General information of the sequencing approach and methods include a genomic DNA (gDNA) preparation of high quality and length for long length sequencing by Oxford Nanopore Sequencing (ONT) with about 150 x as expected genome coverage and Illumina short read sequencing (150 PE) of gDNA (with approximately 90 x coverage) to polish the OTN reads. Furthermore, to facilitate the mapping of the coding sequences (CDSs) onto the newly predicted genes, a *de novo* mRNA approach starting from cDNA was carried out by using a Trinity assembler (Haas et al., 2013). Detailed information for genomic sequencing is described starting from a four-day-old culture of *P. oleae* isolate VK10A grown in Potato Dextrose Agar (PDA) which was subjected to gDNA extraction by using DNeasy PowerSoil Pro kit (Qiagen, Denmark) according to the manufacturer's protocol. The obtained gDNA fragments were in the range of 14-22 kbp with no discernible small fragments judging from Bioanalyzer analysis

(Agilent Technologies, Denmark). DNA concentrations and purities were measured with the Qubit dsDNA HS Assay kit (Thermo Fisher Scientific, USA) and the NanoDrop One (Thermo Fisher Scientific, USA). DNA size distributions were evaluated using the Genomic DNA ScreenTapes on the Agilent Tapestation 4200 (Agilent, USA).

Library preparation was carried out using the ligation sequencing kits (Oxford Nanopore Technologies, UK) on a barcoded SQK-LSK114.24 DNA library prepared according to the manufacturer's protocol, with minor modifications (DNAsense ApS, Aalborg, Denmark) (Sereika et al., 2022). The barcoded DNA library (approximately 10-20 fmol) was loaded onto a primed FLO-MIN114 flow cell and sequenced on a MinION Mk1b device, running MinKNOW v. 23.04.5. FAST5 signal data was base-called and demultiplexed with Guppy v. 6.5.7 (Oxford Nanopore Technologies, Oxford, United Kingdom) using the super-accurate algorithm (dna_r10.4.1_e8.2_400bps_5khz_sup.cfg). Removal of low-quality reads and generation of basic sequencing data statistics were obtained using Nanoq v. 0.9.0 (Steinig and Coin, 2022). Filtered reads were de novo assembled with Flye (Kolmogorov et al., 2019; Kolmogorov et al., 2020) polished once with the help of the Medaka v. 1.8.0 software (https://github.com/nanoporetech/medaka). Subsequently, the ONT data errors were polished with Illumina 350 PE, 1-2Gb (approximately 4-7M reads) data using Racon (via Minimap and Samtools). The draft assembly was subsequently polished twice with Medaka v. 1.8.0. Assembly graphs were inspected with Bandage v. 0.8.1 (Wick et al., 2015). Contigs below 1000 bp were removed with SeqKit v. 2.2.0 (Shen et al., 2016). BUSCO v. 5.2.2 (Manni et al., 2021) was used to evaluate genome completion. Quality-filtered Illumina and Nanopore reads were classified with Kaiju v. 1.9.2 (Menzel et al., 2016) against the subset of GenBank proteins *nr* eukaryotic database. For Illumina RNAseq, *P. oleae* VK10A was grown on PDA and V8 medium and incubated at 20 °C respectively for 10 and 5 days. Total RNA was extracted from mycelia using 1.5 ml of TRI Reagent (Zymo Research, Nordic BioSite, Sweden) using ZR BashingBead Lysis (0.5 mm Y_2O_3 Stabilized Zirconia Beads; Zymo Research, Nordic BioSite, Sweden) and the FastPrep-24™ 5G bead beating grinder and lysis system (MP Biomedicals, Fischer Scientific, Denmark). DNA gDNA and Total RNA samples were sequenced at Novogene (Cambridge, UK) with Illumina Hiseq 4000 and 150 pair end read length (PE), at 30 million of read depths. Data quality control revealed a Q30 [(Base count of Phred value > 30) / (Total base count)] average of 93% for a total of 98% of clean reads.

The quantitative assessment of the assembly was carried out calculating assembly statistics by using the BUSCO (Benchmarking Universal Single-Copy Orthologs) scores (Manni et al., 2021). BUSCO evaluates the completeness of assemblies by looking for the

presence or absence of highly conserved genes (BUSCO orthologs). The *P. oleae* genome assembly was 99% complete relative to an identified ortholog (*P. plurivora*) that covers the entire length of the alignment sequence of the corresponding BUSCO benchmarking. *P. oleae* genome assembly was 1% fragmented which is related to identified orthologs that only partially covers the length of the sequence alignment. Figure 1 shows the Flye v. 2.9.1-b1780 generated *P. oleae* genome draft assembly graph. One of the contigs was clearly showing the entire mitochondrial genome, that has been annotated (65 genes of which 38 CDS, 2 rRNA and 25 tRNA) and submitted to GenBank (PQ510212). However, due to many repetitive regions we could not split the assembly into chromosomes. The Flye Quality-filtered Illumina and Nanopore reads were also classified with Kaiju v. 1.9.2, against the GenBank nr protein database (2023-05-10 database, 321 M protein sequences from both prokaryotes and microbial eukaryotes). When blasted against known *Phytophthora* genomes using GeneBank deposited genomes, the *P. oleae* genome gave as top blastn hits the *P. plurivora* (NCBI:txid639000) genome (with around 93% of genome similarity. This latter also possesses a small genome of 46.9 Mbp (ASM3002794v1).

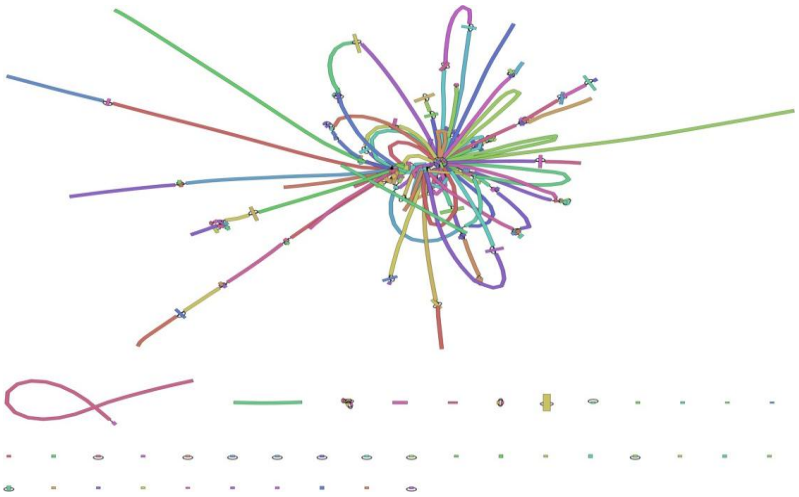

Fig 1 *P. oleae* genome draft assembly graph. Draft assembly graph resulting from the draft *de novo* genome assembly using Flye v. 2.9.1-b1780, highlighting assembly content and contiguity. Only 167 contigs were found in this first draft. However, due to the known *Phytophthora* microsatellite highly repetitive Simple Sequence Repeat (SSR) regions, the contigs in future assembly might be shorter and hopefully better organized into chromosomes. Coloured lines denote size-scaled contiguous DNA elements. Line thickness is proportional to contig coverage. Thin black lines denote connectivity between segments

P. oleae genome annotation was performed using Funannotate 1.8.17 (Stanke and Waack, 2003; Jensen et al., 2008; Ter-Hovhannisyan et al., 2008; Eddy, 2011; Palmer and Stajich, 2020), which started with a filtering out of scaffolds containing mitochondrial DNA sequences and finally 156 scaffolds remained. Afterwards, a RepeatMasking RepeatMasking (Tarailo-Graovac and Chen, 2009) of the genome was made and these soft masked scaffolds were used for the *ab initio* prediction using AUGUSTUS (Stanke and Waack, 2003; Stanke and Morgenstern, 2005) trained with *Fusarium graminearum* intron-exon was made. The funannotate "annotate" pipeline was combined with the Trinity *de novo* mRNA assembly of the cDNA. Prediction of open reading frames (ORFs) from *de novo* mRNA assembly was performed both on the sense and antisense strand by GeneMark (Borodovsky and McIninch, 1993a; Borodovsky and McIninch, 1993b) and GeneMark-ES, version 2 (Ter-Hovhannisyan et al., 2008). For getting the genomic coding sequences (gCDS) we found that besides the (A/C)AG|GT(A/G)AGT consensus sequence (the exon|intron boundary) whereas the first two nucleotides of the intron are underlined, another rare exon|intron consensus, CG|GC as boundary with exons|intron was observed while GT|TG, GT|AC, and AT|AG rare intron|exon consensus was also found at low percentage. In total for the *P. oleae* first draft assembled genome, represented by 43.7 Mbp, we have annotated 19089 genes, of which 18841 gCDS/mRNA and 865 tRNA. A comparison with Trinity *de novo* assembly (Haas et al., 2013) and GeneMark prediction, less proteins were predicted using the cDNA (Table 1).

Table 1. *P. oleae* VK10A ONT genomic DNA plus *de novo RNA* sequencing and assembly statistics together gene prediction and proteome annotation. Using a combination of ONT sequencing and Illumina DNA and RNA sequencing we have produced the first draft of P. oleae VK10A genome and proteome annotation. The table shows both DNA sequencing and assembly data as well as gene prediction by AUGUSTUS (Funanotate) or Trinity (in both sense and antisense orientation). Legend: The Data (Mb) denotes the data yield and the number of generated reads. Read N50 (bp) is the value where half of the data is contained within reads of length N50 or greater. Quality score denotes the median Phred-scaled read quality score. Contigs denote the number of contiguous DNA elements associated with the assembly. Assembly size (Mbp) and Largest contig (Mbp) denote the size of the final assembly and the length of the longest contig, respectively. Contig n50 (kbp) is the value where half of the assembly is contained within contigs of length N50 or greater. GC content (%) denotes the mean content of the G and C nucleotides.

	Raw			Trimmed		
ONT DNA sequencing data	**Data (Mbp)**	**Read N50 (bp)**	**Quality score**	**Data (Mbp) 150 X**	**Read N50 (bp)**	**Quality score**
	10358	7364	18.6	6701	7562	20.5
Assembly data	**Scaffolds**	**Assembly length (Mbp)**	**Largest contig (Mbp)**	**GC content (%)**	**Contig N50 (kbp)**	
	156	43.16	2.05	51.82	684	
Gene prediction data	**Funannotate nuclear genes**	**TRINITY de novo mRNA**	**Funannotate gCDS/mRNA**	**tRNA**	**Secretome**	**Apoplastic effectors**
	19089	13547	18841	865	1995	605
	Funannotate mitochondrion genes	**Mitochondrion CDS**	**Mitochondrion rRNA**	**Mitochondrion tRNA**		
	65	38	2	25		
Proteome annotation data	**CAZy enzymes**	**Glycoside Hydrolases (GHs)**	**Glycosyl Transferases (GTs)**	**Polysaccharide Lyases (PLs)**	**Carbohydrate Esterases (CEs)**	**Auxiliary Activities (AAs)**
	553	248	117	45	29	104
	Secreted (SignalP)	**Proteolytic enzymes (MEROPS)**	**Peptidases**	**Proteases**	**InterPro annotated**	**GO annotated**
	1995	472	270	202	11526	8769
	NPP1 proteins	**RxLR effectors**	**Elicitins**	**Crinkler**		
	39	236	78	264		

The *P. oleae* VK10A genome (43.7 Mbp) as genome size in comparison to other *Phytophthora* species genome size spanning from 228.5 Mbp (e.g. *P. infestants*, reference genome ASM14294v1), to 165.6 Mbp (e. g. *P. palmivora*, PpalZC01v1) or from 101.5 Mbp (e. g. *P. megakarya*, ASM221536v1) to 59 Mbp (e. g. *P. nicotianae*, ASM332846v1) place itself in the bottom of this classification.

Initially, the *P. oleae* VK10A related proteome was annotated by blasting it against most of the GenBank phytophthora species proteins, Mercator4 v7.0 (Lohse et al., 2014). With funannotate "annotate" function, most of the proteins were hierarchical, functionally and phylogenetically annotated using hmmscan/search, diamond and using eggnog database ver. 5.0 (Jensen et al., 2008; Huerta-Cepas et al., 2018). Furthermore, by the blasting into the automated Carbohydrate-active enzyme ANnotation (dbCAN) we identified 553 CAZy enzymes (Yin et al., 2012) which details are presented in different Tabs of the excel file related to the annotation of *P. oleae* NCBI genome (GCA_046127205.1) on Zenodo (https://doi.org/10.5281/zenodo.13254492). InterProScan ver 5.0 (Jones et al., 2014) and gene ontology GO annotation was also performed by the Funannotate annotate pipeline. About 472 proteases (270 peptidases and 202 proteases) were detected belonging to MEROPS databases of which some of those correspond to known pathogenic cysteine and subtilisin proteases. From the secretome point of view, 1995 proteins were predicted to be having a secretion type leader peptide using signalp version 4.0 (Petersen et al., 2011) (Table 1).

From the effectors and pathogenicity proteins point of view, we have blasted among several Phytophthora species with annotated protein our *P. oleae* proteins and discovered 236 RxLR effectors, of which 26 were top blast hits to known avirulence (Avh) proteins, 78 Elicitins, 264 Crinkler proteins and 39 necrosis inducing proteins (NPP). Therefore, our first draft genome sequencing efforts provide strong theoretical basis for elucidating *P. oleae* pathogenic effectors and further studies based on it might contribute to the development of sustainable control approaches against *P. oleae* rot disease.

Data availability: The Whole Genome Shotgun (WGS) of *P. oleae* genome assembly project has been deposited at DDBJ/ENA/GenBank under the accession JBIMZQ000000000 (assembly DJ1425, https://www.ncbi.nlm.nih.gov/datasets/genome/GCA_046127205.1/), along the mitochondrion genome under PQ510212 as accession number. The proteome annotation table has been deposited to Zenodo databases: https://doi.org/10.5281/zenodo.13254492

.

CRediT author statement.

Sebastiano Conti Taguali: Conceptualization, Investigation, Methodology, Data Curation, Writing - Original Draft, Writing - Review & Editing

Mario Riolo: Conceptualization, Investigation, Methodology, Writing - Review & Editing,

Federico La Spada: Conceptualization, Methodology, Writing - Review & Editing.

Giuseppe Dionisio: Conceptualization, Methodology, Software, Data Curation, Formal analysis, Validation, Writing - Original Draft, Writing - Review & Editing, SupervisionResources, Project administration

Santa Olga Cacciola: Conceptualization, Writing - Original Draft, Validation, Writing - Review & Editing, Resources, Supervision, Funding acquisition, Project administration.

FUNDS

This study was supported by the University of Catania, Italy, "Investigation of Phytopathological problems of the main Sicilian productive contexts and eco-sustainable defense strategies (MEDIT-ECO)"- PiaCeRi-PIAno di inCEntivi per la Ricerca di Ateneo 2020-22 linea 2" "5A722192155"; the European Union (NextGeneration EU), through the MUR-PNRR project SAMOTHRACE (ECS00000022).

Conflict of interest: Authors declare no conflict of interest.

Results of this study have been submitted as a scientific article to the Journal of Plant Pathology -Springer

Results of this study have been submitted as a scientific article to the Journal of Plant Pathology -Springer

References

Abad, Z.G., Burgess, T.I., Bourret, T., Bensch, K., Cacciola, S.O., Scanu., B., Mathew, R., Kasiborski, B., Srivastava, S., Kageyama, K., Bienapfl, J.C., Verkleij, G., Broders, K., Schena, L., Redford, A.J. (2023) *Phytophthora*: taxonomic and phylogenetic revision of the genus. Stud Mycol 106:259. https://doi.org/10.3114/SIM.2023.106.05

Borodovsky, M., McIninch, J. (1993a) GENMARK: Parallel gene recognition for both DNA strands. Comput Chem 17:123–133. https://doi.org/10.1016/0097-8485(93)85004-V

Borodovsky, M., McIninch, J. (1993b) Recognition of genes in DNA sequence with ambiguities. Biosystems 30:161–171. https://doi.org/10.1016/0303-2647(93)90068-N

Brasier, C., Scanu, B., Cooke, D., Jung, T. (2022) *Phytophthora*: an ancient, historic, biologically and structurally cohesive and evolutionarily successful generic concept in need of preservation. IMA Fungus 13:1–25. https://doi.org/10.1186/S43008-022-00097-Z

Davison, E.M. (1998). *Phytophthora* diseases worldwide. Plant Pathology, 47(2): 224-225. https://doi.org/10.1046/j.1365-3059.1998.0179a.x

Eddy, S.R. (2011) Accelerated profile hmm searches. PLoS Comput Biol, 7(10): e1002195.

González M, Pérez-Sierra A, Sánchez ME (2019). *Phytophthora oleae*, a new root pathogen of wild olives. Plant Pathology, 68(5): 901-907. https://doi.org/10.1111/ppa.13024

Haas, B.J, Papanicolaou, A., Yassour, M., Grabherr, M., Blood, P.D., Bowden, J., Couger M.B., Eccles, D., Li, B., Lieber, M., MacManes, M.D., Ott, M., Orvis, J., Pochet, N., Strozzi, F., Weeks, N., Westerman, R., William, T., Dewey, C.N., Henschel, R., LeDuc, R.D., Friedman, N., Regev, A. (2013) De novo transcript sequence reconstruction from rna-seq using the trinity platform for reference generation and analysis. Nat Protoc, 8(8): 1494-1512.

Huerta-Cepas, J., Szklarczyk, D., Heller, D., Hernández-Plaza, A., Forslund, S.K., Cook, H., Mende, D.R., Letunic, I., Rattei, T., Jensen, L.J., von Mering, C., Bork, P. (2018) Eggnog 5.0: A hierarchical, functionally and phylogenetically annotated orthology resource based on 5090 organisms and 2502 viruses. Nucleic Acids Research, 47(D1): D309-D314.

Jensen, L.J., Julien, P., Kuhn, M., von Mering, C., Muller, J., Doerks, T., Bork, P. (2008) Eggnog: Automated construction and annotation of orthologous groups of genes. Nucleic Acids Res, 36(Database issue): D250-254.

Jones, P., Binns, D., Chang, H.Y., Fraser, M., Li, W., McAnulla, C., McWilliam, H., Maslen, J., Mitchell, A., Nuka, G., Pesseat, S., Quinn, A.F., Sangrador-Vegas A, Scheremetjew M, Yong SY, Lopez R, Hunter S (2014) Interproscan 5: Genome-scale protein function classification. Bioinformatics, 30(9): 1236-1240.

Jung ,T., Milenković, I., Balci, Y., Janoušek, J., Kudláček, T., Nagy, Z.Á., Baharuddin, B., Bakonyi, J., Broders, K.D., Cacciola, S.O., Chang, T-T., Chi, N.M., Corcobado, T., Cravador,. A., Đorđević., B, Durán, A., Ferreira, M., Fu, C-H., Garcia, L., Hieno, A., Ho, H-H., Hong, C., Junaid, M., Kageyama, K., Kuswinanti, T., Maia, C., Májek, T., Masuya, H., Magnano di San Lio, G., Mendieta-Araica, B., Nasri, N., Oliveira, L.S.S., Pane, A., Pérez-Sierra, A., Rosmana, A., Sanfuentes von Stowasser, E., Scanu, B., Singh, R., Stanivuković, Z., Tarigan, M., Thu, P.Q., Tomić, Z., Tomšovský, M., Uematsu, S.,

Webber, J.F., Zheng, H-C., Zheng, F-C., Brasier, C.M., Horta Jung, M. (2024) Worldwide forest surveys reveal forty-three new species in *Phytophthora* major Clade 2 with fundamental implications for the evolution and biogeography of the genus and global plant biosecurity. Stud Mycol 107:251–388. https://doi.org/10.3114/SIM.2024.107.04

Kolmogorov, M., Bickhart, D.M., Behsaz, B., Gurevich, A., Rayko, M., Shin, S.B., Kuhn, K., Yuan, J., Polevikov, E., Smith, T.P.L., Pevzner, P.A. (2020) metaFlye: scalable long-read metagenome assembly using repeat graphs. Nat Methods 17:1103–1110. https://doi.org/10.1038/s41592-020-00971-x

Kolmogorov, M., Yuan, J., Lin, Y., Pevzner, P.A. (2019) Assembly of long, error-prone reads using repeat graphs. Nat. Biotechnol. 37, 540–546. https://doi.org/10.1038/s41587-019-0072-8

Lohse, M., Nagel, A., Herter, T., May, P., Schroda, M., Zrenner, R., Tohge, T., Fernie, A.R., Stitt, M., Usadel, B. (2014) Mercator: a fast and simple web server for genome scale functional annotation of plant sequence data. Plant Cell Environ 37:1250–1258. https://doi.org/10.1111/PCE.12231

Manni, M., Berkeley, M.R., Seppey, M., Zdobnov, E.M. (2021) BUSCO: Assessing Genomic Data Quality and Beyond. Curr Protoc 1:e323. https://doi.org/10.1002/CPZ1.323

Menzel P, Ng KL, Krogh A (2016) Fast and sensitive taxonomic classification for metagenomics with Kaiju. Nat Commun 7:11257. https://doi.org/10.1038/ncomms11257

Palmer, J.M., Stajich, J. (2020). Funannotate v1. 8.1: Eukaryotic genome annotation. Zenodo, 4054262.

Petersen, T.N., Brunak, S., Von Heijne, G., Nielsen, H. (2011) Signalp 4.0: Discriminating signal peptides from transmembrane regions. Nat Methods, 8(10): 785-786.

Ruano-Rosa, D., Schena, L., Agosteo, G.E., Magnano di San Lio, G., Cacciola, S.O. (2018) *Phytophthora oleae* sp. nov. causing fruit rot of olive in southern Italy. Plant Pathol 67:1362–1373. https://doi.org/10.1111/ppa.12836

Sereika, M., Kirkegaard, R.H., Karst, S.M., Michaelsen, T.Y., Sørensen, E.A., Wollenberg, R.D., Albertsen, M. (2022) Oxford Nanopore R10.4 long-read sequencing enables the generation of near-finished bacterial genomes from pure cultures and metagenomes without short-read or reference polishing. Nat Methods 19:823–826. https://doi.org/10.1038/s41592-022-01539-7

Shen, W., Le, S., Li, Y., Hu, F. (2016) SeqKit: A Cross-Platform and Ultrafast Toolkit for FASTA/Q File Manipulation. PLoS One 11:e0163962.

https://doi.org/10.1371/JOURNAL.PONE.0163962

Sperschneider, J., Dodds P.N. (2022) EffectorP 3.0: Prediction of Apoplastic and Cytoplasmic Effectors in Fungi and Oomycetes. Mol Plant-Microbe Interact 35:146–156. https://doi.org/10.1094/MPMI-08-21-0201-R/ASSET/IMAGES/LARGE/MPMI-08-21-0201-RT6.JPEG

Stanke, M., Morgenstern, B. (2005) AUGUSTUS: a web server for gene prediction in eukaryotes that allows user-defined constraints. Nucleic Acids Res 33:W465–W467. https://doi.org/10.1093/NAR/GKI458

Steinig, E., Coin. L, (2022) Nanoq: ultra-fast quality control for nanopore reads. J Open Source Softw 7:2991. https://doi.org/https://doi.org/10.21105/joss.02991

Ter-Hovhannisyan, V., Lomsadze, A., Chernoff, Y.O., Borodovsky, M. (2008) Gene prediction in novel fungal genomes using an ab initio algorithm with unsupervised training. Genome Res 18:1979–1990. https://doi.org/10.1101/GR.081612.108

Wick, R.R., Schultz, M.B., Zobel, J., Holt, K.E. (2015) Bandage: interactive visualization of de novo genome assemblies. Bioinformatics 31:3350–3352. https://doi.org/10.1093/BIOINFORMATICS/BTV383

Yin, Y., Mao, X., Yang, J., Chen, X., Mao, F., Xu, Y. (2012) Dbcan: A web resource for automated carbohydrate-active enzyme annotation. Nucleic Acids Research, 40(W1): W445-W451. https://doi.org/10.1093/nar/gks479

3. Exploring the impact of various treatments on gene expression in olive (*Olea europaea* L.) drupes infected by *Phytophthora oleae*: Insights from RNA sequencing-based transcriptome analysis

Sebastiano Conti Taguali[1,2], Mario Riolo[1], Federico La Spada[1], Giuseppe Dionisio[3]*, Santa Olga Cacciola[1]*

[1] University of Catania, Department of Agriculture, Food and Environment (UniCT, Di3A), Via Santa Sofia 100, 95123 Catania (Italy).

[2] Mediterranea University of Reggio Calabria, Department of Agricultural Science, Località Feo di Vito, 89122 Reggio di Calabria (Italy).

[3] Aarhus University, Department of Agroecology, section of Crop Biotechnology and Genetics, Forsoegsvej 1, 4200 Slagelse (Denmark)

* Corresponding authors: giuseppe.dionisio@agro.au.dk; olga.cacciola@unict.it .

3.1 Abstract

Phytophthora oleae is a pathogen recently reported to cause fruit rot on olive orchards in Italy and root rot in a natural wild-olive forest in Spain. RNAseq analysis was conducted to gain insight into the molecular mechanisms that trigger a plant defense response upon the inoculation of drupes with *P. oleae* and the pre-treatment with the antagonistic yeast *Candida oleophila* or with culture filtrates of the antagonistic filamentous fungus *Trichoderma atroviride*. Both treatments were applied to the olive drupes 24 h before the inoculation with the pathogen. Although no full resistance was observed, the virulence of *P. oleae* was reduced when the drupes were co-inoculated with the yeast or treated with culture filtrates of *Trichoderma*. Severity of *Phytophthora* rots in olive drupes was assessed at 24, 72, and 168 hours post pathogen inoculation (hpi) and rated based on an empirical scale. The most effective in reducing the disease severity of *P. oleae* infection on olive fruit was the treatment with *T. atroviride* filtrate (56% reduction), followed by *C. oleophila* (52%). Results showed that 2,466, 1,883, and 1,757 genes were differentially expressed in

response to *P. oleae*, to the binary pathosystem *C. oleophila* and *P. oleae*, and *T. atroviride* and *P. oleae*, respectively, as compared to wound alone (control). Differential RNAseq by DESeq2, performed at 72 hours post-inoculation, and qPCR validation, at 24, 72, and 168 hpi, of the top differentially expressed genes defined a new pattern of plant defense mechanisms involving both PAMP and ETI immunity, with production of ROS and PRs.

Keywords: RNAseq, Gene expression, Oomycete, Pathogenesis, Defense responses, Biological control agent, *Candida oleophila*, *Trichoderma atroviride*.

3.2 Introduction

Phytophthora oleae, the only known species comprised in subclade 2d of *Phytophthora* clade 2d (Abad et al., 2023; Jung et al., 2024), was for the first time reported as an emergent pathogen of olive (*Olea europaea* L.) in southern Italy (Ruano-Rosa et al., 2018). Infection by this oomycete causes a soft rot of mature drupes whose symptoms often overlap with those of anthracnose caused by diverse *Colletotrichum* species, which is regarded as the most serious disease of olive fruit worldwide (Agosteo et al., 2023; Cacciola et al., 2012; Moral et al., 2021; Riolo et al., 2023c; Talhinhas et al., 2018). Other *Phytophthora* species were reported to cause rots of olive fruit (Nigro and Ippolito, 2002). Pre- and post-harvest rots of olive drupes incited by fungi and oomycetes may cause severe yield losses and have detrimental effects on oil quality (Chattaoui et al., 2011; Leoni et al., 2018; Moral et al., 2008). Management strategies to prevent spoilage of olive production, caused by infectious diseases of fruit, have mainly focused on anthracnose. Although those strategies have prevalently relied on the use of synthetic fungicides, alternative means, such as the natural substances and biological control agents (BCAs) have been also considered (Cacciola et al., 2012; Moral et al., 2018; Pangallo et al., 2017; Riolo et al., 2023a). By contrast, minor fungal diseases and emerging diseases of olive fruit caused by oomycetes have so far received little attention. The search for more sustainable alternatives to conventional synthetic fungicides is a new frontier of modern plant pathology. In the olive oil supply chain, the objective of substituting or reducing the use of synthetic fungicides is of particular relevance due to the risk that residues on fruit pass into the oil during the extraction process. It is noteworthy the olive fruit itself is a reservoir of microorganisms that can be exploited as BCAs (Riolo et al., 2023a; Riolo et al., 2024). Among BCAs, *Trichoderma* species have been extensively tested against pre- and post-harvest fruit pathogens, including diverse species of *Phytophthora* (Batta, 2004;

Dukare et al., 2019; Ferreira et al., 2020; González-Estrada et al., 2018; Martinez et al., 2023; Mbarga et al., 2014; Stracquadanio et al., 2020). It has been also envisaged the possibility of using bioactive metabolites produced by *Trichoderma* species as natural fungicides (Stracquadanio et al., 2020; Stracquadanio et al., 2021). In field applications, the efficacy of metabolites would be less conditioned by environmental factors than the living microorganism. A more rapid effect would be an additional advantage of metabolites over the living microorganism, as in the olive oil supply chain the post-harvest phase preceding the oil extraction is very brief. Yeasts are other effective BCAs of post-harvest fruit diseases (Droby et al., 1993; Hammami et al., 2022; Liu et al., 2013; Oztekin et al., 2023; Spadaro and Droby, 2016; Xiaokang Zhang et al., 2020). A very interesting antagonistic yeast is *Candida oleophila*, which has showed a biocontrol activity against several post-harvest diseases of diverse fruit crops (Droby et al., 2002; Rovetto et al., 2024). Strains of this yeast have been exploited as commercial bioproducts (Dukare et al., 2019; Lahlali et al., 2004; Lassois et al., 2008; Sui et al., 2020).

Several lines of evidence indicate multiple modes of action contribute to the effectiveness of BCAs in suppressing plant diseases, including the elicitation of plant immune system (Freimoser et al., 2019). However, few studies have addressed the transcriptomic analysis of the complex interaction pathogen/host/BCA. *Phytophthora* species are known to secrete a large array of effectors during infection of the plant host. In recent decades, significant progresses have been made in identifying numerous *Phytophthora* effectors, broadly categorized into two main types: CRN and RxLR effectors (Wang and Jiao, 2019). The CRN proteins are a family of effectors that cause necrosis in the cells of the host and also induce further intracellular effectors that target the host nucleus during infection. RxLR effectors play a central role in pathogen–plant interactions. They are secreted proteins that manipulate the host's immune responses, allowing the pathogen to establish infection (Huang et al., 2019; S., Wang et al., 2023). Although several studies have already elucidated the role of CRN and RxLR proteins in several *Phytophthora* spp., there is a lack of knowledge about the role of these effectors in the pathosystem *P. oleae*/olive drupes.

Successful *Phytophthora* pathogens have evolved and adapted to a specific host range, developing a set of effector proteins and phytotoxins that either directly induce plant cell death or suppress pattern-triggered immunity (PTI) and trigger susceptibility of the host. Nevertheless, some pathogenesis-related proteins (PR-proteins) are constitutive in some plants and represent a first barrier to the pathogen conveying a sort of innate immunity. Most of the time, even such constitutive levels of PR-proteins might be triggered by the

ecto-symbiosis with microorganisms, such as *Trichoderma* spp., or their metabolites known to trigger both growth promotional effects and plant defense mechanisms by the elicitation of salicylic acid (SA)-, ethylene (ET)-, and jasmonic acid (JA)-dependent processes (La Spada et al., 2020; Stracquadanio et al., 2020).

The aims of this study were: i. to evaluate the effectiveness of either *Trichoderma atroviride* culture filtrates or *C. oleophila* strain O in suppressing rot of olive drupes inoculated with *P. oleae*; ii. to examine the differential gene expression in *P. oleae* and olive drupes, treated/non treated with *C. oleophila* or *T. atroviride*-culture filtrate by high throughput technologies (*i.e.* Illumina RNA sequencing).

3.3 Materials and methods

3.3.1 Microorganisms and plant material

Microorganisms included in this study were: the ex-type of the yeast *C. oleophila* Montrocher strain O, ii. the ascomycete *T. atroviride* strain TS and iii. the oomycete *P. oleae* isolate VK10A. C. *oleophila* strain O, *T. atroviride* strain TS and *P. oleae* isolate VK10A were sourced from the culture collection of the Molecular Plant Pathology Laboratory of the Department of Agriculture, Food and Environment of the University of Catania (Catania, Italy) and were identified in previous studies (Riolo et al., 2020; Stracquadanio et al., 2021).

'Coratina' olive fruits were collected from 15-year-old olive trees from an orchard in Calabria (southern Italy), in the municipality of Mirto-Crosia, province of Cosenza (DATUM WGS 84, 39°36′54.5″ N 16°46′11.7″ E). Drupes were used to both determine the incidence of the disease following post-harvest treatments and to study the defense mechanisms triggered in the presence of the pathogen in relation to the applied treatments. Overall, 540 drupes at maturation index (MI) (Riolo et al., 2023c) 4 (MI4) were collected from five trees and stored for 3 hours inside a refrigerated bag while being transported to the laboratory and stored at 8°C until used in experiments.

3.3.2 Preparation of *P. oleae*-inoculum

Phytophthora oleae isolate VK10A was preliminary grown on V8-Agar (V8A) at 20 ± 2°C. Then, inoculum used in following tests was represented by culture fragments (size 2 mm) cut from the growing edge of seven-day-old cultures.

3.3.3 Preparation of *T. atroviride*-culture filtrate

Trichoderma atroviride was grown in the dark in a 500 mL Erlenmeyer flask containing 200 mL of potato dextrose broth (PDB) at pH 7.0 under constant stirring in an orbital shaker

for 30 days (28 ± 2 °C, 140 rpm) (Stracquadanio et al., 2021). After incubation, the supernatant was collected, filtered through a 13-mm/0.22-µm nylon syringe filter and used as treatment for olive drupes in following tests.

3.3.4 Preparation of *C. oleophila* cell suspension

C. oleophila was grown in 500 ml shake flask cultures containing nutrient yeast broth (NYDB) at 24°C for 48 hours. Cells of *C. oleophila* were collected by centrifugation at 5000×g for 10 minutes at 4°C; then, collected cells were suspended in sterile distilled water to reach the concentration to 1×10^8 CFU/ml (a hemacytometer was used). Obtained *C. oleophila* cell suspension was used as treatment for olive drupes in following tests.

3.3.5 Evaluating the effectiveness of *C. oleophila* and *Trichoderma*-culture filtrate in controlling rots of drupes by *P. oleae*

Olive drupes were preliminarily subjected to surface-sterilization by immersion in a 0.5 % NaClO for 30s, rinsing in sterile distilled water (sdw) and air drying for 24 hours. Once dried, olive drupes were punctured once with a sterile needle in an equatorial position and a 20 µl droplet of *C. oleophila* cell suspension, *T. atroviride*-culture filtrate or sdw (control) was pipetted onto the wound. After 24 h of incubation at 21 ± 1°C, the wound of each drupe was inoculated with a 2 mm agar plug collected from a V8A culture of *P. oleae* isolate VK10A. After inoculation, drupes were incubated at 21 ± 1°C, with 80% relative humidity and a photoperiod of 16 h light / 8 h dark. Severity of *Phytophthora* rots in olive drupes was assessed at 24, 72, and 168 hours post pathogen inoculation (hpi) and rated based on the following empirical scale: (0) no symptoms; (1) 0-25% of fruit rot around inoculation point; (2) 26-50% fruit rot; (3) 50-75 % of the fruit covered by mycelium; (4) 100 % fruit covered from mycelium. These values were used to calculate the rAUDPC according to Riolo and other authors (Riolo et al., 2023b; Riolo et al., 2023c; Talhinhas et al., 2005). Overall, the experimental assay included the following three treatments: i. *P. oleae*-inoculated olive drupes treated with sdw (control, IDA); ii. *P. oleae*-inoculated olive drupes treated with *T. atroviride*-culture filtrate (IDB); iii. *P. oleae*-inoculated olive drupes treated with *C. olephila* cell suspension (IDC). The experimental assay was designed as a completely randomized block, with each treatment comprising three biological replicates, each consisting of 20 drupes.

3.3.6. Assessing the experimental assay to study the transcriptome of olive drupes and *P. oleae* in the system olive drupe-*P. oleae*-*C. oleophila*/ *T. atroviride*-culture filtrate

Olive drupes were preliminary surface sterilized, treated with either *C. oleophila* cell suspension or *T. atroviride*-culture filtrate and *P. oleae*-inoculated as described in 4.5. Then, drupes were incubated at 21 ± 1°C, with 80% relative humidity and a photoperiod of 16 h light / 8 h dark. The experimental assay included the following seven treatments: (i) non-wounded drupes treated with 20 µl of sdw (ID1); (ii) wounded drupes treated with 20 µl of sdw (ID2); (iii) wounded drupes inoculated with *P. oleae* (ID3); (iv) wounded drupes treated with *T. atroviride*-culture filtrate and inoculated with *P. oleae* (ID4); (v) wounded drupes treated with *C. oleophila* and inoculated with *P. oleae* (ID5); (vi) wounded drupes treated with *T. atroviride*-culture filtrate (ID6); (vii) wounded drupes treated with *C. oleophila* (ID7). The experimental assay was designed as a completely randomized block, with each treatment comprising three biological replicates, each consisting of 20 drupes. In order to proceed to transcriptomic analyses, at each of the above-mentioned time points, fresh olive fragments from each treatment were collected and immediately frozen in liquid nitrogen and stored at -80°C.

3.3.7 RNA isolation from infected olive drupes and cDNA synthesis for RT-PCR

Total RNA was extracted using RNeasy Plant Mini Kit (Qiagen, Hilden, Germany). Drupes from each treatment (100 mg) were ground to a fine powder with liquid nitrogen, following the manufacturer's protocol and treated with TURBO DNA-free Kit (ThermoFisher Scientific, Italy). The RNA concentration was then adjusted to 200 ng/µl, and its quality was verified by performing denaturing RNA electrophoresis gel in TAE agarose (Masek et al., 2005). First-strand cDNA was synthesized with an oligo d(T)21 primer and reverse transcription was performed using High-Capacity cDNA Reverse Transcription Kit (Applied Biosystems, Foster City, CA, United States) according to the manufacturer's instructions.

3.3.8 Quantitative Real Time-PCR (RT-qPCR) analysis of gene expression

The RT-qPCR for validating expression levels of selected genes of olive drupes and *P. oleae* (Supplementary Table 13) was performed using the QuantGene 9600 system (Bioer Technology, Hangzhou, China). Reactions were performed in a total volume of 20 µl with 10 ng of cDNA, 1 µl of 10 µM of each primer, and 10 µl of PowerUp™ SYBR™ Green Master Mix (2X, Applied Biosystems™, Foster City, CA, United States). For each

treatment, three biological replicates were analysed, with triplicate RT-qPCR experiments per replicate. Thermocycling conditions included 2 min at 50°C for UDG activation, 2 min at 95°C (Dual-Lock™ DNA polymerase), followed by 40 cycles of two steps: 95°C for 15 s (denaturation) and 60°C (annealing/extension) for 1 min. Expression levels of selected genes were calculated using the $2^{-\Delta\Delta Ct}$ method(Livak and Schmittgen, 2001), where $\Delta\Delta Ct$ = (Ct of target gene – Ct of reference gene)$_{sample}$ – (Ct of target gene – Ct of reference gene)$_{calibrator}$ and Ct is the threshold cycle of each transcript, defined as the point at which the amount of amplified target reaches a fixed threshold above the background fluorescence. *O. europaea* tubulin alpha-3 chain (LOC111371391, XM_022993342.1) was used as an internal reference gene. For *P. oleae*, the tubulin beta chain (g8215.t2 (TRINITY_DN6095_c0_g1_i1) gene expression has been used to normalize the RT-qPCR data. The relative expression level of each gene obtained through RT-qPCR was compared to the RNA-seq data. Expression values of the $2^{-\Delta\Delta Ct}$ were represented as boxplots using Python script wit "seaborn", "pandas" and "matplotlib.pyplot" libraries. Dunnett's test was used to calculate the significance (*p-value*) relative to the expression level ($2^{-\Delta\Delta Ct}$) of each sample to wounded olive fruit condition by computing a Student's t-statistic for each experimental conditions and time points (hpi).

3.3.9 Total RNA preparation and Illumina mRNA sequencing

Withdrawal of plant-fungal-oomycete material was carried out around the wounded area from the non-infected and infected drupes. The material was pulverized in liquid nitrogen and stored at -80°C until RNA extraction. Total RNA extraction was performed using the Direct-zol RNA Miniprep kit (Zymo Research, Nordic BioSite, Sweden) with a modified protocol. Frozen samples were extracted with 1.5 ml of TRI Reagent (Zymo Research, Nordic BioSite, Sweden) using ZR BashingBead Lysis (0.5 mm Y_2O_3 Stabilized Zirconia Beads; Zymo Research, Nordic BioSite, Sweden) and the FastPrep-24™ 5G bead beating grinder and lysis system (MP Biomedicals, Fischer Scientific, Denmark). After homogenizing, samples were spin at 21000 ×g for 1 minute and then, phenol:chloroform:isoamyl alcohol 25:24:1 (Sigma-Aldrich, Merck, Germany) extraction was performed. Further steps were performed according to the Direct-zol RNA Miniprep kit. Eluted total RNA quality check was performed using a 2100 Bioanalyzer system (Agilent, Denmark). Two biological samples were extracted in technical triplicate and samples with RNA Integrity Number (RIN) above 8 were selected for RNAseq. Samples were sequenced at Novogene (Cambridge, UK) with Illumina hiseq 4000 and 150 pair end

read length (PE), at 30 million of read depths. Data quality control revealed a Q30 [(Base count of Phred value > 30) / (Total base count)] average of 93% for a total of 98% of clean reads.

3.3.10 *De novo* mRNA analysis

Illumina 150 PE, 30 M reads fastq (Cock et al., 2010) files were processed for removal of the adapters with Trimmomatic Version 0.39 (Bolger et al., 2014). For maximizing and diversifying the mRNA expression of *Phytophthora oleae*, the Trinity *de novo* mRNA assembly algorithm (Haas et al., 2013) was applied to RNA samples of cultures of the isolate VK10A grown in three different substrates, including CZAPEK, MEA and PDA. Annotation of both trinity derived cDNA and AUGUSTUS predicted genes was performed against using Mercator4v6(Lohse et al., 2014) analysis cross-evaluation. AUGUSTUS web prediction gave 20547 proteins of which only 12117 were containing unique scaffold represented of more than 75% as protein identity, the remaining not unique proteins represented alternate proteins or differently spliced or start (ATG) derived proteins. The same number of proteins, 20094 was found by using Trinity ORF prediction software unfiltered and after removing duplicates. Filtering the Trinity accessions for proteins capable of finding a blast hit with other Phytophthora species, then, the real number of de novo mRNA transcript was down to 13373 proteins. It needs to be considered that the Trinity prediction include partial protein/mRNA sequences due to incomplete full-length cDNA. The fasta/excel files related to AUGUSTUS and Trinity protein/CDS/mRNA prediction and annotation can be found at Zenodo (https://zenodo.org/records/11092245).

3.3.11 RNAseq data analysis

The raw Illumina sequence reads of fastaq format were processed as above by removing the adapters. The reference genome and gene model annotation files of *O. europaea* var. *sylvestris* were downloaded from NCBI (*Olea europaea* var. *sylvestris* reference genome O_europaea_v1, accession number GCF_002742605.1) and *P. oleae* reference genome VK10A, from Zenodo (https://zenodo.org/records/11092245). The filtered fastaq files were aligned to the reference genome using Hisat2 v2.0.5 (Kim et al., 2019). The reads with low alignment quality values or unpaired alignments, and alignments to multiple regions of the genome were filtered out by using samtools (Ramirez-Gonzalez et al., 2012) to generate duplicate checked and sorted binary BAM files of mapped reads to the genome. The number of reads and fragments per kilobase per million reads (FPKM) for each gene was calculated using Stringtie v2.2.0 (Pertea et al., 2015). Differential gene

expression analysis between the pathogen-inoculated and control samples at different time points was performed in R studio using the DESeq2 R package in a script (https://bioconductor.org/packages/DESeq2/) customized on the basis of the total normalized reads counts(Love et al., 2014). Corrections for false positives and false negatives were made using the Benjamini-Hochberg procedures (Benjamini et al., 2001) to generate the false discovery rate (FDR).

Fold changes (L2FC, log2Ratio) were estimated from normalized gene expression levels in each sample by using the ratio of the sample Log2 of FPKM and the wounded olive fruit Log2 of FPMK as denominator. The mapped genes with an adjusted false discovery rate (FDR) ≤0.05 and |log2(FoldChange)| > 1 were considered differentially expressed, from L2FC < 0.5 were considered downregulated. To reduce the amount of differentially expressed genes according to 0.05 and 0.001 FDR, shrinkage of log2 (Fold Change) was performed using the R 'apeglm' function (Zhu et al., 2019). Differentially expressed genes (DEGs) clustering heatmaps were generated by the pheatmap and clusterProfiler R packages (Yu et al., 2012). Multiple correlation of the variance of L2FC for all the sample was analyzed by principal components analysis (PCA).

3.3.12 LC-MS identification of proteins in protein filtrate

T. atroviride strain TS was cultured *in vitro* in a YPD liquid media supplemented with malt extract to 1%. After three days, the cultures (in triplicate) were filtered through a Whatman® qualitative filter paper, Grade 1 (WHA1001325 Sigma-Aldrich, Merck, Germany) to retain the mycelia. The filtrate was further centrifuged at 20,000 ×g for 15 minutes then sterile filtered through 0.2 µm vacuum filters. The protein preparation for proteomics including digestion by trypsin and the LC-MS conditions and identification by Waters PLGS software has been described previously (Dionisio et al., 2018).

3.4 Results

3.4.1 Evaluating the effectiveness of *C. oleophila* strain O and *T. atroviride*-culture filtrate in controlling the rot of olive drupes incited by *P. oleae*

This section reports the results of tests aimed at evaluating the effectiveness of either *C. oleophila* strain O cell suspension or *T. atroviride*-culture filtrate in controlling the rot of olive drupes inoculated with *P. oleae* isolate VK10A. Overall, drupes treated with *T. atroviride*-culture filtrate (IDB) or *C. oleophila* cell suspension (IDC) reported values of disease severity significantly lower than control drupe treated with sterile distilled water (sdw) (IDA) (Figure 1). In particular, the mean value of the relative area under the disease

progress curve (rAUDPC) was 0.43 for the control (IDA), 0.21 (i.e. 52% reduction compared to the control) and 0.19 (i.e. 56% reduction compared to the control) for the drupes treated with *C. oleophila* (IDC) and *T. atroviride*-culture filtrate (IDB), respectively. *In vitro* inhibitory activity of liquid culture extracts of *T. atroviride* against *Phytophthora* species (*P. nicotianae* and *P. parvispora*) had been demonstrated in a previous study (Stracquadanio et al., 2020). By contrast, no previous studies reported any data on the efficacy of *C. oleophila* against *Phytophthora* species.

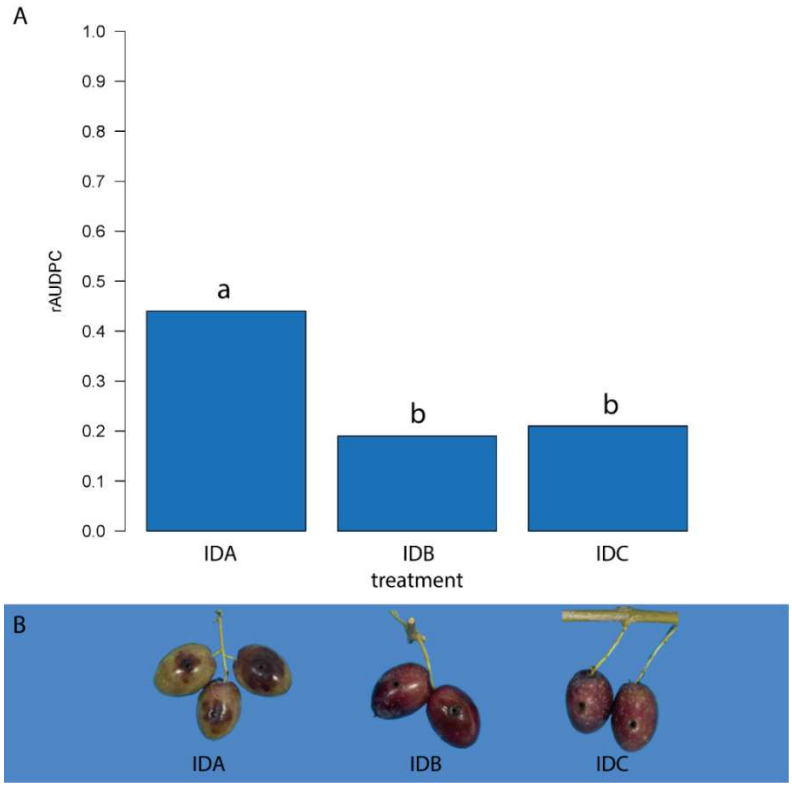

Figure 1. Mean values of the relative area under the disease progress curve (rAUDPC) in olive drupes inoculated with *Phytophthora oleae* and treated with sterile distilled water (control) (IDA), *Candila oleophila* suspension (IDB) or *Trichoderma* atroviride-culture filtrate (IDC). Panel A, rAUDPC values of treatments IDA, IDB and IDC calculated based on % rot severity value recorded at 24, 72 and 168 hours after inoculation (hpi). Values sharing the same letter do not statistically differ according to Tukey's honestly significant difference (HSD) test ($p \leq 0.05$). Panel B, Drupes at 72 hpi showing the different size of necrotic lesion: (IDA) wounded drupes inoculated with *P. oleae*; (IDB) wounded drupes inoculated with *P. oleae* and treated with culture filtrate of *T. atroviride*; (IDC) wounded drupes inoculated with *P. oleae* and *C. oleophila*.

3.4.2 Differential RNA analysis at 72 hours post inoculation with *P. oleae*

This section describes the transcriptomic responses of both olive drupes and *P. oleae* in the system olive drupe-*P. oleae*-*C. oleophila* or olive drupe-*P. oleae*-*T. atroviride*-culture filtrate. To this purpose, the following seven treatments were established: (i) non-wounded drupes treated with 20 µl of sdw (ID1); (ii) wounded drupes treated with 20 µl of sdw (ID2); (iii) wounded drupes inoculated with *P. oleae* (ID3); (iv) wounded drupes treated with *T. atroviride*-culture filtrate and inoculated with *P. oleae* (ID4); (v) wounded drupes treated with *C. oleophila* and inoculated with *P. oleae* (ID5); (vi) wounded drupes treated with *T. atroviride*-culture filtrate (ID6); (vii) wounded drupes treated with *C. oleophila* (ID7). Pre-treatment with *C. oleophila* cell suspension or *T. atroviride*-culture filtrate was performed 24h before *P. oleae* inoculation. Drupe fragments were collected at 24-, 72- and 168-hours post inoculation of *P. oleae* (hpi). However, as in the experiment described at paragraph 2.1., 72 hpi was found to be the best timing for the RNAseq evaluation, as the symptoms of *P. oleae* infection were evident (values of rot severity of about 25%).

The following paragraphs describe the RNAseq analysis of olive fruit performed by analyzing binary conditions (see paragraphs: comparisons 1, 2, 3, 4, 6 and 7). A cluster analysis was also carried out among all the treatments for the olive genes in all the conditions analyzed (see paragraph: comparison 5). Finally, a RNAseq analysis was carried out in the same samples to highlight the differential mRNA changes of *P. oleae* versus the different treatments with either *C. oleophila* cell suspension or *T. atroviride*-culture filtrate; to this aim, pairwise comparisons (see paragraphs: comparisons 8 and 9) or PCA plots were elaborated.

3.4.2.1 Comparison 1: intact olive drupes (treatment ID1) vs. wounded drupes treated with sterile distilled water (treatment ID2)

Only 243 (192 upregulated and 51 downregulated) differentially expressed genes (DEGs) of the olive fruit were detected after filtering with a false discovery rate (FDR) p-value of 0.001 (Figure 2). The upregulated genes included enzymes involved in secondary metabolite production, particularly berberine bridge enzymes (BBE; LOC111391703 and LOC111391702), a subgroup of the superfamily of FAD-linked oxidases that could either be involved in isoquinone alkaloid biosynthesis or in the oxidation of carbohydrates at the anomeric center to the appropriate lactones. Besides, oligogalacturonides (OGs), small fragments coming from the hydrolysis of pectin-homogalacturonan, represent the best example of damage-associated molecular patterns (DAMP) which activate immunity

(Davidsson et al., 2017). However, once the DAMP immunity has been established, the excess of OG accumulation has a negative impact on the plant recovery, which could lead to cell death. BBEs are probably involved in oxidizing oligosaccharide fragments that might be released during mechanical wounds or pathogenesis and could act as DAMPs (Vega-Muñoz et al., 2020). Thus, BBE can efficiently neutralize the OGs by oxidation to the lactone counterparts (Locci et al., 2019), terminating the DAMP activation response(Benedetti et al., 2018). Other top DEGs include the ethylene biosynthetic isogenes of 1-aminocyclopropane-1-carboxylate synthase-like (ACC synthases; LOC111390291, LOC111392037, and LOC111370655). Indeed, their enzyme activity is involved in the synthesis of the precursor, 1-aminocyclopropane 1-carboxylic acid (ACC), synthesized from S-adenosyl-L-methionine (SAM) by ACC synthases (ACSs) and finally oxidized to ethylene (ET) by ACC oxidases (ACOs)(Hoffman et al., 1982). It is known that gaseous ET can trigger and enhance host resistance and basal resistance to fungal pathogens (Helliwell et al., 2016). The ET perception and activation of the defense mechanism pass through the ET receptors and ET transcription factors (TFs) that mediate the signal transduction until the ethylene-insensitive EIN TF (EIN2 and EIN3) hubs mediated by the F-box genes (e.g. EBF1 and EBF2)(Wang et al., 2009). ET receptors are represented by a family of receptors localized in the (ER) membrane. Two main types of ethylene receptors are known; Ethylene response1 (ETR1) and ERS1, belong to subfamily 1c, and ETR2, EIN4, and ERS2 belong to subfamily 2 (Shakeel et al., 2013). Other TFs are activated by ET, such as APETALA2-ethylene responsive factors (AP2-ERFs) which are mediators of stress responses and developmental programs(Licausi et al., 2013). Many ET-related TFs here were DEGs as the ETR TF 1B-like (LOC111378715) which belong to the AP2 DNA-binding TFs in plants such as APETALA2 and EREBPs(Ohme-Takagi and Shinshi, 1995). The elicitin INF-1 of *P. infestans* induced several defense responses in *Nicotiana* spp., including reactive oxygen species (ROS) and ET production with consequent hypersensitive cell death (HCD) and accumulation of the sesquiterpenoid phytoalexin capsidiol (Imano et al., 2022). In this specific case, the production of phytoalexins is regulated by the AP2/ERF TF, NbERF-IX-33 (Imano et al., 2022). Dirigent (DIR) protein 22-like (LOC111383984) was also a highly upregulated DEG, probably involved in catalyzing regio- and stereoselectivity of bimolecular phenoxy radical coupling during lignin or lignan biosynthesis. Dirigent proteins in plants modulate cell wall homeostasis during abiotic and biotic stress (Paniagua et al., 2017). Another top DEG, which is typically expressed after wounding, is beta-amyrin 28-oxidase-like (LOC111396592), a cytochrome CYP716A244 which is implicated in the biosynthesis of

oleanane-type saponin biosynthesis(Jo et al., 2017). Beta-amyrin synthase and beta-amyrin oxidase were characterized in a yeast, where they were able to form not only α-amyrin 6, but also β-amyrin 1, butyrospermol 23, and Ψ-taraxasterol 19 (Jo et al., 2017). Nonsterol triterpenoids of *O. europaea* are then metabolized into multioxygenated compounds and these could represent the precursors of triterpene saponins (Stiti and Hartmann, 2012). Triterpenoids as well as saponins isolated from various plant organs from different species are known to possess antimicrobial as well as antioxidant activities (Topçu, 2006).

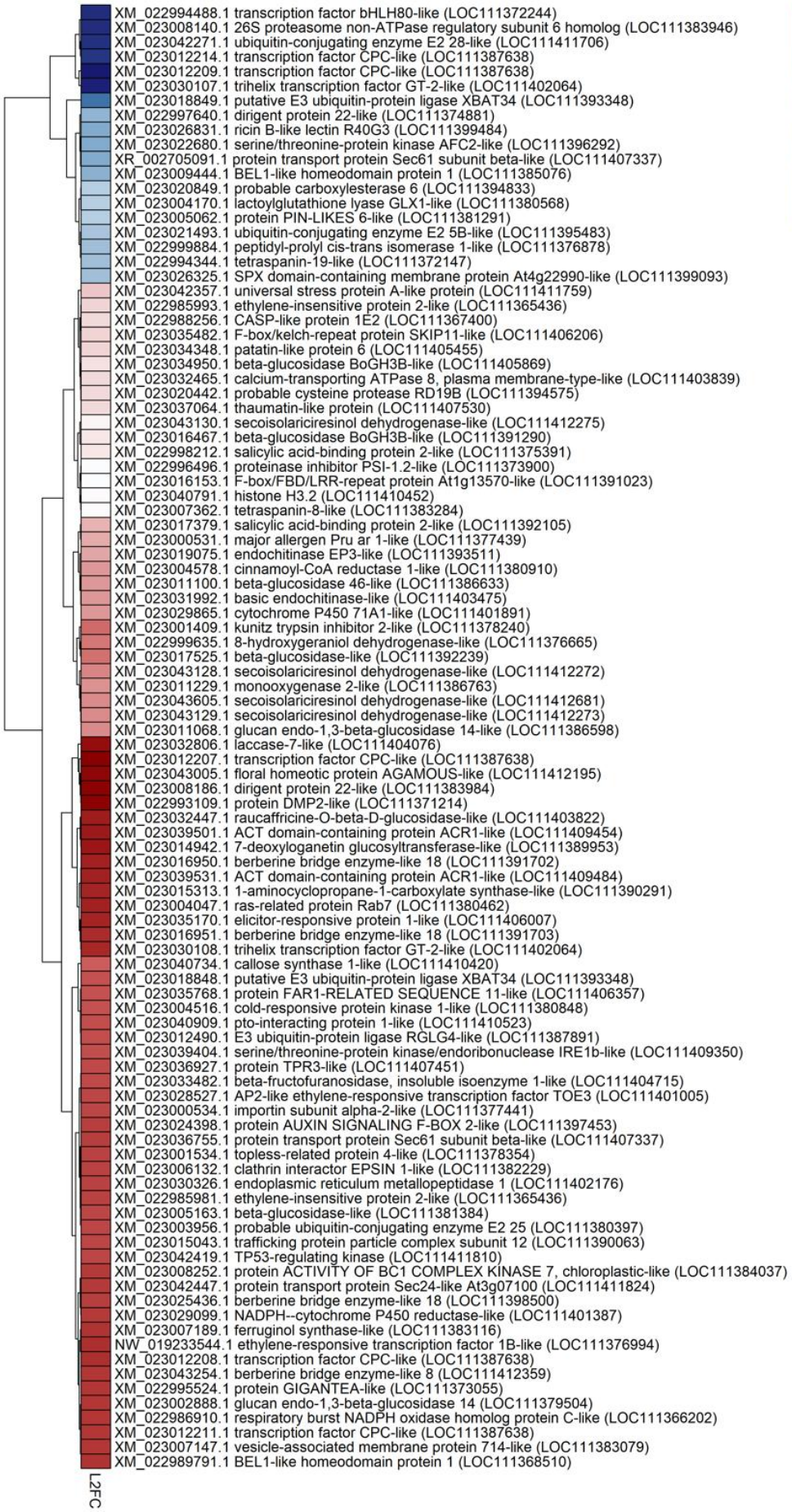
XM_022994488.1 transcription factor bHLH80-like (LOC111372244)
XM_023008140.1 26S proteasome non-ATPase regulatory subunit 6 homolog (LOC111383946)
XM_023042271.1 ubiquitin-conjugating enzyme E2 28-like (LOC111411706)
XM_023012214.1 transcription factor CPC-like (LOC111387638)
XM_023012209.1 transcription factor CPC-like (LOC111387638)
XM_023030107.1 trihelix transcription factor GT-2-like (LOC111402064)
XM_023018849.1 putative E3 ubiquitin-protein ligase XBAT34 (LOC111393348)
XM_022997640.1 dirigent protein 22-like (LOC111374881)
XM_023026831.1 ricin B-like lectin R40G3 (LOC111399484)
XM_023022680.1 serine/threonine-protein kinase AFC2-like (LOC111396292)
XR_002705091.1 protein transport protein Sec61 subunit beta-like (LOC111407337)
XM_023009444.1 BEL1-like homeodomain protein 1 (LOC111385076)
XM_023020849.1 probable carboxylesterase 6 (LOC111394833)
XM_023004170.1 lactoylglutathione lyase GLX1-like (LOC111380568)
XM_023005062.1 protein PIN-LIKES 6-like (LOC111381291)
XM_023021493.1 ubiquitin-conjugating enzyme E2 5B-like (LOC111395483)
XM_022999884.1 peptidyl-prolyl cis-trans isomerase 1-like (LOC111376878)
XM_022994344.1 tetraspanin-19-like (LOC111372147)
XM_023026325.1 SPX domain-containing membrane protein At4g22990-like (LOC111399093)
XM_023042357.1 universal stress protein A-like protein (LOC111411759)
XM_022985993.1 ethylene-insensitive protein 2-like (LOC111365436)
XM_022988256.1 CASP-like protein 1E2 (LOC111367400)
XM_023035482.1 F-box/kelch-repeat protein SKIP11-like (LOC111406206)
XM_023034348.1 patatin-like protein 6 (LOC111405455)
XM_023034950.1 beta-glucosidase BoGH3B-like (LOC111405869)
XM_023032465.1 calcium-transporting ATPase 8, plasma membrane-type-like (LOC111403839)
XM_023020442.1 probable cysteine protease RD19B (LOC111394575)
XM_023037064.1 thaumatin-like protein (LOC111407530)
XM_023043130.1 secoisolariciresinol dehydrogenase-like (LOC111412275)
XM_023016467.1 beta-glucosidase BoGH3B-like (LOC111391290)
XM_022998212.1 salicylic acid-binding protein 2-like (LOC111375391)
XM_022996496.1 proteinase inhibitor PSI-1.2-like (LOC111373900)
XM_023016153.1 F-box/FBD/LRR-repeat protein At1g13570-like (LOC111391023)
XM_023040791.1 histone H3.2 (LOC111410452)
XM_023007362.1 tetraspanin-8-like (LOC111383284)
XM_023017379.1 salicylic acid-binding protein 2-like (LOC111392105)
XM_023000531.1 major allergen Pru ar 1-like (LOC111377439)
XM_023019075.1 endochitinase EP3-like (LOC111393511)
XM_023004578.1 cinnamoyl-CoA reductase 1-like (LOC111380910)
XM_023011100.1 beta-glucosidase 46-like (LOC111386633)
XM_023031992.1 basic endochitinase-like (LOC111403475)
XM_023029865.1 cytochrome P450 71A1-like (LOC111401891)
XM_023001409.1 kunitz trypsin inhibitor 2-like (LOC111378240)
XM_022999635.1 8-hydroxygeraniol dehydrogenase-like (LOC111376665)
XM_023017525.1 beta-glucosidase-like (LOC111392239)
XM_023043128.1 secoisolariciresinol dehydrogenase-like (LOC111412272)
XM_023011229.1 monooxygenase 2-like (LOC111386763)
XM_023043605.1 secoisolariciresinol dehydrogenase-like (LOC111412681)
XM_023043129.1 secoisolariciresinol dehydrogenase-like (LOC111412273)
XM_023011068.1 glucan endo-1,3-beta-glucosidase 14-like (LOC111386598)
XM_023032806.1 laccase-7-like (LOC111404076)
XM_023012207.1 transcription factor CPC-like (LOC111387638)
XM_023043005.1 floral homeotic protein AGAMOUS-like (LOC111412195)
XM_023008186.1 dirigent protein 22-like (LOC111383984)
XM_022993109.1 protein DMP2-like (LOC111371214)
XM_023032447.1 raucaffricine-O-beta-D-glucosidase-like (LOC111403822)
XM_023039501.1 ACT domain-containing protein ACR1-like (LOC111409454)
XM_023014942.1 7-deoxyloganetin glucosyltransferase-like (LOC111389953)
XM_023016950.1 berberine bridge enzyme-like 18 (LOC111391702)
XM_023039531.1 ACT domain-containing protein ACR1-like (LOC111409484)
XM_023015313.1 1-aminocyclopropane-1-carboxylate synthase-like (LOC111390291)
XM_023004047.1 ras-related protein Rab7 (LOC111380462)
XM_023035170.1 elicitor-responsive protein 1-like (LOC111406007)
XM_023016951.1 berberine bridge enzyme-like 18 (LOC111391703)
XM_023030108.1 trihelix transcription factor GT-2-like (LOC111402064)
XM_023040734.1 callose synthase 1-like (LOC111410420)
XM_023018848.1 putative E3 ubiquitin-protein ligase XBAT34 (LOC111393348)
XM_023035768.1 protein FAR1-RELATED SEQUENCE 11-like (LOC111406357)
XM_023004516.1 cold-responsive protein kinase 1-like (LOC111380848)
XM_023040909.1 pto-interacting protein 1-like (LOC111410523)
XM_023012490.1 E3 ubiquitin-protein ligase RGLG4-like (LOC111387891)
XM_023039404.1 serine/threonine-protein kinase/endoribonuclease IRE1b-like (LOC111409350)
XM_023036927.1 protein TPR3-like (LOC111407451)
XM_023033482.1 beta-fructofuranosidase, insoluble isoenzyme 1-like (LOC111404715)
XM_023028527.1 AP2-like ethylene-responsive transcription factor TOE3 (LOC111401005)
XM_023000534.1 importin subunit alpha-2-like (LOC111377441)
XM_023024398.1 protein AUXIN SIGNALING F-BOX 2-like (LOC111397453)
XM_023036755.1 protein transport protein Sec61 subunit beta-like (LOC111407337)
XM_023001534.1 topless-related protein 4-like (LOC111378354)
XM_023006132.1 clathrin interactor EPSIN 1-like (LOC111382229)
XM_023030326.1 endoplasmic reticulum metallopeptidase 1 (LOC111402176)
XM_022985981.1 ethylene-insensitive protein 2-like (LOC111365436)
XM_023005163.1 beta-glucosidase-like (LOC111381384)
XM_023003956.1 probable ubiquitin-conjugating enzyme E2 25 (LOC111380397)
XM_023015043.1 trafficking protein particle complex subunit 12 (LOC111390063)
XM_023042419.1 TP53-regulating kinase (LOC111411810)
XM_023008252.1 protein ACTIVITY OF BC1 COMPLEX KINASE 7, chloroplastic-like (LOC111384037)
XM_023042447.1 protein transport protein Sec24-like At3g07100 (LOC111411824)
XM_023025436.1 berberine bridge enzyme-like 18 (LOC111398500)
XM_023029099.1 NADPH--cytochrome P450 reductase-like (LOC111401387)
XM_023007189.1 ferruginol synthase-like (LOC111383116)
NW_019233544.1 ethylene-responsive transcription factor 1B-like (LOC111376994)
XM_023012208.1 transcription factor CPC-like (LOC111387638)
XM_023043254.1 berberine bridge enzyme-like 8 (LOC111412359)
XM_022995524.1 protein GIGANTEA-like (LOC111373055)
XM_023002888.1 glucan endo-1,3-beta-glucosidase 14 (LOC111379504)
XM_022986910.1 respiratory burst NADPH oxidase homolog protein C-like (LOC111366202)
XM_023012211.1 transcription factor CPC-like (LOC111387638)
XM_023007147.1 vesicle-associated membrane protein 714-like (LOC111383079)
XM_022989791.1 BEL1-like homeodomain protein 1 (LOC111368510)
L2FC
5
0
-5

Figure 2. Selection of top up/down-regulated genes present at 72h post mechanical wounding in mature olive cv. Coratina fruits versus intact drupes. The DESeq2 algorithm has been used to calculate the statistics and the differentially expressed genes were sorted according to the log2FoldChange (L2FC). Filtering by FDR with p-value of 0.01 has been applied. Heatmap colors with similar LF2C have been clustered. The complete set of up- down-regulated genes is present in Supplementary Table 1.

Among top DEGs, it is noteworthy the presence of elicitor-responsive protein 1-like (LOC111406007), which encodes a protein possessing C2 domains which confer a Ca^{2+}-dependence or binding activity. Usually, such C2 domains bind a wide variety of substances including bound phospholipids, inositol polyphosphates, and intracellular proteins probably acting as signal transduction enzymes. The excess of calcium release during the wound or infection can disrupt the calcium signaling. In *Arabidopsis*, its homologue, NP_001078296.1, is annotated as a calcium-dependent lipid-binding (CaLB domain) family protein, and it acts as a novel repressor of abiotic stress response by chelating the excess free Ca^{2+} (De Silva et al., 2011). Among the innate immunity activated defense genes/proteins which have been detected here as DEGs are protease inhibitors (e.g., glu, ase, PSI, potato proteinase inhibitor I, kunitz trypsin inhibitor 2), endo-1,3-beta-glucosidases, endo- and exo-chitinases, pathogenesis-related protein STH-2-like, thaumatin-like protein, cysteine proteinase inhibitor B-like, and defensin-like protein (Supplementary Table 1)

3.4.2.2 Comparison 2: *Phytophthora oleae*-inoculated wounded drupes (treatment ID3) vs. sterile distilled water-treated wounded drupes (treatment ID2)

About 2466 (854 upregulated and 1612 downregulated) genes were differentially expressed with a FDR p-value of 0.001; top upregulated genes are shown in Figure 2. However, when differentially expressed genes are analyzed by the DESeq2 algorithm, a base PFKM mean is also given. Both log2FoldChange and the baseMean of the FPKM counts are not high enough to have a real biological significance in the differential RNAseq data. Therefore, both log2FoldChange (L2FC) and PFKM (baseMean) have been further filtered by a baseMean value above 2.5 (Figure 3).The top differentially expressed transcripts were mRNA encoding many EXORDIUM-like proteins (e.g. LOC111408846, LOC111402133, LOC111389937, etc.), presumably involved in cell proliferation. EXORDIUM proteins were first identified as mediators of brassinosteroid (BR)-promoted growth in *Arabidopsis* (Schröder et al., 2009), but they can be negatively regulated by exogenous cytokinin (Farrar et al., 2003). EXORDIUM 2 like (EXL2, Glyma15g06010) was upregulated and classified among the incompatible interaction genes (IIGs) in the case of

P. sojae infecting soya bean near isogenic lines (NILs) and associated with resistance (Lin et al., 2014).

Figure 3. Heatmap of filtered mRNA DEGs present at 72 h post *P. oleae* inoculation of wounded drupes vs. non-inoculated wounded drupes. The wounded L2FC has been calculated between wounded vs not wounded drupes. The DESeq2 algorithm has been used to calculate the statistics and the DEGs were sorted and clustered according to *P. oleae* infection triggering the highest olive mRNAs (positive values L2FC). Filtering by FDR with p-value of 0.001 has been applied. Heatmap shows filtered mRNA as FPKM > 50 as baseMean. The complete set of up- and down-regulated genes is shown in Supplementary Table 2.

Another differentially expressed gene was the BON1-associated protein 2 (LOC111391572) which is part of the regulatory complex formed by the BONZAI1 (BON1):BON1-associated protein (BAP1) proteins (Hua et al., 2001). BON1-associated proteins seem to exert a negative regulator role related to cell death and defense responses. In plants, BON1 and BAP1 protein-protein interaction sends a negative activation signal to a suppressor of npr1-1, constitutive 1 (SNC1), a nuclear R protein (Zhu et al., 2010). The product of R gene SNC1 represents a hub of different signaling events coming from many different protein receptor kinases at the plasma membrane, which mediate the final event leading to the activation, or not, of plant PTI or effector-triggered immunity (Zhu et al., 2010).

Ethylene biosynthesis is also highly upregulated in the case of *P. oleae* infection, since the final enzyme involved in its biosynthesis, the 1-aminocyclopropane-1-carboxylate oxidase 1-like (ACO, LOC111366119), is markedly upregulated as compared to wounded fruit treated with sdw (L2FC≥ 7.6). Two other ACO isogenes were detected as differentially expressed genes (e.g. LOC111370655 LF2C≥4 and LOC111370659 L2FC≥1.9), suggesting that this final step of ET biosynthesis occurs to a high degree during infection (Houben and Van de Poel, 2019; Iwai et al., 2006).

As mentioned before, Ca^{2+} signaling is very active during wounding. Coupled with pathogen attack, Ca^{2+} signaling is further amplified, as inferred by the fact that a higher number of upregulated calcium binding proteins are differentially expressed during *P. oleae* infection: calcium-binding protein CML38-like (LOC111365847), calmodulin-like protein 6 (LOC111406833), calcium-binding protein CML19 (LOC111378369), probable calcium-binding protein CML30 (LOC111406832), calcium-binding protein PBP1-like (LOC111402783), calmodulin-binding protein 60 C-like (LOC111409968), and others. In particular, calmodulin-binding protein 60 C-like (CBP60, LOC111409968) and calmodulin-binding protein 60 C-like (LOC111370556), as well as the transcription activator SAR DEFICIENT 1-like (LOC111402349) and protein SAR DEFICIENT 1 (SARD1) (LOC111377821)

are known to bind directly to the promoter of ISOCHORISMATE SYNTHASE 1 (ICS1), increasing the production of salicylic acid (SA) and/or binding to the promoter of ABERRANT GROWTH AND DEATH2 (AGD2)-LIKE DEFENSE RESPONSE PROTEIN 1 (ALD1) and SAR DEFICIENT 4 (SARD4), which leads to the biosynthesis of pipecolic acid (Pip)(Sun et al., 2018). In turn, SA and Pip lead to the activation of immune-related genes, such as PATHOGENESIS-RELATED GENES 1 (PRs)(Peng et al., 2018). CBP60 is also known to bind the promoter region of SARD1, suggesting that it directly promotes SARD1 expression (Huang et al., 2021). Activation of PTI and effector-triggered immunity at local infection sites leads to the development of systemic acquired resistance (SAR) in distal parts of the plant, of which SA and Pip represent the signaling molecules (Sun and Zhang, 2021).

Another differentially expressed gene, which encodes the protein SRC2 homolog (LOC111386812), is a calcium binding protein localized in the plasma membrane which possesses a C2 domain. This latter is known to be involved in protein–protein interactions, binding of phospholipids, and targeting of proteins to the membrane in response to Ca^{2+} signaling (Rupwate and Rajasekharan, 2012). However, in the case of pepper infection, when *Phytophthora capsici* secretes a protein elicitor 1 (PcINF1) with homology to the elicitor of the hypersensitive reaction (HR), it induces a cell death response in pepper leaves mediated by the SRC2 protein (Liu et al., 2015). In this case, the upregulation of olive SRC2 could represent a negative factor for plant immunity, but act as a positive mediator of the *P. oleae* INF1 effector by increasing its cell death efficacy.

A huge transcriptional remodeling during *P. oleae* infection is suggested by the massive upregulation of olive histones (Supplementary Table 2): histone H3.2 (LOC111381491), histone H2AX-like (LOC111369819), histone H4 (LOC111408016), histone H2AX-like (LOC111379587), and histone H2B.5-like (LOC111399700). Genome remodeling via epigenetics (changes in methylation level) and transposases activity are known to occur during pathogen attack and the development of plant immunity (Ramirez-Prado et al., 2018). In plants, acetylation of histones H3 and H4 (H3ac and H4ac), trimethylation on lysine residues, and mono-ubiquitination of H2B (H2Bub1) are normally signs of heterochromatin formation with enhanced transcriptional activation(Alvarez et al., 2010). Transcriptional remodeling and genome rearrangement including retrotransposon jumping within the chromatin play a central role in plant defense mechanisms (Jiménez-Ruiz et al., 2020; Kang et al., 2022). Based on *de-novo* synthesis of histones alone, it cannot be possible to discern their epigenetic post-translational

modification, but certainly, artificial treatment of plants with SA induces acetylation of histones H3 and H4 (Jaskiewicz et al., 2011).

Other differentially expressed genes are the product of the genes encoding olive E3 ubiquitin-protein ligases. Some of those could be the homologue of Arabidopsis RING E3 ligase HUB1 which mediates histone mono-ubiquitination with the subsequent activation of heterochromatin and probably contributes to enhancement of the defense mechanism (Dhawan et al., 2009).

That genome rearrangement could be linked to the induction of plant resistance that is evident when DDE-type transposases (containing a DD[E/D]-motif) are involved(Nesmelova and Hackett, 2010). In this study, it is highly probable that *P. oleae* induced a high expression of the protein ALP1-like (LOC111383726), which possesses a N-terminal RNase H domain, a DNA binding domain and a known transposase DDE C-terminal domain. Demethylation of transposable elements (TEs) makes them jump in heterochromatin genes, which, in this case, could be associated with mediating a 'long-term memory', since their insertion into the promoter of these genes makes them constitutively expressed. This epigenetic stress memory can be transmitted to subsequent generations and involves changes in the silencing of transposable elements (TEs) by DNA methylation, histone modifications, and non-coding RNAs. At late infection stages, the DNA jumping activities of functional class I ('copy and paste') and class II ('cut and paste') TEs, might result in small and large mutations at the sites of excision (class 2) and insertion (class 1 and 2). TE-induced insertion/excision accelerates the evolution of novel defense regulatory genes and, because TEs are somewhat regulated by epigenetic mechanisms, the derived defense genes will remain under stress-dependent epigenetic control and potentially able to resist to biotic stresses (Ashapkin et al., 2020).

Transcription factors (TFs) known to be involved during both wound response and pathogen attack are the WRKY TFs (Pandey and Somssich, 2009). These TFs contain a 60-70 amino acid protein domain composed of a conserved WRKYGQK motif and a zinc-finger region (C2HC). Both domains contribute to the capability of DNA to bind with W-box and/or other cis-acting elements, such as in R-genes (Wang et al., 2006) or biosynthetic genes related to specialized metabolism (Chen et al., 2019). Upon *P. oleae* infection, it has been recorded an upregulated (L2FC≥ 3.4) olive WRKY TF 33 (LOC111405948) homologue of AtWRKY33, which functions as a positive regulator of resistance toward some necrotrophic fungi (Zheng et al., 2006). However, the olive WRKY

TF 18-like (LOC111377241) was even more differentially expressed (L2FC≥ 4.6) and, according to the homology function with AtWRKY18, could enhance certain defense signaling, boosting the transcription of PR genes and resistance against certain pathogens(Chen and Chen, 2002). Other upregulated WRKY TFs include WRKY TF 53 (LOC111367778. L2FC>6.1), WRKY transcription factor 23 (LOC111388449, L2FC>4.7), WRKY transcription factor 70 (LOC111392938, L2FC>4.3), and WRKY transcription factor 57 (LOC111373803, L2FC>1.2).

The main differentially upregulated R-genes were the LEAF RUST 10 DISEASE-RESISTANCE LOCUS RECEPTOR-LIKE PROTEIN KINASE-like 1.1 (LOC111390435, L2FC>5.2), the protein ENHANCED DISEASE RESISTANCE 2 (LOC111389201, L2FC>5), the disease resistance protein At5g63020 (LOC111397442, L2FC>5), receptor-like protein kinase HERK 1 (LOC111407351, L2FC>5.5; LOC111407714, L2FC>2.3), the rust resistance kinase Lr10-like (LOC111411655, L2FC>3.6), the disease resistance RPP13-like protein 1 (LOC111400669, L2FC>3.6), the disease resistance protein RGA1 (LOC111392054, L2FC>3.2), and the disease resistance RPP13-like protein 4 (LOC111379833, L2FC>2.2). These plasma membrane-located receptors possess a nucleotide-binding site–leucine-rich repeat (NBS-LRR) and a protein kinase C domain for intracellular signal transduction and are probably involved in the signaling cascade of pathogen sensing(DeYoung and Innes, 2006). On the other hand, upregulated F-box/LRR-repeat proteins might be associated with resistance to *Phytophthora* species, since for instance, in cacao (*Theobroma cacao*), similar genes were differentially upregulated in response to *P. megakarya* only in a resistant cultivar(Pokou et al., 2019). Here, upregulated F-box/LRR-repeat proteins were represented by F-box/FBD/LRR-repeat protein At1g13570-like (LOC111386658) and the F-box/kelch-repeat protein At1g67480-like (LOC111406244) (Supplementary Table 2). Other differentially expressed TFs during *P. oleae* infection are the ethylene-responsive TFs ERF104-like (LOC111386758), ERF017-like (LOC111373863), ERF017-like (LOC111373875), ERF118-like (LOC111403203), ERF071-like (LOC111406367), RAP2-3-like (LOC111403560), ERF4-like (LOC111395465), and ERF04 (LOC111381486). Ethylene induced immunity involves sensing and TF-responsive transcription; this ET-pathway interacts both positively and negatively with the SA-pathway, in relation to the type of plant and pathogen(Van Der Ent and Pieterse, 2012). The APETALA2 (AP2)/ETHYLENE RESPONSE FACTOR (ERF) transcription factor ORA59 is a major positive switch of the ET/JA-mediated defense pathway in *A. thaliana*. In *Arabidopsis*, biosynthetic genes responsible for the formation of hydroxycinnamic acid amides

(HCAAs), known as phytoalexins, are regulated by ORA59 and other ET-responsive TFs (Huang et al., 2022).

Jasmonic acid (JA) and its precursors and derivatives, referred to as jasmonates (Jas), are important molecules in the regulation of plant responses to biotic and abiotic stresses(Ali and Baek, 2020). JA-dependent defense responses are predominantly effective against necrotrophic pathogens and their downstream signaling pathway is typically targeted by fungal effectors to prevent the expression of JA-related defense genes. Coronatine-insensitive protein 1 (COI1) is an F-box protein essential for all the jasmonate responses. COI1 interacts with multiple proteins to form the SCF:COI1:E3 ubiquitin ligase complex which recruits jasmonate ZIM-domain (JAZ) proteins for degradation by the 26S proteasome. *Phytophthora sojae* uses an RXLR effector, Avh94, to manipulate host JA signaling to promote infection hijacking-JA signaling(Zhao et al., 2022). Zhao et al. have demonstrated that Avh94 interacts with soybean JAZ1 or JAZ2, which is a repressor of jasmonic acid (JA) signaling (Zhao et al., 2022). Methyl jasmonate (MeJA)-triggered JAZ1 protein degradation could be inhibited by the proteasome inhibitor MG132, suggesting that JAZ1 is consistently degraded by the 26S proteasome. Avh94 bind JAZ1 and protect it against methyl jasmonate-induced degradation. In turn, the JAZ proteins act as repressors of JA TFs such as AtMYC2, which is involved in the induction of JA biosynthetic genes. In the case of *P. oleae* infection, the coronatine-insensitive protein 1-like (LOC111390662) is a differentially expressed gene and could represent a jasmonate receptor. The highly differential expression of COI1 is accompanied by other upregulated differentially expressed genes encoding F-box proteins: F-box protein At3g07870-like (LOC111409106), F-box protein At1g61340-like (LOC111407155), and F-box protein PP2-A12-like (LOC111408420).

Among differentially expressed genes related to the PR proteins, in the case of *P. oleae* infection, two genes are predominating, the PR proteins STH-2-like (LOC111388408, L2FC≥5) and STH-1-like (LOC111388885, L2FC≥2.3). LOC111388408 was a gene upregulated in response to wounding, but it is even more upregulated in response to the pathogen. Furthermore, another upregulated gene, as compared to the wound condition itself, is the cysteine proteinase inhibitor B-like (LOC111390855, L2FC≥6) and the cysteine proteinase inhibitor A-like (LOC111411928, L2FC>3) which could act in defense, trying to block several *P. oleae* cysteine proteases. An upregulated gene related to the apoplastic immunity/defense protease was the cysteine protease RD19B (LOC111394575) of the *O. europaea* homologue of RD19, an *Arabidopsis* cysteine protease that modulates

RESISTANT TO RALSTONIA SOLANACEARUM 1-R (RRS1-R) (Bernoux et al., 2008). Other differentially expressed genes related to defense response, from highest to lowest L2FC, respectively, are pollen allergen Che a 1-like (LOC111394816, L2FC≥4.7), subtilisin inhibitor CLSI-I-like (LOC111374455, L2FC≥4.5), and kirola-like proteins (LOC111411103, and LOC111410001). On the other hand, a defense response can be represented by the upregulated expression of proteases such as aspartic proteinase Asp1-like (LOC111394357, L2FC>2.2), subtilisin-like protease SBT1.6 (LOC111374885, L2FC>2.1), and SBT3.15 (LOC111386418, L2FC>1.7).

For most of the common differentially expressed genes detected in this comparison, a higher level of upregulation was generally observed. Importantly, tetraspanin-2 (LOC111399506) and tetraspanin-8-like (LOC111403728, and LOC111383284) are genes related to the wounding condition itself (Figure 1). Tetraspanins are transmembrane specific proteins of extracellular vesicles (EVs) or exosomes (EXOs) (Cui et al., 2020), which possess the function of cargo vesicle shipping molecules involved in plant–pathogen interaction. Exosomes transport lipids, proteins (e.g. PR proteins), messenger RNA, and especially microRNAs (Bailey et al., 2011). Silencing of the pathogens by miRNA is a recent trend in pathogen resistance (Zhou et al., 2022). Indeed, plant EVs inhibit fungal growth and virulence by transferring their cargo content into fungal cells at the appressoria/haustoria (Regente et al., 2017). Another role of tetraspanins is in moving the EVs through infection hot spots and allowing the exosomal NADPH oxidase (NOX) to release ROS molecules locally (e. g. H_2O_2 production).

It is also worth mentioning the differential expression of the gene encoding for the receptor-like protein kinase FERONIA (FER; LOC111374777, L2FC≥5.5) (Supplementary Table 2). FER negatively regulates plant immunity by inhibiting JA and coronatine (COR) signaling. It phosphorylates and destabilizes MYC2, the master regulator of JA signaling, which otherwise activates SA biosynthesis (Guo et al., 2018). FER, in response to abiotic and biotic stress, acts as a sensor of cell wall integrity which could be challenged by pathogen secreted enzymes (Ji et al., 2020). FER may negatively regulate plant immunity to biotrophic pathogens (Kessler et al., 2010). The plant rapid alkalinization factor (RALF) are secreted peptides that were first identified through their ability to trigger a rapid increase in extracellular pH [a]. Their mechanism of action is through binding to FERONIA, that once activated triggers extracellular alkalinization, to favor pathogenic subtiliases (alkaline proteases) or alkaline cysteine proteases and inhibits the defense response (Kessler et al., 2010).

3.4.2.3 Comparison 3: wounded olive drupes pre-treated with *C. oleophila* and inoculated with *P. oleae* (treatment ID5) vs. wounded olive drupes inoculated with *P. oleae* (treatment ID3).

A total of 1883 (1018 upregulated and 865 downregulated) olive differentially expressed genes were detected in this comparison (Supplementary Table 3). It is known that *C. oleophila* secretes various cell wall-degrading enzymes, exo-β-1,3-glucanases, chitinases, and proteases, which are especially active against filamentous fungi (Bar-Shimon et al., 2004). *C. oleophila* has an *in vitro* effect on the inhibition of mycelial growth of several *Phytophthora* species (Hammami et al., 2022). Due to this beneficial effect, some of the genes in *O. europaea* related to the pathogen response could be downregulated, since the pre-treatment ameliorates the pathogenic index (rAUDPC = 0.21; Figure 1, IDC). Thus, the downregulated genes, in this comparison, could represent the olive genes that help to counteract the pathogen invasion, or which are no longer needed since the pathogenic effect of *P. oleae* decreased due to *C. oleophila* pre-treatment. Among the top downregulated genes with L2FC>-21 were ALA-interacting subunit 1-like (LOC111368552), the ras-related protein Rab7 (LOC111380462), and protein YIF1B-like (LOC111391136), all localized into the Golgi apparatus, regulating endomembrane dynamics and involved in secretory vesicle formation (Tripathy et al., 2021). In the specific case here, RABs, which are the largest family of small guanosine triphosphate (GTP)-binding proteins, are involved in intracellular trafficking and in autophagy or plant microbe interactions, and in biotic and abiotic stress responses (Tripathy et al., 2021), for instance, the secretion of PATHOGENESIS-RELATED 1 (PR1) protein to the apoplast. *Phytophthora capsici* RxLR effector RxLR242 has been found to bind RABE1-7, a ras-related protein, and inhibits vesicle trafficking (Li et al., 2022). This detected decrease of vesicle trafficking is accompanied by the strong downregulation of the WRKY TF 18-like (LOC111377241) here with L2FC>-8.5 instead of +3.5 as for *P. oleae* infection itself. Otherwise, WRKY 18, as mentioned, could have further enhanced another defense signaling (Chen et al., 2019).

One of the possible mechanisms by which *O. europaea* counteracts *P. oleae* infection is through synthesis of sesquiterpenoid phytoalexins. In potato challenged by *P. infestans*, it has been found that the infected tissue produces antimicrobial sesquiterpenoid phytoalexins (*e.g.* lubimin and rishitin) which might have been implicated in a resistance mechanism in some cultivars (Yoshioka et al., 2019). Here, there is a clear downregulation of sesquiterpenoid phytoalexin biosynthesis when drupes are pre-treated with *C. oleophila* and inoculated with *P. oleae* (treatment ID5) as compared to drupes inoculated

with *P. oleae* (treatment ID3) (Supplementary Table 3). Vetispiradiene synthases or sesquiterpene cyclases and cytochrome P450 premnaspirodiene oxygenases catalyze several key biosynthetic steps in the synthesis of antimicrobial (phytoalexins) sesquiterpenes (Takahashi et al., 2007). Indeed, the expression of olive vetispiradiene synthase 2-like (LOC111371938, L2FC>-7.1), vetispiradiene synthase 2-like (LOC111372151, L2FC>-7), premnaspirodiene oxygenase-like (LOC111369993, L2FC>-6.5; LOC111383354, L2FC>-5.9; LOC111375139, L2FC>-5.2; LOC111374442, L2FC>-4.6), vetispiradiene synthase 2-like (LOC111394812, L2FC>-6.3), vetispiradiene synthase 2-like (LOC111394298, L2FC>-5.7), and (-)-isopiperitenol/(-)-carveol dehydrogenase (LOC111388383, L2FC>-5.7; LOC111388380, L2FC>-5.0) clearly points to the production of sesquiterpenoid defense compounds. These enzymes are upregulated in treatment with the only inoculation of *P. oleae* (ID3) (Supplementary Table 3) but also during *P. infestants* infection in potato. Associated with decreased infectivity of *P. oleae* due to *C. oleophila* pre-treatment, production of these phytoalexins is downregulated. However, the amount of phytoalexins produced also depends on the amount of the precursor mevalonate and hence, the expression level of 3-hydroxy-3-methylglutaryl CoA reductase (HMGR) (Yoshioka et al., 1999).

Lignan biosynthesis is also regulated differentially from that occurring during wounding and plant defense responses in this comparison. Many phytoalexins in plants are represented by complex dimeric substituted lignan (Okazaki et al., 2007). Dimerization of two coniferyl alcohol units produces pinoresinol, which is then reduced to lariciresinol and secoisolariciresinol by pinoresinol/lariciresinol reductase (PLR), and finally into matairesinol by secoisolariciresinol dehydrogenase (SIRD) (Hano et al., 2006). Here, opposite to what was observed in olive drupes only inoculated with *P. oleae* (treatment ID3) (Supplementary Table 2), the biosynthetic enzymes of the lignan biosynthesis are also downregulated with *C. oleophila* co-infection: dirigent protein 22-like (LOC111374881, L2FC>-3.5), dirigent protein 19-like (LOC111376314, L2FC>-3), dirigent protein 22-like (LOC111383984, L2FC>-2), and the secoisolariciresinol dehydrogenase-like (LOC111412270, L2FC>-3.6; LOC111412278, L2FC>-1.3) (Supplementary Table 3).

On the other hand, *C. oleophila* pre-treatment also triggered the upregulation of beneficial genes/proteins that help to counteract the *P. oleae* infection. For instance, the PR proteins STH-21-like (LOC111388400) and STH-2-like (LOC111388410) showed L2FC≥1.09 and =1.7, respectively, but baseMean (PFKM) counts of 4032 and 2646. This means that even a small log2-fold increase with elevated high expression counts could be significant if the *p*-value and *p*-adj value are small. The lowest *p*-value and *p*-adj value of

the upregulated mRNA/genes during *C. oleophila* co-infection were also filtered by high baseMean and L2FC (Figure 4). Many differentially expressed genes related to defense proteins are also upregulated, such as proteinase inhibitor PSI-1.2-like (LOC111373900), xylanase inhibitor thaumatin-like protein 1b (LOC111367584), chitinase hevamine-A-like (LOC111402962), basic endochitinase-like (LOC111379188), aquaporin PIP1-3-like (LOC111408442), TIP1-1 (LOC111403122), and PIP2-2-like (LOC111372815) (Figure 4, Supplementary Table 3).

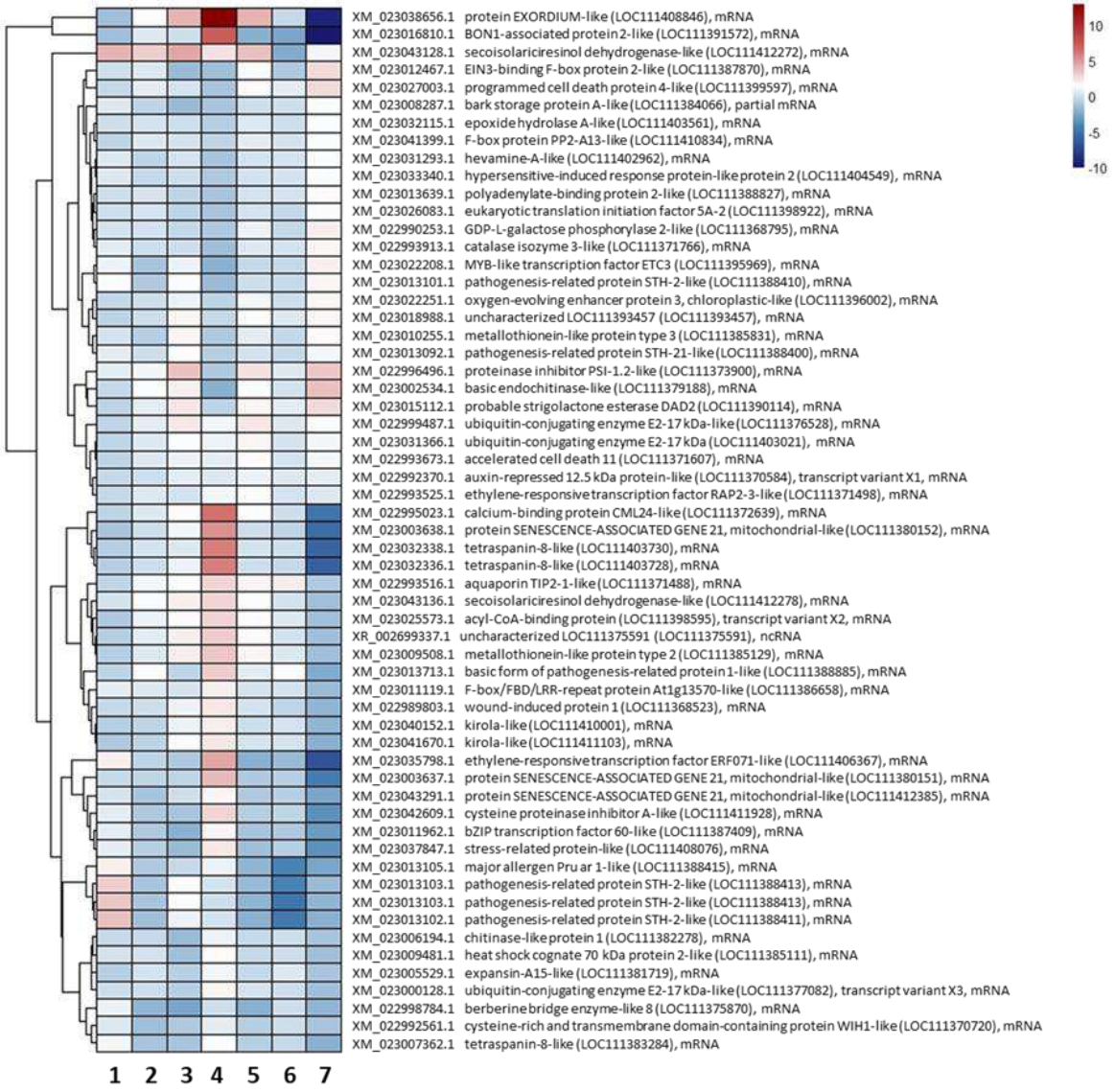

Figure 4. Cluster heatmap analysis of the top mRNAs related to DEGs of *O. europaea* detected 72 hpi from the significative upregulated genes during *C. oleophila* co-infection with *P. oleae* vs. infection with *P. oleae* alone (lane 7). Filtering after DESeq2 analysis was applied to the DEGs in Supplementary Table 3 by sorting for the lowest *p*-value/*p*-adj-value and highest baseMean or L2FC. Lane 1, L2FC of wounded drupes vs. intact drupes; lane 2, L2FC of wounded drupes with *T. atroviride* extract vs. wounded drupes; lane 3,

L2FC of wounded drupes plus *C. oleophila* vs. wounded drupes; lane 4, L2FC of wounded drupes plus *P. oleae* vs. wounded drupes; lane 5, L2FC of wounded drupes plus *C. oleophila* and *P. oleae*; lane 6, L2FC of wounded drupes plus *T. atroviride* extract plus *P. oleae* vs. wounded drupes; lane 7, L2FC of wounded drupes plus *C. oleophila* and *P. oleae* vs. wounded drupes and *P. oleae*.

The involvement of the aquaporins (AQPs) is not immediate, but it has been shown that they also transport H_2O_2(Smirnoff and Arnaud, 2019). Hydrogen peroxide acts as a ROS signaling molecule and can be produced by various oxidases, superoxide and superoxide dismutase, plasma membrane NADPH oxidases, and peroxisomal oxidases, by electron transport in chloroplasts and mitochondria, or by other apoplastic oxidases. In wheat (*Triticum aestivum* L.), TaPIP2;10 transports the pathogen-induced apoplastic H_2O_2 into the cytoplasm of the infected cell and this signal induces PTI immunity (X., Wang et al., 2021). Consequently, in this comparison, the olive AQPs expressed here might have a function of stimulating the H_2O_2 signaling and accelerate the PTI response. Besides, the non-symbiotic hemoglobins have been implicated in the scavenging of nitric oxide signaling (Wendehenne et al., 2004). In this comparison, the possible role of the upregulation of the non-symbiotic hemoglobin 2-like (LOC111376313) could be that of neutralizing the excess of NO produced during the pre-treatment (Supplementary Table 3).

3.4.2.4 Comparison 4: wounded olive drupes pre-treated with *Trichoderma atroviride*-culture filtrate and inoculated with *Phytophthora oleae* (treatment ID4) versus wounded drupes inoculated with *P. oleae* (treatment ID3).

A total of 1757 (914 upregulated and 843 downregulated) olive DEGs differentially expressed genes were detected in comparison 'olive drupes pre- treated with *Trichoderma atroviride*-culture filtrate (treatment ID4) and inoculated with *Phytophthora oleae*' versus 'olive drupes inoculated with *P. oleae* (treatment ID3)' (Supplementary Table 4). Biocontrol fungi, such as *Trichoderma* spp., are known to induce systemic resistance (ISR) and prime their host plants to become more resistant to future attack from pathogenic microorganisms (Shoresh et al., 2010). For example, *Trichoderma viride* produces the peptide antibiotic alamethicin (Mathew and Balaram, 1983), that forms PM-pores and alters the membrane potential and ion permeability, and acts against other fungi or bacteria (Aidemark et al., 2010). The *T. atroviride*-culture filtrate used in this study was checked by proteomics for evaluating its composition in proteins. To this aim, the culture filtrate was subjected to Liquid Chromatographic – Mass Spectrometry (LC-MS) proteomic analysis and the top abundant proteins were identified (Table 1).

Table 1. Proteins with the highest concentration in *Trichoderma atroviride* strain TS-culture filtrate. Identification of the tryptic peptides was made by LC-MS and runs were analyzed by the software Protein Lynx Global Server (PLGS v3.0, Waters, Milford, USA).

Accession	Description	mW (Da)	PLGS Score	Peptides	Theoretical Peptides	Protein Coverage (%)	RMS Mass Error (ppm)
XP_013937770.1	Epl1 Cerato-platanin (eliciting plant response like protein)	14537	3428.453	10	8	44.9275	2.664
XP_013947697.1	Fungal specific cysteine rich protein TRIATDRAFT 297515	14227	2068.27	8	6	21.3333	2.6779
XP_013947323.1	SSCRP homologue to *Alternaria alternata* allergen 1 (TRIATDRAFT 297835)	21243	929.0758	2	7	7.0707	2.8815
XP_013944816.1	FAD-binding containing oxidase TRIATDRAFT 299189	65421	588.5992	17	37	31.9079	2.7963
XP_013947876.1	Calmodulin-like TRIATDRAFT 297616	16971	429.0748	8	24	48.3221	2.9071

XP_013947715.1	Glycoside hydrolase family 72 protein	57251	336.4076	8	28	19.3015	2.3381
XP_013944241.1	Heterokaryon incompatibility protein (HET) TRIATDRAFT 292246	41924	316.7303	8	32	15.2406	2.7148
XP_013938290.1	Collagen triple helix repeat-containing protein TRIATDRAFT 89284	14635	264.8594	7	20	23.2558	2.6052
XP_013938761.1	Coiled-coil domain-containing protein TRIATDRAFT 29005	17709	215.9985	8	15	21.7391	1.7383

The most abundant protein was the Epl1 elicitin, which is a member of the Cerato-platanin family that contains several phytotoxic proteins of about 150 AA residues. Cerato-platanin contains a cysteine-rich domain (four cysteine residues that form two disulfide bonds). *Trichoderma viride* and *T. atroviride* secrete the proteins Sm1 (XP_013943617.1) and Epl1 (XP_013937770.1), respectively, which elicit local and systemic disease resistance in plants (Zhou et al., 2010). Deletion of epl1 in *T. atroviride* resulted in reduced systemic protection against *Alternaria solani* and *Botritis cinerea*, whereas the *T. virens* sm1 KO strain was less effective in protecting tomato against *Pseudomonas syringae* and *B. cinerea*. Upregulation of epl1 and sm1 led to enhanced basal resistance in tomato i.e., systemic acquired resistance (SAR) and induced systemic resistance (ISR) (Salas-Marina et al., 2015).

Results from this study suggest that the impact of *T. atroviride*-culture filtrate pre-treatment on *P. oleae* was significative, as it has been observed the lowest reduction in pathogenic index (rAUDPC = 0.19; Figure 1, IDB). Furthermore, RNAseq results strongly suggest that the pre-treatment of olive drupes with this culture filtrate determined a marked reduction of expression of the *P. oleae* infection marker proteins.

The data in Figure 5 many pairwise comparisons have been selected and filtered according to the most significant upregulated differentially expressed genes (lane 7 describe the comparison 4).

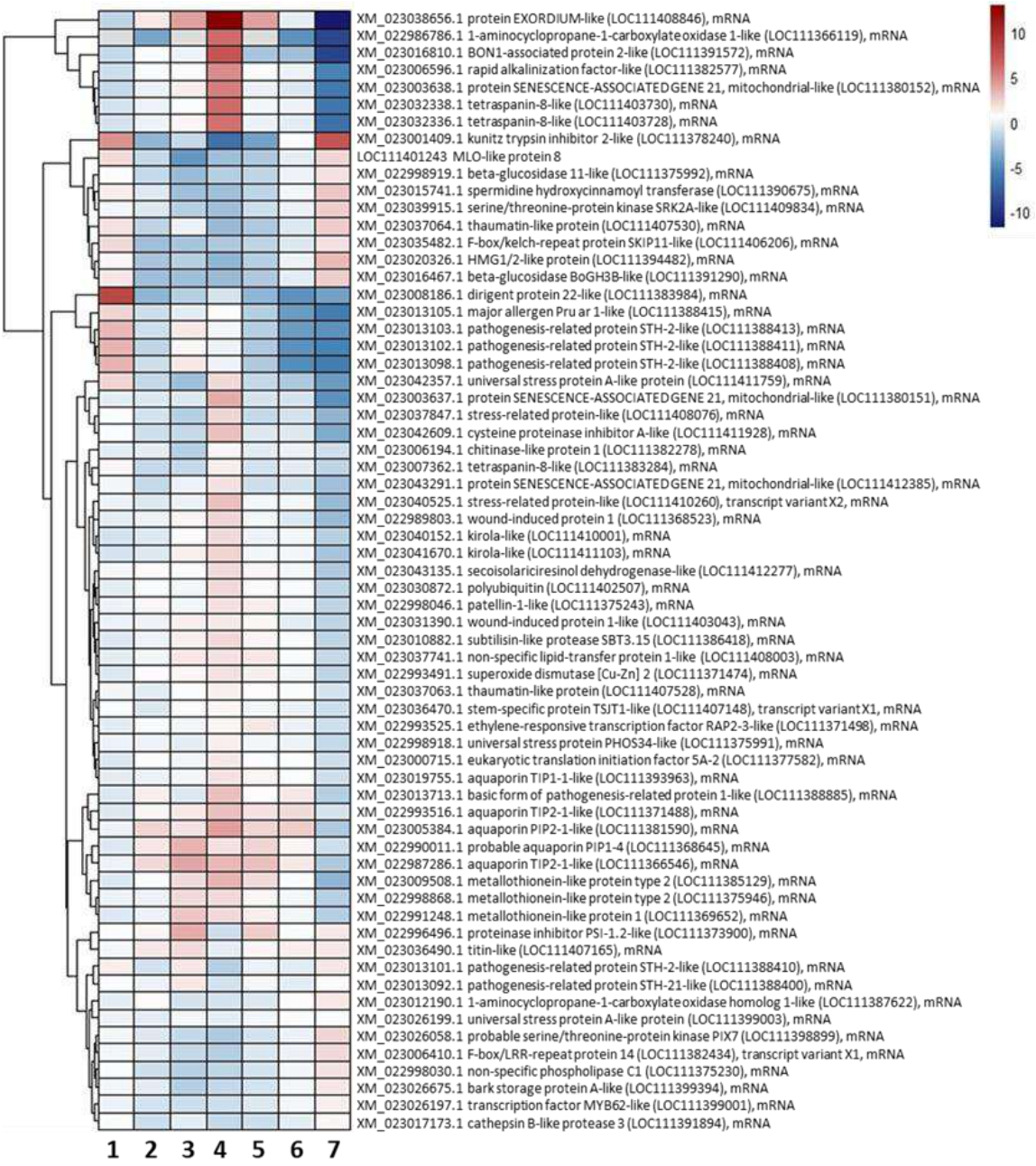

Figure 5. Cluster heatmap analysis of the top mRNAs related to DEGs genes of *O. europaea* detected during 72 hpi from the significant upregulated genes during *T. atroviride culture filtrate* pre-treatment plus *P. oleae* vs infection with *P. oleae* alone (lane 7). The DESeq2 data have been filtered first by lowest pvalue/padj value and then highest baseMean and L2FC from Supplementary Table 4. Lane 1: L2FC of wounded olives vs intact ones; lane 2: L2FC of wounded plus *T. atroviride* extract vs wounded; lane 3: L2FC of wounded plus *C. oleophila* vs wounded; lane 4: L2FC of wounded plus *P. oleae* vs wounded; lane 5: L2FC of wounded plus *C. oleophila* and *P. oleae*; lane 6: L2FC of wounded plus *T. atroviride extract* plus *P. oleae* vs wounded; lane 7: L2FC of wounded plus *T. atroviride* culture filtrate pre-inoculation plus *P. oleae* vs infection with *P. oleae* alone.

By associating differentially expressed genes resulting from comparison 4 with results from LC-MS analysis, it can be speculated that the pre-treatment of olive drupes with of *T. atroviride*-culture filtrate alerts the plant tissues to pathogen attack. Indeed, one of the top upregulated gene, the HR protein-like protein 2, OeHIR-2 (LOC111404549) (Supplementary Table 4), is responsible for alerting the tissues(Zhou et al., 2010). In this study, two F-box/LRR-repeat proteins 14 (LOC111382434) and (LOC111405202) were also upregulated, but not in stoichiometric amounts as for OeHIR-2 (LOC111404549) (Supplementary Table 4). Therefore, OeHIR-2 should instead be responsible for the disease resistance response, perhaps triggered by *T. atroviride* culture filtrate, which gave the lowest pathogenicity index in this comparison.

Unexpectedly, there were two possibly slightly upregulated resistance genes: LRR, leucine-rich repeat receptor-like serine/threonine-protein kinase homologue of At1g06840 (LOC111371641) and MLO-like protein 8 (LOC111401243) (Supplementary Table 4). Using the Arabidopsis eFP Browser(Winter et al., 2007), it is possible to visualize that the expression of At1g06840 mRNA is very high 48 hpi after *Botrytis cinerea* inoculation of leaves. MLO-like protein 8 (LOC111401243) is also overexpressed (Figure 5; Supplementary Table 4).In the barley, the *Mlo* gene, is involved in particular mutation(s) that can cause the misfunction of the MLO protein, resulting in a correlation with resistance to the fungal pathogen *Erysiphe graminis* f. sp. *hordei*(Büschges et al., 1997). It can be inferred that the same mutations are also present in olive *MLO* germplasm and if those contribute to the partial/total resistance to Oomycetes.

3.4.2.5 Comparison 5: overall differential mRNA expression of olive genes

Following the pairwise comparisons of olive mRNA in the previous conditions (Figures 2, 3, 4 and 5), it was performed, in addition, the overall changes in mRNA, better summarized by cluster analysis (Figure 6). The following three groups of treatments were used for this cluster analysis: (i) the control groups, including wounded drupes treated with 20 µl of sterile distilled water (treatment ID2), wounded drupes treated with either *T. atroviride*-culture filtrate (treatment ID6) or *C. oleophila* cell suspension (treatment ID7); (ii) olive drupes inoculated with *P. oleae* (treatment ID3); and (iii) *P. oleae*-inoculated olive drupes pre-treated with either *T. atroviride*-culture filtrate (treatment ID4) or *C. oleophila* cell suspension (treatment ID5). In olive drupes inoculated with *P. oleae* (ID3), 739 olive genes were exclusively upregulated (in red in Figure 6) (L2FC > 1) (Figure 6B; Supplementary Table 5).

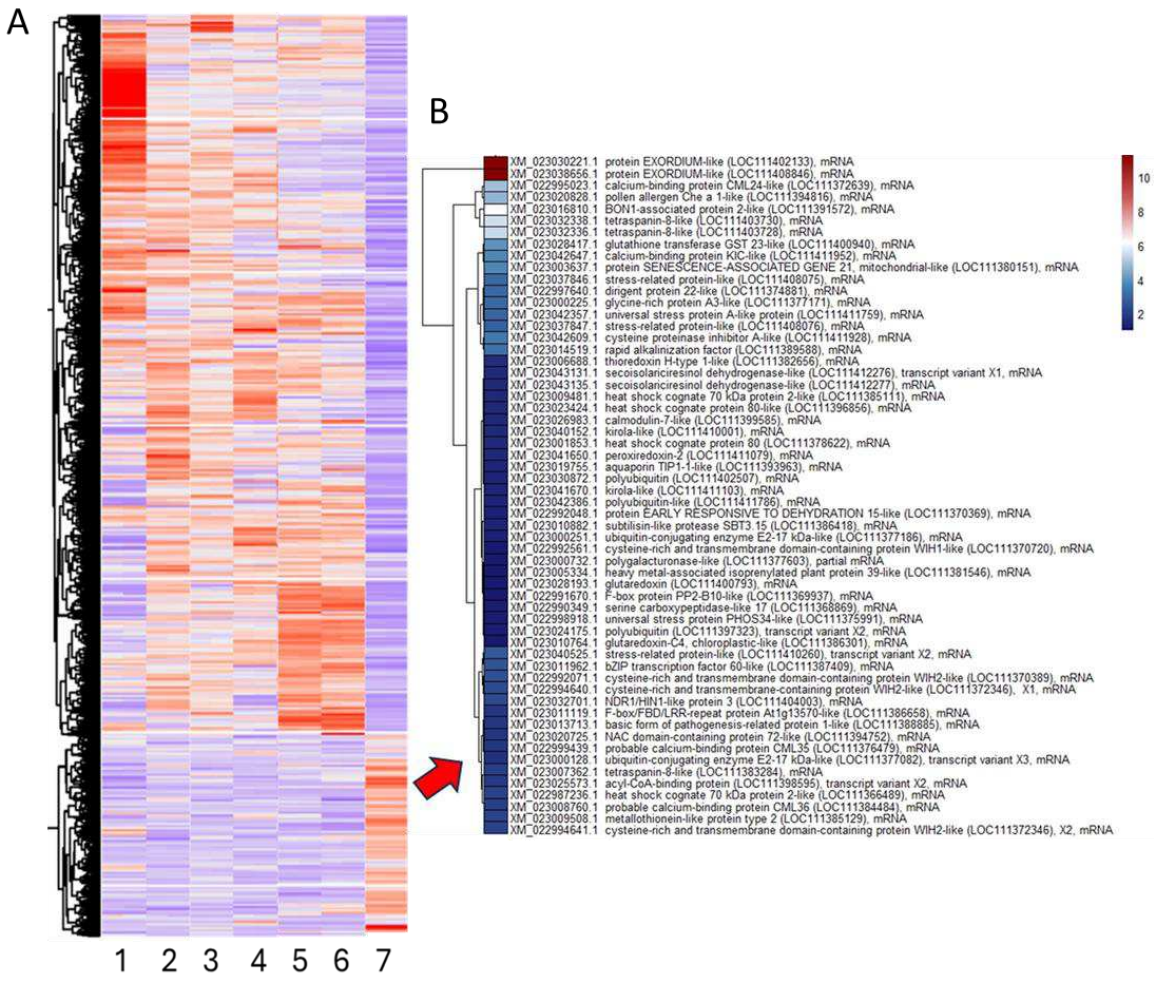

Figure 6. Cluster heatmap analyses of the differential RNAseq related to olive genes among all treatments at 72 hpi. This heatmap has been constructed assuming three groups of samples (all with technical duplicates and some of them with more biological repeats). Panel A (left) cluster analysis in which the wounded drupe treatment LF2C has been normalized to "not wound" ones, while the rest of conditions has been normalized to the "wound" condition. The data has been normalized with L2FC being = +/-4 by Z score. Legend: 1) intact olive drupes (ID1); 2) wounded drupes (ID2); 3) wounded drupes pre-treated with *C. oleophila* cells (ID7); 4) wounded drupes pre-treated with *T. atroviride* culture filtrate (ID6); 5) wounded drupes pre-treated with *C. oleophila* cells and inoculated with *P. oleae* (ID5); 6) wounded drupes pre-treated with *T. atroviride* culture filtrate and inoculated with *P. oleae* (ID4); 7) wounded drupes inoculated with *P. oleae* (ID3). Panel B (right) list of FPKM base mean filtered (>100 counts) upregulated and L2Fc sorted genes in the *P. oleae* alone condition (the total 739 genes are listed in Supplementary Table 5).

The general trend of top upregulated genes triggered by *P. oleae* are described above (Figs. 3 and 4). However, the plant response to the attack of the oomycete, even though this strain of *P. oleae* could not be fully blocked, showed a differential defense response as

indicated by the relative expressions of the pathogenic related (PR) proteins (Supplementary Figure 1).

The expression level of PR proteins has been evaluated based on their L2FC (Supplementary Table 6), and their overall comparison are shown in Supplementary Figure 1. The PR proteins were selected by blasting with PR reported in the literature (van Loon et al., 1994). For the class of PR-1, results obtained here strongly suggest that some of them are pre-activated by *T. atroviride*-culture filtrate or *C. oleophila* cells pre-treatment (e. g. LOC111385823, LOC111385823, and LOC111384285); however, only the basic form of pathogenesis-related protein 1-like (LOC111384285) remained expressed in drupes only inoculated with *P. oleae* (treatment ID3) or when the pre-treatment with *C. oleophila* was also provided (treatment ID5) (Supplementary Figure 1). For β-1,3-glucanase (PR-2), the trend is more complex, being LOC111378392 the only one shared among the treatments and that could represent a threat to the target oomycete. The expression levels of the olive chitinases (PR-3, PR-4, PR-8, and PR-11) seem to have a better trend: the chitinase 10 (LOC111407547) and endochitinase EP3-like (LOC111393512) upregulation during the treatments with either *C. oleophila* or *T. atroviride*-culture filtrate seems to be a marker for the PR-3 weapons against the oomycete.

Among the PR-5 highly induced by *P. oleae* infection, the pathogenesis-related protein 5-like (LOC111397298) and the thaumatin-like protein (LOC111398526) were markedly differentially overexpressed (Supplementary Figure 1), but the pre-treatment with either *C. oleophila* or *T. atroviride*-culture filtrate slightly contributed to trigger the expression of the thaumatin-like protein (LOC111398526). The group of PR-6 includes important proteinase inhibitors, such as the cysteine protease inhibitors (relevant for blocking fungal cysteine proteases) and other enzyme inhibitors related to different classes of enzymes involved in the defense response (Valueva et al., 1998; Walsh and Twitched, 1991). Among these PR-6, as shown in Supplementary Figure 1, the polygalacturonase inhibitor LOC111382121 is the main PR-6 gene transcribed in response to fungal polygalacturonase. In this study, *C. oleophila* resulted to be an effective inducer of the expression of this gene, in contrast with *T. atroviride*-culture filtrate treatment. Neither *C. oleophila* or *T. atroviride*-culture filtrate could trigger the expression of the cysteine proteinase inhibitor B-like (LOC111390855), which was only induced by *P. oleae* infection itself. On the other hand, a set of inhibitors (proteinase inhibitor PSI-1.2-like LOC111390049 and LOC111373900, pectinesterase inhibitor 9-like LOC111377531, and kunitz trypsin inhibitor 2-like LOC111405411), including the cysteine proteinase inhibitor A-like (LOC111412304), were exclusively induced by *C. oleophila*.

Among the subtilisin-like protease (PR-7), serine protease belonging to the peptidases_S8 subfamily, which are already upregulated upon wounding alone, the highest upregulation was recorded for the gene encoding the subtilisin-like protease SBT1.9 (LOC111394370) in all the treatments. Previous studies demonstrated that the tomato P69 subtilase, which is a subtilisin, activates plant immunity since it can cut the pathogen-secreted apoplastic "small cysteine-rich secreted protein" PC2 (Wang et al., 2021). Downstream fragments are alerting the plant immunity by intracellular signaling. To evade the plant surveillance system, *Phytophthora* may have evolved protease inhibitors, such as the Kazal-like, protease inhibitors (EPIs) to block PC2 extracellular processing. Furthermore, *Phytophthora* may secrete cytoplasmic effectors to block the secretion of proteases (i.e., subtilisins and cysteine proteases) into the apoplast and, indirectly, block PC2-triggered immunity (Bozkurt et al., 2011; Guo et al., 2019). For PR-8, the acidic endochitinase-like (LOC111391829) was the main upregulated PR protein in response to *P. oleae* or *C. oleiphila* alone as compared the wound control. However, when both *P. oleae* and *C. oleophila* were present then it was downregulated. Other PR-8 expressed were hevamine-A-like (LOC111402962 and LOC111402963). The upregulation of PR-8 alone is hence not impressive to claim an active role in contrasting the infection.

The PR-9 proteins are lignin-forming peroxidases that fortify the cell wall by increasing the crosslinking of lignin. Results obtained here evidence that *P. oleae* infection determined the up-regulation of many PR-9 peroxidases (Supplementary Figure 1), but the treatment with either *C. oleophila* or *T. atroviride*-culture filtrate also contributed to increase the PR-9 expression level, especially for the lignin-forming anionic peroxidase-like (LOC111385717).

The PR-10 class is quite versatile in their biological action due to a loop that has small-chemical binding capabilities and diverse role in stress signaling(Agarwal and Agarwal, 2013). In this study, the upregulation of some of them (e.g. pathogenesis-related protein STH-2-like - LOC111388404, LOC111388408, LOC111388411, and LOC111388413) is significative in olive drupes pre-treated with either *C. oleophila* or *T. atroviride*-culture filtrate as compared to olive drupes inoculated with *P. oleae* (Supplementary Figure 1). The highly expressed PR-11 are the acidic mammalian chitinases-like (LOC111382479, LOC111382480, and LOC111382484), but their expression is controversial, since wounding itself can trigger their higher expression and *T. atroviride* culture filtrate downregulated their expression.

Among the PR-12 class, the defensins-like protein 1 were not expressed. Some genes encoding PR-13 and PR-14 showed a slight upregulation in all the treatments.

The germin-like oxalate oxidases (PR-15) were also downregulated by *P. oleae* infection, even though treatment with either *C. oleophila* or *T. atroviride*-culture filtrate had the effect of upregulating some of them (Supplementary Figure 1).

Finally, the expression of PR-17 in olive drupes, which include important zinc apoplastic metalloproteinases, was relevant for the LOC111379582 and LOC111391744 in case of olive drupes only inoculated with *P. oleae* (treatment ID3) or drupes only pre-treated with *C. oleophila* (treatment ID7). Unfortunately, the combination of the pretreatment with either *C. oleophila* or *T. atroviride*-culture filtrate and *P. oleae* infection had the effect of reducing their expression (Supplementary Figure 1).

3.4.2.6. Comparison 6: wounded olive drupes pre-treated with *C. oleophila* cell suspension (treatment ID7) versus wounded drupes pre-treated with sterile distilled water (treatment ID2)

In olive drupes, the treatment with *C. oleophila* (treatment ID7) triggered the differential upregulation of the lignin/lignan biosynthetic pathway, possibly to fortify the cell wall and produce anti-fungal compounds. Indeed, a lot of secoisolariciresinol dehydrogenase genes (LOC111412681, LOC111412273, LOC111412272, and LOC111412275) were overexpressed (Supplementary Table 7). Two kunitz trypsin inhibitors (LOC111405411 and LOC111373900), two basic endochitinases (LOC111403475 and LOC111379188), and two pathogenesis-related proteins STH-like (LOC111388400 and LOC111388410) were highly upregulated as compared to the wound condition (treatment ID2). Meanwhile, the upregulation of metallothioneins (LOC111369652, LOC111375946, LOC111385831, and LOC111385129), thioredoxins (LOC111370790 and LOC111370789) and aquaporins (LOC111368643, LOC111408442, LOC111368644, and LOC111368645) might help the olive drupe to sustain a high level of ROS scavenging intracellularly and ROS export to the extracellular environment, such as superoxide (O_2^-), hydrogen peroxide (H_2O_2) and the hydroxyl radical (•OH) (Israel et al., 2022; Rodrigues et al., 2017).

3.4.2.7 Comparison 7: wounded olive drupes pre-treated with *T. atroviride*-culture filtrate (treatment ID6) versus wounded drupes pre-treated with sterile distilled water (treatment ID2)

It is known that *Trichoderma* spp. produce metabolites able to trigger plant defense response against fungal pathogens (Adnan et al., 2019; Marra et al., 2020; La Spada et al., 2020). In olive drupes pre-treated with *T. atroviride*-culture filtrate only 60 genes were upregulated and 176 downregulated (Supplementary Table 8). As for the treatment ID3 (*P. oleae* infection alone) also here the biosynthetic enzymes of the lignan biosynthesis was highly upregulated in particular the secoisolariciresinol dehydrogenase-like genes

with L2FC≥3 (LOC111412681, LOC111412273, LOC111412272).In addition, polygalacturonase inhibitor (PR-6, LOC111385823), proteinase inhibitor PSI-1.2-like (LOC111390049), acidic glucan endo-1,3-beta-glucosidase (LOC111378392), kirola-like (PR-10, LOC111392831) and a basic endochitinase-like (LOC111379188) were also induced (Supplementary Table 8). In this study, it has been also found the induction of ethylene biosynthesis (1-aminocyclopropane-1-carboxylate oxidase-like LOC111370659). The activation of numerous disease-resistance- (Ethylene Responsive Factor, ERF, NAC, bHLH, and STK) and defense-response genes (DRP, ABC, and HSP) following treatment with *Trichoderma* spp. has been reported previously (Ji et al., 2021). The NAC transcription factor 56-like (LOC111393458) and the protein DOWNY MILDEW RESISTANCE 6-like (LOC111393985) were also upregulated.

3.4.2.8. Comparison 8: *P. oleae* differentially expressed genes during olive fruit infection (treatment ID3) as compared to its in vitro growth in several culture media

About 4513 that *Trichoderma* spp. produce metabolites able to trigger plant defense response against fungal pathogens (Adnan et al., 2019; Marra et al., 2020; La Spada et al., 2020). In olive drupes pre-treated with *T. atroviride*-culture filtrate only 60 genes were upregulated and 176 downregulated (Supplementary Table 8). As for the treatment ID3 (*P. oleae* infection alone) also here the biosynthetic enzymes of the lignan biosynthesis was highly upregulated in particular the secoisolariciresinol dehydrogenase-like genes with L2FC≥3 (LOC111412681, LOC111412273, LOC111412272).In addition, polygalacturonase inhibitor (PR-6, LOC111385823), proteinase inhibitor PSI-1.2-like (LOC111390049), acidic glucan endo-1,3-beta-glucosidase (LOC111378392), kirola-like (PR-10, LOC111392831) and a basic endochitinase-like (LOC111379188) were also induced (Supplementary Table 8). In this study, it has been also found the induction of ethylene biosynthesis (1-aminocyclopropane-1-carboxylate oxidase-like LOC111370659). The activation of numerous disease-resistance- (Ethylene Responsive Factor, ERF, NAC, bHLH, and STK) and defense-response genes (DRP, ABC, and HSP) following treatment with *Trichoderma* spp. has been reported previously(Ji et al., 2021). The NAC transcription factor 56-like (LOC111393458) and the protein DOWNY MILDEW RESISTANCE 6-like (LOC111393985) were also upregulated.

Table 2. Selected upregulated mRNA related to *P. oleae* effectors differentially expressed into olive drupes during 72h of infection as compared to the mRNA expression during the growth in PDA (FDR =0.001). The gene expression has been filtered by the highest baseMean FPKM counts from Supplementary Table 11.

gene_id	baseMean	log2FoldChange	nr_accession	description
g8411.t1	11029.8423	-3.4545	AFY98083.1	elicitin protein INF1 [*Phytophthora capsici*]
g8407.t1	8980.9793	-3.1698	AFY98083.1	elicitin protein INF1 [*Phytophthora capsici*]
g8435.t1	1273.8463	-2.0990	KAG1694610.1	Acidic elicitin DVH05_028658 [*Phytophthora capsici*]
g8431.t1	884.7458	-2.1785	KAG1694610.1	Acidic elicitin DVH05_028658 [*Phytophthora capsici*]
g15852.t1	665.5780	1.0264	KAG7377058.1	Crinkler domain containing protein PHYPSEUDO_012238 [*Phytophthora pseudosyringae*]
g723.t1	521.1116	1.5093	XP_009516255.1	Crinkler domain containing protein PHYSODRAFT_250419 [*Phytophthora sojae*]
g17200.t1	492.0255	0.9111	KAG2775728.1	Crinkler (CRN) protein Pcac1_g13827 [*Phytophthora cactorum*]
g9420.t1	444.7386	0.7532	ETM53299.1	Crinkler effector protein L914_03213 [*Phytophthora parasitica*]
g8427.t1	427.0925	-3.2409	KAG1694610.1	Acidic elicitin DVH05_028658 [*Phytophthora capsici*]
g9425.t1	407.7032	0.8020	ETL34626.1	Crinkler effector protein L916_13176 [*Phytophthora parasitica*]

g16268.t1	364.1512	1.2954	XP_009523239.1	Crinkler domain containing protein PHYSODRAFT_328631 [*Phytophthora sojae*]
g23121.t1	345.5128	1.0980	KAG2759001.1	Crinkler (CRN) protein Pcac1_g28927 [*Phytophthora cactorum*]
g23192.t1	332.1388	1.0418	KAG2759001.1	Crinkler (CRN) protein Pcac1_g28927 [*Phytophthora cactorum*]
g24529.t1	270.2418	1.8162	GMF21132.1	Crinkler (CRN) protein [*Phytophthora lilii*]
g202.t1	259.0405	0.7907	KAG1704798.1	Apoplastic effector (Aspartic Peptidase A1) DVH05_004825 [*Phytophthora capsici*]
g4561.t1	251.1319	3.1599	GMF31732.1	Protease DDE [*Phytophthora fragariaefolia*]
g12968.t1	211.1898	1.3185	ETP25357.1	Crinkler effector protein F441_01749 [*Phytophthora parasitica* CJ01A1]
g23731.t1	208.4466	-0.9947	KAG1702536.1	RxLR effector protein DVH05_009486 [*Phytophthora capsici*]
g17483.t1	207.6982	6.7996	OWZ24715.1	Elicitin [*Phytophthora megakarya*]
g8438.t1	196.5607	-3.2032	KAF1780997.1	Elicitin [*Phytophthora cactorum*]
g585.t1	178.7704	1.4733	KAG1697742.1	Ubiquitin-dependent protease (DA1) DVH05_015699 [*Phytophthora capsici*]

g11723.t1	163.7110	-6.3604	KAG1698237.1	Elicitin protein DVH05_015225 [*Phytophthora capsici*]
g8405.t1	145.8855	-1.8859	GMF34482.1	Acidic elicitin [*Phytophthora lilii*]
g21188.t1	144.3538	-2.7376	KAG1697993.1	Elicitor transglutaminase protein DVH05_015477 [*Phytophthora capsic*i]
g3030.t1	134.9453	2.5023	KAG1692710.1	PPPDE thiol peptidase DVH05_025188 [*Phytophthora capsici*]
g14300.t1	126.2690	0.7730	KAG3233470.1	Crinkler domain containing protein PI124_g21451 [*Phytophthora idaei*]
g23107.t2	119.6059	0.8056	ETL34626.1	Crinkler effector protein L916_13176, partial [*Phytophthora parasitica*]
g23119.t1	113.2387	0.8713	ETP00001.1	Crinkler effector protein F441_22572, partial [*Phytophthora parasitica* CJ01A1]
g6404.t1	110.4554	1.1941	KAG3126550.1	Crinkler domain containing protein PC128_g27212 [*Phytophthora cactorum*]
g3543.t1	108.9492	1.1206	XP_009525765.1	Crinkler domain containing protein PHYSODRAFT_285836 [*Phytophthora sojae*]

g1666.t1	98.3432	1.0580	KAG3050369.1	Crinkler domain containing protein PI125_g26450 [*Phytophthora idaei*]
g11549.t1	91.7458	1.0846	ETI44683.1	Cystatin cysteine protease inhibitor EPIC [*Phytophthora parasitica* P1569]
g1938.t1	87.6575	9.8643	KAG1691739.1	Elicitin protein DVH05_026749 [*Phytophthora capsici*]
g19255.t1	85.2815	-1.0839	KAG1698440.1	Elicitin protein DVH05_014982 [*Phytophthora capsici*]
g20938.t1	79.1749	3.7683	OWZ17931.1	RxLR effector protein [*Phytophthora megakarya*]
g24013.t1	78.5695	-1.7169	KAG1690006.1	Secreted RxLR effector protein DVH05_001833 [*Phytophthora capsici*]
g2412.t1	78.0523	5.7525	XP_009517714.1	RxLR effector protein PHYSODRAFT_470423, partial [*Phytophthora sojae*]
g21215.t1	75.0605	1.1873	XP_009525765.1	Crinkler domain containing protein PHYSODRAFT_285836 [*Phytophthora sojae*]
g3199.t1	69.5818	1.4011	OWZ21632.1	Crinkler (CRN) [*Phytophthora megakarya*]
g21724.t1	68.8456	1.3974	OWZ21632.1	Crinkler (CRN) [*Phytophthora megakarya*]
g9756.t1	67.2585	1.4343	KAF1781372.1	Serine protease (peptidase S1) [*Phytophthora cactorum*]

g16483.t1	63.3187	0.7658	KAG1699076.1	RxLR effector protein DVH05_014446 [*Phytophthora capsici*]
g9111.t1	62.2498	1.0313	KAG6613212.1	RxLR-like protein [*Phytophthora cinnamomi*]
g9424.t1	59.2075	4.2622	QST87862.1	Crinkler CRN125_11 protein, partial [*Phytophthora capsici*]
g21067.t1	58.7755	1.7041	KAG6613212.1	RxLR-like protein [*Phytophthora cinnamomi*]
g9419.t1	58.3041	4.3746	QST87862.1	Crinkler CRN125_11 protein, partial [*Phytophthora capsici*]
g676.t1	56.3898	1.2711	OWZ21632.1	Crinkler (CRN) [*Phytophthora megakarya*]
g24615.t1	55.9194	0.8335	OWZ21632.1	Crinkler (CRN) [*Phytophthora megakarya*]
g20317.t1	54.3757	0.7280	KAG7377828.1	Elicitin protein PHYPSEUDO_010934 [*Phytophthora pseudosyringae*]
g11433.t1	54.0197	1.0609	OWZ21632.1	Crinkler (CRN) [*Phytophthora megakarya*]
g14655.t1	53.7483	0.9118	KAG1684410.1	Cysteine peptidase C1 DVH05_011155 [*Phytophthora capsici*]
g20315.t1	52.3149	3.8751	XP_009517714.1	RxLR effector protein PHYSODRAFT_470423, partial [*Phytophthora sojae*]
g19973.t1	50.6314	1.0442	XP_002997237.1	Crinkler (CRN) family protein [*Phytophthora infestans* T30-4]

g13239.t1	48.1890	0.7862	KAG3105523.1	Crinkler domain containing protein Pl125_g13422 [*Phytophthora idaei*]
g5831.t1	45.8712	0.6652	KAG1713044.1	RxLR protein DVH05_000772 [*Phytophthora capsici*]
g19206.t1	42.3917	-2.7982	KAG1698404.1	Elicitin protein DVH05_014946 [*Phytophthora capsici*]
g4307.t1	41.8255	-1.9681	KAG1705445.1	Elicitin protein DVH05_004375 [*Phytophthora capsici*]
g8773.t1	37.0533	3.4176	KAG7380604.1	RxLR effector protein PHYPSEUDO_006998 [*Phytophthora pseudosyringae]*
g16251.t1	31.9605	8.4079	KAG1693317.1	Secreted RxLR effector peptide proteinDVH05_023781 [*Phytophthora capsici*]
g20157.t1	22.6564	5.2388	A0A8T1VW52	RxLR effector protein [*Phytophthora pseudosyringae*]
g8439.t1	21.8038	-6.5190	OWZ01960.1	Elicitin [*Phytophthora megakarya*]
g13418.t1	20.3765	1.2881	AIU99520.1	Elicitin 113574 [*Phytophthora capsici*]
g10032.t1	16.6270	-7.5518	AIU99526.1	Elicitin 510832 [*Phytophthora capsici*]
g11722.t1	15.8853	-4.8215	KAG1698238.1	Elicitin protein DVH05_015226 [*Phytophthora capsici*]
g14657.t1	14.4881	1.9889	KAG1684411.1	Cysteine peptidase C1 DVH05_011156 [*Phytophthora capsici*]

g16516.t1	11.8968	-1.8912	POM73746.1	Avr1b-1 Avirulence-like protein (RxLR protein) [*Phytophthora palmivora* var. *palmivora*]
g22048.t1	10.1113	-6.8316	KAG2767785.1	Elicitor transglutaminase protein Pcac1_g20938 [*Phytophthora cactorum*]
g19132.t1	8.0089	6.4152	POM65797.1	Secreted RxLR effector peptide protein [*Phytophthora palmivora* var. *palmivora*]
g19245.t1	6.8210	-5.7677	KAG1698428.1	Elicitin protein ral13e DVH05_014970 [*Phytophthora capsici*]
g19253.t1	5.5695	-1.9078	KAG7376623.1	Elicitin protein PHYPSEUDO_013036 [*Phytophthora pseudosyringae*]
g11296.t1	3.3055	3.6026	AUD40032.1	Necrosis inducing protein (Nep1-like Pc118551) [*Phytophthora capsici*]
g22046.t1	1.9340	-4.4446	KAG1705011.1	Elicitor transglutaminase protein DVH05_005036 [*Phytophthora capsici*]

As As for *P. oleae* proteases and protease inhibitors differentially expressed genes (statistically filtered; FDR=0.001), including cysteine proteases and serine protease types (Peptidase S10, serine carboxypeptidase, and chymotrypsin type), were downregulated. The cystatin cysteine protease inhibitor EPIC and the Kazal-like serine protease inhibitor were also downregulated (Supplementary Table 9). Necrosis inducing protein NPP1 or Nep-1 (g11296.t1) was upregulated while all the remaining homologues were downregulated (Supplementary Table 9).

As already mentioned, *Phytophthora* species. also secrete elicitins, whose function is to facilitate the onset of infection and its progress, because they are toxic proteins and most of the time induce necrotic and systemic hypersensitive response (HR) in the infected tissues. The interpretation of the less expressed elicitin protein INF1, known for its high toxicity, is that in certain cases INF-1 is responsible for the high virulence but it is also known to be highly expressed in artificial media as compared to biotroph growth in infected tissues (Kamoun et al., 1997). Virulent races of fungal and bacterial pathogens are generally defined by their failure to express particular avirulence genes (Petit-Houdenot and Fudal, 2017). However, the loss or lack of elicitin production in *P. parasitica* was shown to increase its virulence on sensitive plants (Kamoun et al., 1994). Here, the downregulation of *P. oleae* INF-1 (g8411.t1 and g8407.t1) and others (g8435.t1, g8431.t1, g8427.t1, g11723.t1, and g8405.t1) might instead have a strategic role to favor its virulence, since, for example, the *in vitro* elicitin production by *Phytophthora* spp. is strongly negatively correlated with their pathogenicity on tobacco (Ryan et al., 1995). The most upregulated elicitins, instead, were g8411.t1, g8407.t1, g1938.t1, g17483.t1, and g18550.t1 (Supplementary Table 9). Other avirulent effectors were also highly upregulated, like cysteine peptidase C1 domain containing protein (g14657.t1) and cystatin cysteine protease inhibitor EPIC-like (g11549.t1) (Table 2).

3.4.2.9 Comparison 9: differentially expressed genes of *P. oleae* during olive drupe infection (treatment ID3) as compared to olive drupe inoculated with *P. oleae* and pre-treated with either *C. oleophila* (treatment ID5) or *T. atroviride*-culture filtrate (treatment ID4)

Supplementary Table 10 shows 3716 (2116 upregulated and 1600 downregulated) and differentially expressed mRNAs related to *P. oleae* during pre-treatment of olive drupes with either *C. oleophila* (treatment ID5) or *T. atroviride*-culture filtrate (treatment ID4) versus olive drupes infected with *P. oleae* (treatment ID3), 72 hpi (FDR =0.001). Supplementary Tables 11 and 12 show the *P. oleae* differential mRNA expression in the comparisons 'olive drupes pre-treated with *C. oleophila* and inoculated with *P. oleae*

(treatment ID5)' versus 'olive drupes only inoculated with *P. oleae* (treatment ID3)', and 'olive drupes pre-treated with *T. atroviride*-culture filtrate and inoculated with *P. oleae* (treatment ID4)' versus 'olive drupes only inoculated with *P. oleae* (treatment ID3)', respectively.

In the pre-treatment with *T. atroviride*-culture filtrate, the gene-encoding for the elicitin proteins INF-1 (g8411.t1 and g8407.t1) have been slightly upregulated as compared to drupes only inoculated with *P. oleae*; however, *P. oleae*-inoculated drupes pre-treated with *C. oleophila* showed a slight downregulation (L2FC= -0.8) (Supplementary Table 11). The differentially expressed elicitin genes that were not down-regulated in *P. oleae*-inoculated olive drupes pre-treated with either *C. oleophila* or *T. atroviride*-culture filtrate were g21198.t1, g10684.t1, g17483.t1, g24094.t1, and g4307.t1 (Supplementary Tables 10, 11); other genes-encoding for elicitins were downregulated by pre-treatment with either *C. oleophila* or *T. atroviride*-culture filtrate (e. g. g13418.t1, g1938.t1, g19255.t1).

To evaluate the efficacy of the antagonistic effect of the treatment with either *C. oleophila* or *T. atroviride*-culture filtrate versus the infection of *P. oleae* alone and, for comparison purposes, genes, vs. axenic cultures of *P. oleae* grown in PDA, MEA and CZ (CZAPEK) the DESeq2 results at 72 hpi were analyzed using the Principal Component Analysis (PCA)(Figure 7). The sum of all these components (PC) accounted for 76% of the total variance, while PC1 and PC2 represented 53% and 23%, respectively. Although PCA analysis is usually significant when the percentage of variance in the first three components is at least 80%, it may be used to find correlations based on the co-variance matrix. Figure 7 shows that four distinct groups were grouped apart. Specifically, olive drupes inoculated with *P. oleae* were clearly separated from *P. oleae*-inoculated drupes pre-treated with either *C. oleophila* or *T. atroviride*-culture filtrate, as well as from the axenic cultures of *P. oleae* on CZ and MEA media. Only the culture of *Phytophthora oleae* on PDA medium is singularly grouped in the quadrant with negative values on the abscissa and ordinate.

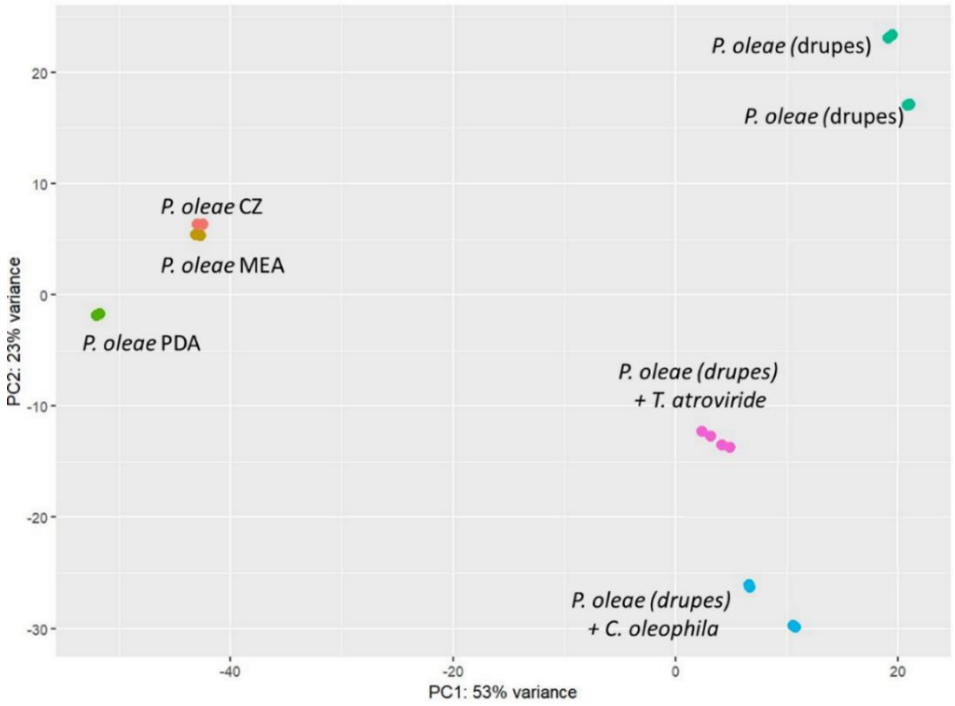

Figure 7. PCA plot including all the *P. oleae* samples alone or with either *C. oleophila* or *T. atroviride*-culture filtrate from 72hpi DESEq2 data. The horizontal axis (PC1) represents the distance from *P. oleae* grown in artificial media (CZ, MEA, or PDA) proportional to the variance of pathogenicity (rAUDPC) starting from the coordinates 0, 0. Negative PC1 variance means no infection. The closer the horizontal distance from 0, 0, the less is the degree of infectivity for the cases where infection is ongoing. The vertical variance of this PCA describes the variation of genes involved in severity of the disease as compared to original characteristics (no infection) of *P. oleae* grown in artificial media (CZ, MEA, or PDA). The distance/variance in PC2 between *P. oleae* infecting the drupe alone has a positive value while the distance/variance in PC2 of *P. oleae* infecting the drupe plus either *C. oleophila* or *T. atroviride*-culture filtrate is proportional to the reduction of infectivity detected in each mixed condition (*P. oleae* + either *C. oleophila* or *T. atroviride*-culture filtrate variance) where was observed a negative variance in PC2.

Furthermore, several cluster analyses have been performed to evaluate the changes in genes-encoding for a number of pathogenic enzymes and effectors. To this aim, elicitins, crinkler, peptidases, and RxLR effectors LF2C from DESeq2 data expression were chosen (Figure 8). Some examples include peptidases as the cysteine peptidase C1 (g9173.t1), which are downregulated when *P. oleae* is inoculated in olive drupes, but upregulated when either *C. oleophila* or *T. atroviride*-culture filtrate are included as pre-treatment. This could mean that perhaps the cysteine peptidase C1 (g9173.t1) could serve as weapon against other surrounding fungi. An opposite trend was observed for the Peptidase s59 (g4376.t1) (Figure 8A) and for the RxLR effectors (Figure 8C).

The genes-encoding for the RxLR effector proteins g6343.t1, g19400.t1, g16251.t1, g19132.t1, g24597.t1, g7454.t1, and g6774.t1, for example, were clearly upregulated in *P. oleae*-inoculated and non-treated olive drupes (treatment ID3) but downregulated when either *C. oleophila* (ID5) or *T. atroviride*-culture filtrate (ID4) where provided as pre-treatment (Figure 8C). Most of those highly expressed *P. oleae* RxLR effectors might attenuates the responses to SA like including of PR1 as in the case of *Arabidopsis* infected with *Hyaloperonospora arabidopsidis* (Hpa Emoy2) (Asai et al., 2014). In facts, g6343.t1, and g7454.t1 are homologous respectively to HaRxLL465b (BAP69127.1) and HaRxL24b (CCC55787.1) highly expressed in Hpa Emoy2 [p]. Besides, *P. oleae* RxLR effector g19132.t1 possesses also one WY motifs, known for being necessary for the infection and RNA silencing suppression activity (Zhang et al., 2019).

The trend of the *P. oleae* CRN78 homologous isogenes (g11433.t1, g676.t1, g3199.t1, g21724.t1, g24615.t1) was characterized by an up-regulation when *P. oleae* was inoculated in non-pre-treated olive drupes (L2FC > 1.2) (ID3) and by a downregulation in drupes pre-treated with either *C. oleophila* (L2FC<-1.2) (ID5) or *T. atroviride* (L2FC<0.4) (ID4) (Figure 6B). The Crinkler effector CRN78 of *P. soja* (XP_009521873.1) is known to enhance oomycete pathogen infection by inhibiting plant immunity through a unique mechanism (Ai et al., 2021). *P. sojae* effector CRN78 contains a secretion signal peptide (SP), a typical LXLFLAK and HVLVVVP motifs at its N terminal; this latter is predicted to be a serine/threonine kinase domain. It has been demonstrated that CRN78 mediates phosphorylation of NbPIP2;2 at Ser279 and induces its degradation via a 26S-dependent pathway (Ai et al., 2021). Since the aquaporin PIP2;2 acts as a H_2O_2 transporter into the apoplast, its degradation substantially decreases extracellular ROS.

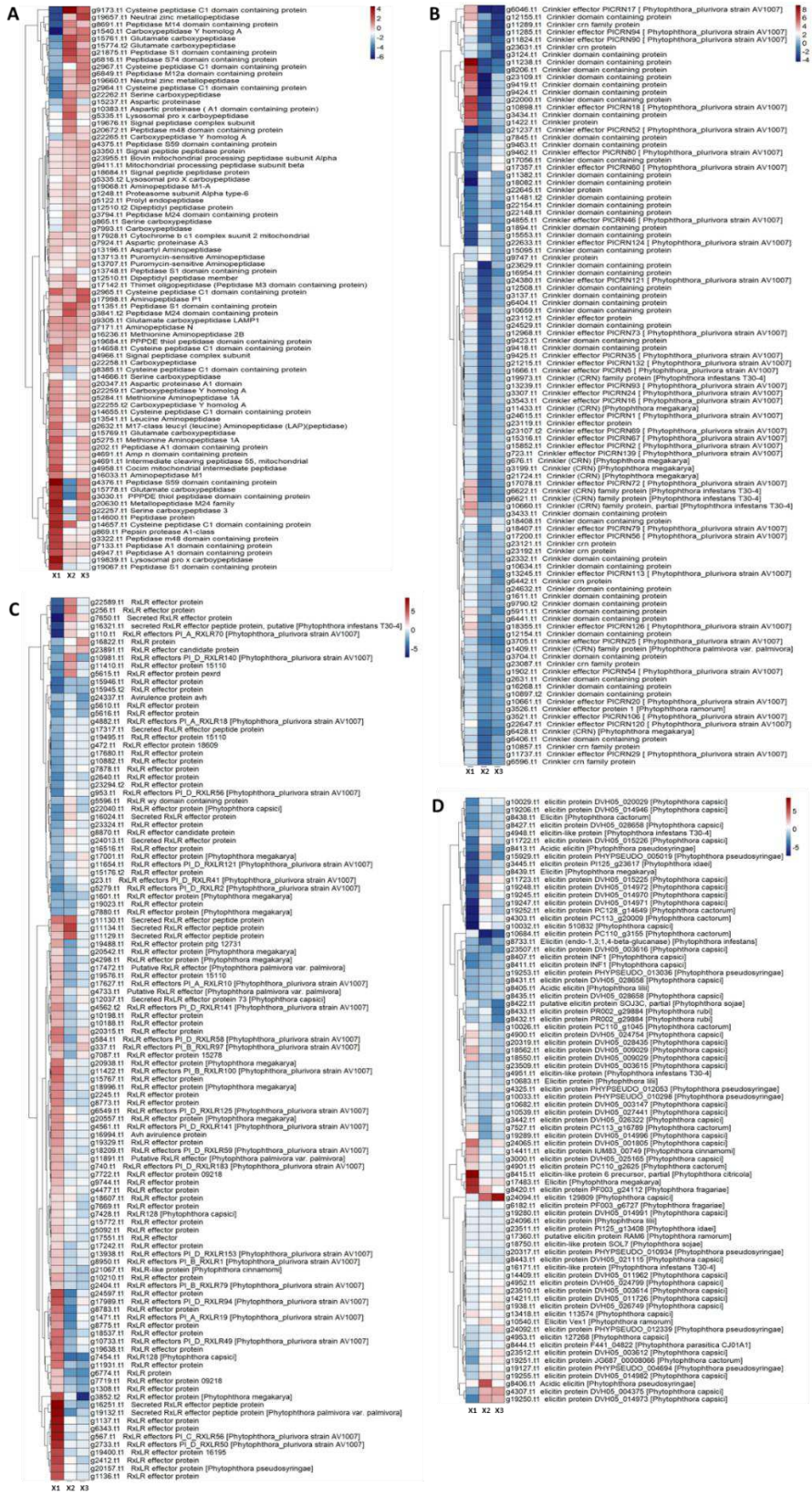

Figure 8. Cluster heatmap analyses of *P. oleae* peptidases, Crinkler, RxLR effectors and elicitins differentially expressed in three conditions tested. X1= L2FC of *P. oleae* grown on olive drupes vs. *P. oleae* grown on artificial media; X2= L2FC of *P. oleae* grown on drupes plus *C. oleophila* vs. *P. oleae* grown on drupes; X3= L2FC of *P. oleae* grown on drupes plus *T. atroviride* filtrate vs. *P. oleae* grown on drupes.

3.4.2.10 RT-qPCR validation of selected genes of *Olea europaea* and *Phytophthora oleae*.

A selection of differentially expressed genes of olive drupes (Supplementary Table 15), as analyzed by RNAseq at 72 hpi, have been validated during the entire time course considered (24, 72, and 168 hpi). Figure 9 shows the trend of expression of those genes. At 24 hpi, the gene-encoding for the pathogenesis-related protein STH-2-like (XM_023013103.1, LOC111388413) (Figure 9A) was significantly up-regulated in all the treatments, but in wounded drupes; thus, indicating that this gene is positively transcribed as a consequence of biotic stresses. Furthermore, *P. oleae* inoculated drupes pre-treated with either *T. atroviride*-culture filtrate or *C. oleophila* showed the highest upregulation values. A similar trend was also observed at 72 hpi, although less marked in olive drupes only inoculated with *P. oleae* (ID3) and those also pre-treated with *T. atroviride*-culture filtrate (ID4). Finally, at 168 hpi, the most significant up-regulation of the gene-encoding for the pathogenesis-related protein STH-2-like was recorded in *P. oleae*-inoculated olive drupes pre-treated with *T. atroviride*-culture filtrate. Overall,, throughout all the infection period considered, it is constant the higher upregulation of this PR protein in the presence of both *C. oleophila* and *T. atroviride* culture filtrate, phenomenon already known for *T. harzianum* in case of sunflower challenged by *Rhizoctonia solani*(Singh et al., 2014). The gene-encoding for the BON1-associated protein 2-like (LOC111391572, XM_023016810.1) (Figure 9B) showed a marked upregulation in drupes only inoculated with *P. oleae* (ID03) at the three time points of measurement. BON1 is a calcium-dependent phospholipid-binding protein interacting with the leucine-rich-repeat receptor-like kinases BIR1 (BAK1-interacting receptor-like kinase 1) and pathogen-associated molecular pattern (PAMP) receptor regulator BAK1(Wang et al., 2011). BON1-associated protein participates to the protein-protein regulation of the PAMP signaling of which BAK1 represent a hub of signals functioning as negative regulator role related to cell death and defense responses(Yang et al., 2006). Results obtained in this study suggest that the infection by *P. oleae* caused the upregulation of BON1-associated protein, probably suppressing both cell death and reducing the PAMP response in activating the defense response. Notably, all the treatments that included either *C. oleophila* or *T. atroviride*-culture filtrate showed a generalized low up-regulation or a down-regulation. This study also analyzed the trend of the gene-encoding for FERONIA (Figure 9C), an LRK-receptor-like protein kinase (LOC111374777, XM_022997515.1), involved in the plant immunity by inhibiting JA signaling(Guo et al., 2018). Hence, the transcription of this gene is supposed to exert a negative function toward *P. oleae* pathogenicity. Results

obtained here show that at 24 hpi the FERONIA encoding-gene was significantly up-regulated in *P. oleae*-inoculated olive drupes pre-treated with *T. atroviride*-culture filtrate (ID_4) and in olive drupes only pre-treated with *C. oleophila* (ID_5); at 72 hpi the modulation in the transcription of the gene was significant just in *P. oleae*-inoculated olive drupes pre-treated with *T. atroviride*-culture filtrate (ID_4); at 168 hpi, no-significant differential transcriptions were recorded in drupes from any treatment.

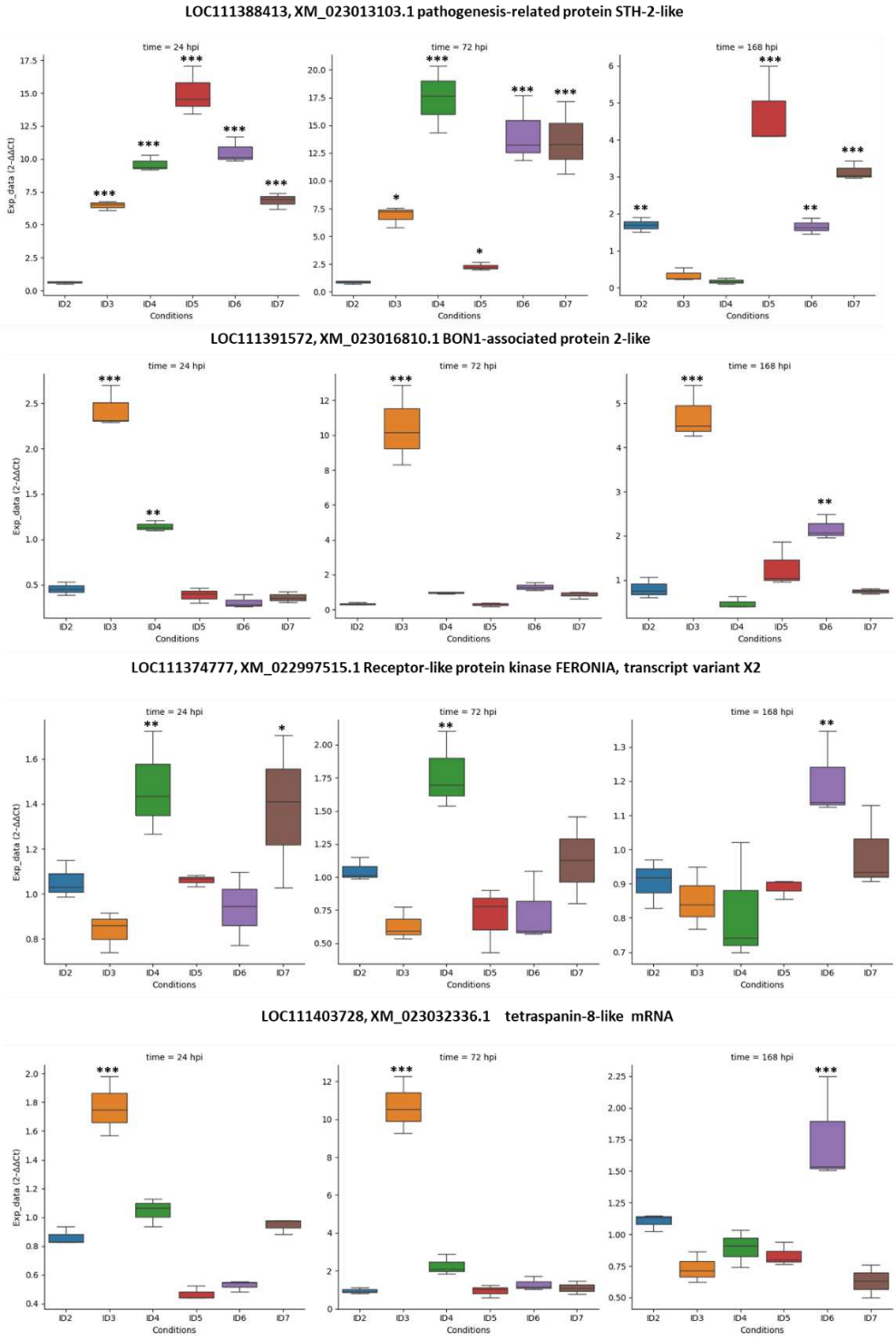

Figure 9. RT-qPCR validation of chosen DEGs for *Olea europaea* at three time points and under different conditions. Asterisks represents statistically different samples according to Dunnett's test (* = $p < 0.05$, ** = $p < 0.01$, and *** = $p < 0.001$), as compared to unwounded fruits. The normalization has been performed according to the tubulin alpha-3 chain (LOC111371391, XM_022993342.1). The RT-qPCR primers are shown in Supplementary Table 15. The bars represent the standard deviation (SD). Conditions legend: ID2, wound; ID3, wound + *P. oleae*; ID4, wound + *T. atroviride* + *P. oleae*; ID5, wound + *C. oleophila* + *P. oleae*; ID6, wound + *T. atroviride*; ID7, wound + *C. oleophila*.

As mentioned, the plant small extracellular vesicles (EVs) or exosomes (EXOs) that carry plant defense enzymes, PRs and the ROS generating machine, were supposed accumulating toward the pathogen entrance hot spot. Plant exosomes contain DADPH oxidases, PM-ATPases, and tetraspanins that mediate PM-fusion (unloading of content). Many tetraspanins are involved in EXOs trafficking and here, the gene-encoding for the tetraspanin-8-like (LOC111403728, XM_023032336.1) was chosen as a top differentially expressed gene for RT-qPCR-analysis (Figure 9D). At the time points 24- and 72-hpi, the significant upregulation of the tetraspanin-8-like in drupes only inoculated with *P. oleae* (ID3), was interpreted as the attempt of plant cells to counteract the oomycete pathogen by ROS and PRs. Conversely, the downregulation in *P. oleae* inoculated drupes pre-treated with either *C. oleophila* (ID5) or *T. atroviride*-culture filtrate (ID4), although non-significant, suggests that the presence of either *C. oleophila* or *T. atroviride*-culture filtrate could have downregulated the ROS and PRs mediated mechanism by their own extracellular enzymes/effectors to help the plant immunity by by-passing the exosomes mechanism of defense. This interpretation of the results is supported by the fact that at 168-hpi, drupes only inoculated with *P. oleae* (ID3) exhibited a downregulation of tetraspanin-8-like gene, indicating that the advanced stage of infection could have completely compromised any plant defense response. At this time point, the only significant up-regulation was recorded in olive drupes treated with *T. atroviride*-culture filtrate.

In this study, the RT-qPCR validation of some selected *P. oleae* differentially expressed encoding effectors (Supplementary Table 15) at all time points considered was also carried out. As comparison, the mean value of expression level of the *P. oleae* genes grown in artificial media (PDA, MEA, or Czapek) was used.

The Crinkler (CRN) gene g723.t1 (TRINITY_DN5906_c2_g5_i1) (Figure 10A) is homologous of the Crinkler effector of *P. soja* (XP_009516255.1) and the Crinkler effector protein 5 of *P. infestans* (Q2M408.1) The CRN proteins are supposed to be secreted by the oomycete into the host apoplast and, by an unknown mechanism, they can penetrate and exert their toxic necrotic function against the host. Results of this study strongly suggest that the presence of either *C. oleophila* (ID5) or *T. atroviride*-culture filtrate (ID4) smoothed the upregulation of the Crinkler (CRN) gene g723.t1, as it is markedly upregulated in the treatment where *P. oleae* is alone (ID3) (Figure 10A). A similar trend was recorded for the Elicitin g17483.t1 (Figure 10B). The expression trend of the INF-1 elicitin encoding-genes (g8411.t1 and g8407.t1) (Figure 10C) aligns with the RNAseq analysis findings at 72 hpi. In

the treatment where *P. oleae* is alone (ID3), the INF-1 elicitin is down-regulated at 24 hpi. Additionally, at 72 and 168 hpi, its upregulation was significantly lower than in drupes that also included pre-treatment with either *C. oleophila* (ID5) or *T. atroviride*-culture filtrate (ID4). This INF-1 elicitin gene trend in treatment ID3, which overall exhibited consistently lower positive regulation compared to the other two treatments, might be attributed to the potential establishment of an 'infection barrier' by the presence of either *C. oleophila* or *T. atroviride*-culture filtrate. Hence, to overcome this barrier, *P. oleae* might have increased the synthesis of INF-1 elicitin.

Another host-translocated effector belonging to the RxLR family, the *P. oleae* g24837.t1 (TRINITY_DN8100_c0_g1_i1) (Figure 10D) homologous to HaRxLL438 (BAP69100.1) of *H. arabidopsidis* Emoy2, upregulated upon infection, has also been detected as highly expressed in the case of infection with *P. oleae* alone, but downregulated over time following treatments with either *C. oleophila* or *T. atroviride*-culture filtrate.

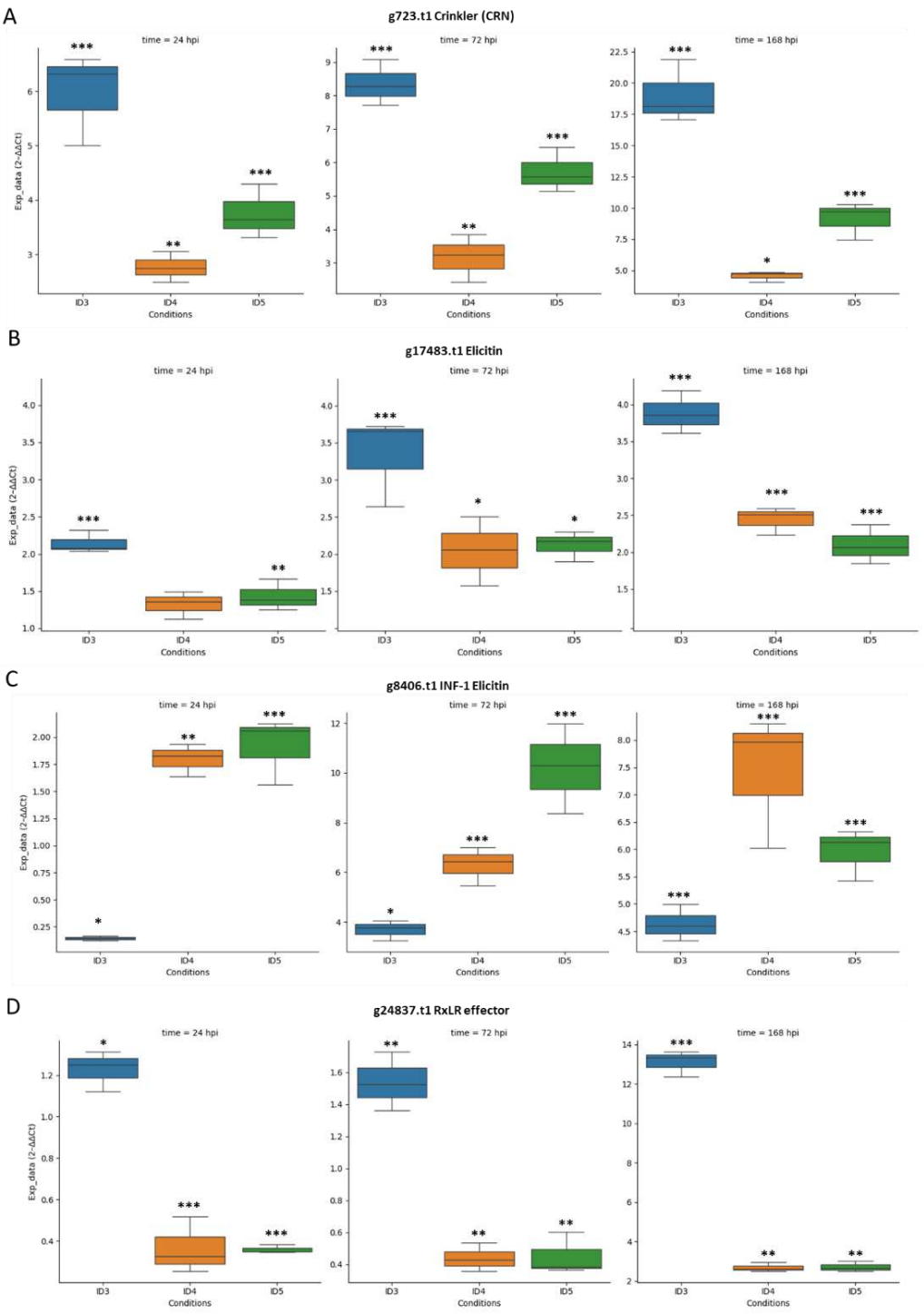

Figure 10. RT-qPCR validation of chosen DEGs for *P. oleae* during the three time points and different conditions. Asterisks represent statistically different responses as compared to the expression in artificial media, according to Dunnett's test (* = $p < 0.05$, ** = $p < 0.01$, and *** = $p < 0.001$). The normalization has been performed according to the tubulin beta chain g8215.t2 (TRINITY_DN6095_co_g1_i1). The RT-qPCR primers are shown in Supplementary Table 15. The bars represent the standard deviation (SD).

3.5 Discussion

This study demonstrated the yeast *C. oleophila* and the culture filtrate of the filamentous fungus *T. atroviride* were effective in reducing the severity of symptoms of soft rot in olive drupes infected by *P. oleae*. To the best of our knowledge, this is the first report of *in planta* efficacy of these treatments, a BCA and a culture filtrate of an antagonistic fungus. Results are promising, also in the light of the transcriptome analysis, indicating the activation of plant immune system by the yeast and culture filtrate tested in this study. This would suggest the possibility that both *C. oleophila* and *T. atroviride* culture filtrate can be effective against a broad spectrum of fruit diseases caused by necrotrophic pathogens. Indeed, *C. oleophila* strain O is already available as a commercial bioproduct registered for treatments of post-harvest fungal rots of several fruit crops, while the practical application of *Trichoderma atroviride* metabolites as natural substances for the biocontrol of plant diseases is almost unexplored. Moreover, the pathosystem *P. oleae*/olive drupe treated with either *Trichoderma* culture filtrate or *C. oleophila* cell suspension proved to be an interesting model to analyze the gene expression in a multiple-actor (pathogen/host plant/treatment) interaction. The transcriptome analysis of this interaction provided a better understanding of the defense responses of olive to stressors, including the abiotic stress provoked by wound inoculation, and the mechanisms underlying the biocidal activity of two very diverse means. The components of the model were chosen and assembled in various combinations based on a rationale. *Phytophthora oleae* is an emergent olive pathogen and the genus *Phytophthora* includes numerous species that are responsible of serious diseases of crop, forest, ornamental and landscape plants. 'Coratina', originating from the Apulia region (southern Italy), is one of the most popular Italian olive varieties for oil production. It is an ancient variety thought to express many wild resistance genes and to be closer to *O. europaea* var. *sylvestris* (taxid:158386), the wild relative of *O. europaea* var. *sativa*, in genomic sequence. Hence, RNAseq analysis has been performed using the O_europaea_v1 genome assembly (GCF_002742605.1). As in many studies it was demonstrated the strong efficacy of different strains of *C. oleophila* against post-harvest fungal diseases of edible fruit crops such as apples, bananas, citrus and strawberries(Hammami et al., 2022; Lima et al., 1997), this BCA was selected for the treatment of olive drupes. The choice of evaluating *T. atroviride* culture filtrate as an eco-friendly treatment was suggested by the high efficient production of bioactive secondary metabolites in liquid culture with antifungal activity by other *Trichoderma* spp. (Chóez-Guaranda et al., 2023; Guzmán-Guzmán et al., 2023; Li et al., 2019; Stracquadanio et al., 2020; Stracquadanio et al., 2021). The elicitation of the

plant immune system by liquid culture filtrate of *T. atroviride*, in this study, has perhaps been triggered by the elicitin Epl1 (XP_013937770.1) Cerato-platanin, which was found the most highly expressed protein by proteomics analysis (Table 1). Ep1 potential in triggering plant defense responses is well known(Salas-Marina et al., 2015; Zhou et al., 2010).

The time course of olive rot severity for each treatment, as represented by rAUDPC, is in somewhat in agreement with the PCA plot (Figure 7), which shows the variance of the expression of genes involved in pathogenicity as compared to the *P. oleae* growth in artificial medium (baseline or zero variance) or during infection (positive variance) or infection and pre-treatment with either *C. oleophila* or *T. atroviride*-culture filtrate (negative variance). In both cases, pre-treatment with *T. atroviride*-culture filtrate had the effect of attenuating the virulence of *P. oleae*. *P. oleae* effectors had a marked downregulation as a consequence of pre-treatment with *T. atroviride*-culture filtrate. This down regulation was probably due to a combined effect of the plant tissue pre-elicited by *T. atroviride* elicitin (e.g. Epl1 Cerato-platanin) and other bioactive metabolites of the culture filtrate.

The RNAseq analysis of olive gene differentially expressed during the infection by *P. oleae* showed the most upregulated genes were EXORDIUM-like isogenes, known to inhibit cell proliferation(Schröder et al., 2009) and which in soybean are associated with resistance to *P. sojae*(Lin et al., 2014). In inoculated olives the ethylene biosynthesis occurred very early during the infection process and was triggered by wounding itself, as revealed by the expression of 1-aminocyclopropane-1-carboxylate synthase-like genes (ACC synthases; LOC111390291, LOC111392037 and LOC111370655) (Figure 2; Supplementary Table 1). In olive drupes only inoculated with *P. oleae*, 1-aminocyclopropane-1-carboxylate oxidase 1-like (ACO, LOC111366119) was also highly upregulated (Figure 3; Supplementary Table 2) and represented the last step in ET biosynthesis. Infection by *P. oleae* upregulated significantly also Ca^{2+} signaling, more than wounding itself as shown by the upregulation of protein SRC2 homolog (LOC111386812; Figure 3), which is the target of the main *P. oleae* elicitin INF-1 (g8411.t1 and g8407.t1).

The most upregulated gene in olive fruit during *P. oleae* infection, the BON1-associated protein 2 (LOC111391572), function as a negative regulator of cell death and defense responses in association with BAP1 and negatively regulating the R-protein "suppressor of npr1-1, constitutive 1" (SNC1)(Houben and Van de Poel, 2019; Zhu et al., 2010). Infection by *P. oleae* led to suppression of the natural immunity response by regulating BON1/SNC1

at the site of infection, but perhaps was not sufficient to inhibit the production of salicylic acid and pipecolic acid by maintaining the upregulated expression of SAR DEFICIENT 1-like (LOC111402349 and LOC111377821), initiating the systemic acquired resistance (SAR) in distal parts of the plant(Peng et al., 2018; Sun and Zhang, 2021). As already reminded, SA and Pip trigger the activation of immune-related genes, such as many pathogenesis-related protein genes (PRs), including pathogenesis-related proteins STH-21-like, kirola-like proteins, hevamine-A-like, thaumatin-like proteins, cysteine proteinase inhibitors A/B-like, kunitz trypsin inhibitor 2-like, chitinases, endoglucanases, and β-1,3-glucanases. These are upregulated during *P. oleae* infection (Figure 3; Supplementary Table 2) and significantly even more following treatment with *C. oleophila* (Table 1; Supplementary Table 3) and *T. atroviride*-culture filtrate (Supplementary Table 4).

The receptor kinase FERONIA is downregulated by *P. oleae* infection and upregulated by the presence of *C. oleophila* and *T. atroviride* extracts as also validated over time by qPCR(Figure 9). During cell elongation, RALF23 plant peptides, when cleaved by the site-1 protease (S1P, a serine protease of the family of proprotein convertase subtilisin/kexins), can create a complex with FER and the binding activate it kinase activity resulting in phosphorylation of plasma membrane H^+-ATPase 2 at serine-899, causing inhibition of proton transport and in general an arrest of root growth(Pearce et al., 2001). The FER activation suppresses also flg22-induced reactive oxygen species (ROS) burst and immune responses. This suppression is achieved by destabilizing the complex formation of EFR and FLS2 with their co-receptor BAK1, illustrating how RALF-FER signaling can modulate immune signaling pathways(Xin Zhang et al., 2020). Pathogens, such as fungi, have evolved strategies to manipulate plant signaling pathways to facilitate infection. The discovery of potential RALF peptides in fungal and bacterial genomes suggests that pathogens might exploit RALF-FER signaling to manipulate plant immune responses and facilitate infection. Some fungal pathogens (e. g. *Fusarium oxysporum*) produce peptides that mimic plant signaling molecules, known as RALFs-like peptides, which can interact with FER by activating it and hence promote infection. These pathogen-derived RALF mimics can hijack the FER signaling pathway, leading to increased virulence and successful colonization of the plant host. The interaction between RALF peptides and FER triggers a signaling cascade that can inhibit cell growth, as seen in the inhibition of primary root growth in *Arabidopsis* upon binding of RALF1 to FER(Du et al., 2016). For instance, *F. oxysporum f. sp. lycopersici* RALF-like peptides inhibited the growth of tomato seedlings and elicited responses in tomato and *Nicotiana benthamiana* typical of

endogenous plant RALF peptides (reactive oxygen species burst, induced alkalinization and mitogen-activated protein kinase activation)(Thynne et al., 2017). To make the hypothesis that FER is upregulated due to its inhibition by *P. oleae* effectors, we searched into a group of small proteins, top differentially expressed, in case of *P. oleae* infection (Supplementary Table 9) and aligned their protein sequence to known RALF peptides from *O. europaea* and/or fungal RALF-like peptide homologues (Supplementary Figure 2). The alignment revealed a conservation of critical cysteine residues and FER binding motifs even if those were more similar to the *Colletotrichum higginsianum* RALF-like protein (CCF44719) rather than *F. graminearum* (FG05_30327). *P. oleae* putative RALF-like homologues, differentially expressed, were: g3545.t1, g8557.t1 and g5663.t1. The hypothesis here is that *P. oleae* putative RALF-like proteins/peptides might activate FERONIA, and hence *P. oleae* could block the JA, COR and SA signaling, facilitating its pathogenesis. We need, of course, to confirm by other experiments whether the putative bioinformatics identified *P. oleae* RALF-like proteins here (Supplementary Figure 2) really interact with FERONIA.

Many R-genes were upregulated during *P. oleae* infection (Figure 3; Supplementary Table 2), probably acting in conjunction with WRKY TFs and F-box/LRR-repeat proteins to express such PRs. During 72hpi of *T. atroviride*-culture filtrate pre-treatment followed by *P. oleae* infection, the R-genes were particularly upregulated: LRR receptor-like serine/threonine-protein kinase At1g06840 (LOC111371641), LEAF RUST 10 DISEASE-RESISTANCE LOCUS RECEPTOR-LIKE PROTEIN KINASE-like 1.1 (LOC111390435), MLO-like protein 2 (LOC111370597), rust resistance kinase Lr10-like (LOC111411655), pto-interacting protein 1-like (LOC111410523), WRKY transcription factor 20 (LOC111391535), and the LRR receptor-like serine/threonine-protein kinase At1g06840 (LOC111393227). Calcium (Ca^{2+}) signaling plays a pivotal role in plant immunity, functioning as a key secondary messenger in response to various stimuli, including pathogen attack. In plants, Ca^{2+} signaling is central to both pattern-triggered immunity (PTI) and effector-triggered immunity (ETI), with the generation of characteristic cytoplasmic Ca^{2+} elevations being common to both(Köster et al., 2022). The interaction between FERONIA and MLO-like proteins (e.g. NORTIA, NTA) is known in pollen tube reception and fungal invasion causing a release of intracellular Ca^{2+} and related signaling(Kessler et al., 2010). Here, FERONIA and MLO-like protein2 might have interacted and triggered the same Ca^{2+} release and signaling followed by upregulation of many Ca^{2+} binding proteins for further signaling and immunity activation. On another hand, *T. atroviride*-culture filtrate pre-

treatment triggered the upregulated of other R-genes: the LRR receptor-like serine/threonine-protein kinase At1g06840 (LOC111371641), LRR receptor-like serine/threonine-protein kinase At1g06840 (LOC111393227), and the MLO-like protein 8 (LOC111401243). Besides, BON1-associated protein 2 (LOC111391572) was downregulated following pre-treatment with either *C. oleophila* or *T. atroviride*-culture filtrate (Supplementary Tables 3, and 4).

Necrotrophic pathogens and beneficial antagonist microorganisms induce or prime ET- and JA-dependent signaling pathways. For example, the necrotrophic pathogen *Botrytis cinerea* causes a rapid activation of ET biosynthesis in *Arabidopsis* by the action of Mitogen Activated Protein Kinase3 (MAPK3) and MAPK6 that phosphorylate the ET biosynthesis proteins 1-Aminocyclopropane-1-Carboxilic Acid (ACC) Synthase 2 (ACS2) and ACS6(Han et al., 2010). In the case of *P. oleae* infection alone, ethylene biosynthesis was highly upregulated since it was found that the final step involving biosynthetic enzyme 1-aminocyclopropane-1-carboxylate oxidase 1-like (ACO, LOC111366119), was very highly upregulated as compared to wounded fruit (L2FC≥ 7.6; Figure 3; Supplementary Table 2). Besides the boost to ET biosynthesis, it was observed a significant increase in JA biosynthesis and an upregulation of many ET responsive genes. The Apetala 2 (AP2)/Ethylene Response Factor (ERF) seems to be the driver of the ET/JA-mediated defense pathway. Its homologue in olive is the ethylene-responsive TF 1B-like (ERF-1B) of which many isogenes are present in the genome. Upon *P. oleae* infection, many ERF-1B like factors were upregulated (Supplementary Table 2). As described above, JA binds to the JA receptor Coronatine Insensitive 1 (COI1, LOC111390662 in *O. europaea*), which results in the degradation of JAZ repressor proteins by the 26S proteasome and subsequent release of activating TFs. ET binds to the receptor ETR1, and this in turn stabilizes the EIN3/EIL1 TFs which bind to the promoters of both JA and ET responsive/defense genes, activating the ERF branch of the JA defense pathway(Broekgaarden et al., 2015).

On the other hand, to link *P. oleae* effectors with known *Phytophthora* avirulence genes, for instance, we could not find a homologue of *P. sojae* RxLR effector avh94 in the *P. oleae* genome/proteome. RxLR effector avh94 was shown to interact with soybean JAZ1/2, which is a repressor of JA signaling(Zhao et al., 2022). However, by genome sequencing and annotation, *P. oleae* was shown to possess more than 350 effectors (RxLR, crinklers, elicitins, etc.) whose function is unknown and whose identity has only been confirmed by annotation pipelines.

Here we have performed simultaneously a dual RNA-seq, with a total RNA extraction, of both host (*O. europaea*) and pathogen (*P. oleae*), with or without treatment with either *C. oleophila* or *T. atroviride*-culture filtrate. The outcome of the *P. oleae* gene expression on the host has revealed a expression pattern that was modulated by either *C. oleophila* or *T. atroviride*-culture. For instance, the cluster analysis for top DEGs of elicitins (Figure 8D) revealed that g8415.t1, g17483.t1, and g8420.t1 were upregulated upon *P. oleae* infection and downregulated by the effect of either *C. oleophila* or *T. atroviride*-culture filtrate (Figure 8D). The trend of expression for the elicitin g17483.t1 as monitored by RT-qPCR confirmed that biocontrol agents constantly over time downregulated such important elicitin (Figure 8B). Opposite trend of expression was observed for the elicitins g24094.t1, g4307.t1 and g19250.t1, which were upregulated upon treatment with either *C. oleophila* or *T. atroviride*-culture filtrate and which role is unknown. The same opposite trend was observed at 72 hpi for the INF-1 elicitins (g8407.t1 and g8411.t1), known inducer of HR (Figure 8D).

Our cluster analysis on *P. oleae* effectors (Figure 8) revealed a group of Crinkler highly differentially expressed during the infection with *P. oleae* alone (e. g. g11238.t1, g8206.t1, g23109.t1, g9419.t1, g9424.t1, g22000.t1, g10898.t1, g3434.t1 and g1422.t1) but downregulated by the treatment with either *C. oleophila* or *T. atroviride*-culture filtrate (Figure 8B). RNAseq revealed the same trend for Crinkler g723.t1 and RT-qPCR confirmed downregulation of this gene overtime as a consequence of the treatment with the BCAs (Figure 10A).

The same trend was observed for the RxLR effectors. In detail, the differentially expressed genes upregulated upon infection with *P. oleae* alone and downregulated by the treatment with either *C. oleophila* or *T. atroviride*-culture filtrate, having the highest L2FC, were g3852.t1, g16251.t1, g19132.t1, g1137.t1, g6343.t1, g567.t1, g2733.t1, g19400.t1, g24837.t1, g2412.t1, g20157.t1, and g1136.t1 respectively. For the RxLR effector g24837.t1 this trend of qPCR expression remained unchanged over time (Figure 10C).

Results obtained here strongly support the hypothesis that the molecular counteraction exerted by either *C. oleophila* or *T. atroviride*-culture filtrate applied one day before *P. oleae* inoculation, reduced significantly the pathogenicity of *P. oleae* by lowering the most effective effectors/exoenzymes by a still unclear mechanism. However, despite its action was long lasting (up to 168 hpi), it did not halt but only slowed the invasion of olive drupes

by *P. oleae*. Further research will be needed to increase the effectiveness and extend further the duration of the inhibitory activity exerted by agents of biological control.

3.6 Conclusion

In conclusion, this study unveiled the transcriptomic events of the two- and three-actors interactions of *P. oleae* with olive fruits and each of the two evaluated biocontrol agents. Genome sequencing of *P. oleae* has strongly contributed to the study of its transcriptomics and description of the annotated pathogenesis-related genes. The olive cultivar 'Coratina' can be regarded as a susceptible host, despite several R-genes described here were upregulated in response to the infection (compatible host), and the two biocontrol agents only temporarily restricted the growth of the pathogen inside the drupes. However, over time (up to 168 hpi) these treatments were not able to stop *P. oleae* infection progression

CRediT author statement.

Sebastiano Conti Taguali: Investigation, Methodology, Software, Data Curation, Formal analysis, Validation, Writing - Original Draft, Writing - Review & Editing

Mario Riolo: Conceptualization, Investigation, Methodology, Software, Formal analysis, Validation, Writing - Original Draft, Writing - Review & Editing.

Federico La Spada: Conceptualization, Investigation, Methodology, Writing - Review & Editing.

Giuseppe Dionisio: Conceptualization, Methodology, Software, Data Curation, Formal analysis, Validation, Writing - Original Draft, Writing - Review & Editing, SupervisionResources, Project administration

Santa Olga Cacciola: Conceptualization, Writing - Original Draft, Validation, Writing - Review & Editing, Resources, Supervision, Funding acquisition, Project administration.

FUNDS

This study was supported by the University of Catania, Italy, "Investigation of Phytopathological problems of the main Sicilian productive contexts and eco-sustainable defense strategies (MEDIT-ECO)"- PiaCeRi-PIAno di inCEntivi per la Ricerca di Ateneo 2020-22 linea 2" "5A722192155"; the project "Smart and innovative packaging, postharvest rot management, and shipping of organic citrus fruit (BiOrangePack)" under Partnership for Research and Innovation in the Mediterranean Area (PRIMA) – H2020 (E69C20000130001); the European Union (NextGeneration EU), through the MUR-PNRR

project SAMOTHRACE (ECS00000022) and Ministero dell'agricoltura, della sovranità alimentare e delle foreste (MASAF), project title: Difesa degli Agrumeti Italiani dal Malsecco – AGRIVITA (CUP: C83C23000650006).

Conflict of interest: Authors declare no conflict of interest.

Declaration of availability of supplementary material

The supplementary data of this study will be available to the evaluators upon request to the corresponding authors.

3.7 References

Abad, Z.G., Burgess, T.I., Bourret, T., Bensch, K., Cacciola, S.O., Scanu, B., et al. (2023) *Phytophthora*: taxonomic and phylogenetic revision of the genus. *Studies in Mycology*, 106, 259. https://doi.org/10.3114/SIM.2023.106.05.

Adnan, M., Islam, W., Shabbir, A., Khan, K.A., Ghramh, H.A., Huang, Z., et al. (2019) Plant defense against fungal pathogens by antagonistic fungi with *Trichoderma* in focus. *Microbial Pathogenesis*, 129, 7–18. https://doi.org/10.1016/J.MICPATH.2019.01.042.

Agarwal, P. & Agarwal, P.K. (2013) Pathogenesis related-10 proteins are small, structurally similar but with diverse role in stress signaling. *Molecular Biology Reports*, 41, 599–611. https://doi.org/10.1007/S11033-013-2897-4.

Agosteo, G.E., Ragazzi, A., Surico, G. & Cacciola, S.O. (2023) Olive diseases. In: Fabbri, A., Baldoni, L., Caruso, T., and Famiani, F. (Eds.) The Olive: Botany and Production. Wallingford, UK: CABI Publishing, pp. 565–610.

Ai, G., Xia, Q., Song, T., Li, T., Zhu, H., Peng, H., et al. (2021) A *Phytophthora sojae* CRN effector mediates phosphorylation and degradation of plant aquaporin proteins to suppress host immune signaling. *PLOS Pathogens*, 17, e1009388. https://doi.org/10.1371/JOURNAL.PPAT.1009388.

Aidemark, M., Tjellström, H., Sandelius, A.S., Stålbrand, H., Andreasson, E., Rasmusson, A.G., et al. (2010) *Trichoderma viride* cellulase induces resistance to the antibiotic pore-forming peptide alamethicin associated with changes in the plasma membrane lipid composition of tobacco BY-2 cells. *BMC Plant Biology*, 10, 1–13. https://doi.org/10.1186/1471-2229-10-274/FIGURES/8.

Ali, M.S. & Baek, K.H. (2020) Jasmonic Acid Signaling Pathway in Response to Abiotic Stresses in Plants. *International Journal of Molecular Sciences*, 21, 621. https://doi.org/10.3390/IJMS21020621.

Alvarez, M.E., Nota, F. & Cambiagno, D.A. (2010) Epigenetic control of plant immunity. *Molecular plant pathology*, 11, 563–576. https://doi.org/10.1111/J.1364-3703.2010.00621.X.

Asai, S., Rallapalli, G., Piquerez, S.J.M., Caillaud, M.C., Furzer, O.J., Ishaque, N., et al. (2014) Expression Profiling during Arabidopsis/Downy Mildew Interaction Reveals a Highly-Expressed Effector That Attenuates Responses to Salicylic Acid. *PLOS Pathogens*, 10, e1004443. https://doi.org/10.1371/JOURNAL.PPAT.1004443.

Ashapkin, V. V., Kutueva, L.I., Aleksandrushkina, N.I. & Vanyushin, B.F. (2020) Epigenetic Mechanisms of Plant Adaptation to Biotic and Abiotic Stresses. *International Journal of Molecular Sciences*, 21, 1–32. https://doi.org/10.3390/IJMS21207457.

Bailey, R.L., Herbert, J.M., Khan, K., Heath, V.L., Bicknell, R. & Tomlinson, M.G. (2011) The emerging role of tetraspanin microdomains on endothelial cells. *Biochemical Society Transactions*, 39, 1667–1673. https://doi.org/10.1042/BST20110745.

Bar-Shimon, M., Yehuda, H., Cohen, L., Weiss, B., Kobeshnikov, A., Daus, A., et al. (2004) Characterization of extracellular lytic enzymes produced by the yeast biocontrol agent *Candida oleophila*. *Current Genetics*, 45, 140–148. https://doi.org/10.1007/S00294-003-0471-7/FIGURES/6.

Batta, Y.A. (2004) Postharvest biological control of apple gray mold by *Trichoderma harzianum* Rifai formulated in an invert emulsion. *Crop Protection*, 23, 19–26. https://doi.org/10.1016/S0261-2194(03)00163-7.

Benedetti, M., Verrascina, I., Pontiggia, D., Locci, F., Mattei, B., Lorenzo, G. De, et al. (2018) Four Arabidopsis berberine bridge enzyme-like proteins are specific oxidases that inactivate the elicitor-active oligogalacturonides. *The Plant Journal*, 94, 260–273. https://doi.org/10.1111/TPJ.13852.

Benjamini, Y., Drai, D., Elmer, G., Kafkafi, N. & Golani, I. (2001) Controlling the false discovery rate in behavior genetics research. *Behavioural Brain Research*, 125, 279–284. https://doi.org/10.1016/S0166-4328(01)00297-2.

Bernoux, M., Timmers, T., Jauneau, A., Brière, C., Wit, P.J.G.M. De, Marco, Y., et al. (2008) RD19, an *Arabidopsis* Cysteine Protease Required for RRS1-R–Mediated Resistance, Is Relocalized to the Nucleus by the *Ralstonia solanacearum* PopP2 Effector. *The Plant Cell*, 20, 2252–2264. https://doi.org/10.1105/TPC.108.058685.

Bolger, A.M., Lohse, M. & Usadel, B. (2014) Trimmomatic: a flexible trimmer for Illumina sequence data. *Bioinformatics*, 30, 2114–2120. https://doi.org/10.1093/BIOINFORMATICS/BTU170.

Bozkurt, T.O., Schornack, S., Win, J., Shindo, T., Ilyas, M., Oliva, R., et al. (2011)

Phytophthora infestans effector AVRblb2 prevents secretion of a plant immune protease at the haustorial interface. *Proceedings of the National Academy of Sciences of the United States of America*, 108, 20832–20837. https://doi.org/10.1073/PNAS.1112708109/SUPPL_FILE/PNAS.201112708SI.PDF.

Broekgaarden, C., Caarls, L., Vos, I.A., Pieterse, C.M.J. & Wees, S.C.M. Van (2015) Ethylene: Traffic Controller on Hormonal Crossroads to Defense. *Plant Physiology*, 169, 2371–2379. https://doi.org/10.1104/PP.15.01020.

Büschges, R., Hollricher, K., Panstruga, R., Simons, G., Wolter, M., Frijters, A., et al. (1997) The Barley *Mlo* Gene: A Novel Control Element of Plant Pathogen Resistance. *Cell*, 88, 695–705. https://doi.org/10.1016/S0092-8674(00)81912-1.

Cacciola, S.O., Faedda, R., Sinatra, F., Agosteo, G.E., Schena, L., Frisullo, S., et al. (2012) Olive anthracnose. *Journal of Plant Pathology*, 94, 29–44.

Chattaoui, M., Rhouma, A., Krid, S., Triki, M.A., Moral, J., Msallem, M., et al. (2011) First Report of Fruit Rot of Olives Caused by *Botryosphaeria dothidea* in Tunisia. *Plant Disease*, 95, 770–770. https://doi.org/10.1094/PDIS-11-10-0827.

Chen, C. & Chen, Z. (2002) Potentiation of Developmentally Regulated Plant Defense Response by AtWRKY18, a Pathogen-Induced Arabidopsis Transcription Factor. *Plant Physiology*, 129, 706–716. https://doi.org/10.1104/PP.001057.

Chen, X., Li, C., Wang, H. & Guo, Z. (2019) WRKY transcription factors: evolution, binding, and action. *Phytopathology Research*, 1, 1–15. https://doi.org/10.1186/S42483-019-0022-X.

Chóez-Guaranda, I., Espinoza-Lozano, F., Reyes-Araujo, D., Romero, C., Manzano, P., Galarza, L., et al. (2023) Chemical Characterization of *Trichoderma* spp. Extracts with Antifungal Activity against Cocoa Pathogens. *Molecules*, 28, 3208. https://doi.org/10.3390/MOLECULES28073208.

Cock, P.J.A., Fields, C.J., Goto, N., Heuer, M.L. & Rice, P.M. (2010) The Sanger FASTQ file format for sequences with quality scores, and the Solexa/Illumina FASTQ variants. *Nucleic Acids Research*, 38, 1767–1771. https://doi.org/10.1093/NAR/GKP1137.

Cui, Y., Gao, J., He, Y. & Jiang, L. (2020) Plant extracellular vesicles. *Protoplasma*, 257, 3–12. https://doi.org/10.1007/S00709-019-01435-6/TABLES/2.

Davidsson, P., Broberg, M., Kariola, T., Sipari, N., Pirhonen, M. & Palva, E.T. (2017) Short oligogalacturonides induce pathogen resistance-associated gene expression in *Arabidopsis thaliana*. *BMC Plant Biology*, 17, 1–17. https://doi.org/10.1186/S12870-016-0959-1/FIGURES/9.

DeYoung, B.J. & Innes, R.W. (2006) Plant NBS-LRR proteins in pathogen sensing and host

defense. *Nature immunology*, 7, 1243–1249. https://doi.org/10.1038/NI1410.

Dhawan, R., Luo, H., Foerster, A.M., Abuqamar, S., Du, H.N., Briggs, S.D., et al. (2009) HISTONE MONOUBIQUITINATION1 Interacts with a Subunit of the Mediator Complex and Regulates Defense against Necrotrophic Fungal Pathogens in *Arabidopsis*. *The Plant Cell*, 21, 1000–1019. https://doi.org/10.1105/TPC.108.062364.

Dionisio, G., Uddin, M.N. & Vincze, E. (2018) Enrichment and Identification of the Most Abundant Zinc Binding Proteins in Developing Barley Grains by Zinc-IMAC Capture and Nano LC-MS/MS. *Proteomes*, 6, 3. https://doi.org/10.3390/PROTEOMES6010003.

Dou, D., Kale, S.D., Wang, X., Jiang, R.H.Y., Bruce, N.A., Arredondo, F.D., et al. (2008) RXLR-Mediated Entry of *Phytophthora sojae* Effector Avr1b into Soybean Cells Does Not Require Pathogen-Encoded Machinery. *The Plant Cell*, 20, 1930. https://doi.org/10.1105/TPC.107.056093.

Droby, S., Hofstein, R., Wilson, C.L., Wisniewski, M. , Fridlender, B., Cohen, L., et al. (1993) Pilot testing of *Pichia guilliermondii*: A biocontrol agent of postharvest diseases of citrus fruit . *Biol. Control*, 3, 47 52, https://doi.org/10.1006/bcon.1993.1008

Droby, S.,. Vinokur, V., Weiss, B., Cohen, L., Daus, A., Goldschmidt, E.E,. Porat, R.(2002) Induction of resistance to *Penicillium digitatum* in grapefruit by the yeast biocontrol agent *Candida oleophila*. *Phytopathology*, 92, 393-399, https://doi.org/10.1094/PHYTO.2002.92.4.393

Du, C., Li, X., Chen, J., Chen, W., Li, B., Li, C., et al. (2016) Receptor kinase complex transmits RALF peptide signal to inhibit root growth in *Arabidopsis*. *Proceedings of the National Academy of Sciences of the United States of America*, 113, E8326–E8334. https://doi.org/10.1073/PNAS.1609626113/SUPPL_FILE/PNAS.201609626SI.PDF.

Dukare, A.S., Paul, S., Nambi, V.E., Gupta, R.K., Singh, R., Sharma, K., et al. (2019) Exploitation of microbial antagonists for the control of postharvest diseases of fruits: a review. *Critical reviews in food science and nutrition*, 59, 1498–1513. https://doi.org/10.1080/10408398.2017.1417235.

Ent, S. Van Der & Pieterse, C.M.J. (2012) Ethylene: Multi-Tasker in Plant–Attacker Interactions. Annual Plant Reviews Volume 44: The Plant Hormone Ethylene. John Wiley & Sons, Ltd, pp. 343–377.

Farrar, K., Evans, I.M., Topping, J.F., Souter, M.A., Nielsen, J.E. & Lindsey, K. (2003) *EXORDIUM*– a gene expressed in proliferating cells and with a role in meristem function, identified by promoter trapping in *Arabidopsis*. *The Plant Journal*, 33, 61–73.

https://doi.org/10.1046/J.1365-313X.2003.01608.X.

Ferreira, F. V., Herrmann-Andrade, A.M., Calabrese, C.D., Bello, F., Vázquez, D. & Musumeci, M.A. (2020) Effectiveness of *Trichoderma* strains isolated from the rhizosphere of citrus tree to control *Alternaria alternata*, *Colletotrichum gloeosporioides* and *Penicillium digitatum* A21 resistant to pyrimethanil in post-harvest oranges (Citrus sinensis L. (Osbeck)). *Journal of Applied Microbiology*, 129, 712–727. https://doi.org/10.1111/jam.14657.

Freimoser, F.M., Rueda-Mejia, M.P., Tilocca, B. & Migheli, Q. (2019) Biocontrol yeasts: mechanisms and applications. *World journal of microbiology & biotechnology*, 35, 154. https://doi.org/10.1007/S11274-019-2728-4.

González-Estrada, R., Blancas-Benítez, F., Montaño-Leyva, B., Moreno-Hernández, C., Romero-Islas, L.D.C., Romero-Islas, J., et al. (2018) A Review Study on the Postharvest Decay Control of Fruit by *Trichoderma*. Trichoderma - The Most Widely Used Fungicide. IntechOpen.

Guo, B., Wang, H., Yang, B., Jiang, W., Jing, M., Li, H., et al. (2019) *Phytophthora sojae* Effector PsAvh240 Inhibits Host Aspartic Protease Secretion to Promote Infection. *Molecular Plant*, 12, 552–564. https://doi.org/10.1016/J.MOLP.2019.01.017.

Guo, H., Nolan, T.M., Song, G., Liu, S., Xie, Z., Chen, J., et al. (2018) FERONIA Receptor Kinase Contributes to Plant Immunity by Suppressing Jasmonic Acid Signaling in *Arabidopsis thaliana*. *Current Biology*, 28, 3316-3324.e6. https://doi.org/10.1016/J.CUB.2018.07.078.

Guzmán-Guzmán, P., Kumar, A., los Santos-Villalobos, S. de, Parra-Cota, F.I., Orozco-Mosqueda, M. del C., Fadiji, A.E., et al. (2023) *Trichoderma* Species: Our Best Fungal Allies in the Biocontrol of Plant Diseases—A Review. *Plants*, 12, 432. https://doi.org/10.3390/PLANTS12030432.

Haas, B.J., Papanicolaou, A., Yassour, M., Grabherr, M., Blood, P.D., Bowden, J., et al. (2013) *De novo* transcript sequence reconstruction from RNA-seq using the Trinity platform for reference generation and analysis. *Nature Protocols*, 8, 1494–1512. https://doi.org/10.1038/nprot.2013.084.

Hammami, R., Oueslati, M., Smiri, M., Nefzi, S., Ruissi, M., Comitini, F., et al. (2022) Epiphytic Yeasts and Bacteria as Candidate Biocontrol Agents of Green and Blue Molds of Citrus Fruits. *Journal of Fungi*, 8, 818. https://doi.org/10.3390/jof8080818.

Han, L., Li, G.J., Yang, K.Y., Mao, G., Wang, R., Liu, Y., et al. (2010) Mitogen-activated protein kinase 3 and 6 regulate *Botrytis cinerea*-induced ethylene production in Arabidopsis. *The Plant Journal*, 64, 114–127. https://doi.org/10.1111/J.1365-

313X.2010.04318.X.

Hano, C., Martin, I., Fliniaux, O., Legrand, B., Gutierrez, L., Arroo, R.R.J., et al. (2006) Pinoresinol-lariciresinol reductase gene expression and secoisolariciresinol diglucoside accumulation in developing flax (*Linum usitatissimum*) seeds. *Planta*, 224, 1291–1301. https://doi.org/10.1007/S00425-006-0308-Y/TABLES/2.

Helliwell, E.E., Wang, Q. & Yang, Y. (2016) Ethylene biosynthesis and signaling is required for rice immune response and basal resistance against *Magnaporthe oryzae* infection. *Molecular Plant-Microbe Interactions*, 29, 831–843. https://doi.org/10.1094/MPMI-06-16-0121-R/ASSET/IMAGES/LARGE/MPMI-06-16-0121-R_F7.JPEG.

Hoffman, N.E., Yang, S.F. & McKeon, T. (1982) Identification of 1-(malonylamino)cyclopropane-1-carboxylic acid as a major conjugate of 1-aminocyclopropane-1-carboxylic acid, an ethylene precursor in higher plants. *Biochemical and Biophysical Research Communications*, 104, 765–770. https://doi.org/10.1016/0006-291X(82)90703-3.

Houben, M. & Poel, B. Van de (2019) 1-Aminocyclopropane-1-Carboxylic Acid Oxidase (ACO): The Enzyme That Makes the Plant Hormone Ethylene. *Frontiers in Plant Science*, 10, 464815. https://doi.org/10.3389/FPLS.2019.00695/BIBTEX.

Hua, J., Grisafi, P., Cheng, S.H. & Fink, G.R. (2001) Plant growth homeostasis is controlled by the *Arabidopsis BON1* and *BAP1* genes. *Genes & development*, 15, 2263–2272. https://doi.org/10.1101/GAD.918101.

Huang, G., Liu, Z., Gu, B., Zhao, H., Jia, J., Fan, G., et al. (2019) An RXLR effector secreted by *Phytophthora parasitica* is a virulence factor and triggers cell death in various plants. *Molecular Plant Pathology*, 20, 356–371. https://doi.org/10.1111/MPP.12760.

Huang, L.J., Zhang, J., Lin, Z., Yu, P., Lu, M. & Li, N. (2022) The AP2/ERF transcription factor ORA59 regulates ethylene-induced phytoalexin synthesis through modulation of an acyltransferase gene expression. *Journal of Cellular Physiology*. https://doi.org/10.1002/JCP.30935.

Huang, W., Wu, Z., Tian, H., Li, X. & Zhang, Y. (2021) *Arabidopsis* CALMODULIN-BINDING PROTEIN 60b plays dual roles in plant immunity. *Plant Communications*, 2, 100213. https://doi.org/10.1016/j.xplc.2021.100213.

Imano, S., Fushimi, M., Camagna, M., Tsuyama-Koike, A., Mori, H., Ashida, A., et al. (2022) AP2/ERF Transcription Factor NbERF-IX-33 Is Involved in the Regulation of Phytoalexin Production for the Resistance of Nicotiana benthamiana to Phytophthora infestans. *Frontiers in Plant Science*, 12, 821574.

https://doi.org/10.3389/FPLS.2021.821574/FULL.

Israel, D., Lee, S.H., Robson, T.M. & Zwiazek, J.J. (2022) Plasma membrane aquaporins of the PIP1 and PIP2 subfamilies facilitate hydrogen peroxide diffusion into plant roots. *BMC plant biology*, 22, 566. https://doi.org/10.1186/S12870-022-03962-6.

Iwai, T., Miyasaka, A., Seo, S. & Ohashi, Y. (2006) Contribution of Ethylene Biosynthesis for Resistance to Blast Fungus Infection in Young Rice Plants. *Plant Physiology*, 142, 1202–1215. https://doi.org/10.1104/PP.106.085258.

Janků, M., Jedelská, T., Činčalová, L., Sedlář, A., Mikulík, J., Luhová, L., et al. (2022) Structure-activity relationships of oomycete elicitins uncover the role of reactive oxygen and nitrogen species in triggering plant defense responses. *Plant science : an international journal of experimental plant biology*, 319, 111239. https://doi.org/10.1016/J.PLANTSCI.2022.111239.

Jaskiewicz, M., Conrath, U. & Peterhälnsel, C. (2011) Chromatin modification acts as a memory for systemic acquired resistance in the plant stress response. *EMBO Reports*, 12, 50–55. https://doi.org/10.1038/EMBOR.2010.186/SUPPL_FILE/EMBR2010186-SUP-0001.PDF.

Ji, D., Chen, T., Zhang, Z., Li, B. & Tian, S. (2020) Versatile Roles of the Receptor-Like Kinase Feronia in Plant Growth, Development and Host-Pathogen Interaction. *International Journal of Molecular Sciences*, 21, 7881. https://doi.org/10.3390/IJMS21217881.

Ji, S., Liu, Z. & Wang, Y. (2021) *Trichoderma*-Induced Ethylene Responsive Factor MsERF105 Mediates Defense Responses in *Malus sieversii*. *Frontiers in plant science*, 12, 708010. https://doi.org/10.3389/FPLS.2021.708010.

Jiménez-Ruiz, J., Ramírez-Tejero, J.A., Fernández-Pozo, N., Leyva-Pérez, M. de la O., Yan, H., Rosa, R. de la, et al. (2020) Transposon activation is a major driver in the genome evolution of cultivated olive trees (*Olea europaea* L.). *The Plant Genome*, 13, e20010. https://doi.org/10.1002/TPG2.20010.

Jo, H.J., Han, J.Y., Hwang, H.S. & Choi, Y.E. (2017) β-Amyrin synthase (EsBAS) and β-amyrin 28-oxidase (CYP716A244) in oleanane-type triterpene saponin biosynthesis in *Eleutherococcus senticosus*. *Phytochemistry*, 135, 53–63. https://doi.org/10.1016/J.PHYTOCHEM.2016.12.011.

Jung, T., Milenković, I., Balci, Y., Janoušek, J., Kudláček, T., Nagy, Z.Á., et al. (2024) Worldwide forest surveys reveal forty-three new species in *Phytophthora* major Clade 2 with fundamental implications for the evolution and biogeography of the

genus and global plant biosecurity. *Studies in Mycology*, 107, 251–388. https://doi.org/10.3114/SIM.2024.107.04.

Kamoun, S., West, P. Van, Jong, A.J. De, Groot, K.E. De, Vleeshouwers, V.G.A.A. & Govers, F. (1997) A Gene Encoding a Protein Elicitor of *Phytophthora infestans* Is Down-Regulated During Infection of Potato. *Molecular Plant-Microbe Interactions*, 10, 13–20. https://doi.org/10.1094/MPMI.1997.10.1.13.

Kamoun, S., Young, M., Forster, H., Coffey, M.D. & Tyler, B.M. (1994) Potential Role of Elicitins in the Interaction between *Phytophthora* Species and Tobacco. *Applied and Environmental Microbiology*, 60, 1593–1598. https://doi.org/10.1128/AEM.60.5.1593-1598.1994.

Kang, H., Fan, T., Wu, J., Zhu, Y. & Shen, W.H. (2022) Histone modification and chromatin remodeling in plant response to pathogens. *Frontiers in Plant Science*, 13, 986940. https://doi.org/10.3389/FPLS.2022.986940/BIBTEX.

Kawamura, Y., Hase, S., Takenaka, S., Kanayama, Y., Yoshioka, H., Kamoun, S., et al. (2009) INF1 Elicitin Activates Jasmonic Acid- and Ethylene-mediated Signalling Pathways and Induces Resistance to Bacterial Wilt Disease in Tomato. *Journal of Phytopathology*, 157, 287–297. https://doi.org/10.1111/J.1439-0434.2008.01489.X.

Kessler, S.A., Shimosato-Asano, H., Keinath, N.F., Wuest, S.E., Ingram, G., Panstruga, R., et al. (2010) Conserved Molecular Components for Pollen Tube Reception and Fungal Invasion. *Science (New York, N.Y.)*, 330, 968–971. https://doi.org/10.1126/SCIENCE.1195211.

Kim, D., Paggi, J.M., Park, C., Bennett, C. & Salzberg, S.L. (2019) Graph-based genome alignment and genotyping with HISAT2 and HISAT-genotype. *Nature Biotechnology*, 37, 907–915. https://doi.org/10.1038/s41587-019-0201-4.

Köster, P., DeFalco, T.A. & Zipfel, C. (2022) Ca2+ signals in plant immunity. *The EMBO journal*, 41, e110741. https://doi.org/10.15252/EMBJ.2022110741.

Lahlali, R., Serrhini, M.N. & Jijakli, M.H. (2004) Efficacy assessment of *Candida oleophila* (strain O) and *Pichia anomala* (strain K) against major postharvest diseases of citrus fruits in Morocco. *Communications in agricultural and applied biological sciences*, 69, 601–609.

La Spada, F., Stracquadanio, C., Riolo, M., Pane, A. & Cacciola, S.O. (2020) *Trichoderma* Counteracts the Challenge of *Phytophthora nicotianae* Infections on Tomato by Modulating Plant Defense Mechanisms and the Expression of Crinkler, Necrosis-Inducing Phytophthora Protein 1, and Cellulose-Binding Elicitor Lectin Pathogenic Effecto. *Frontiers in Plant Science*, 11, 1653. https://doi.org/10.3389/fpls.2020.583539.

Lassois, L., Lapeyre de Bellaire, L. de & Jijakli, M.H. (2008) Biological control of crown rot of bananas with *Pichia anomala* strain K and *Candida oleophila* strain O. *Biological Control*, 45, 410–418. https://doi.org/10.1016/J.BIOCONTROL.2008.01.013.

Leoni, C., Bruzzone, J., Villamil, J.J., Martínez, C., Montelongo, M.J., Bentancur, O., et al. (2018) Percentage of anthracnose (*Colletotrichum acutatum* s.s.) acceptable in olives for the production of extra virgin olive oil. *Crop Protection*, 108, 47–53. https://doi.org/10.1016/J.CROPRO.2018.02.013.

Li, M.F., Li, G.H. & Zhang, K.Q. (2019) Non-Volatile Metabolites from *Trichoderma* spp. *Metabolites*, 9, 58. https://doi.org/10.3390/METABO9030058.

Li, T., Ai, G., Fu, X., Liu, J., Zhu, H., Zhai, Y., et al. (2022) A *Phytophthora capsici* RXLR effector manipulates plant immunity by targeting RAB proteins and disturbing the protein trafficking pathway. *Molecular Plant Pathology*, 23, 1721–1736. https://doi.org/10.1111/MPP.13251.

Licausi, F., Ohme-Takagi, M. & Perata, P. (2013) APETALA2/Ethylene Responsive Factor (AP2/ERF) transcription factors: mediators of stress responses and developmental programs. *New Phytologist*, 199, 639–649. https://doi.org/10.1111/NPH.12291.

Lima, G., Ippolito, A., Nigro, F. & Salerno, M. (1997) Effectiveness of *Aureobasidium pullulans* and *Candida oleophila* against postharvest strawberry rots. *Postharvest Biology and Technology*, 10, 169–178. https://doi.org/10.1016/S0925-5214(96)01302-6.

Lin, F., Zhao, M., Baumann, D.D., Ping, J., Sun, L., Liu, Y., et al. (2014) Molecular response to the pathogen *Phytophthora sojae* among ten soybean near isogenic lines revealed by comparative transcriptomics. *BMC Genomics*, 15, 1–13. https://doi.org/10.1186/1471-2164-15-18/FIGURES/6.

Liu, J., Sui, Y., Wisniewski, M., Droby, S. & Liu, Y. (2013) Review: Utilization of antagonistic yeasts to manage postharvest fungal diseases of fruit. *International journal of food microbiology*, 167, 153–160. https://doi.org/10.1016/J.IJFOODMICRO.2013.09.004.

Liu, T., Ye, W., Ru, Y., Yang, X., Gu, B., Tao, K., et al. (2011) Two Host Cytoplasmic Effectors Are Required for Pathogenesis of *Phytophthora sojae* by Suppression of Host Defenses. *Plant Physiology*, 155, 490–501. https://doi.org/10.1104/PP.110.166470.

Liu, Z.Q., Qiu, A.L., Shi, L.P., Cai, J. Sen, Huang, X.Y., Yang, S., et al. (2015) SRC2-1 is required in PcINF1-induced pepper immunity by acting as an interacting partner of PcINF1. *Journal of Experimental Botany*, 66, 3683–3698. https://doi.org/10.1093/JXB/ERV161.

Livak, K.J. & Schmittgen, T.D. (2001) Analysis of Relative Gene Expression Data Using

Real-Time Quantitative PCR and the 2−ΔΔCT Method. *Methods*, 25, 402–408. https://doi.org/10.1006/METH.2001.1262.

Locci, F., Benedetti, M., Pontiggia, D., Citterico, M., Caprari, C., Mattei, B., et al. (2019) An Arabidopsis berberine bridge enzyme-like protein specifically oxidizes cellulose oligomers and plays a role in immunity. *The Plant Journal*, 98, 540–554. https://doi.org/10.1111/TPJ.14237.

Lohse, M., Nagel, A., Herter, T., May, P., Schroda, M., Zrenner, R., et al. (2014) Mercator: a fast and simple web server for genome scale functional annotation of plant sequence data. *Plant, cell & environment*, 37, 1250–1258. https://doi.org/10.1111/PCE.12231.

Loon, L.C. van, Pierpoint, W.S., Boller, T. & Conejero, V. (1994) Recommendations for naming plant pathogenesis-related proteins. *Plant Molecular Biology Reporter*, 12, 245–264. https://doi.org/10.1007/BF02668748/METRICS.

Love, M.I., Huber, W. & Anders, S. (2014) Moderated estimation of fold change and dispersion for RNA-seq data with DESeq2. *Genome Biology*, 15, 1–21. https://doi.org/10.1186/S13059-014-0550-8/FIGURES/9.

Marra, R., Coppola, M., Pironti, A., Grasso, F., Lombardi, N., D'errico, G., et al. (2020) The Application of *Trichoderma* Strains or Metabolites Alters the Olive Leaf Metabolome and the Expression of Defense-Related Genes. *Journal of Fungi*, 6, 369. https://doi.org/10.3390/JOF6040369.

Martinez, Y., Ribera, J., Schwarze, F.W.M.R. & France, K. De (2023) Biotechnological development of *Trichoderma*-based formulations for biological control. *Applied Microbiology and Biotechnology*, 107, 5595–5612. https://doi.org/10.1007/S00253-023-12687-X.

Masek, T., Vopalensky, V., Suchomelova, P. & Pospisek, M. (2005) Denaturing RNA electrophoresis in TAE agarose gels. *Analytical Biochemistry*, 336, 46–50. https://doi.org/10.1016/J.AB.2004.09.010.

Mathew, M.K. & Balaram, P. (1983) Alamethicin and related membrane channel forming polypeptides. *Molecular and Cellular Biochemistry*, 50, 47–64. https://doi.org/10.1007/BF00225279/METRICS.

Mbarga, J.B., Begoude, B.A.D., Ambang, Z., Meboma, M., Kuate, J., Schiffers, B., et al. (2014) A new oil-based formulation of *Trichoderma asperellum* for the biological control of cacao black pod disease caused by *Phytophthora megakarya*. *Biological Control*, 77, 15–22. https://doi.org/10.1016/J.BIOCONTROL.2014.06.004.

Moral, J., Agustí-Brisach, C., Agalliu, G., Oliveira, R. de, Pérez-Rodríguez, M., Roca, L.F.,

et al. (2018) Preliminary selection and evaluation of fungicides and natural compounds to control olive anthracnose caused by *Colletotrichum* species. *Crop Protection*, 114, 167–176. https://doi.org/10.1016/J.CROPRO.2018.08.033.

Moral, J., Agustí-Brisach, C., Raya, M.C., Jurado-Bello, J., López-Moral, A., Roca, L.F., et al. (2021) Diversity of *Colletotrichum* Species Associated with Olive Anthracnose Worldwide. *Journal of Fungi*, 7, 741. https://doi.org/10.3390/JOF7090741.

Moral, J., Luque, F. & Trapero, A. (2008) First Report of *Diplodia seriata*, the Anamorph of *"Botryosphaeria" obtusa*, Causing Fruit Rot of Olive in Spain. *Plant Disease*, 92, 311–311. https://doi.org/10.1094/PDIS-92-2-0311C.

Nesmelova, I. V. & Hackett, P.B. (2010) DDE transposases: Structural similarity and diversity. *Advanced Drug Delivery Reviews*, 62, 1187–1195. https://doi.org/10.1016/J.ADDR.2010.06.006.

Nigro, F. & Ippolito, A. (2002) Occurrence of new rots of olive drupes in Apulia. *Acta Horticulturae*, 586, 777–780. https://doi.org/10.17660/ActaHortic.2002.586.168.

Ohme-Takagi, M. & Shinshi, H. (1995) Ethylene-inducible DNA binding proteins that interact with an ethylene-responsive element. *The Plant Cell*, 7, 173. https://doi.org/10.1105/TPC.7.2.173.

Okazaki, Y., Ishizuka, A., Ishihara, A., Nishioka, T. & Iwamura, H. (2007) New Dimeric Compounds of Avenanthramide Phytoalexin in Oats. *Journal of Organic Chemistry*, 72, 3830–3839. https://doi.org/10.1021/JO0701740/SUPPL_FILE/JO0701740SI20070305_124746.PDF.

Oztekin, S., Dikmetas, D.N., Devecioglu, D., Acar, E.G. & Karbancioglu-Guler, F. (2023) Recent Insights into the Use of Antagonistic Yeasts for Sustainable Biomanagement of Postharvest Pathogenic and Mycotoxigenic Fungi in Fruits with Their Prevention Strategies against Mycotoxins. *Journal of agricultural and food chemistry*, 71, 9923–9950. https://doi.org/10.1021/ACS.JAFC.3C00315.

Pandey, S.P. & Somssich, I.E. (2009) The Role of WRKY Transcription Factors in Plant Immunity. *Plant Physiology*, 150, 1648–1655. https://doi.org/10.1104/PP.109.138990.

Pangallo, S., Li Destri Nicosia, M.G., Agosteo, G.E., Abdelfattah, A., Romeo, F. V., Cacciola, S.O., et al. (2017) Evaluation of a Pomegranate Peel Extract as an Alternative Means to Control Olive Anthracnose. *Phytopathology*, 107, 1462–1467. https://doi.org/10.1094/PHYTO-04-17-0133-R.

Paniagua, C., Bilkova, A., Jackson, P., Dabravolski, S., Riber, W., Didi, V., et al. (2017) Dirigent proteins in plants: modulating cell wall metabolism during abiotic and

biotic stress exposure. *Journal of Experimental Botany*, 68, 3287–3301. https://doi.org/10.1093/JXB/ERX141.

Pearce, G., Moura, D.S., Stratmann, J. & Ryan, C.A. (2001) RALF, a 5-kDa ubiquitous polypeptide in plants, arrests root growth and development. *Proceedings of the National Academy of Sciences of the United States of America*, 98, 12843–12847. https://doi.org/10.1073/PNAS.201416998/ASSET/50F2B588-C2B5-4C1C-8AFE-3F6B18278504/ASSETS/GRAPHIC/PQ2014169006.JPEG.

Peng, Y., Wersch, R. Van & Zhang, Y. (2018) Convergent and Divergent Signaling in PAMP-Triggered Immunity and Effector-Triggered Immunity. *Molecular Plant-Microbe Interactions*, 31, 403–409. https://doi.org/10.1094/MPMI-06-17-0145-CR/ASSET/IMAGES/LARGE/MPMI-06-17-0145-CR_F1.JPEG.

Pertea, M., Pertea, G.M., Antonescu, C.M., Chang, T.C., Mendell, J.T. & Salzberg, S.L. (2015) StringTie enables improved reconstruction of a transcriptome from RNA-seq reads. *Nature Biotechnology*, 33, 290–295. https://doi.org/10.1038/nbt.3122.

Petit-Houdenot, Y. & Fudal, I. (2017) Complex Interactions between Fungal Avirulence Genes and Their Corresponding Plant Resistance Genes and Consequences for Disease Resistance Management. *Frontiers in Plant Science*, 8, 1072. https://doi.org/10.3389/FPLS.2017.01072.

Pokou, D.N., Fister, A.S., Winters, N., Tahi, M., Klotioloma, C., Sebastian, A., et al. (2019) Resistant and susceptible cacao genotypes exhibit defense gene polymorphism and unique early responses to *Phytophthora megakarya* inoculation. *Plant Molecular Biology*, 99, 499–516. https://doi.org/10.1007/S11103-019-00832-Y.

Ramirez-Gonzalez, R.H., Bonnal, R., Caccamo, M. & MacLean, D. (2012) Bio-samtools: Ruby bindings for SAMtools, a library for accessing BAM files containing high-throughput sequence alignments. *Source Code for Biology and Medicine*, 7, 6. https://doi.org/10.1186/1751-0473-7-6/TABLES/4.

Ramirez-Prado, J.S., Abulfaraj, A.A., Rayapuram, N., Benhamed, M. & Hirt, H. (2018) Plant Immunity: From Signaling to Epigenetic Control of Defense. *Trends in Plant Science*, 23, 833–844. https://doi.org/10.1016/J.TPLANTS.2018.06.004.

Regente, M., Pinedo, M., Clemente, H.S., Balliau, T., Jamet, E. & La Canal, L. De (2017) Plant extracellular vesicles are incorporated by a fungal pathogen and inhibit its growth. *Journal of Experimental Botany*, 68, 5485–5495. https://doi.org/10.1093/JXB/ERX355.

Riolo, M., Aloi, F., Spada, F. La, Sciandrello, S., Moricca, S., Santilli, E., et al. (2020) Diversity of *Phytophthora* Communities across Different Types of Mediterranean

Vegetation in a Nature Reserve Area. *Forests*, 11, 1–21. https://doi.org/10.3390/F11080853.

Riolo, M., Luz, C., Santilli, E., Meca, G. & Cacciola, S.O. (2023a) Antifungal activity of selected lactic acid bacteria from olive drupes. *Food Bioscience*, 52, 102422. https://doi.org/10.1016/J.FBIO.2023.102422.

Riolo, M., Luz, C., Santilli, E., Meca, G. & Cacciola, S.O. (2023b) Secondary metabolites produced by four *Colletotrichum* species *in vitro* and on fruits of diverse olive cultivars. *Fungal Biology*, 127, 1118–1128. https://doi.org/10.1016/J.FUNBIO.2023.06.003.

Riolo, M., Pane, A., Santilli, E., Cacciola, S.O. & Moricca, S. (2023c) Susceptibility of Italian olive cultivars to various *Colletotrichum* species associated with fruit anthracnose. *Plant Pathology*, 72, 255–267. https://doi.org/10.1111/ppa.13652.

Riolo, M., Villena, A.M., Calpe, J., Luz, C., Meca, G., Tuccitto, N., et al. (2024) A circular economy approach: A new formulation based on a lemon peel medium activated with lactobacilli for sustainable control of post-harvest fungal rots in fresh citrus fruit. *Biological Control*, 189, 105443. https://doi.org/10.1016/J.BIOCONTROL.2024.105443.

Rodrigues, O., Reshetnyak, G., Grondin, A., Saijo, Y., Leonhardt, N., Maurel, C., et al. (2017) Aquaporins facilitate hydrogen peroxide entry into guard cells to mediate ABA- and pathogen-triggered stomatal closure. *Proceedings of the National Academy of Sciences of the United States of America*, 114, 9200–9205. https://doi.org/10.1073/PNAS.1704754114/SUPPL_FILE/PNAS.1704754114.SM04.WMV.

Rovetto, E.I., La Spada, F., El boumlasy, S., Conti Taguali, S., Riolo, R., Pane, A. et al. (2024) Biological control of green mold in simulated post-harvest chain of citrus Fruit: Efficacy of *Candida oleophila* strain O and molecular insight into elicitation of host immune system, *Biological Control*, 193, 105531. https://doi.org/10.1016/j.biocontrol.2024.105531.

Ruano-Rosa, D., Schena, L., Agosteo, G.E., Magnano di San Lio, G. & Cacciola, S.O. (2018) *Phytophthora oleae* sp. nov. causing fruit rot of olive in southern Italy. *Plant Pathology*, 67, 1362–1373. https://doi.org/10.1111/ppa.12836.

Rupwate, S.D. & Rajasekharan, R. (2012) C2 domain is responsible for targeting rice phosphoinositide specific phospholipase C. *Plant Molecular Biology*, 78, 247–258. https://doi.org/10.1007/S11103-011-9862-1/FIGURES/10.

Ryan, C.A., Lamb, C.J., Jagendorf, A.T., Kolattukudy, P.E. & Yu, L.M. (1995) Elicitins from

Phytophthora and basic resistance in tobacco. *Proceedings of the National Academy of Sciences*, 92, 4088–4094. https://doi.org/10.1073/PNAS.92.10.4088.

Salas-Marina, M.A., Isordia-Jasso, M.I., Islas-Osuna, M.A., Delgado-Sánchez, P., Jiménez-Bremont, J.F., Rodríguez-Kessler, M., et al. (2015) The Epl1 and Sm1 proteins from *Trichoderma atroviride* and *Trichoderma virens* differentially modulate systemic disease resistance against different life style pathogens in *Solanum lycopersicum*. *Frontiers in Plant Science*, 6, 119981. https://doi.org/10.3389/FPLS.2015.00077/ABSTRACT.

Schröder, F., Lisso, J., Lange, P. & Müssig, C. (2009) The extracellular EXO protein mediates cell expansion in Arabidopsis leaves. *BMC Plant Biology*, 9, 1–12. https://doi.org/10.1186/1471-2229-9-20/TABLES/5.

Shakeel, S.N., Wang, X., Binder, B.M. & Schaller, G.E. (2013) Mechanisms of signal transduction by ethylene: overlapping and non-overlapping signalling roles in a receptor family. *AoB Plants*, 5, plt010. https://doi.org/10.1093/AOBPLA/PLT010.

Shoresh, M., Harman, G.E. & Mastouri, F. (2010) Induced Systemic Resistance and Plant Responses to Fungal Biocontrol Agents. *Annual Review of Phytopathology*, 48, 21–43. https://doi.org/10.1146/annurev-phyto-073009-114450.

Silva, K. De, Laska, B., Brown, C., Sederoff, H.W. & Khodakovskaya, M. (2011) *Arabidopsis thaliana* calcium-dependent lipid-binding protein (AtCLB): a novel repressor of abiotic stress response. *Journal of Experimental Botany*, 62, 2679–2689. https://doi.org/10.1093/JXB/ERQ468.

Singh, B.N., Singh, A., Singh, B.R. & Singh, H.B. (2014) *Trichoderma harzianum* elicits induced resistance in sunflower challenged by *Rhizoctonia solani*. *Journal of Applied Microbiology*, 116, 654–666. https://doi.org/10.1111/JAM.12387.

Smirnoff, N. & Arnaud, D. (2019) Hydrogen peroxide metabolism and functions in plants. *New Phytologist*, 221, 1197–1214. https://doi.org/10.1111/NPH.15488.

Spadaro, D., Droby, S. (2016) Development of Biocontrol Products for Postharvest Diseases of Fruit: The Importance of Elucidating the Mechanisms of Action of Yeast Antagonists. *Trends in Food Science & Technology.*, 47, 39-49. https://doi.org/10.1016/j.tifs.2015.11.003.

Stiti, N. & Hartmann, M.-A. (2012) Nonsterol Triterpenoids as Major Constituents of *Olea europaea*. *Journal of lipids*, 2012, 1–13. https://doi.org/10.1155/2012/476595.

Stracquadanio, C., Luz, C., Spada, F. La, Meca, G. & Cacciola, S.O. (2021) Inhibition of Mycotoxigenic Fungi in Different Vegetable Matrices by Extracts of *Trichoderma* Species. *Journal of Fungi*, 7, 445. https://doi.org/10.3390/jof7060445.

Stracquadanio, C., Quiles, J.M., Meca, G. & Cacciola, S.O. (2020) Antifungal Activity of Bioactive Metabolites Produced by *Trichoderma asperellum* and *Trichoderma atroviride* in Liquid Medium. *Journal of Fungi*, 6, 263. https://doi.org/10.3390/jof6040263.

Sui, Y., Wisniewski, M., Droby, S., Piombo, E., Wu, X. & Yue, J. (2020) Genome Sequence, Assembly, and Characterization of the Antagonistic Yeast *Candida oleophila* Used as a Biocontrol Agent Against Post-harvest Diseases. *Frontiers in Microbiology*, 11, 518395. https://doi.org/10.3389/FMICB.2020.00295/BIBTEX.

Sun, T., Busta, L., Zhang, Q., Ding, P., Jetter, R. & Zhang, Y. (2018) TGACG-BINDING FACTOR 1 (TGA1) and TGA4 regulate salicylic acid and pipecolic acid biosynthesis by modulating the expression of *SYSTEMIC ACQUIRED RESISTANCE DEFICIENT 1 (SARD1)* and *CALMODULIN-BINDING PROTEIN 60g (CBP60g)*. *New Phytologist*, 217, 344–354. https://doi.org/10.1111/NPH.14780.

Sun, T. & Zhang, Y. (2021) Short- and long-distance signaling in plant defense. *The Plant Journal*, 105, 505–517. https://doi.org/10.1111/TPJ.15068.

Takahashi, S., Yeo, Y.S., Zhao, Y., O'Maille, P.E., Greenhagen, B.T., Noel, J.P., et al. (2007) Functional Characterization of Premnaspirodiene Oxygenase, a Cytochrome P450 Catalyzing Regio- and Stereo-specific Hydroxylations of Diverse Sesquiterpene Substrates. *Journal of Biological Chemistry*, 282, 31744–31754. https://doi.org/10.1074/JBC.M703378200.

Talhinhas, P., Loureiro, A. & Oliveira, H. (2018) Olive anthracnose: a yield- and oil quality-degrading disease caused by several species of *Colletotrichum* that differ in virulence, host preference and geographical distribution. *Molecular Plant Pathology*, 19, 1797–1807. https://doi.org/10.1111/mpp.12676.

Talhinhas, P., Sreenivasaprasad, S., Neves-Martins, J. & Oliveira, H. (2005) Molecular and phenotypic analyses reveal association of diverse *Colletotrichum acutatum* groups and a low level of *C. gloeosporioides* with olive anthracnose. *Applied and Environmental Microbiology*, 71, 2987–2998. https://doi.org/10.1128/AEM.71.6.2987-2998.2005.

Thynne, E., Saur, I.M.L., Simbaqueba, J., Ogilvie, H.A., Gonzalez-Cendales, Y., Mead, O., et al. (2017) Fungal phytopathogens encode functional homologues of plant rapid alkalinization factor (RALF) peptides. *Molecular Plant Pathology*, 18, 811–824. https://doi.org/10.1111/MPP.12444.

Topçu, G. (2006) Bioactive triterpenoids from *Salvia* species. *Journal of Natural Products*, 69, 482–487. https://doi.org/https://doi.org/10.1021/np0600402.

Tripathy, M.K., Deswal, R. & Sopory, S.K. (2021) Plant RABs: Role in Development and in Abiotic and Biotic Stress Responses. *Current Genomics*, 22, 26–40. https://doi.org/10.2174/1389202922666210114102743.

Valueva, T.A., Revina, T.A., Kladnitskaya, G. V. & Mosolov, V. V. (1998) Kunitz-type proteinase inhibitors from intact and *Phytophthora*-infected potato tubers. *FEBS Letters*, 426, 131–134. https://doi.org/10.1016/S0014-5793(98)00321-4.

Vega-Muñoz, I., Duran-Flores, D., Fernández-Fernández, Á.D., Heyman, J., Ritter, A. & Stael, S. (2020) Breaking Bad News: Dynamic Molecular Mechanisms of Wound Response in Plants. *Frontiers in Plant Science*, 11, 610445. https://doi.org/10.3389/FPLS.2020.610445/BIBTEX.

Walsh, T.A. & Twitched, W.P. (1991) Two Kunitz-Type Proteinase Inhibitors from Potato Tubers. *Plant Physiology*, 97, 15. https://doi.org/10.1104/PP.97.1.15.

Wang, D., Amornsiripanitch, N. & Dong, X. (2006) A Genomic Approach to Identify Regulatory Nodes in the Transcriptional Network of Systemic Acquired Resistance in Plants. *PLOS Pathogens*, 2, e123. https://doi.org/10.1371/JOURNAL.PPAT.0020123.

Wang, H., Wang, S., Wang, W., Xu, L., Welsh, L.R.J., Gierlinski, M., et al. (2023) Uptake of oomycete RXLR effectors into host cells by clathrin-mediated endocytosis. *The Plant cell*, 35, 2504–2526. https://doi.org/10.1093/PLCELL/KOAD069.

Wang, S., McLellan, H., Boevink, P.C. & Birch, P.R.J. (2023) RxLR Effectors: Master Modulators, Modifiers and Manipulators. *Molecular plant-microbe interactions*, 36, 754–763. https://doi.org/10.1094/MPMI-05-23-0054-CR.

Wang, S., Xing, R., Wang, Yan, Shu, H., Fu, S., Huang, J., et al. (2021) Cleavage of a pathogen apoplastic protein by plant subtilases activates host immunity. *New Phytologist*, 229, 3424–3439. https://doi.org/10.1111/NPH.17120.

Wang, W. & Jiao, F. (2019) Effectors of *Phytophthora* pathogens are powerful weapons for manipulating host immunity. *Planta*, 250, 413–425. https://doi.org/10.1007/S00425-019-03219-X.

Wang, X., Kong, H. & Hong, M. (2009) F-box proteins regulate ethylene signaling and more. *Genes & development*, 23, 391–396. https://doi.org/10.1101/GAD.1781609.

Wang, X., Lu, K., Yao, X., Zhang, L., Wang, F., Wu, D., et al. (2021) The Aquaporin TaPIP2;10 Confers Resistance to Two Fungal Diseases in Wheat. *Phytopathology*, 111, 2317–2331. https://doi.org/10.1094/PHYTO-02-21-0048-R.

Wang, Z., Meng, P., Zhang, X., Ren, D. & Yang, S. (2011) BON1 interacts with the protein kinases BIR1 and BAK1 in modulation of temperature-dependent plant growth and

cell death in Arabidopsis. *The Plant Journal*, 67, 1081–1093. https://doi.org/10.1111/J.1365-313X.2011.04659.X.

Wendehenne, D., Durner, J. & Klessig, D.F. (2004) Nitric oxide: a new player in plant signalling and defence responses. *Current Opinion in Plant Biology*, 7, 449–455. https://doi.org/10.1016/J.PBI.2004.04.002.

Winter, D., Vinegar, B., Nahal, H., Ammar, R., Wilson, G. V. & Provart, N.J. (2007) An "Electronic Fluorescent Pictograph" Browser for Exploring and Analyzing Large-Scale Biological Data Sets. *PLOS ONE*, 2, e718. https://doi.org/10.1371/JOURNAL.PONE.0000718.

Yang, H., Li, Y. & Hua, J. (2006) The C2 domain protein BAP1 negatively regulates defense responses in Arabidopsis. *The Plant Journal*, 48, 238–248. https://doi.org/10.1111/J.1365-313X.2006.02869.X.

Yoshioka, H., Yamada, N. & Doke, N. (1999) cDNA Cloning of Sesquiterpene Cyclase and Squalene Synthase, and Expression of the Genes in Potato Tuber Infected with *Phytophthora infestans*. *Plant and Cell Physiology*, 40, 993–998. https://doi.org/10.1093/OXFORDJOURNALS.PCP.A029633.

Yoshioka, M., Adachi, A., Sato, Y., Doke, N., Kondo, T. & Yoshioka, H. (2019) RNAi of the sesquiterpene cyclase gene for phytoalexin production impairs pre- and post-invasive resistance to potato blight pathogens. *Molecular Plant Pathology*, 20, 907–922. https://doi.org/10.1111/MPP.12802.

Yu, G., Wang, L.G., Han, Y. & He, Q.Y. (2012) clusterProfiler: an R Package for Comparing Biological Themes Among Gene Clusters. *OMICS: a Journal of Integrative Biology*, 16, 284–287. https://doi.org/10.1089/OMI.2011.0118.

Zhang, P., Jia, Y., Shi, J., Chen, C., Ye, W., Wang, Y., et al. (2019) The WY domain in the *Phytophthora* effector PSR1 is required for infection and RNA silencing suppression activity. *New Phytologist*, 223, 839–852. https://doi.org/10.1111/NPH.15836.

Zhang, Xiaokang, Li, B., Zhang, Z., Chen, Y. & Tian, S. (2020) Antagonistic Yeasts: A Promising Alternative to Chemical Fungicides for Controlling Postharvest Decay of Fruit. *Journal of Fungi*, 6, 158. https://doi.org/10.3390/JOF6030158.

Zhang, Xin, Yang, Z., Wu, D. & Yu, F. (2020) RALF–FERONIA Signaling: Linking Plant Immune Response with Cell Growth. *Plant Communications*, 1, 100084. https://doi.org/10.1016/J.XPLC.2020.100084.

Zhao, Y., Yang, B., Xu, H., Wu, J., Xu, Z. & Wang, Y. (2022) The *Phytophthora* effector Avh94 manipulates host jasmonic acid signaling to promote infection. *Journal of Integrative Plant Biology*, 64, 2199–2210.

https://doi.org/10.1111/JIPB.13358/SUPPINFO.

Zheng, Z., Qamar, S.A., Chen, Z. & Mengiste, T. (2006) Arabidopsis WRKY33 transcription factor is required for resistance to necrotrophic fungal pathogens. *The Plant Journal*, 48, 592–605. https://doi.org/10.1111/J.1365-313X.2006.02901.X.

Zhou, L., Cheung, M.Y., Li, M.W., Fu, Y., Sun, Z., Sun, S.M., et al. (2010) Rice Hypersensitive Induced Reaction Protein 1 (OsHIR1) associates with plasma membrane and triggers hypersensitive cell death. *BMC Plant Biology*, 10, 1–10. https://doi.org/10.1186/1471-2229-10-290/FIGURES/4.

Zhou, Q., Ma, K., Hu, H., Xing, X., Huang, X. & Gao, H. (2022) Extracellular vesicles: Their functions in plant–pathogen interactions. *Molecular Plant Pathology*, 23, 760–771. https://doi.org/10.1111/MPP.13170.

Zhu, A., Ibrahim, J.G. & Love, M.I. (2019) Heavy-tailed prior distributions for sequence count data: removing the noise and preserving large differences. *Bioinformatics*, 35, 2084–2092. https://doi.org/10.1093/BIOINFORMATICS/BTY895.

Zhu, Z., Xu, F., Zhang, Yaxi, Cheng, Y.T., Wiermer, M., Li, X., et al. (2010) Arabidopsis resistance protein SNC1 activates immune responses through association with a transcriptional corepressor. *Proceedings of the National Academy of Sciences of the United States of America*, 107, 13960–13965. https://doi.org/10.1073/PNAS.1002828l0.

4. Physiological and biochemical responses of olive fruit to *Colletotrichum* infection: A metabolomic Insight

Sebastiano Conti Taguali[1,2], Federico La Spada[1], Mario Riolo[1*], Elena Santilli[3], Antonella Pane[1], Biancaelena Maserti[4], Santa Olga Cacciola[1*]

[1] University of Catania, Department of Agriculture, Food and Environment (UniCT, Di3A), Via Santa Sofia 100, 95123 Catania (Italy).

[2] Mediterranea University of Reggio Calabria, Department of Agricultural Science, Località Feo di Vito, 89122 Reggio di Calabria (Italy).

[3] CREA-OFA - Council for Agricultural Research and Economics, Research Centre for Olive, Fruit and Citrus crops, 87036 Rende, Cosenza, Italy

[4] CNR- IPSP- Institute for the Sustainable Plant Protection -Area Della Ricerca, Via Madonna Del Piano 10, 50019, Sesto Fiorentino, Firenze, Italy

* Corresponding authors: mario.riolo@unict.it; olga.cacciola@unict.it.

4.1 Abstract

This study investigated the physiological and biochemical responses of three olive cultivars, 'Ottobratica', 'Dolce Agogia', and 'Leccino', to infection by four *Colletotrichum* species, *C. acutatum*, *C. gloeosporioides*, *C. godetiae*, and *C. karsti*, all commonly associated with olive fruit anthracnose but with diverse levels of virulence. Pathogenicity assays confirmed significant differences in disease susceptibility and virulence among cultivars and *Colletotrichum* species. 'Ottobratica' was the most susceptible to all *Colletotrichum* species, exhibiting a Disease Severity Index of 100% at 168 hours post-inoculation with *C. acutatum*, the most virulent among the species tested. 'Dolce Agogia' showed intermediate susceptibility, while 'Leccino' was the least susceptible. *C. karsti* was the least virulent. Chlorophyll a, chlorophyll b, and total carotenoid concentrations in olive drupes at different time intervals after inoculation revealed significant variations among cultivars. 'Dolce Agogia' exhibited the highest constitutive levels of the three photosynthetic pigments and the most relevant increase in their concentration following infection, whereas 'Leccino' showed the lowest, suggesting cultivar specificity in response

to infection. Analysis of oxidative stress markers, malondialdehyde (MDA) and hydrogen peroxide (H_2O_2), in olive drupes showed differential changes depending on cultivar and pathogen species. It revealed a strong oxidative burst in all cultivar/*Colletotrichum* species, particularly in 'Dolce Agogia' and in response to *C. acutatum*. This oxidative burst occurred earlier in drupes infected by the more virulent *C. acutatum* and *C. gloeosporioides*, while it was delayed in drupes infected by *C. godetiae* and *C. karsti*. Sugar levels also showed noticeable variations depending on cultivar and fungal species.

Key words: olive anthracnose; *Colletotrichum* spp.; olive cultivars; chlorophyll; carotenoids; lipid peroxidation; disease susceptibility/tolerance.

4.2 Introduction

Olive anthracnose (OA) is a major disease affecting olive (*Olea europaea* L.) crops in many olive-growing regions worldwide (Cacciola et al., 2012; Riolo et al., 2023b; Talhinhas et al., 2018; Talhinhas and Baroncelli, 2021). This disease is caused by several species of the genus *Colletotrichum*, mainly belonging to the *C. acutatum*, *C. boninense*, and *C. gloeosporioides* species complexes (Moral et al., 2021; Riolo et al., 2023b; Talhinhas et al., 2018). The severity of the damage caused to drupes by OA depends on various factors, including environmental conditions, the virulence of the *Colletotrichum* species involved, the amount of inoculum and the susceptibility of the olive cultivar (Cacciola et al., 2012; Riolo et al., 2023b; Talhinhas et al., 2015; Talhinhas et al., 2018). Indeed, previous studies have shown a significant variability in the susceptibility of different olive cultivars to OA (Moral et al., 2017). For instance, among Italian cultivars 'Leccino' exhibits relative resistance, whereas 'Ottobratica' is highly susceptible (Riolo et al., 2023b). Morever, an interaction has been also observed between olive cultivar susceptibility and *Colletotrichum* species virulence (Cacciola et al., 2012; Moral and Trapero, 2009; Riolo et al., 2023b; Talhinhas et al., 2015).

In general, the impact of biotic stresses, such as pathogen infections on photosynthesis has been well-documented across various plant species. Studies have shown that pathogens tend to induce a more pronounced decline in net photosynthesis (Pn) compared to other biotic stressors like insect herbivory, primarily due to the pathogen-induced reduction in stomatal conductance (gs), chlorophyll content and water transport impairment (Zhang et al., 2022). This decline in photosynthesis is often accompanied by an increase in dark respiration (Rd) and a reduction in carotenoids and other pigments,

exacerbating the oxidative damage caused by reactive oxygen species (ROS) (Zhang et al., 2022).

Photosynthetic pigments, such as carotenoids and chlorophylls, play crucial roles in plant responses to pathogen infections, especially carotenoids, including lutein and β-carotene, which function as both accessory pigments in photosynthesis and antioxidants, mitigating damage caused by ROS, such as hydrogen peroxide (H_2O_2) (Eloy et al., 2015; Maoka, 2020).

Chlorophylls, especially chlorophyll a, undergo a significant reduction during the development and ripening of olive fruit, while carotenoids degrade at a slower rate. This differential trend of degradation of the two types of pigments helps maintain some protective capacity against oxidative stress during pathogen outbreaks, as lutein and other carotenoids act as important scavengers of ROS (Criado et al., 2006). Furthermore, several studies have also shown that certain enzymes, such as chlorophyllase (Chlase) and lipoxygenase (Lox), play a role in pigment degradation during fruit maturation. These enzymes contribute to the breakdown of chlorophyll and the oxidation of fatty acids, further affecting the plant's ability to manage oxidative stress (Criado et al., 2006).

Among the various ROS, H_2O_2, plays a critical role in plant-pathogen interactions. It is often produced as part of the plant's defence mechanism, acting both as an antimicrobial agent and a signaling molecule to promote the hypersensitive responses (HR) and systemic acquired resistance (SAR). However, excessive H_2O_2 production can lead to cellular damage, promoting lipid peroxidation (Criado et al., 2006; Eloy et al., 2015). This balance between H_2O_2's defensive role and its potential for causing oxidative damage is crucial in determining the outcome of the pathogen infection. For example, studies on *Colletotrichum gloeosporioides* in cowpea plants showed that manipulating H_2O_2 levels can alter the pathogen's lifestyle from biotrophic to necrotrophic, influencing disease progression (Eloy et al., 2015). Similarly, Alkan and Fortes (2015) emphasized that fruit-specific metabolic adjustments strongly influence the outcome of fungal infections, highlighting the dual role of ROS in both signaling and damage.

Under environmental stress or developmental signals, ROS or lipoxygenases produce malondialdehyde (MDA) from the lipid peroxidation of polyunsaturated fatty acids (PUFAs). MDA is a small and reactive organic molecule that occurs ubiquitously among eukaryotes, whose levels are widely used as an indicator of damage in plant membranes. The increase of this aldehyde levels, leads to protein carbonylation, and this mechanism may either result in defense signaling if MDA accumulates transiently, or trigger cell

death if there is sustained accumulation of MDA and carbonylated proteins accumulate in the cells (Tagnon and Simeon, 2017).

However, if the elimination of MDA and redox signaling regulation work correctly, MDA increase may represent acclimation processes rather than damage, since MDA can exert a positive role by activating regulatory genes involved in plant defence and development acting as a protection mechanism rather than being an indicator of damage (Tounekti et al., 2011).

Sugars have an important role as energy and carbon sources and also have regulatory functions influencing all phases of the plant life cycle, both growth and development (Rolland et al., 2006). Several researches also reported that sugars are involved in plant defense responses to various abiotic and biotic stresses, enhancing the immune response against fungal pathogens (Bolouri Moghaddam and Van den Ende, 2012; Keunen et al., 2013; Morkounas andRatajczak, 2014; Rojas et al., 2014).

The aim of this study was to evaluate the physiological and biochemical response of the fruit of three olive cultivars, 'Ottobratica', 'Dolce Agogia', and 'Leccino' to the infection of various *Colletotrichum* species, examining in particular the changes in chlorophyll, carotenoid and sugar concentrations in fruits at different time intervals after inoculation, along with oxidative stress indicators, such as MDA and H_2O_2 levels.

4.3 Material and methods

4.3.1 Plant material and experimental design

Olive drupes from three cultivars of *Olea europaea* L., with different susceptibility to olive anthracnose (Riolo et al., 2023b), 'Leccino', 'Ottobratica' and 'Dolce Agogia', were included in this study. Drupes were collected from 15-year-old olive trees at a medium ripening stage (MI 3-4) (Guzmán et al., 2015). Before inoculation, drupes were surface disinfected by immersion in a 0.5% NaOCl solution for 30 seconds, rinsed in sterile distilled water (SDW), blotted dry, and placed in incubation trays. Olives were punctured with a sterile needle at an equatorial position, and a 10 µl droplet of the conidial suspension (10^6 conidia/ml), prepared as described in the next sub-section, was pipetted onto the surface of the wound. Controls received a 10 µl droplet of SDW. Overall, 225 drupes per cultivar x *Colletotrichum* species, including the controls, were inoculated. After inoculation, drupes were incubated for 7 days in a humid chamber at 23 ± 1°C, with a photoperiod of 16 hours of light and 8 hours of dark, and 80% relative humidity. Symptom severity on inoculated drupes was rated daily using an empirical scale from 0 to 6 (Riolo et al., 2023a; Riolo et al., 2023b) where 0= no symptoms; 1= mycelium only; 2= small

necrosis (<5 mm diameter) and absence of sporulation; 3= large necrosis (>5 mm diameter) and absence of sporulation; 4= few spore masses on the inoculation point; 5= abundant spore masses expanding around the inoculation point; 6= spore masses entirely covering the fruit. The disease severity index (DSI) was calculated for each replication using the following formula: $DSI = [(\Sigma ni \times i)/ (N \times 6)] \times 100$, where i represents the severity (0–6), ni is the number of fruits with the severity i, and N is the total number of fruits (Varveri et al., 2024). For metabolomic analysis, flesh fragments (± 5 mm diameter) were sampled from inoculated olives at four different time intervals: 24, 72, 120, and 168 hours post-inoculation (hpi). Fragments were excised from around the inoculation site and transferred into 2 ml Eppendorf tubes (three fragments from three distinct olives of the same batch per tube). Each combination of cultivar and pathogen was assigned a unique code, as detailed in Table 1.

Table 1. Experimental setup for the inoculation of *Olea europaea* cultivars ('Dolce Agogia', 'Ottobratica', and 'Leccino') with four *Colletotrichum* species at different time points post-inoculation. The codes represent the combination of cultivar, pathogen, and time point."

Time intervals post inoculation (hours)	*Colletotrichum* species and controls	Olive cultivars and codes		
		'Dolce agogia'	'Ottobratica'	'Leccino'
24	*Colletotrichum acutatum*	DaCa1	OtCa1	LcCa1
72	*C. acutatum*	DaCa2	OtCa2	LcCa2
120	*C. acutatum*	DaCa3	OtCa3	LcCa3
168	*C. acutatum*	DaCa4	OtCa4	LcCa4
24	*C. gloeosporioides*	DaCg1	OtCg1	LcCg1
72	*C. gloeosporioides*	DaCg2	OtCg2	LcCg2
120	*C. gloeosporioides*	DaCg3	OtCg3	LcCg3
168	*C. gloeosporioides*	DaCg4	OtCg4	LcCg4
24	*C. godetiae*	DaCg01	OtCg01	LcCg01
72	*C. godetiae*	DaCg02	OtCg02	LcCg02

120	*C. godetiae*	DaCg03	OtCg03	LcCg03
168	*C. godetiae*	DaCg04	OtCg04	LcCg04
24	*C. karsti*	DaCk1	OtCk1	LcCk1
72	*C. karsti*	DaCk2	OtCk2	LcCk2
120	*C. karsti*	DaCk3	OtCk3	LcCk3
168	*C. karsti*	DaCk4	OtCk4	LcCk4
24	Control (sdw)*	DaCrt1	OtCrt1	LcCrt1
72	Control (sdw)	DaCrt2	OtCrt2	LcCrt2
120	Control (sdw)	DaCrt3	OtCrt3	LcCrt3
168	Control (sdw)	DaCrt4	OtCrt4	LcCrt4

*Sterile distilled water

4.3.2 Fungal isolates and inoculum

Isolates of four different *Colletotrichum* species, *C. acutatum* (C9D2C isolate), *C. gloeosporioides* (RD9B isolate), *C. godetiae* (OLP12 isolate) and *C. karsti* (C12D1A isolate), were used in this study. The isolates were identified molecularly in previous studies (Faedda et al., 2011; Riolo et al., 2023a; Riolo et al., 2023b). All isolates included in this study were sourced from the culture collection of the Molecular Plant Pathology Laboratory of the Department of Agriculture, Food and Environment of the University of Catania, Italy. A conidial suspension of each isolate (10^6 conidia ml^{-1}) in sterile distilled water (SDW) was prepared from 10-day old cultures in potato dextrose agar (PDA; Oxoid Ltd., Basingstoke, UK) and used as inoculum. The inoculum concentration of each isolate tested was quantified using a Neubauer chamber (BLAUBRAND®, Merck KGaA, Darmstadt, Germany).

4.3.3 Determination of photosynthetic pigments content

Three independent aliquots (500 mg) were homogenized (500 mg) of olive tissue ground in liquid nitrogen was homogenized with inert sand, in 5 ml of 95% EtOH (Merck) with mortar and pestle. Each homogenate was independently centrifuged at 15,000 rpm for 15 min twice. The supernatant was separated collected and 0.05ml were mixed with 0.95 ml of 95% ethanol in a test tube. The solution mixture was analyzed for Chlorophyll-a (Chl-

a), Chlorophyll-b (Chl-b) and Carotenoids (Cart) content by a UV-VIS spectrophotometer (Agilent Cary 3500 UV-Vis Multicell) at 664 nm, 649 nm, and 470 nm wavelength in a 1 mL cuvette. The equations used for the quantification of Chl-a, Chl-b and Cart are reported in the table 2 (Lichtenthaler, 1987).

Table 2. Equations used to calculate the concentration (µg/ml) of chlorophyll a (Ch-a). chlorophyll b (Ch-b) and carotenoids (Cart).

Solvent	Equations/Formula
95% Ethanol	Ch-a=13.36A664 – 5.19 A649
	Ch-b=27.43A649 – 8.12 A664
	Cart=(1000A470 –2.13Ca - 97.63Cb)/209

Note: A=Absorbance at

4.3.4 Determination of lipid peroxidation

Lipid peroxidation as malondialdehyde (MDA) equivalent was determined via the reaction of thiobarbituric acid (TBA) as described by Hodges et al. (1999) . Briefly, three independent aliquots (500 mg) of ground olive biomass were homogenized with inert sand in 1:25 (g FW:mL) of a 80:20 (v:v) ethanol:water solution with mortar and pestle. After centrifugation at 15,000 g for 10 min, 1 mL of supernatant was added to a test tube with 1 mL of either (i) -TBA, 20.0% (w/v) trichloroacetic acid solution, or (ii) +TBA solution containing the above plus 0.65% TBA. The mixtures were heated at 95 °C for 25 min. After centrifugation at 15,000 g for 5 min, the absorbance of the samples was recorded at 440, 532, and 600nm in a 1mL cuvette by a UV-VIS spectrophotometer (Agilent Cary 3500 UV-Vis Multicell). The MDA concentration was calculated in mg/mL using the following equations as in Hodges et al. (1999):

1) $[(Abs\ 532_{+TBA}) - (Abs\ 600_{+TBA}) - (Abs\ 532_{-TBA} – Abs\ 600_{-TBA})] = A$

2) $[(Abs\ 440_{+TBA} - Abs\ 600_{+TBA})\ 0.0571] = B$

3) MDA equivalents (nmol * mL^{-1}) = (A-B) /157.000) 10^6

4.3.5 Hydrogen peroxide analysis

Hydrogen peroxide (H_2O_2) content was determined following the method of Catola et al., (2016), with slight modifications. Briefly, olive tissue samples (0.25 g) were homogenized in 3 mL of 5% trichloroacetic acid (TCA) at 4°C. The homogenate was then centrifuged at 12,000g for 15 minutes. For the assay, a 0.5 mL aliquot of the supernatant was mixed with

0.5 mL of 10 mM potassium phosphate buffer (pH 7.0) and 0.75 mL of 1 M potassium iodide (KI). Absorbance was measured at 390 nm in a 1mL cuvette by a UV-VIS spectrophotometer (Agilent Cary 3500 UV-Vis Multicell). H_2O_2 content was calculated by comparing the relative absorbance (sample absorbance minus that of a control sample without KI) against a standard curve prepared using known concentrations of H_2O_2. Results were expressed as nmol/mL of extract.

4.3.6 Total carbohydrate assay

The total carbohydrate content was determined using the phenol-sulfuric acid method according to Dubois et al. (1956), using D+ glucose as a standard.

4.3.7 Statistical analysis

Statistical analysis was conducted using R software (version 4.3.1) to assess the significance of differences in the values of photosynthetic pigments (Chl-a, Chl-b, carotenoids), malondialdehyde (MDA), and hydrogen peroxide (H_2O_2) content in olive drupes across different pathogen infections and olive cultivars. Tukey's honestly significant difference (HSD) test was applied to analyze these values, and bar plots were generated to visualize the results. Statistical significance was calculated to compare the effects of pathogen infection on each cultivar.

Metabolomic data analysis was also performed using R software. Data were grouped by variety and pathogen, and mean values for each metabolite were calculated across replicates using the dplyr package. This averaging reduced individual sample variability and provided representative metabolomic profiles for each variety-pathogen combination. To mitigate the influence of different scales among metabolites and ensure equal contribution to the analyses, the averaged metabolite data were normalized by centering and scaling each variable using the scale function. For data visualization and pattern recognition, two complementary analyses were performed: hierarchical clustering with heatmap visualization and Principal Component Analysis (PCA).

A heatmap was generated using the pheatmap package to visualize patterns of metabolite accumulation across the different variety-pathogen combinations. Hierarchical clustering was applied to both samples (rows) and metabolites (columns), facilitating the identification of groups with similar metabolomic profiles. The heatmap utilized a reversed "RdYlBu" (Red-Yellow-Blue) color palette from the RColorBrewer package to represent metabolite concentration levels, with colors transitioning from blue (low concentration) to red (high concentration). This visual representation highlighted

distinct patterns and enabled the identification of clustering patterns among samples and metabolites.

Additionally, PCA was performed using the prcomp function to explore the main sources of variation in the metabolomic data. The analysis was conducted on the normalized, averaged metabolite data without the grouping variables (variety and pathogen). The proportion of variance explained by each principal component was calculated to interpret the importance of each component. The PCA results were visualized using ggplot2, plotting the first two principal components (PC1 and PC2). Samples were represented as points, with colors indicating the variety and shapes indicating the pathogen treatment or the control without pathogen infection. Custom colour schemes and shape symbols were defined for each variety and pathogen using manual scales in ggplot2. The PCA provided insights into the relationships between samples based on their metabolite composition, facilitating the identification of key factors contributing to variations in the data.

4.4 Results

4.4.3 Pathogenicity assays

Pathogenicity assays confirmed significant differences in susceptibility to the infection of *C. acutatum*, *C. gloeosporioides*, *C. godetiae*, and *C. karsti* among olive cultivars ('Ottobratica', 'Dolce Agogia', and 'Leccino') (Figure 1). Whereas, the four *Colletotrichum* species in turn showed noticeable differences in virulence. Among the tested cultivars, 'Ottobratica' was the most susceptible to *C. acutatum*, with the Disease Severity Index (DSI) reaching a maximum of 100% at 168 hours post-inoculation (hpi). 'Leccino' inoculated with this *Colletotrichum* species showed the lowest DSI values throughout the infection period examined with a final DSI value of 45 % at 168 hpi, demonstrating to be resistant in comparison with the other two cultivars. 'Dolce Agogia' exhibited an intermediate susceptibility between the other two cultivars, with a DSI value of 82% at 168 hpi. A similar pattern was observed in drupes inoculated with *C. gloeosporioides*, with final (at 168 hpi) DSI values of 83%, 50% and 7% for 'Ottobratica', 'Dolce Agogia' and 'Leccino', respectively. Drupes of 'Ottobratica' inoculated with *C. godetiae* showed a DSI of 45% at 168 hpi while drupes of both 'Dolce Agogia' and 'Leccino' inoculated with this *Colletotrichum* species showed very low final DSI values (7 % and 10%, respectively). No significant difference was observed among the final values of DSI in the drupes of the three olive cultivars inoculated with *C. karsti*. This *Colletotrichum* species was confirmed to

be weakly virulent on olive drupes, with final values of 21 % for both 'Ottobratica' and 'Dolce Agogia' and 7%, for 'Leccino'

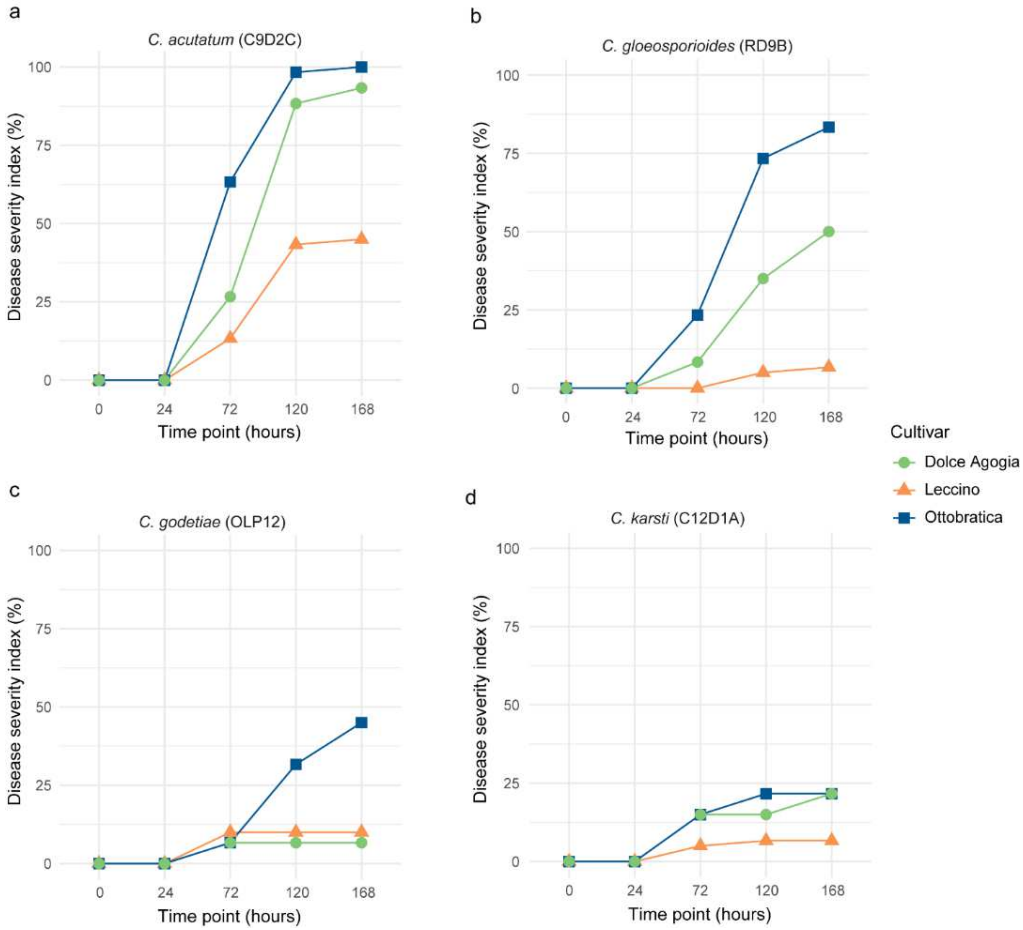

Figure 1. Mean values of disease severity index (DSI) in the drupes of 'Ottobratica', 'Dolce Agogia' and 'Leccino' inoculated with four *Colletotrichum* species, at progressive time intervals post inoculation (in hours).

4.4.4 Photosynthetic pigment analysis

The analysis of photosynthetic pigments reveals notable variations in chlorophyll a, chlorophyll b, and total carotenoid content depending on the olive cultivar, the time interval after inoculation and the *Colletotrichum* species involved. As regards chlorophyll a, drupes of 'Dolce Agogia' showed higher intrinsic values compared to the drupes of 'Leccino' and 'Ottobratica' (Fig, 2a). Moreover, drupes of this cultivar inoculated with *C. acutatum* showed a significant increase in chlorophyll a content compared to the control since 24 hpi (T1), with a peak (2.22 mg/mL) at 72 hpi (T2) (Fig. 2a-1). At T2 chlorophyll a content increased also in drupes inoculated with *C. godetiae*, *C. gloeosporioides* and *C. karsti*. The highest values of chlorophyll a (2.22 and 1.96 mg/mL, respectively) were

observed in drupes inoculated with *C. acutatum* and *C. gloeosporioides* (Fig. 2a-1). At 120 and 168 hpi (T_3 and T_4, respectively) chlorophyll a content in drupes inoculated with all *Colletotrichum* species remained higher than in control, with the only exception of drupes inoculated with *C. gloeosporioides* at T_3 (Fig. 2a-1). In general, however, the absolute values showed a progressive decline (Fig. 2a-1). No particular trend in chlorophyll a content was observed in drupes of the other two olive cultivars,'Ottobratica' (Fig.2a-2) and 'Leccino' (Fig.2a-3) characterized by an inherently lower chlorophyll a content than 'Dolce Agogia', as a consequence of the infection with *Colletotrichum*. As regards chlorophyll b, 'Dolce Agogia' drupes again exhibited the highest content compared to the other cultivars (Fig. 2 b). With few exceptions, chlorophyll b content in drupes inoculated with *Colletotrichum* was higher than in the respective control throughout the entire infection process (from T_1 to T_4), irrespective of the cultivar and the *Colletotrichum* species. The highest peak of chlorophyll b content for 'Dolce Agogia' (5.44 mg/mL) was detected at T_2 in drupes inoculated with *C. acutatum* (Fig. 2b-1) while the highest peaks for 'Ottobratica' (2.73 mg/mL) and 'Leccino' (2.18 mg/mL) were detected in drupes also inoculated with *C. acutatum* at T_3 and T_2, respectively, suggesting a possible relationship between the virulence of *Colletotrichum* species and the production of this pigment (Figs. 2b-2 and 2b-3). Similarly to what was observed for chlorophyll a and b, in general the total carotenoid content in the drupes of 'Dolce Agogia' was higher than in the drupes of 'Ottobratica' and 'Leccino' (Fig. 2c). At T_1 and T_2, i.e. in the initial phases of infection process, the total carotenoid content of 'Dolce Agogia' drupes inoculated with *Colletotrichum* was significantly ($p \leq 0.05$) higher than the control, irrespective of the *Colletotrichum* species involved. At T_1, control drupes of 'Dolce Agogia' exhibited a total carotenoid content of 3.573 mg/mL, drupes inoculated with *C. acutatum* showed a significantly ($p \leq 0.05$) higher content than the control, with a value of 6.437 mg/mL, followed by those inoculated with *C. godetiae* and *C. gloeosporioides*, with values of 5.304 mg/mL and 5.558 mg/mL, respectively, while total carotenoid content of drupes inoculated with *C. karsti* was significantly lower than the control, with a value of 0.219 mg/mL (Fig. 2c-1). The highest peak (10.869 mg/mL) was observed at T_2 in drupes inoculated with *C. gloeosporioides*. In the successive phases of the infection process (T_3 and T_4) the total carotenoid content of 'Dolce Agogia' drupes inoculated with the three more virulent *Colletotrichum* species, *C. acutatum*, *C. gloeosporioides* and *C. godetiae*, declined sharply, while it remained high (6.28 and 4.76 mg/mL at T_3 and T_4, respectively) in drupes inoculated with *C. karsti* (Fig. 2c-1).

No particular trend in total carotenoid content was observed in 'Ottobratica' and 'Leccino' drupes during the infection process (Figs. 2c-2 and 2c-3).

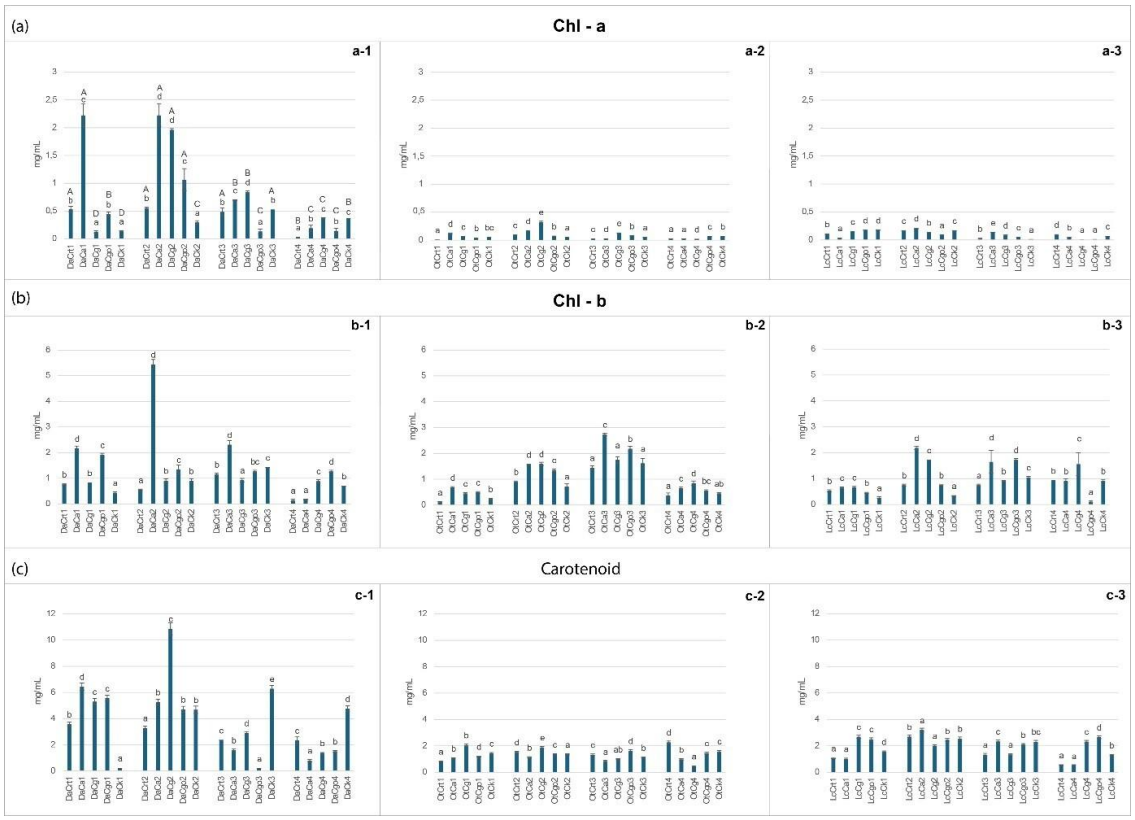

Figure 2. Mean content of chlorophyll a (a-1, a-2, a-3), chlorophyll b (b-1, b-2, b-3), and total carotenoids (a-1,a-2,a-3) in the drupes of three olive cultivars, 'Dolce Agogia' (Da), 'Ottobratica' (ot) and 'Leccino (Lc), inoculated with different *Colletotrichum* species at progressive time intervals after inoculation (24, 72, 120 and 168 hours post-inoculation). The values are presented as mean concentrations (mg/mL). Values for each treatment sharing a common letter are not statistically different according to Tukey's honestly significant difference (HSD) test ($p \leq 0.05$).

4.4.5 MDA and H_2O_2 analysis

The analysis of malondialdehyde (MDA) and hydrogen peroxide (H_2O_2) levels in fruit of the three olive cultivars at progressive time intervals (24, 72, 128, and 168 hpi, T1, T2, T3 and T4, respectively) after inoculation with diverse *Colletotrichum* species revealed significant variations indicative of transient oxidative stress responses as a consequence of inoculation, which varied depending on the cultivar and the *Colletotrichum* species involved (Figure 3).

At T1, 'Dolce Agogia' drupes inoculated with all four *Colletotrichum* species showed MDA levels significantly ($p \leq 0.05$) higher than the control (Fig. 3a-1). In particular, drupes inoculated with *C. acutatum* exhibited a peak (3.23 MDA equivalents/mL of extract) of MDA level significantly higher compared to both the control and the MDA level of drupes inoculated with other *Colletotrichum* species (Figure 3a-1), indicating a rapid oxidative response following infection by this virulent *Colletotrichum* species. Also, drupes inoculated with *C. gloepsporioides* exhibited a peak of MDA level (2.90 equivalents/mL of extract) at T1. However, at T2 MDA level of both groups of drupes dropped sharply exhibiting values (0.97 and 0.94 equivalents/mL, respectively) significantly ($p \leq 0.05$) lower than the control (Fig. 3 a-1). Conversely, MDA level of drupes inoculated with *C. godetiae* reached its maximum (2.04 equivalents/mL) at T2, while MDA level of drupes inoculated with *C. karsti* increased progressively up to T3, reaching a maximum of 3.46 equivalents/mL (Fig. 3a-1). The MDA level of drupes inoculated with *C. gloeosporioide*s showed a second peak (2.31 equivalents/mL) at T3. However, in an advanced stage of infection process, at T4, only MDA levels of drupes inoculated with *C. acutatum* and *C. karsti* were still significantly higher than the control (Fig. 3 a-1).

The MDA level of 'Ottobratica' drupes inoculated with the four *Colletotrichum* species remained lower than or equal to that of the control throughout the infection process (Fig. 3 a-2), suggesting no substantial oxidative response occurred in drupes of this cultivar as a consequence of the infection. Also, MDA level of 'Leccino' drupes inoculated with the four *Colletotrichum* species remained lower than or equal to that of the control, but only initially (T1) (Fig. 3 a-3). At T2 (72 hpi), all four groups of drupes, each inoculated with a diverse *Colletotrichum* species, showed significantly ($p \leq 0.05$) higher MDA levels than the control. Maximum value (0.61 equivalents/mL) was detected in drupes inoculated with *C. acutatum*. Subsequently, MDA levels declined progressively in all four groups of inoculated drupes but at T3 they were still significantly ($p \leq 0.05$) higher than in control, with the only exception of the group inoculated with *C. gloeosporioides* (Fig. 3 a-3). Maximum value (1.13 equivalents/mL) was detected in drupes inoculated with *C. karsti*. At T4, only drupes inoculated with *C. karsti* showed a MDA level (0.81 equivalents/mL) higher than that of the control, indicating a prolonged oxidative stress as a consequence of the infection by this *Colletotrichum* species (Fig. 3 a-3).

As regards H_2O_2 accumulation, significant ($p \leq 0.05$) differences were noticed between inoculated drupes and the respective controls (Fig. 3b). However, the trend of H_2O_2 accumulation in drupe tissues during the infection process varied greatly depending on both the olive cultivar and the *Colletotrichum* species involved. As for 'Dolce Agogia' only

drupes inoculated with *C. acutatum* and *C. gloeosporioides* exhibited significant higher levels (9.58 and 16.13 nmol/mL, respectively) compared to the control (8.90 nmol/mL) at T1, indicating an early oxidative stress as a consequence of the infection by these two species of *Colletotrichum*. The same trend, but with a reduced value for drupes inoculated with *C. gloeosporioides* and *C. acutatum* (10.58 and 9.53 nmol/mL) was observed at T2 (Fig. 3 b-1). The level of H_2O_2 declined progressively in drupes inoculated with *C. gloeosporioides* but increased in drupes inoculated with the other three *Colletotrichum* species, particularly in drupes inoculated with *C. godetiae*, and at T3 it was significantly higher than in control in all inoculated drupes, except those inoculated with *C. gloeosporioides* (Fig. 3 b-1). Maximum value (16.52 nmol/mL) was observed in drupes inoculated with *C. godetiae*. However, at T_4, all groups of drupes inoculated with *Colletotrichum*, including also those inoculated with *C. gloeosporioides*, showed a significantly higher level of H_2O_2 than the control (Fig. 3 b-1). Maximum value (16.60 nmol/mL) was observed in drupes inoculated with *C. karsti.* As for 'Ottobratica', the level of H_2O_2 in all inoculated drupes was significantly ($p \leq 0.05$) higher than the control throughout the infection process (from T1 to T_4) and irrespective of the *Colletotrichum* species (Fig. 3 b-2), indicating both an early and prolonged oxidative burst as a consequence of the infection by *Colletotrichum* in this cultivar very susceptible to anthracnose. As for the level of H_2O_2 in drupes of 'Leccino', it was both substantially and constantly higher than in control throughout the entire infection process in drupes inoculated with *C. acutatum* (varying from 16.71 nmol/mL at T_4 to 18.26 nmol/mL at T_4) (Fig. 3 b-3) . Conversely, it showed a bimodal trend in drupes inoculated with *C. gloesporioides* and *C. karsti* . The H_2O_2 level in drupes inoculated with each of these two species was significantly ($p \leq 0.05$) lower than the control at T1 and T3 and significantly ($p \leq 0.05$) higher than the control at T2 and T_4, varying from 7.16 nmol/mL at T3 to 19.62 nmol/mL at T2 for *C. gloeosporioides* and from 7.78 nmol/mL at T1 to 15.31 nmol/mL at T2 for *C. karsti*. In drupes inoculated with *C. godetiae* it was significantly ($p \leq 0.05$) higher than the control at T1, T2 and T_4 (9.13, 7.43 and 8.6 nmol/mL, respectively) while did not differ significantly from the control at T3 (9.53 nmol/mL).

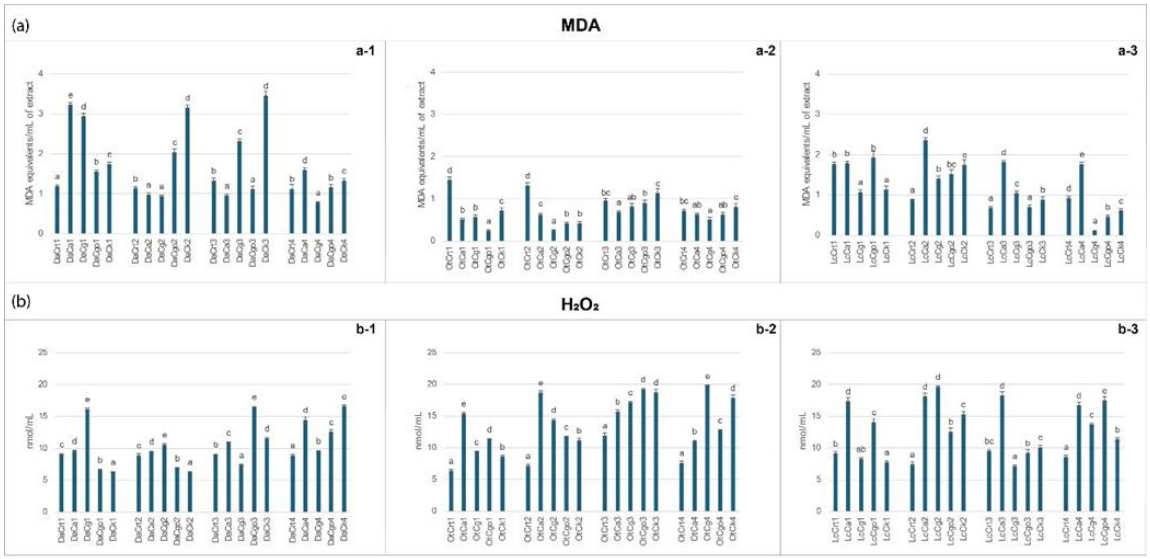

Figure 3. Mean content of malondialdehyde (MDA) (a-1, a-2, a-3) and hydrogen peroxide (H_2O_2) in the drupes of three olive cultivars inoculated with different *Colletotrichum* species at four progressive time intervals after inoculation (24, 72, 120 and 168 hours post-inoculation). The values are presented as mean concentrations (MDA equivalents/mL extract and nmol/mL, respectively). Values for each treatment sharing a common letter are not statistically different according to Tukey's honestly significant difference (HSD) test ($p \leq 0.05$).

4.4.6 Total carbohydrates analysis

The analysis of total carbohydrates in fruit of the three olive cultivars at progressive time intervals after inoculation (24, 72, 128, and 168 hpi, T1, T2, T3 and T4, respectively) with the three different *Colletotrichum* species revealed different responses as a consequence of inoculation, depending on the cultivar and the *Colletotrichum* species involved (Figure 4). At T1, 'Dolce Agogia' drupes inoculated with *C. acutatum* (DaCa1) showed carbohydrates levels significantly ($p \leq 0.05$) higher (9875 mg/L) than the control (7017 mg/L) (Fig. 4a-1). Conversely, the values decreased when drupes were inoculated with *C. godetiae* and *C. gloepsporioides* or remained similar to those measured in the control after inoculation with *C. karsti*, the less susceptible fungi species. At T1 total sugars in 'Leccino' (Fig. 4a-2) decreased after inoculation with *C. acutatum*, showed similar values after inoculation with *C. gloepsporioides* (LeCg1) and increased after inoculation with *C. godetiae* and *C. karsti* when compared with the control. No modulation of total carbohydrates was observed in 'Ottobratica' (Fig. 4a-3), except a slight increase after inoculation with *C. godetiae* (Otg04).

Interesting, at T2 the carbohydrates level in 'Dolce Agogia' shoed values similar to the control when the drupes were inoculated with all the fungi species, expect the noticeable

increase observed after *C. godetiae* inoculation. Only the most virulent species *C. acutatum* triggered a noticeable increase of the values in 'Leccino', whereas decreased of the carbohydrates levels were recordered in 'Ottobratica' after inoculation with all the fungi species.

At T_3 and T_4 in 'Dolce Agogia', the total carbohydrates were lower than the respective control after inoculation with all the fungi species except the values similar to the respective control at T_4 after inoculation with *C. godetiae* and *C. gloepsporioides*. 'Leccino' showed increase of the values at T_3 after inoculation of all the species except *C. acutatum*, and values similar to the respective control at T_4 after inoculation with all the fungi species. At T_3, in 'Ottobratica' the carbohydrate concentration significantly dropped respect to the control after inoculation with *C. acutatum* *C. gloepsporioides* and *C. karsti*, and increased when infected by *C. godetiae*. Conversely, at T_3 the levels in 'both 'Dolce Agogia' and 'Leccino' infected by *C. godetiae* dropped respect to the control suggesting a species specific response mechanism of both the drupe variety and fungi species. At T_4 'Ottobratica' showed a slight decrease of the carbohydrates levels respect to the control irrespective of the fungi species

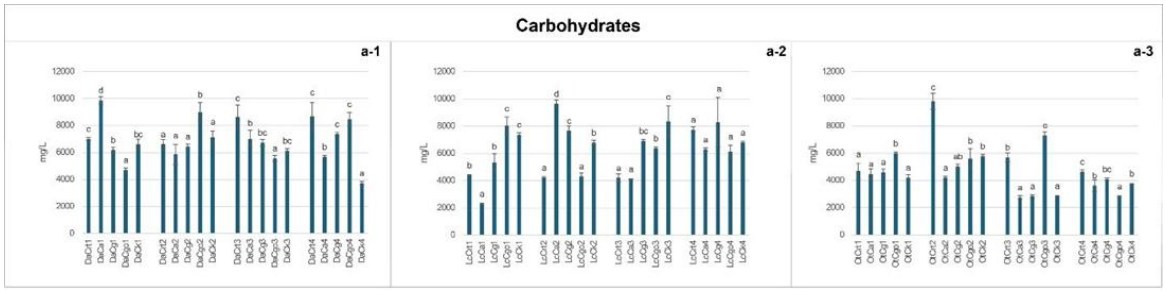

Figure 4. Mean content of carbohydrates (a-1, a-2, a-3) in the drupes of three olive cultivars inoculated with different *Colletotrichum* species at four progressive time intervals after inoculation (24, 72, 120 and 168 hours post-inoculation). The values are presented as mean concentrations (mg/L, fresh weight). Values for each treatment sharing a common letter are not statistically different according to Tukey's honestly significant difference (HSD) test ($p \leq 0.05$).

4.4.7 Heatmap and PCA analysis of metabolic profiles

The analysis and representation of data using the semi-quantitative heatmap method (Fig. 5) made it possible to compare synoptically the metabolic profiles of drupes of the three olive cultivars ('Dolce Agogia', 'Leccino' and 'Ottobratica') inoculated with the four *Colletotrichum* species at progressive time intervals post-inoculation (T_1, T_2, T_3 and T_4).

At T_1 (24h), the metabolic profiles of the three olive cultivars 'Dolce Agogia,' 'Leccino,' and 'Ottobratica' showed distinct responses to *Colletotrichum* infections, highlighting early-stage physiological adjustments (Fig. 5-a).

In 'Dolce Agogia,' *C. acutatum* (DaCa1) induced the most pronounced metabolic changes, characterized by a strong increase in chlorophyll a (Chl-a), as well as elevated levels of chlorophyll b (Chl-b), malondialdehyde (MDA), carbohydrates, and carotenoids. Infection with *C. gloeosporioides* (DaCg1) led to a moderate increase in H_2O_2, MDA, and carotenoids, indicating the onset of oxidative stress. *C. godetiae* (DaCg01) infection resulted in an accumulation of chlorophyll b and carotenoids. Conversely, *C. karsti* (DaCk1) did not trigger significant metabolic changes compared to the control, suggesting a weaker initial metabolic response. In 'Leccino,' *C. acutatum* (LcCa1) infection showed marked increase in H_2O_2 levels and a strong reduction in carbohydrate content. Infection with *C. godetiae* (LcCg01) led to a slight increase in H_2O_2, MDA, and carbohydrate levels, suggesting a moderate stress response, while *C. gloeosporioides* (LcCg1) and *C. karsti* (LcCk1) did not induce substantial metabolic changes.

In 'Ottobratica,' none of the *Colletotrichum* infections caused major metabolic shifts compared to the control, except for a slight increase in H_2O_2 levels in drupes infected with *C. acutatum* (OtCa1), indicating a delayed stress response.

At T2 (72h), the metabolic profiles of the cultivars evolved, reflecting different adaptive strategies (Figure 5-b). In 'Dolce Agogia,' *C. acutatum* (DaCa2) maintained elevated levels of chlorophyll a and b, while MDA, carbohydrate, and carotenoid levels decreased, suggesting a transition from an acute stress response toward metabolic stabilization. Infection with *C. gloeosporioides* (DaCg2) resulted in a significant increase in carotenoid levels and a slight rise in chlorophyll b, whereas H_2O_2 and MDA levels declined, indicating a potential metabolic rebalancing. *C. godetiae* (DaCg02) maintained a stable metabolic profile, with a reduction in H_2O_2 levels. In contrast, *C. karsti* (DaCk2) triggered a pronounced increase in MDA levels alongside a reduction in H_2O_2, highlighting a shift towards lipid peroxidation rather than oxidative stress regulation.

In 'Leccino,' *C. acutatum* (LcCa2) infection caused an increase in carbohydrate and MDA levels, while H_2O_2 levels showed a slight reduction, suggesting the progression of an oxidative stress response. Infection with *C. gloeosporioides* (LcCg2) led to a slight increase in H_2O_2, whereas *C. karsti* (LcCk2) did not significantly alter the metabolic profile, indicating a minimal metabolic impact.

In 'Ottobratica,' metabolic changes remained relatively limited across all treatments. However, compared to T1, control samples exhibited a decrease in H_2O_2 levels and an increase in carbohydrate content, suggesting a natural metabolic adjustment rather than a pathogen-induced effect.

At T3 (120h), the most relevant results were very high levels of MDA and carotenoids in 'Dolce Agogia' drupes inoculated with *C. karsti* and relatively high levels of MDA, carotenoids and chlorophyll a in drupes of this cultivar inoculated with *C. gloeosporioides*, indicating a delayed stress response to infection (Fig.5-c). Conversely, levels of chlorophyll a, chlorophyll b and total carotenoids exhibited by drupes of 'Dolce Agogia' inoculated with *C. acutatum* at T1 and T2 declined, indicating the stress response noticed in the initial stages of infection was subsiding. Moreover, it was registered a moderately high level of H_2O_2 in 'Ottobratica' drupes infected by *C. acutatum*, *C. gloeosporioides*, *C. godetiae* and *C. karsti* as well as in 'Leccino' drupes infected by *C. acutatum*. Drupes of 'Ottobratica' infected by *C. acutatum* and *C. godetiae* also showed relatively high levels of chlorophyll b.

At T_4 (168h), the overall picture was further complicated by the presence of moderately elevated levels of stress markers, which were also present in non-inoculated drupes (controls), possibly due to a process of tissue senescence. Significantly elevated levels of stress markers, including chlorophyll a, MDA, carotenoids and H_2O_2, were detected in 'Dolce Agogia' drupes infected with *C. karsti*. In addition, high levels of other stress markers appeared sporadically across different treatments. For example, high concentrations of MDA were observed in 'Dolce Agogia' and 'Leccino' drupes infected with *C. acutatum*, and high levels of chlorophyll a and b were recovered in 'Dolce Agogia' and 'Leccino' drupes infected with *C. gloeosporioides*, respectively. The level H_2O_2 were also elevated in 'Ottobratica' drupes infected with *C. gloeosporioides* (Fig 5-d).

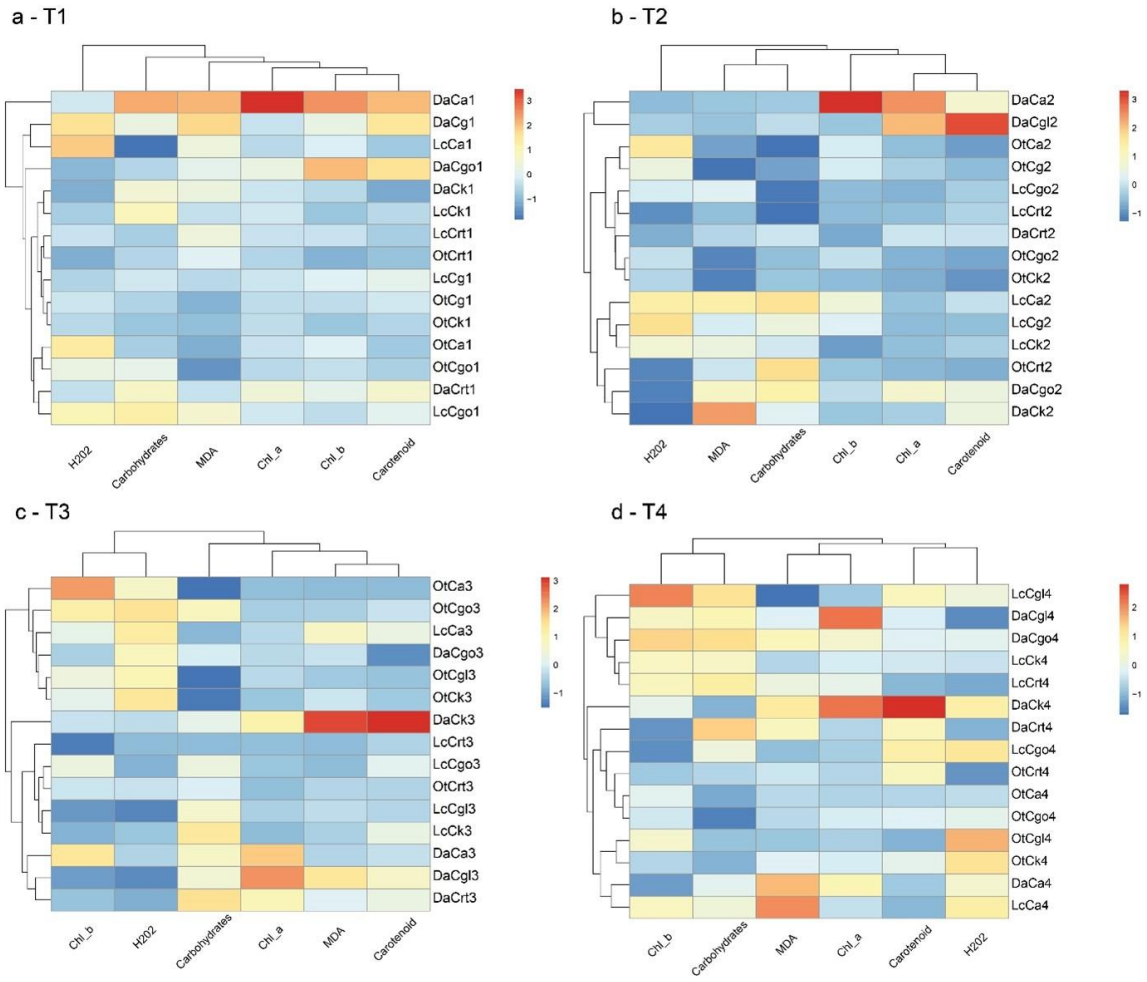

Figure 5. Heat maps of the chlorophyll a, chlorophyll b, carotenoids, H2O2 e MDA produced on drupes of 'Ottobratica' (Ot), 'Dolce Agogia' (Da) and 'Leccino' (Lc) inoculated with four Colletotrichum species. Colors indicate the relative abundance (logarithmic scale) of pigments, H2O2 and MDA produced in each olive cultivar x Colletotrichum species combination during the infection process, at different time intervals after inoculation (T_1, T_2 and T_3, T_4 corresponding to 24, 72, 120 and 168 hours post inoculation, respectively). Red and blue colours represent high and low abundance,

respectively. Drupes inoculated with SDW of each cultivar at T1, T2, T3 and T4 were included as controls.

The metabolic profiles of 'Dolce Agogia', 'Leccino' and 'Ottobratica' drupes inoculated with four *Colletotrichum* species at four time intervals post-inoculation (T1 =24 hours; T2 = 72 hours; T3 = 120 hours; T4 = 168 hours) were analysed using PCA. The PCA results elucidated the dynamic responses of the olive cultivars to pathogen inoculation over time (Figure 6).

At T1 (24 hours), PCA analysis revealed a metabolic differentiation among the inoculated olive cultivars, with PC1 accounting for 57.39% of the total variance and PC2 explaining 19.03%, summing up to 76.42%. This variance suggests an early metabolic response to *Colletotrichum* infection. Notably, 'Dolce Agogia' drupes inoculated with *C. acutatum* and *C. gloeosporioides* clustered separately from the other samples along the principal components, suggesting a distinct metabolic response to infection. This was further evidenced by the broader dispersion of these infected samples along PC1 and PC2 compared to the control (non-inoculated 'Dolce Agogia' drupes). These findings indicate that the presence of the pathogen influenced the metabolic profile as early as 24 hours after inoculation. In contrast, 'Leccino' and 'Ottobratica' drupes displayed a more moderate distribution along PC1 and PC2, suggesting a less pronounced yet detectable metabolic response (Fig.6-a). At T2 (72 hours), PCA analysis revealed a redistribution of metabolic profiles, with PC1 explaining 37.36% of the total variance and PC2 accounting for 27.08%, summing up to 64.44%. Compared to T1, the overall separation among the inoculated cultivars appeared to decrease, suggesting a trend toward partial metabolic convergence over time. However, 'Dolce Agogia' drupes inoculated with *C. acutatum* and *C. gloeosporioides* remained distinguishable, albeit with a reduced dispersion along PC1. Additionally, 'Dolce Agogia' drupes inoculated with *C. karsti* and *C. godetiae* showed a separation from the control, suggesting a pathogen-specific metabolic rearrangement. In contrast, the metabolic profiles of 'Leccino' and 'Ottobratica' tended to move closer to those of the control, suggesting a less pronounced metabolic response compared to 'Dolce Agogia' (Fig. 6-b).

At T3 (120 hours), PCA analysis revealed a new reorganization of metabolic profiles, with PC1 explaining 48.47% of the total variance and PC2 accounting for 24.13%, summing up to 72.60%. Compared to T2, a greater separation among some inoculated groups was observed, while others tended to converge toward the control, suggesting that the metabolic response of the cultivars is evolving differently depending on the pathogen. 'Dolce Agogia' drupes inoculated with *C. karsti* showed a clear separation from the other samples, indicating that the metabolic response to infection remains evident at 120 hours. Similarly, 'Dolce Agogia' drupes inoculated with *C. gloeosporioides*, *C. acutatum*, and *C. godetiae* remained distinct from the control, though with reduced dispersion compared to earlier time points, suggesting a possible onset of metabolic rebalancing while still maintaining distinctive traits compared to non-inoculated olives. In contrast, 'Leccino' and 'Ottobratica' cultivars showed a more pronounced tendency toward convergence with the control, with reduced separation along PC1 and PC2. This suggests that in these cultivars, the metabolic alterations induced by infection are less pronounced, or that adaptation mechanisms are in place, leading them toward a metabolic profile

more similar to that of non-inoculated olives (Fig. 6-c). At T_4 (168 hours), PCA analysis revealed an overall reduction in explained variance compared to previous time points, with PC1 accounting for 27.23% and PC2 for 25.08%, summing up to 52.31%. This decrease suggests a greater homogenization of metabolic profiles among samples, indicating that metabolic differences between cultivars and the control have progressively diminished over time. However, 'Dolce Agogia' drupes inoculated with *C. karsti* and *C. gloeosporioides* remain clearly separated from the other samples, suggesting that the effect of infection persists even at 168 hours. This distinct metabolic profile indicates that these pathogens induced more prolonged metabolic changes compared to the other treatments. On the other hand, 'Dolce Agogia' drupes inoculated with *C. acutatum* and *C. godetiae* show a stronger tendency toward convergence with the control, while still maintaining some metabolic differences. Conversely, 'Leccino' and 'Ottobratica' samples showed a more homogeneous response across all pathogen inoculations, with controls consistently clustering together, confirming that metabolic changes were, indeed, driven by pathogen interaction rather than inherent cultivar traits (Fig. 6-c).

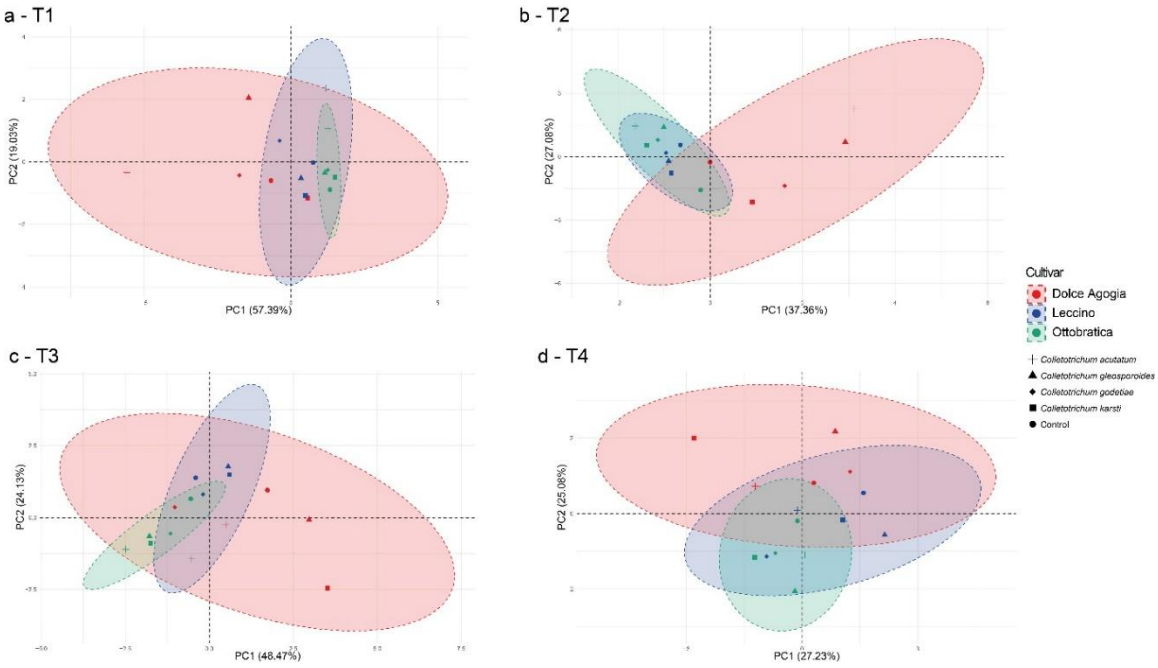

Figure 6. Principal component analysis (PCA), based on Chlorophyll a, Chlorophyll b, Carotenoids, H_2O_2 and MDA content of fruit of 'Ottobratica', 'Coratina' and 'Dolce Agogia' inoculated with four *Colletotrichum* species at different time intervals after inoculation (T_1, T_2, T_3 and T_4).

4.5 Discussion

Due to their sessile nature, plants have evolved well-coordinated defence systems to adapt and survive to abiotic and biotic environmental stresses. These systems modulate growth, photosynthesis, osmotic maintenance, and carbohydrate homeostasis. Previous

studies addressed the metabolic changes in olive fruit infected by *Colletotrichum* species and evidenced they are influenced by both the cultivar susceptibility and the virulence of the *Colletotrichum* species involved. However, these studies focused on either the negative effects of *Colletotrichum* infection on the chemical parameters used to evaluate the commercial and sensorial oil quality or the secondary metabolites produced by the pathogen (Miho et al., 2024; Riolo et al., 2023a). In the present study, the metabolite profiles of three olive cultivars, 'Ottobratica', 'Dolce Agogia', and 'Leccino', were correlated with the different susceptibility of these cultivars to the *Colletotrichum* species commonly associated with olive anthracnose. The pathogenicity tests on detached olive drupes confirmed previous studies indicating the cultivar Ottobratica can be regarded as very susceptible to *Colletotrichum* infection while 'Dolce Agogia' and 'Leccino' were susceptible and relatively resistant, respectively (Riolo et al. 2023a and b). Among the *Colletotrichum* species tested, *C. acutatum* was the most virulent species, followed by *C. gloeosporioides* and *C. godetiae*, in order of virulence, while *Colletotrichum karsti* exhibited only weakly virulent. The low virulence of this latter species masked the difference in susceptibility between 'Ottobratica' and 'Dolce Agogia'. Similarly, no significant difference in susceptibility was observed between the drupes of 'Dolce Agogia' and 'Leccino' inoculated with *C. godetiae*. Conversely, the inoculation with the two most virulent *Colletotrichum* species, *C. acutatum* and *C. gloeosporioides*, amplified the differences in susceptibility making it possible to separate the three olive cultivars into clearly distinct categories, i.e. very susceptible, susceptible and relatively resistant. Quite interestingly, the resistance of 'Leccino' proved to be effective against all *Colletotrichum* species tested. The content of photosynthetic pigments chlorophyll a, chlorophyll b, and carotenoids was a metabolic response of olive drupes to the infection by *Colletotrichum* examined in this study. Yang and Luo, (2021) showed that in wheat infected with the fungal pathogens *Puccinia striiformis* and *Fusarium graminearum*, photosynthesis was inhibited during pathogen infection as part of the plant's defense strategy. Several other studies addressed the effects on fungal infections on photosynthetic pigments of plants and a possible role of these pigments in plant/pathogen interaction. For instance, carotenoids are known for their antioxidant properties (Crupi et al., 2023). Costa Pinto et al. (2000) demonstrated the photosynthesis capacity of maize leaves was inhibited by infection of *C. musae* and *Fusarium moniliforme*, leading to a significant reduction in chlorophyll content. Soleimani et al. (2024) observed a lower chlorophyll concentration in leaves of cucumber seedlings infected by powdery mildew incited by *Podosphaera fusca*, compared to helathy seedlings. Other studies emphasized that resistant plants

often experience a temporary reduction in photosynthesis, reallocating resources toward immune defence (Yang and Luo, 2021; Yang et al., 2021). In the present study, the effect of *Colletotrichum* infection on the content of photosynthesis pigments of olive drupes was significant. It was more marked in the cultivar Dolce Agogia, which also showed a higher inherent content of all three pigments examined, compared to the other two cultivars. The analysis of all three pigment contents and their time course during infection showed a general increase as a consequence of infection. However, chlorophyll a exhibited a distinct pattern: it increased dramatically in 'Dolce Agogia' drupes, but remained relatively stable in the other two cultivars—'Ottobratica', the most susceptible to anthracnose, and 'Leccino', the only cultivar relatively resistant to infection. Also the content of chlorophyll b and total carotenoids in the drupes of 'Dolce Agogia' was higher than in those of both 'Ottobratica' and 'Leccino'. It is noticeable that the most relevant increments of photosynthetic pigments as a consequence of the infection were observed in drupes inoculated with *C. acutatum* and in fewer instances in those inoculated with *C. gloeosporioides*, the two most virulent *Colletotrichum* species tested in this study. Overall, the analysis of the response of photosynthetic pigments to the *Colletotrichum* infection revealed a cultivar-specificity and suggested an activation of metabolism, particularly in the early phases of the infection progress. Moreover, the reaction intensity was correlated with the virulence of the *Colletotrichum* species involved. Conversely, no clear relationship was noticed between the pattern of variation of photosynthetic pigments in response to the infection and any potential mechanism of resistance. The analysis of oxidative stress markers (MDA and H_2O_2) reflected a strong oxidative burst in the tissues of all inoculated drupes irrespective of the olive cultivar and the *Colletotrichum* species involved. However, looking at the intensity of the response and its time course some specificities were noticeable. Basically, in drupes inoculated with *C. acutatum*, one of the two most virulent *Colletotrichum* species tested in this study, it was observed an early and more persistent oxidative stress while in drupes inoculated with the less virulent species, such as *C. karsti* and *C. godetiae*, the response was more delayed and peaks of H_2O_2 level were also observed in the final stage of infection process (T_4). The most relevant cultivar-specificity was observed in the levels of MDA in drupes of the very susceptible 'Ottobratica'. In this cultivar, they remained lower than or at maximum equal to the control during the whole infection process, irrespective of the *Colletotrichum* species involved, suggesting this metabolic pathway might have a role in resistance mechanisms to the infection by these pathogens. The patterns of MDA level in inoculated drupes of 'Leccino' and 'Dolce Agogia' during the infection process did not differ substantially while

the higher absolute values of MDA level in the drupes of the latter cultivar might be imputed, like in the case of photosynthesis pigments, to a cultivar-specificity. Overall these results indicate clearly that reactive oxygen species (ROS) have a crucial role as signals of defence responses (Eloy et al., 2015; Lu and Yao, 2018; Yang and Luo, 2021) also in the olive/*Colletotrichum* pathosystem, as shown by the high levels of H_2O_2 observed in infected drupes. These levels contribute to the increased oxidative damage, and the corresponding elevated levels of MDA. They also provide evidence of a possible role of ROS in resistance mechanisms. Consistently with the findings of the present study, Eloy et al. (2015) demonstrated H_2O_2 plays a dual role in the pathosystem *C. gloeosporioides*/cowpea, functioning as both a defence signal and a damaging agent, depending on the pathogen lifestyle.

The sharp increase in carbohydrates observed in T1 for 'Dolce Agogia' and T2 for 'Leccino' infected by *C. acutatum*, one of the two most virulent species, suggests the activation of a response mechanism to infection, requiring greater energy availability.This hypothesis might be also supported by the observed increasing (Fig. 2) of the photosynthetic pigments in these drupe varieties. Sugars play a key role in stress perception and signaling, acting as a central regulatory hub for stress-mediated gene expression. They contribute to osmotic adjustment, reactive oxygen species (ROS) scavenging, and the maintenance of cellular energy status through carbon partitioning (Morkunas & Ratajczak, 2014; Salam et al., 2023). Additionally, carbohydrates are essential for cell wall synthesis. The polysaccharide-rich fungal cell wall is crucial for maintaining cellular integrity and protecting the cell from external stressors, such as environmental fluctuations and host infection (Geoghegan, 2017). Thus, the observed increase in sugar levels in 'Dolce Agogia' and 'Leccino' may indicate a metabolic adjustment aimed at enhancing stress tolerance and reinforcing defense responses against infection, which requires further investigation. Conversely, the lack of sugar synthesis or its reduction in the most susceptible variety, 'Ottobratica,' may reflect its metabolic inability to mount an effective response to pathogen infection. Finally, the distinct responses elicited by different *Colletotrichum* species within the same drupe variety are particularly intriguing, paving the way for more in-depth research on their mechanisms of action. The analysis of data using heat maps and PCA provided further insight into the complex metabolic responses of olive cultivars to the infection of diverse *Colletotrichum* species and their dynamics during the infection process. Initially, at 24h, responses were cultivar-specific. In particular, 'Dolce Agogia' inoculated with *C. acutatum* and *C. gloeosporioides* reacted

differently from the other cultivars. However, over time, the responses converged progressively, indicating common defense mechanisms were being activated in different cultivars. An exception was 'Dolce Agogia', which remained metabolically distinct indicating lingering pathogen-specific effects in this cultivar. Despite being generally considered a weak pathogen, *C. karsti* elicited a notable response in 'Dolce Agogia', as evidenced by its clear separation from the control at 72 hours (T2). This highlights that even less virulent species can trigger substantial metabolic rearrangements in certain cultivars. The tight clustering of control samples confirmed that the metabolic shifts observed were mostly pathogen-induced, while the distinct spread observed for samples inoculated with *C. acutatum* and *C. gloeosporioides* would suggest these species induce stronger or diverse metabolic responses. Nevertheless, the distinct metabolic footprint observed in 'Dolce Agogia' upon inoculation with *C. karsti* underscores the complexity of host–pathogen interactions, where pathogen virulence does not always directly correlate with the magnitude of the host's metabolic response (Costa Pinto et al., 2000; Kretschmer et al., 2020). Overall this study provided a better insight into the complex biochemical and physiological pathogen/host interactions during the infection process of olive fruit anthracnose and revealed how they can vary depending on olive cultivar and *Colletotrichum* species involved. Most alterations observed in olive fruit to the infection indicate a stress-response, some can be regarded as cultivar-specific while others seem related to either general or more specific defence mechanisms. These findings are preliminary to the investigation of olive tree resistance to this infectious disease.

5. Conclusions

This study provides novel insights into the physiological and biochemical responses of olive fruit to *Colletotrichum* infection, revealing significant cultivar-specific differences. Variations in chlorophyll, carotenoid, and sugar content, along with oxidative stress markers (MDA, H_2O_2), indicate that metabolic adjustments influence susceptibility and pathogen virulence. The early oxidative burst observed in response to aggressive *Colletotrichum* species suggests a key role of stress signaling in disease progression. The distinct responses of *Dolce Agogia* and *Leccino* suggest that pigment retention and sugar accumulation may contribute to defense mechanisms, while the prolonged oxidative stress in *Ottobratica* aligns with its higher susceptibility. The metabolomic approach applied has identified potential biomarkers linked to host response, offering new perspectives for future studies on resistance mechanisms. These findings enhance our understanding of olive anthracnose and may support breeding programs and disease

management strategies. Further research on oxidative stress regulation and metabolic reprogramming could provide valuable insights for improving resistance and mitigating the impact of *Colletotrichum* infections on olive production.

CRediT author statement.

Sebastiano Conti Taguali: Investigation, Methodology, Software, Data Curation, Formal analysis, Validation, Writing - Original Draft, Writing - Review & Editing

Federico La Spada: Investigation, Methodology, Formal analysis.

Mario Riolo: Conceptualization, Investigation, Methodology, Software, Data Curation, Formal analysis, Validation, Writing - Original Draft, Writing - Review & Editing

Elena Santilli: Investigation, Formal analysis, Writing - Review & Editing

Antonella Pane: Investigation, Resources, Supervision.

Biancaelena Maserti: Methodology, Formal analysis, Writing - Original Draft, Writing - Review & Editing, Resources, Supervision.

Santa Olga Cacciola: Conceptualization, Investigation, Writing - Original Draft, Validation, Writing - Review & Editing, Resources, Supervision, Funding acquisition, Project administration.

FUNDS

This study was supported by the University of Catania, Italy, "Investigation of Phytopathological problems of the main Sicilian productive contexts and eco-sustainable defense strategies (MEDIT-ECO)"- PiaCeRi-PIAno di inCEntivi per la Ricerca di Ateneo 2020-22 linea 2" "5A722192155"; the European Union (NextGeneration EU), through the MUR-PNRR project SAMOTHRACE (ECS00000022) and Ministero dell'agricoltura, della sovranità alimentare e delle foreste (MASAF), project title: Difesa degli Agrumeti Italiani dal Malsecco – AGRIVITA (CUP: C83C23000650006); the project "PROMETEO", Strategic project ENI Italy-Tunisia 2014–2020.

Conflict of interest: Authors declare no conflict of interest.

Results of this study have been submitted as a scientific article to the Physiological and Molecular Plant Pathology – ScienceDirect (ELSEVIER)

4.6 References

Alkan N and Fortes AM (2015) Insights into molecular and metabolic events associated with fruit response to post-harvest fungal pathogens. *Front. Plant Sci*. 6:889. doi:

10.3389/fpls.2015.00889

Bolouri Moghaddam M.R. &Van den Ende W. (2012) Sugars and plant innate immunity. *Journal of Experimental Botany*; 63:3989–3998. doi: 10.1093/jxb/ers129.

Cacciola, S.O., Faedda, R., Sinatra, F., Agosteo, G.E., Schena, L., Frisullo, S., et al. (2012) Olive anthracnose. *Journal of Plant Pathology*, 94, 29–44.

Catola, S., Marino, G., Emiliani, G., Huseynova, T., Musayev, M., Akparov, Z., et al. (2016) Physiological and metabolomic analysis of *Punica granatum* (L.) under drought stress. *Planta*, 243, 441–449. https://doi.org/10.1007/s00425-015-2414-1.

Costa Pinto, L.S.R., Azevedo, J.L., Pereira, J.O., Carneiro Vieira, M.L. & Labate, C.A. (2000) Symptomless infection of banana and maize by endophytic fungi impairs photosynthetic efficiency. *New Phytologist*, 147, 609–615. https://doi.org/10.1046/j.1469-8137.2000.00722.x.

Criado, M.N., Motilva, M.J., Ramo, T. & Romero, M.P. (2006) Chlorophyll and carotenoid profile and enzymatic activities (chlorophyllase and lipoxygenase) in olive drupes from the fruit-setting period to harvest time. *Journal of the American Society for Horticultural Science*, 131, 593–600. https://doi.org/10.21273/jashs.131.5.593.

Crupi, P., Faienza, M.F., Naeem, M.Y., Corbo, F., Clodoveo, M.L. & Muraglia, M. (2023) Overview of the Potential Beneficial Effects of Carotenoids on Consumer Health and Well-Being. *Antioxidants*, 12. https://doi.org/10.3390/antiox12051069.

Eloy, Y.R.G., Vasconcelos, I.M., Barreto, A.L.H., Freire-Filho, F.R. & Oliveira, J.T.A. (2015) H2O2 plays an important role in the lifestyle of *Colletotrichum gloeosporioides* during interaction with cowpea [*Vigna unguiculata* (L.) Walp.]. *Fungal Biology*, 119, 747–757. https://doi.org/10.1016/j.funbio.2015.05.001.

Dubois M, Gilles KA, Hamilton JK, Rebers PA, Smith F. Colorimetric method for determination of sugars and related substances. Anal Chem 1956;28:350e6.

Faedda, R., Agosteo, G.E., Schena, L., Mosca, S., Frisullo, S., Magnano Di San Lio, G., et al. (2011) *Colletotrichum clavatum* sp. Nov. identified as the causal agent of olive anthracnose in Italy. *Phytopathologia Mediterranea*, 50, 283–302. https://doi.org/10.14601/Phytopathol_Mediterr-9547.

Geoghegan, I., Gero Steinberg, G. & Gurr S. (2017) The Role of the Fungal Cell Wall in the Infection of Plants, Trends in Microbiology,Volume 25, Issue 12,957-967, https://doi.org/10.1016/j.tim.2017.05.015.

Guzmán, E., Baeten, V., Pierna, J.A.F. & García-Mesa, J.A. (2015) Determination of the olive maturity index of intact fruits using image analysis. *Journal of Food Science and Technology*, 52, 1462–1470. https://doi.org/10.1007/s13197-013-1123-7.

Hodges, D.M., DeLong, J.M., Forney, C.F. & Prange, R.K. (1999) Improving the thiobarbituric acid-reactive-substances assay for estimating lipid peroxidation in plant tissues containing anthocyanin and other interfering compounds. *Planta*, 207, 604–611. https://doi.org/10.1007/s004250050524.

Keunen E., Peshev D., Vangronsveld J., Van Den Ende W.& Cuypers A. (2013) Plant sugars are crucial players in the oxidative challenge during abiotic stress: Extending the traditional concept. *Plant Cell Environment* 36:1242–1255. doi: 10.1111/pce.12061.

Kretschmer, M., Damoo, D., Djamei, A. & Kronstad, J. (2020) Chloroplasts and plant immunity: Where are the fungal effectors? *Pathogens*, 9, 1–16. https://doi.org/10.3390/pathogens9010019.

Lichtenthaler, H.K. (1987) Chlorophylls and Carotenoids: Pigments of Photosynthetic Biomembranes. *Methods in Enzymology*, 148, 350–382. https://doi.org/10.1016/0076-6879(87)48036-1.

Lu, Y. & Yao, J. (2018) Chloroplasts at the crossroad of photosynthesis, pathogen infection and plant defense. *International Journal of Molecular Sciences*, 19, 1–37. https://doi.org/10.3390/ijms19123900.

Maoka, T. (2020) Carotenoids as natural functional pigments. *Journal of Natural Medicines*, 74, 1–16. https://doi.org/10.1007/s11418-019-01364-x.

Miho, H., Expósito-Díaz, A., Marquez-Perez, M.I., Ledesma-Escobar, C., Diez, C.M., Prusky, D., et al. (2024) The dynamic changes in olive fruit phenolic metabolism and its contribution to the activation of quiescent *Colletotrichum infection*. *Food Chemistry*, 450. https://doi.org/10.1016/j.foodchem.2024.139299.

Moral, J. & Trapero, A. (2009) Assessing the susceptibility of olive cultivars to anthracnose caused by *Colletotrichum acutatum*. *Plant Disease*, 93, 1028–1036. https://doi.org/10.1094/PDIS-93-10-1028.

Morkunas I.& Ratajczak L (2014) The role of sugar signaling in plant defense responses against fungal pathogens. A*cta Physiologica Plantarum* 36:1607–1619. doi: 10.1007/s11738-014-1559-z

Riolo, M., Luz, C., Santilli, E., Meca, G. & Cacciola, S.O. (2023a) Secondary metabolites produced by four *Colletotrichum* species in vitro and on fruits of diverse olive cultivars. *Fungal Biology*, 127, 1118–1128. https://doi.org/10.1016/j.funbio.2023.06.003.

Riolo, M., Pane, A., Santilli, E., Moricca, S. & Cacciola, S.O. (2023b) Susceptibility of Italian olive cultivars to various *Colletotrichum* species associated with fruit anthracnose. *Plant Pathology*, 72, 255–267. https://doi.org/10.1111/ppa.13652.

Rojas, C.M., Senthil-Kumar, M., Tzin V and Mysore KS (2014) Regulation of primary plant metabolism during plant-pathogen interactions and its contribution to plant defense. Frontiers in Plant Sciences 5:17. doi: 10.3389/fpls.2014.00017

Rolland F., Baena-Gonzalez E. & Sheen J. (2006) Sugar sensing and signaling in plants: Conserved and novel mechanisms. *Annual Review of Plant Biology,* 57, 675–709. https://doi: 10.1146/annurev.arplant.57.032905.105441.

Salam, U., Ullah, S., Tang, Z.-H., Elateeq, A. A., Khan, Y., Khan, J., Khan, A., & Ali, S. (2023) Plant Metabolomics: An Overview of the Role of Primary and Secondary Metabolites against Different Environmental Stress Factors. *Life*, *13*(3), 706. https://doi.org/10.3390/life13030706

Soleimani, H., Mostowfizadeh-Ghalamfarsa, R., Ghanadian, M., Karami, A., Cacciola, S.O. (2024) Defense Mechanisms Induced by Celery Seed Essential Oil against Powdery Mildew Incited by *Podosphaera fusca* in Cucumber. *Jornal of Fungi* , *10*; 17. https://doi.org/10.3390/jof10010017

Tagnon, M.D. & Simeon, K.O. (2017) Aldehyde dehydrogenases may modulate signaling by lipid peroxidation-derived bioactive aldehydes. Plant Signaling and Behavior, 12, e1387707. https://doi.org/10.1080/15592324.2017.1387707

Talhinhas, P. & Baroncelli, R. (2021) *Colletotrichum* species and complexes: geographic distribution, host range and conservation status. Springer Netherlands.

Talhinhas, P., Gonçalves, E., Sreenivasaprasad, S. & Oliveira, H. (2015) Virulence diversity of anthracnose pathogens (*Colletotrichum acutatum* and *C. gloeosporioides* species complexes) on eight olive cultivars commonly grown in Portugal. *European Journal of Plant Pathology*, 142, 73–83. https://doi.org/10.1007/s10658-014-0590-7.

Talhinhas, P., Loureiro, A. & Oliveira, H. (2018) Olive anthracnose: a yield- and oil quality-degrading disease caused by several species of *Colletotrichum* that differ in virulence, host preference and geographical distribution. *Molecular Plant Pathology*, 19, 1797–1807. https://doi.org/10.1111/mpp.12676.

Tounekti, T., Vadel, A.M., Oñate, M., Khemira, H. & Munné-Bosch, S. (2011) Salt-induced oxidative stress in rosemary plants: Damage or protection? Environmental and Experimental Botany, 71, 298–305. https://doi.org/10.1016/J.ENVEXPBOT.2010.12.016

Varveri, M., Papageorgiou, A.G. & Tsitsigiannis, D.I. (2024) Evaluation of Biological Plant Protection Products for Their Ability to Induce Olive Innate Immune Mechanisms and Control *Colletotrichum acutatum*, the Causal Agent of Olive Anthracnose. *Plants*, 13. https://doi.org/10.3390/plants13060878.

Yang, H. & Luo, P. (2021) Changes in photosynthesis could provide important insight into the interaction between wheat and fungal pathogens. *International Journal of Molecular Sciences*, 22. https://doi.org/10.3390/ijms22168865.

Yang, X., Lu, M., Wang, Yufei, Wang, Yiran, Liu, Z. & Chen, S. (2021) Response mechanism of plants to drought stress. *Horticulturae*, 7. https://doi.org/10.3390/horticulturae7030050.

Zhang, B., Zhou, L., Zhou, X., Bai, Y., Zhan, M., Chen, J., et al. (2022) Differential responses of leaf photosynthesis to insect and pathogen outbreaks: A global synthesis. *Science of the Total Environment*, 832, 155052. https://doi.org/10.1016/j.scitotenv.2022.155052.

5. Environmental and agronomic factors shaping rhizosphere microbial communities in organically and conventionally managed citrus orchards: An omics approach

Sebastiano Conti Taguali[1,2 y], Rhea Pöter [3 y], Francesco Aloi[1], Clara Fernández-Trujillo[4], Alberto Acedo[4], Federico La Spada[1*], Maria Giulia Li Destri Nicosia[2], Leonardo Schena[2], Antonella Pane[1], Santa Olga Cacciola[1*]

[1] University of Catania, Department of Agriculture, Food and Environment (UniCT, Di3A), Via Santa Sofia 100, 95123 Catania (Italy).

[2] Mediterranea University of Reggio Calabria, Department of Agricultural Science, Località Feo di Vito, 89122 Reggio di Calabria (Italy).

[3] Ruhr University Bochum, Department of Soil Science and Soil Ecology, Geographical Institute, Universitaetsstr. 150, 44801 Bochum, Germany

[4] Biome Makers Inc., Davis, CA 95618, USA

[y] These authors contributed equally.

* Corresponding authors: federico.laspada@unict.it; olga.cacciola@unict.it.

5.1 Abstract

In general, cropping systems influence the structure and diversity of rhizosphere microbiota of cultivated plants, impacting soil health and plant productivity. This research examined the effects of farming systems, soil physicochemical properties and season on the rhizosphere microbiota of citrus orchards in diverse municipalities of eastern Sicily, using BeCrop® custom primers for PCR amplification and Illumina sequencing technologies complemented by bioinformatic data processing. Consistently with a parallel metagenomic study, targeting the ITS-1 and rps10 gene DNA regions. Orchard location was found to have the most significant influence on rhizosphere microbial community. Other factors, including seasonality, soil type and chemical characteristics, tillage number and depth, irrigation system and rootstock variety had a lower albeit significant impact on both prokaryotic and fungal communities. Rootstock age and tree vigour had negligible influence on both prokaryotic and fungal communities. Some factors, e.g. the irrigation system, the frequency of soil tillage and the rootstock variety, exerted differential effects on either prokariotic or fungal rhizosphere

communities. Unlike other published studied targeting the ITS-1 and rps10 gene DNA regions, , in the present study the analysis of rhizosphere soil samples demonstrated that the microbial communities, including both prokaryota and fungi, were significantly affected by the farming system. Organic orchards compared to conventionally managed orchards exhibited higher microbial diversity as well as a unique composition of nutrient-cycling microbes, which are crucial for enhancing soil fertility and plant health. Moreover, the study revealed that organic practices promote beneficial microbial functions, such as nitrogen fixation and phosphorus solubilization, more effectively than conventional agronomic practices. By elucidating the dynamic interactions between management practices and microbial assemblages, our findings underscore the potential of microbial diversity as a crucial indicator of ecological sustainability and soil health in agricultural settings. This research highlights the impact of organic management on enhancing microbial ecosystems, thereby supporting more sustainable agricultural outputs.

Key words: citrus; rhizosphere microbiota; fungi; prokaryota; metagenomics; Illumina; BeCrop® indices; organic agriculture; microbioma functions.

5.2 Introduction

Citrus have a prominent role in global fruit production and trade (FAO, 2021; Mukhametzyanov et al., 2024). Spain and Italy are the two major citrus producing countries of the European Union (EU) and among the Italian regions, Sicily (southern Italy) is the first citrus producer, with a total citrus growing area of around 88,000 ha (Spreen et al., 2020; Ciriminna et al., 2024). Since the early 2000s the EU policy has encouraged organic agriculture in order to pursue environmental sustainability and food safety. Presently, the global citrus farmland managed organically is estimated at around 115,000 ha and Italy and Spain, the two leading organic citrus producers worldwide, account for around 31,000 and 25,000 ha, respectively (Willer et al., 2024). Despite the relevant economic importance of organic citriculture, information about the effects of farming system on soil microbial ecology in citrus orchards is scarce and has focused almost exclusively on the bacterial component of microbiota (Lima et al., 2024). Moreover, soil health, differently from air and water health, has been only occasionally tackled by EU regulation. Only recently the European Commission has proposed a directive addressing soil health (Proposal for a directive of the Parliament and Council on soil monitoring and resilience_COM_2023_416), with the ultimate aim of establishing a harmonized soil monitoring system across the member countries. According with the EU soil strategy for 2030, the EU member states will have to define which practices should be implemented

and which should be banned to prevent soil degradation. In this context, a primary objective of the present study was to provide insights into the effects of organic farming system and more generally agronomic practices on soil microbiota associated with citrus tree roots. In recent years, the study of microbial communities associated with the plants has been greatly implemented as a consequence of rapid technological progress of metagenomics and in particular the soil microbiota has gained attention due to its crucial role in soil fertility, plant health and crop productivity (Mercado-Blanco et al-., 2018). However, a substantial knowledge gap persists in understanding how agronomic and environmental factors shape the rhizosphere microbiota in citrus orchards. Agricultural management is a key driver of soil microbial diversity and function, influencing both community composition and microbial activity. Plant associated microorganism communities comprise a wide range of taxa, including fungi, bacteria, prokaryotes, archaea, and viruses which reside in all above ground and below ground plant parts and play key roles in many aspects of plant functions and health status, such as nutrient intake, development, growth, tolerance of biotic and abiotic stresses and disease suppression (Mendes et al., 2011, Richardson and Simpson, 2011; Turner et al., 2013; Pieterse et al., 2014; van der Voort et al., 2016: Martin et al., 2017; Abdelfattah et al., 2019; Carrión et al., 2019; Parasuraman et al., 2019; De Vries et al., 2020; Trivedi et al., 2016 and 2020; Ali et al., 2023; Guo et al., 2024). A few of these studies characterised the pylloplane, rhizosphere and endophytic microbiota of citrus (Abdelfattah et al., 2017; Xu et al., 2018; Faddetta et al., 2021; Zhang et al., 2021: Lombardo et al., 2024; Mo et al., 2024), however no one addressed the effects of organic farming system, as regulated by the EU, on soil microbiome of commercial citrus orchards.

BeCrop® technology, a cutting-edge tool for measuring microbial processes in soil nutrient cycling, is revolutionizing the study of microbial population dynamics. Using the qualitative and quantitative composition of the microbiome as input, this technology employs patented algorithms to predict specific microbial activities that can influence nutrient availability to plants (Imam et al., 2021; Gobbi et al., 2022; Mondello et al., 2022; Acin-Albiac et al., 2023; Adamo et al., 2024; Blanco et al., 2024; Milke et al., 2024; Bansal et al., 2025). By profiling soil microbial communities and their functional potentials, BeCrop® can provide valuable insights into the complex network of interactions within the soil microbiome, linking microbial diversity and functionality to soil health and plant productivity.

The scope of this study was to provide a deeper understanding of the relationships between soil microbiome and soil health in citrus farmland by complementing high-

throughput sequencing with BeCrop® technology. Specific objectives were to evaluate the influence of environmental (geographical area and soil type) and agronomic factors (rootstock genotype, tree age, tillage frequency and depth, irrigation system, and tree health status), season (summer vs. winter), and farming system (organic vs. conventional) on the structure and functionality of the soil microbiota associated with roots of citrus trees in commercial citrus orchards of Sicily.

5.3 Material and methods

5.3.1 sampling sites

Samples were collected in 15 commercial orange [*Citrus* × *sinensis* (L.) Osbeck] orchards (sampling sites) located in the municipalities of Siracusa, Lentini, Carlentini, Ramacca, and Mineo within the provinces of Catania and Siracusa, in southeastern Sicily (Table 1 and Fig. 1). The extension of a single orchard varied from 10 to around 50 ha.

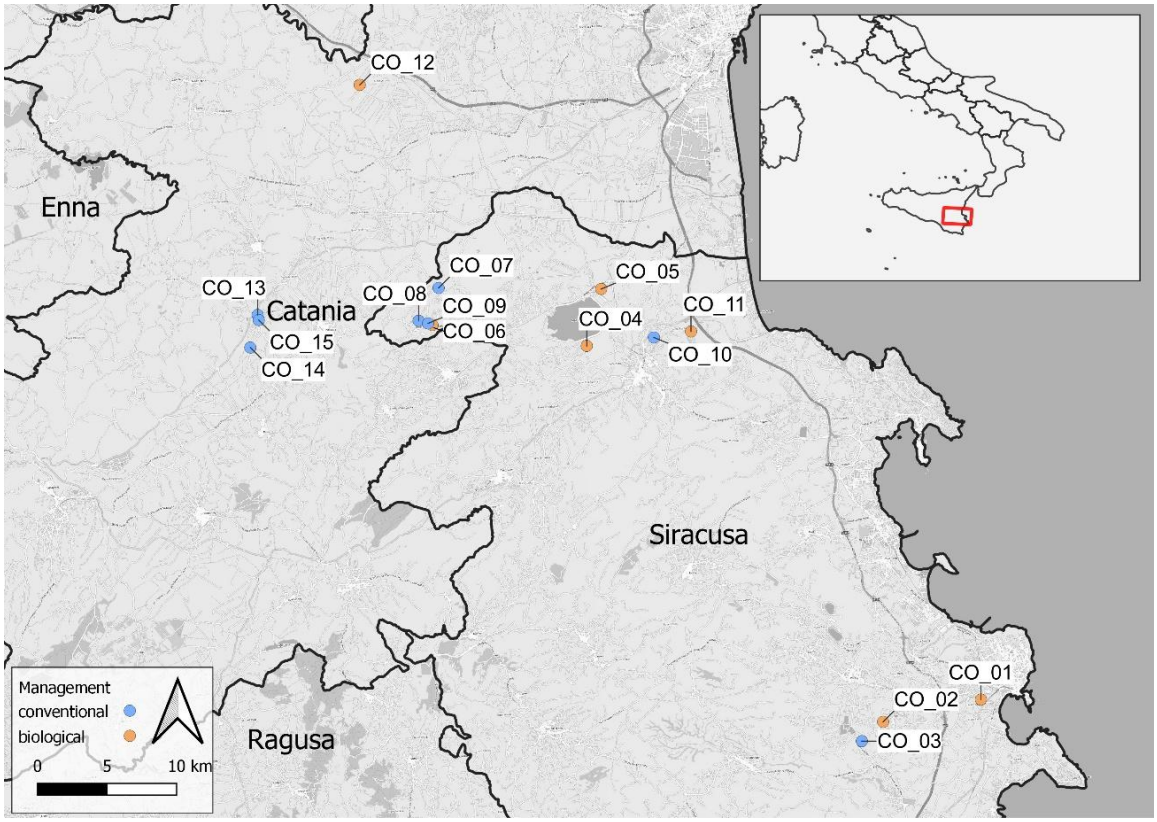

Figure 1. Geographical location of the 15 citrus orchards located in the municipalities of Syracuse (in Italian Siracusa), Lentini, Carlentini, Ramacca, and Mineo in eastern Sicily (Italy).

Table 1. Sampling sites selected in this study along with the citrus producing area, type of plaintation, orange variety, type of rootstock and age, agronomical management, tillage number per year and depth, irrigation system, collected rhizosphere soil samples, soil type, tree vigor.

Localities	Sampling Site – ID coordinates and altitude [a]	Scion species and cultivar	Rootstock[b] and Tree age[c]	Farming system[d]	Tillage number[e] and depth[f]	Irrigation system	Sample-ID	Soil type [h]	Tree health status[g]
Siracusa (Italy)	CO_01 - Tenuta Giardina; 37°03'43.5'' N; 15°15'30.5'' E 1.4 mt a.s.l.	Sweet orange 'Moro'	Sour orange; old	Org	3 S	Drip	CO_1_P1	S	V
							CO_1_P2		V
							CO_1_P3		V
							CO_1_P4		V
							CO_1_P5		V
	CO_02 - Tenuta Giardina; 37°03'11.2'' N; 15°10'35.1'' E 72.9 mt a.s.l.	Sweet orange 'Valencia'	Sour orange; old	Org	3 S	Drip	CO_2_P1	SL	V
							CO_2_P2		V
							CO_2_P3		V
							CO_2_P4		V
							CO_2_P5		V
	CO_03 -Tenuta Cava Donna; 37°02'29.5'' N; 15°09'29.9'' E 78.3 mt a.s.l.	Sweet orange 'Valencia'	Sour orange old	Conv	NT	Sprinklers (T-shaped)	CO_3_P1	S	V
							CO_3_P2		V
							CO_3_P3		V
							CO_3_P4		V
							CO_3_P5		V

Lentini (Syracusa, Italy)	CO_04 – Tenuta Biviere; 37°18'29.2'' N; 14°57'23.7'' E 20 mt a.s.l.	Sweet orange 'Tarocco'	Citrange 'Carrizo' young	Org	3 S	Sprinklers (T-shaped)	CO_4_P1 CO_4_P2 CO_4_P3 CO_4_P4 CO_4_P5	S	V V W V V
	CO_05 – Tenuta Di Cataldo; 37°20'39'' N; 14°58'16'' E 39.5 mt a.s.l.	Sweet orange 'Moro'	Sour orange old	Org	2 D	Sprinkers (T-shaped)	CO_5_P1 CO_5_P2 CO_5_P3 CO_5_P4 CO_5_P5	SL	W V W W V
	CO_06 – Tenuta Mario Grimaldi; 37°19'40'' N; 14°49'58'' E 157.3 mt a.s.l.	Sweet orange 'Tarocco'	Sour orange old	Org	4 D	Sprinklers (T-shaped)	CO_6_P1 CO_6_P2 CO_6_P3 CO_6_P4 CO_6_P5	SL	V V W V V
	CO_07 – Tenuta Grimaldi; 37°21'05'' N; 14°50'22'' E 56.6 mt a.s.l.	Sweet orange 'Tarocco'	Citrange 'Carrizo' young	Conv	3 D	Sprinklers (T-shaped)	CO_7_P1 CO_7_P2 CO_7_P3 CO_7_P4 CO_7_P5	S	V W V W V

	CO_08 – Tenuta Coco; 37°19'53'' N; 14°49'18''E 99.4 mt a.s.l.	Sweet orange 'Tarocco'	Sour orange old	Conv	4 D	Microsprinklers (inter-row)	CO_8_P1 CO_8_P2 CO_8_P3 CO_8_P4 CO_8_P5	SaL	V V V V V
	CO_09 – Tenuta Viglianisi; 37°19'44'' N; 14°49'45'' E 151.5 mt a.s.l.	Sweet orange 'Tarocco'	Sour orange old	Conv	4 D	Microsprinklers (inter-row)	CO_09_P1 CO_09_P2 CO_09_P3 CO_09_P4 CO_09_P5	S	V W V V V
Carlentini (Syracuse, Italy)	CO_10 – Tenuta Guastella; 37°18'39'' N; 15°00'40'' E 10.5 mt a.s.l.	Sweet orange 'Tarocco'	Sour orange young	Conv	3 D	Sprinklers (T-shaped)	CO_10_P1 CO_10_P2 CO_10_P3 CO_10_P4 CO_10_P5	SL	W V W V V
	CO_11 – Tenuta Calvo; 37°18'47'' N; 15°02'30'' E 7 mt a.s.l.	Sweet orange 'Ovale'	Sour orange old	Org	3 D	Sprinklers (T-shaped)	CO_11_P1 CO_11_P2 CO_11_P3 CO_11_P4 CO_11_P5	S	V W W V V

Ramacca (Catania, Italy)	CO_12 – Tenuta Borzi Akiana; 37°29'08'' N; 14°47'09'' E 60.7 mt a.s.l.	Sweet orange 'Tarocco'	Citrange 'Carrizo' young	Org	3 S	Drip	CO_12_P1 CO_12_P2 CO_12_P3 CO_12_P4 CO_12_P5	SL	V V V V W
Mineo (Catania, Italy)	CO_13 - Tenuta Sedati; 37°20'28'' N; 14°41'30'' E 90.5 mt a.s.l.	Sweet orange 'Tarocco'	Sour orange young	C	NT	Drip	CO_13_P1 CO_13_P2 CO_13_P3 CO_13_P4 CO_13_P5	S	V V W V V
	CO_14 - Tenuta Salinella; 37°19'14'' N; 14°41'03'' E 107.5 mt a.s.l.	Sweet orange 'Tarocco'	Citrange 'Carrizo' young	C	3 D	Drip	CO_14_P1 CO_14_P2 CO_14_P3 CO_14_P4 CO_14_P5	SL	V V V V V
	CO_15 - Tenuta Serravalle; 37°20'16'' N; 14°41'33'' E 90.9 mt a.s.l,	Sweet orange 'Tarocco'	Sour orange young	C	3 D	Microsprinklers (inter-row)	CO_15_P1 CO_15_ P2 CO_15_P3 CO_15_P4 CO_15_P5	SL	V V V V V

[a] DATUM WGS84; [b] Sour orange (*Citrus aurantium* L.), 'Carrizo' citrange [*C. sinensis* (L.) Osbeck x *Poncirus trifoliata* (L.) Raf.] [c] young 20÷39 years, old ≥40 years; [d] Org = organic, C = Conventional; [e] Tillage number (NT= No-tillage,alternatively 2÷ 4 per year); [f] Tillage depth (S=shallow **<** 15 cm, D=deep ≥ 15 cm); [g] S = silt, SL = silt loam, SaL = sandy loam, U.S.D.A. soil texture classes (IUSS Working Group WRB, 2022);[g] S = silt, SL = silt loam, SaL = sandy loam, U.S.D.A. soil texture classes (Bridges, 1978); [h]V = vigorous, with a deep green and thick canopy, W = weak, with a pale green and transparent canopy.

5.3.1.1 Features of sampling sites

Samples were collected in eight conventionally and seven organically managed commercial citrus orchards (Table 1). Tree spacing in all orchards was 6x4 m. Conventionally managed orchards used herbicides such as glyphosate, 2,4-dichlorophenoxyacetic acid (1-3 applications per year at 2 kg/ha of a.i. per each application) and oxyfluorfen (a single application per year at 0.15 kg/ha of a.i.), paraffinic oils (30-40 L/ha) and/or synthetic insecticides, such as acetamiprid (1-2 treatments per year at 93 ml/ha of a.i. per each treatment) and/or spirotetramat (a single application per year at 136-200 ml/ha of a.i.), as well as copper fungicides (a single treatment per year at 0.8-1 kg/ha of Cu^{++}) for controlling major diseases caused by fungi and oomycetes (Rovetto et al., 2024). Moreover, conventionally managed orchards were fertilized each year with synthetic commercial NPK (20.10.10) complexes at 800-1000 kg/ha. Organically managed orchards, which received subsides from the regional government, were managed according with the EU rules (basically, EU Council Regulation No. 834/2007, European Commission Regulation No. 889/2008 and EU Regulation No, 2018/848): paraffinic oils (30-40 l/ha) were used for controlling insect pests, copper fungicides (a single treatment per year at 0.8-1 kg/ha of Cu^{++}) for controlling diseases caused by fungi and oomycetes, and a commercial product (Biotris, SIRIAC s.r.l., Acate (RG), Italy), an organic mineral complex containing NPK (Ca-Mg-S) 5-8-12 (11-2-13), at 1500-2000 kg/ha as a fertilizer. Moreover both conventionally and organically and conventionally managed orchards were fertigated once a year with Fe-EDDHA chelate (0.6-1.2 kg/ha of Fe^{++}). As for other variables, either environmental such as the geographical location (sampling site) and soil type (textural class), or agronomic, such as rootstock (sour orange vs.'Carrizo' citrange), tree age (young vs. old), soil tillage frequency (0÷4 times per year) and depth (shallow <15 cm, deep >15 cm), irrigation system (drip, T-shaped sprinklers, microsprinklers), and tree health status as determined by visual observation (vigorous trees with a dense, deep green canopy vs. weak trees with a sparse, i.e. transparent, pale green canopy), detailed information is schematically resumed in Table 1.

5.3.2 Collection of soil samples

Sampling activities were carried out in summer (June-July 2021) and replicated in winter (December 2021-January 2022). A total of 150 composite soil samples (75 samples in summer and 75 in winter) were collected from the 15 citrus orchards listed in Table 1 (five samples from each orchard at each sampling time). A square plot of around 2.1 ha was delimited within each orchard and five trees were randomly selected along the two diagonals of the plot at a distance of at least 100 m from each other, excluding the trees along the perimeter

of the plot. Soil samples were collected beneath the tree canopy. The top 5 cm layer comprising the litter was removed, then, four soil cores, including fine roots (depth of approximately 20–30 cm), were sampled at four cardinal points, at a distance of 40–100 cm from the trunk. The four soil cores were then pooled together into a single composite soil sample of approximately 1 L. For each 1 L sample, sub-samples of 10 ml were promptly placed on ice, and transported to the Molecular Plant Pathology Laboratory at the University of Catania for metagenomic processing. These sub-samples were stored at -80°C until molecular analyses were performed. The remaining soil was weighed on-site and brought immediately to the Molecular Plant Pathology Laboratory of the University of Catania, air-dried, reweighed and stored at room temperature until subsequent analyses to determine physicochemical properties.

5.3.3 Determination of physicochemical soil

The physicochemical properties of the soil samples were analyzed at the Physical Geography Laboratory of the Ruhr-Universität Bochum, Germany. The analyses included the determination of water content (WC), pH, total carbon (TC), total nitrogen (TN), carbon-to-nitrogen ratio (C:N), inorganic carbon (IC), organic carbon (OC), and soil texture class. Before conducting the specific analyses, the soil samples underwent preliminary preparation, which involved air-drying and sieving through a 2 mm mesh to remove larger residues. These residues were weighed and discarded, while the remaining soil was manually crushed using a porcelain mortar. The water content of each sample at the time of sampling was determined by calculating the ratio of the dry weight to the wet weight and expressing the result as a percentage of the sample's wet weight. The pH of the samples was measured using 0.01M calcium chloride ($CaCl_2$), following the standard DIN ISO 10390:2005-12. For the determination of TC, TN, and the C:N ratio, the samples were finely ground using a Pulverisette 7 (Fritsch, Idar-Oberstein, Germany), and approximately 750 mg of each sample was analyzed using a Vario Max Cube elemental analyzer (Elementar, Langenselbold, Germany). The measurement was performed twice to ensure accuracy. Inorganic carbon (IC) was determined by treating 100 mg of soil with 7 mL of phosphoric acid, followed by incineration at 200°C, and quantified using a Solid Sampling Module SSM-5000A of the TOC-L analyzer (Shimadzu, Kyoto, Japan). Organic carbon (OC) was then calculated as the difference between TC and IC. For soil texture analysis, approximately 45 g of soil from each sample were subjected to the removal of carbonates and organic matter, following DIN ISO 11277 and the protocol described by Utermann et al. (2000). After treatment, the soil was washed until conductivity fell below 2.0 mS, then dried at 60°C, gently crushed, and sieved

through a 0.2 mm mesh. The small quantity of material larger than 0.2 mm was considered negligible and not included in the measurements. The particle size distribution (sand, silt, and clay percentages) was analyzed using laser particle diffraction with an Analysette 22 (Fritsch, Idar-Oberstein, Germany). The results were compared to the World Reference Base for Soil Resources (IUSS 2022) to classify soil type.

5.3.4 Soil microbiome analyses

Metagenomic analyses of the microbiome associated with the rhizosphere soil of the selected citrus orchards were conducted by the Biome-Makers laboratory (Valladolid, Spain), where samples were shipped frozen on ice. The detailed procedures for metagenomic processing are outlined in the following paragraphs.

5.3.4.1 Environmental DNA (eDNA) extraction and Illumina libraries preparation

For each 10 mL rhizosphere soil sample (in total, 150 samples were analyzed), total eDNA was extracted from three sub-aliquots using the DNeasy PowerLyzer PowerSoil® kit (Qiagen, Hilden, Germany). To analyze the bacterial and fungal communities in the rhizosphere soils of citrus plants, BeCrop® custom primers (patent publication number: WO2017096385, Biome Makers) were used for PCR amplifications, specifically targeting the 16S rRNA V4 region and the ITS1 region (Becares and Fernandez, 2017). The amplified DNA fragments were then purified using the KAPA Pure Beads kit (Roche, Basel, Switzerland). The amplification of the 16S and ITS regions was confirmed by electrophoresis on a 2% agarose gel. Libraries for both 16S and ITS regions were prepared for Illumina sequencing according to a two-step protocol (Gobbi et al., 2019; Liao et al., 2019). The DNA was quantified using a Qubit fluorometer with the Qubit HS Assay (Thermo Fisher Scientific, Waltham, MA, USA). Finally, the DNA libraries were sequenced using an Illumina MiSeq instrument (Illumina, San Diego, CA, USA) with 2 × 300 paired-end reads.

5.3.4.2 Bioinformatic processing for taxonomical classifications

The paired-end read sequences were processed for primer removal using the Cutadapt software (Martin, 2011). After removing the primers, the sequences were assembled by overlapping at least 100 nucleotides, resulting in longer and more reliable sequences. Then, the assembled sequences underwent a rigorous filtering process based on expected errors, with a maximum threshold value of 1.0, as recommended by (Edgar et al. (2015). Following preprocessing to ensure sequence quality, reads with single nucleotide differences were iteratively clustered to form amplicon sequencing variants (ASVs) using the Swarm method (Mahé et al., 2022). De novo chimeras and singletons were subsequently removed. Chimeras were identified and eliminated to avoid false positives, following the methodologies outlined

by Edgar et al. (2011). Finally, the ASVs were classified taxonomically through global alignment with a 97% identity threshold against reference databases. Specifically, for 16S sequences, the SILVA 138.1 database was used, while the UNITE 8.3 database was employed for ITS sequences (Glöckner et al., 2017; Nilsson et al., 2019).

5.3.4.3 Computation of microbiome indexes and network properties

Local network properties were determined as described by Ortiz-Álvarez et al. (2021). First, microbial community networks were built separately for 16S and ITS samples, following the methodology of Veech (2013). To create presence-absence meta-networks, rarefied species-level counts were used. Then, pairs of species that appeared together significantly more often or less often than expected were identified. These pairs formed co-occurrence networks (species that often occur together) or co-exclusion networks (species that tend not to appear together). Local network properties were then derived by selecting these species pairs from the meta-network for each individual sample.

In addition, BeCrop® indexes were calculated as per Acedo et al. (2022). These indexes evaluate critical soil health characteristics, including microbial processes related to nutrient cycling, such as 'calcium transport', 'carbon', 'carbon fixation', 'fermentation', 'inorganic nitrogen consumption', 'manganese transport equilibrium', 'nitrogen', 'organic phosphorus assimilation', and 'potassium consumption'. These processes were analyzed in relation to the agricultural management of the orchards. By focusing on these specific microbial activities, a deeper understanding was gained of how different management practices and seasonal variations influence the soil microbiome and, consequently, plant health. BeCrop® indexes have been used in previous soil microbiome studies, demonstrating the robustness and quality of the BeCrop® technology (See Table S7) (Milke et al., 2024).

5.3.4.4 Statistical analyses

Statistical analyses were performed using phyloseq and vegan packages in R version 4.3.2 (McMurdie and Holmes, 2013; Oksanen et al., 2024). The alpha diversity of microbial communities was determined on rarefied data using the Shannon and Chao1 biodiversity indices. Unsupervised clustering of ITS and 16S soil microbiome was applied using the k-means algorithm. The optimal number of clusters was assessed using silhouette, WSS, and gap statistics (Table S2). Microbiome indexes, network and physicochemical properties were fitted to a varying set of mixed models. Briefly, these models contained the main effect of environmental factors, including citrus-producing area and soil type, and agronomic factors, including type of rootstock and age of rootstock, tillage practices and depth, irrigation system, and plant vigor, The interactions between management and other factors were

included when possible. ITS or 16S clusters were either fixed or random effects, depending on specific model for microbiome and network indexes. Note that physicochemical properties models did not contain season as a factor since data was available only for summer season. In models that included physicochemical properties as response variables, random effect was always the location. The optimal model for each index was selected based on Akaike's information criterion (AIC) (Table S1). Marginal (random and fixed terms) and conditional (fixed terms only) R-squared for each model were determined. Next, ANOVA on fixed terms was applied and subsequent post-hoc comparison across significant factor levels was performed. P-value was corrected for multiple testing using the FDR procedure.

To investigate beta diversity and visualize variations in community structures, Principal Coordinates Analysis (PCoA) based on Bray-Curtis distance was employed. Permutational Multivariate Analysis of Variance (PERMANOVA) was employed to assess the statistical significance of differences in community composition attributed to experimental factors. Redundancy Analysis (RDA) was performed on summer samples to ascertain which physicochemical properties and experimental variables were significantly correlated with the observed variations in the microbiome.

The prevalence of conserved prokaryotic and fungal phyla and genera within all soil samples (combined data) from either organically or conventionally managed citrus orchards, collected in either the summer or winter season, was determined at a prevalence threshold of 25% and a detection limit of 0.01%. Shared and exclusive taxa numbers at genus level across management practices and seasons were represented in Venn diagrams for both 16S and ITS. Next, differentially abundant (DA) taxa were identified between mainly organic and conventional management practices. Further analyses were performed to examine the effect of tillage depth and frequency on microbiome composition, as illustrated in Tables S4 and S5. All differential abundance analyses were assessed using negative binomial regression at various taxonomic levels utilizing the edgeR package (Robinson Mark et al., 2010).

5.4 Results

5.4.1 Physicochemical properties of soils

The physicochemical properties of soil samples are reported in Tables 1 and 2. As for soil type, 35 soil samples were of the silt texture class while 35 were of the silt loam texture class. The only exception were five soil samples from a conventionally managed orchard (CO_08 – Tenuta Coco) in the municipality of Lentini, which were of the sandy loam texture class (Table 1). In Table 2, chemical soil properties are grouped according with the farming system

(organic vs. conventional). The only parameter that differed significantly between organically and conventionally managed orchards was the TC content, which was higher in organically managed orchards (Table 2).

Water content. The mean WC content was 0.15 ± 0.04 and 0.13 ± 0.04 for organically and conventionally managed orchards, respectively. In organically managed orchards, soil WC ranged from 10.04 % (CO_12; Ramacca, Catania) to 21.77 % (CO_04; Lentini, Siracusa), while in conventionally managed orchards it ranged from 8.29 % (CO_15; Mineo, Catania) to 18.92 % (CO_08; Lentini, Siracusa).

pH. Mean pH was 7.66 ± 0.04 and 7.58 ± 0.1 in soil of organically and conventionally managed orchards. In organically managed orchards values ranged from 7.61 (CO_11; Lentini, Syracuse) to 7.70 (CO_06; Ramacca, Catania), while in soils from conventionally managed orchards ranged they from 7.11 (CO_08; Lentini, Siracusa) to 7.80 (CO_14; Mineo, Catania).

Total carbon and total nitrogen content. In soil of organically managed orchards the mean content of TC was significantly higher than in soils from conventionally managed orchards. Mean values were 4.61 ± 1.67 and 3.85 ± 1.21 in organically and conventionally managed orchards, respectively. In organically managed orchards values ranged between 2.37 % (CO_12; Ramacca, Catania) and 6.68 % (CO_06; Lentini, Siracusa), while in conventionally managed orchards they ranged between 2.07 % (CO_07; Lentini, Siracusa) and 5.32 % (CO_09; Lentini, Siracusa). TN content was only slightly higher in soils of organically managed orchards, ranging from 0.12 % (CO_12; Ramacca, Catania) to 0.22 % (CO_05; Lentini, Siracusa) in organically managed orchards, and from 0.10 % (CO_14, from Mineo) to 0.27 % (CO_09 from Lentini, Siracusa) in conventionally managed orchards. However the means (0.18 ± 0.03 and 0.17 ± 0.06, respectively) were not significantly different.

Inorganic carbon. In soils of organically managed orchards, IC levels were slightly higher than in conventionally managed orchards. They ranged from 1.44 % (CO_04, Lentini, Siracusa) to 5.44 % (CO_06, Lentini, Siracusa) in soils of organically managed orchards, while in soils from conventionally managed orchards they ranged from 0.47 % (CO_08, Lentini, Siracusa) to 4.18 % (CO_14, Mineo, Catania). However, differences between the means (3.15 ± 1.61 and 2.58 ± 1.5, respectively) were not statistically significant.

Organic carbon. Similarly to IC, OC levels were slightly higher in organically managed soil. However, differences between the means (1.46 ± 0.49 and 1.39 ± 0.68, respectively) were not significant. IC values ranged between 0.85 % (CO_12, Ramacca, Catania) and 2.07 % (CO_05, Lentini, Siracusa) in soils from organically managed orchards, and between 0.55 % (CO_14, Mineo, Catania) and 2.34 % (CO_03, Siracusa) in soils from conventionally managed orchards.

C:N ratio. This parameter showed a great variability, irrespective of the farming system and the geographic location of the orchards. In organically managed orchards the C:N values varied from 16.01 (CO_04, Lentini, Siracusa) to 42.24 (CO_06, Lentini, Siracusa), while in conventionally managed orchards they varied from 10.49 (CO_08, Lentini, Siracusa) to 43.73 (CO_14, Mineo, Catania), with no substantial difference between the means of the two groups of soils (25.7 ± 9.99 and 25.6 ± 12.4, respectively).

Table 2. Chemical properties of soil samples from conventionally and organically managed citrus orchards. Data are means ± SD of 40 and 35 replicate soil samples for organically and conventionally managed orchards, respectively. Statistically significant differences between management systems were determined using an independent Student's t-test ($p < 0.05$ considered significant).

	Organic	Conventional	t-test	p-value
pH	7.66 ± 0.04	7.58 ± 0.1	1.75	0.08
TN[a] %	0.18 ± 0.03	0.17 ± 0.06	0.23	0.81
TC[b] %	4.61 ± 1.67	3.85 ± 1.21	2.23	**0.02**
C:N	25.7 ± 9.99	25.6 ± 12.4	0.04	0.97
IC[c] %	3.15 ± 1.61	2.58 ± 1.50	1.59	0.11
OC[d] %	1.46 ± 0.49	1.39 ± 0.68	0.50	0.61
WC[e] %	0.15 ± 0.04	0.13 ± 0.04	1.47	0.14

[a] Total nitrogen; [b] Total Carbon; [c] Inorganic carbon: [d] Organic carbon; [e] Water content.

5.4.2 Variability of core microbiome in soil of organically and conventionally managed citrus orchards

The metagenomic analysis of microbiome of soil samples from organically managed citrus orchards yielded a total 1,632,434 16S- and 997,214 ITS-reads in summer, and 2,754,628 16S- and 2,853,156 ITS-reads in winter, respectively. The metagenomic analysis of soil samples from conventionally managed citrus orchards yielded a total of 1,868,359 16S- and 1,933,049 ITS-reads in summer, and 3,334,785 16S- and 1,158,030 ITS-reads in winter, respectively.

The prevalence of conserved prokaryotic and fungal phyla and genera across all soil samples from both organically or conventionally managed citrus orchards in either summer or winter season was determined at a threshold of 25% and a detection limit of 0.01%.

5.4.2.1 Microbiome structure (prokaryotic and fungal phyla)

The comparative analysis of the core microbiome of organically and conventionally managed citrus orchards (Figs. 2 and 3) evidenced that in samples collected in summer, *Proteobacteria*, *Actinobacteriota*, *Crenarchaeota*, and *Acidobacteriota* were the predominant bacterial phyla irrespective of the farming system (Fig. 2, a and b), while in organically managed orchards, differently from conventionally managed orchards (Fig. 2a), the phylum *Planctomycetota* prevailed on *Firmicutes* (Fig. 2b),

In winter, the phylum *Chloroflexi* was detected exclusively in samples from conventionally managed orchards (Figs. 2e and 2f). However, similarly to the samples collected in summer, *Proteobacteria*, *Actinobacteriota*, and *Crenarchaeota* were dominant, irrespective of the farming system.

The analysis of fungal community in soil collected in summer showed that the phylum *Ascomycota* was dominant in both organically and conventionally managed orchards (Figs. 2c and 2d), while *Basidiomycota* and *Mortierellomycota* were comparatively more represented, albeit with minor differences, in soil from conventionally managed orchards (Figs. 2c and 2d).

In soil samples collected in winter, *Ascomycota* was the most prevalent phylum in both conventionally and organically managed orchards (Figs. 2g and 2h). In conventionally managed orchards, the *Basidiomycota* phylum was as prevalent as the *Ascomycota* phylum (Fig. 2g), while in organically managed orchards it was slightly less represented than *Ascomycota* (Fig. 2h). *Mortierellomycota* was the third prevalent fungus phylum in soil from both organically and conventionally managed orchards (Figs. 2g and 2h). The

analysis focused on these three main phyla as they were by far the most prevalent ones in soil microbiome. The presence of other phyla was negligible.

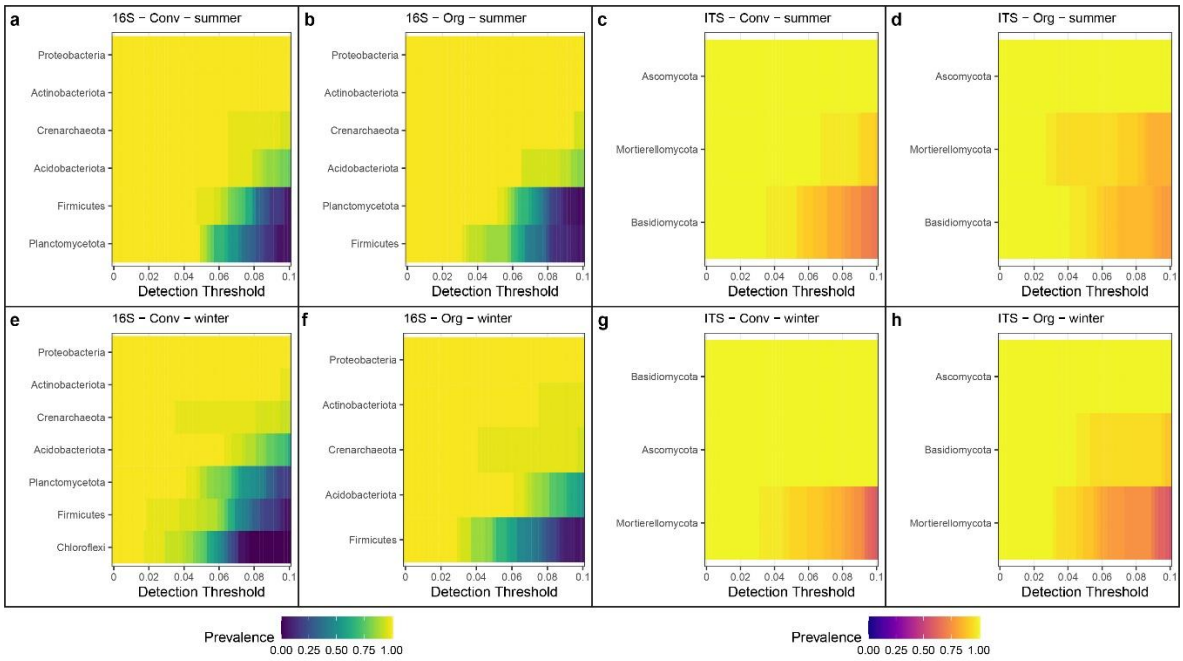

Figure 2. Heatmaps showing the phylum prevalence proportion across different detection thresholds in organic (Org) and conventional (Conv) management at summer (top) and winter (bottom) for 16S (left) and ITS (right) markers.

5.4.2.2 Microbiome structure (prokaryiotic and fungal genera)

Heatmaps in Fig. 3 depict the prevalence of genera in soil samples from organically (B) and conventionally (C) managed citrus orchards in summer and winter, for prokaryotic (16S region) and fungal (ITS region) communities, respectively.

As for prokaryotic communities, the most represented genera, irrespective of farming system or season, included *Crenarchaeota Nitrososphaera*, *Lutetiella*, *Candidatus Nitrosocosmicus*, *Gaiella*, *Solirubrobacter*, *Rubrobacter*, *Iamia*, *Bacillus*, *Neobacillus*, *Crossiella*, and *Rhodoplanes* (Figs. 3a, b, e and f and Fig. 4). However, seasonal differences were observed between farming systems. In soil microbiome of conventionally managed orchards, all genera detected in summer were also present in winter (Figs. 3a and e and Fig. 4). In addition, in winter other genera, such as *Ilumatobacter*, *Sphingomonas*, *Steroidobacter*, and *Bryobacter*, were detected (Fig. 3e and Fig. 4). A seasonal pattern, was also observed in microbiome of soil samples from organically managed orchards. *Pirellula* and *Vicinamibacter* were exclusively detected in summer (Fig. 3b and Fig. 4), while *Nitrospira, Bryobacter*, and *Sphingomonas* were exclusively detected in winter (Fig. 3f and

Fig. 4). In summer, *Vicinamibacter* and *Pirellula* were exclusive to samples from organically managed orchards, while no exclusive genera were recorded in microbiome of samples from conventionally managed orchards (Figs. 3a and b and Fig. 4).

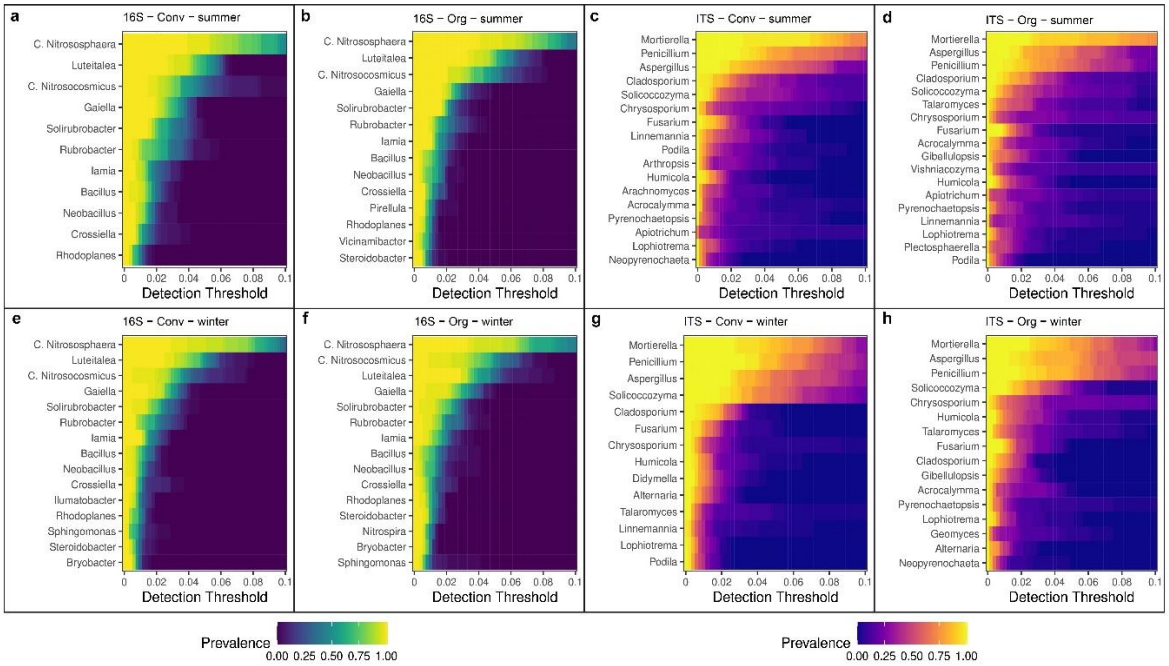

Figure 3. Heatmaps showing the genus prevalence proportion across different detection thresholds in organic (Org) and conventional (Conv) management at summer (top) and winter (bottom) for 16S (left) and ITS (right) markers (panel a).

In winter, *Ilumatobacter* was exclusively detected in microbiome soil of conventionally managed orchards, while *Nitrospira* was exclusive to samples from organically managed orchards (Figs. 3e and f and Fig. 4). As for fungal communities, *Mortierella*, *Penicillium*, *Aspergillus*, *Solicoccozyma*, *Cladosporium*, *Fusarium*, *Lophiotrema*, and *Chrysosporium* were consistently present, irrespective of farming system or season (Figs. 3c, d, g, and h, and Fig. 4). However, some differences were observed between farming systems and seasons. In soil microbiome of conventionally managed orchards, genera such as *Arthropsis*, *Arachnomyces,* and *Apiotrichum* were detected exclusively in summer, while genera such as *Didymella*, *Alternaria*, *Talaromyces*, and *Linnemannia* were exclusively detected in winter (Figs. 3c and g and Fig. 4). Genera, such as *Vishniacozyma*, *Plectosphaerella*, *Apiotrichum* and *Linnemannia*, were detected exclusively in citrus orchards under organic management, in summer. *Geomyces*, *Gibellulopsis*, *Alternaria*, and *Talaromyces* were exclusive to the winter season (compare Fig. 3d and h and Fig. 4). Focusing on fungal communities recorded in summer with respect to agricultural management, *Vishniacozyma*, *Plectosphaerella* and *Linnemannia* were exclusive to

samples from orchards under organic management, while *Arthropsis* and *Arachnomyces* were exclusive records in samples from conventional management (compare Fig. 3c and d and Fig. 4). In winter, *Didymella* and *Linnemannia* were exclusively detected in conventionally managed orchards, whereas *Gibellulopsis* and *Geomyces* were exclusive to samples from organically managed orchards (Fig. 3g and h, and Fig. 4).

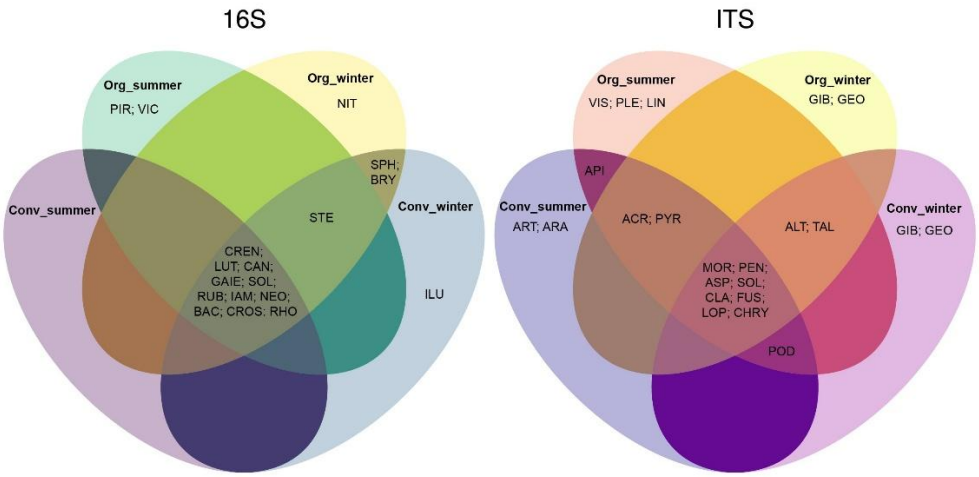

Figure 4. Comparison among the different members of prokaryote (left) and fungal (right) taxa at summer and winter seasons at genus level. Members of prokaryote (CREN = *Crenarchaeota Nitrososphaera*, LUT= *Lutetiella*, CAN = *Candidatus Nitrosocosmicus*, GAIE = *Gaiella*, SOL = *Solirubrobacter*, RUB=*Rubrobacter*, IAM= *Iamia*, BAC= *Bacillus*, NEO= *Neobacillus*,CROS= *Crossiella*, RHO= *Rhodoplanes*, ILU= *Ilumatobacter*, SPH= *Sphingomonas*, STE = *Steroidobacter*, BRY= *Bryobacter*, PIR= *Pirellula*, VIC= *Vicinamibacter* and NIT= *Nitrospira*). Members of fungal (MOR= *Mortierella*, PEN= *Penicillium*, ASP= *Aspergillus*, SOL = *Solicoccozyma*, CLA = *Cladosporium*, FUS=*Fusarium*, LOP= *Lophiotrema*, CHRY= *Chrysosporium*, ART= *Arthropsis*, ARA= *Arachnomyces*, API= *Apiotrichum*, DID= *Didymella*, ALT= *Alternaria*, TAL= *Talaromyces*, VIS= *Vishniacozyma*, PLE= *Plectosphaerella*, GEO= *Geomyces*, DID= *Didymella*, GIB= *Gibellulopsis*, ACR= *Acrocalymma*, and LIN= *Linnemannia*)

5.4.2.3 Variability of microbiome structure in relation to seasonality and farming system

Venn diagrams (Fig. 5a) depict the frequency of diverse prokaryotic and fungal genera recorded in soil samples based on farming system of orchards (organic versus conventional) and soil sampling season (summer versus winter). As for the seasonal variability of soil prokaryotic communities in relation to the farming system (Fig. 5a), in

summer four and two exclusive taxa characterized the soil microbiome of organically and conventionally managed citrus orchards, respectively. No taxa were shared between the soil microbiome of orchards differing in farming system. In winter, 18 bacterial taxa were exclusive to the microbiome of either organically or conventionally managed orchards, while 15 taxa were shared between the soil micorbiome of differently managed orchards. When considering the interaction between farming system and seasonality on the assembly of prokaryotic communities, the microbiome of organically managed orchards showed four exclusive taxa in summer and 18 in winter, with nine taxa common to both seasons. In conventionally managed orchards, two exclusive taxa were recorded in summer and 18 in winter, with six taxa common to both seasons. Finally, 340 prokaryotic taxa did not vary with the farming system or season. They were recorded in soil microbiome of both organically and conventionally managed orchards in winter as well as in summer (Fig. 5a).

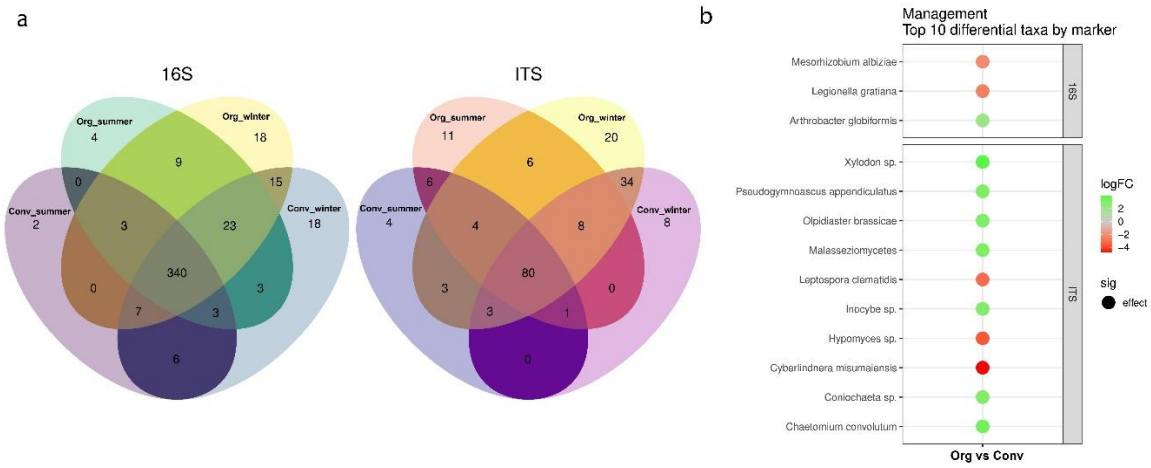

Figure 5. Number of shared and exclusive members of prokaryote (left) and fungal (right) taxa at summer and winter seasons at genus level (panel a). Top 10 differentially abundant taxa (panel b) found when comparing biological and conventional managements at species level (adjusted p-value <0.05) for 16S (top) and ITS (bottom).

As for the seasonal variability of fungal communities in relation to the farming system (Fig. 5a), in summer, 11 and four taxa were exclusive to the microbiome of organically and conventionally managed orchards, respectively, while six taxa were shared between the two groups of orchards as separated on the basis of farming system. In winter, 20 and eight taxa were exclusive to the soil microbiome of organically and conventionally managed orchards, respectively, while 34 taxa were shared between the two groups of orchards managed differently. Six out of 31 taxa unique to the soil microbiome of

organically managed orchards were detected both in summer and winter, while no taxon out of 12 taxa unique to the soil microbiome of conventionally managed orchards was detected in both seasons. Overall, 80 fungal taxa were not influenced by either agricultural management or seasonality and consequently were recorded in soil microbiome of both organically and conventionally managed orchards as well as in both summer and winter (Fig. 5a).

5.4.2.4 Microbiome structure (prokaryotic and fungal species)

The top-ranked differentially abundant species in soil microbiome of surveyed citrus orchards are reported in Fig. 5b and Supplementary Table S3. In the prokaryotic dataset (16S-reads), the top three differentially abundant species were *Mesorhizobium albiziae*, *Legionella gratiana*, and *Arthrobacter globiformis*. These taxa exhibited significant differences in abundance between organically and conventionally managed orchards, with *Arthrobacter globiformis* showing higher abundance in soil microbiome of organically managed orchards (logFC green, p-value < 0.05), while *Mesorhizobium albiziae* and *Legionella gratiana* were the most abundant in soil microbiome of conventionally managed orchards (logFC red, p-value < 0.05). In the fungal dataset (ITS-reads), 10 taxa were the most abundant, including *Xylodon* sp., *Pseudogymnoascus appendiculatus*, *Olpidiaster brassicae*, *Malasseziomycetes*, *Leptospora clenmidis*, *Inocybe* sp., *Hypomyces* sp., *Cyberlindnera misumaiensis*, *Coniochaeta* sp., and *Chaetomium convolutum*. Among them, *L. clenmidis*, *Hypomyces* sp. and *C. misumaiensis* were more abundant in conventionally managed soils (logFC red, p-value < 0.05), while the remaining taxa were more abundant in organically managed orchards (logFC green, p-value < 0.05).

5.4.3 Modelling of microbiome indexes and microbiome network indicators

5.4.3.1 Farming system and network properties: co-exclusion and co-occurrence

The analyses of data indicated an increase in the proportion of co-exclusion within the prokaryotic and fungal microbial networks of the soil microbiome from organically managed orchards compared to the soil microbiome from conventionally managed orchards (Figs. 6, a1 and a3). The co-occurrence networks were significant only for prokaryotic communities, which showed the highest modularity in soils from organically managed orchards (Fig. 6, a2).

5.4.3.2 Influence of management on α-diversity, Chao1 and Shannon indexes

Data processing for alpha diversity indicated that prokaryotic records did not show a significant relationship with the type of farming system.

As a result, prokaryotic alpha diversity could not be calculated. Therefore, Fig. 1b presents only the results for fungal alpha diversity. Specifically, the analysis revealed that the highest value of the Shannon diversity index was recorded in soils from organically managed orchards, while the Chao1 index suggested greater species richness in soils from organically managed orchards compared to those from conventionally managed ones.

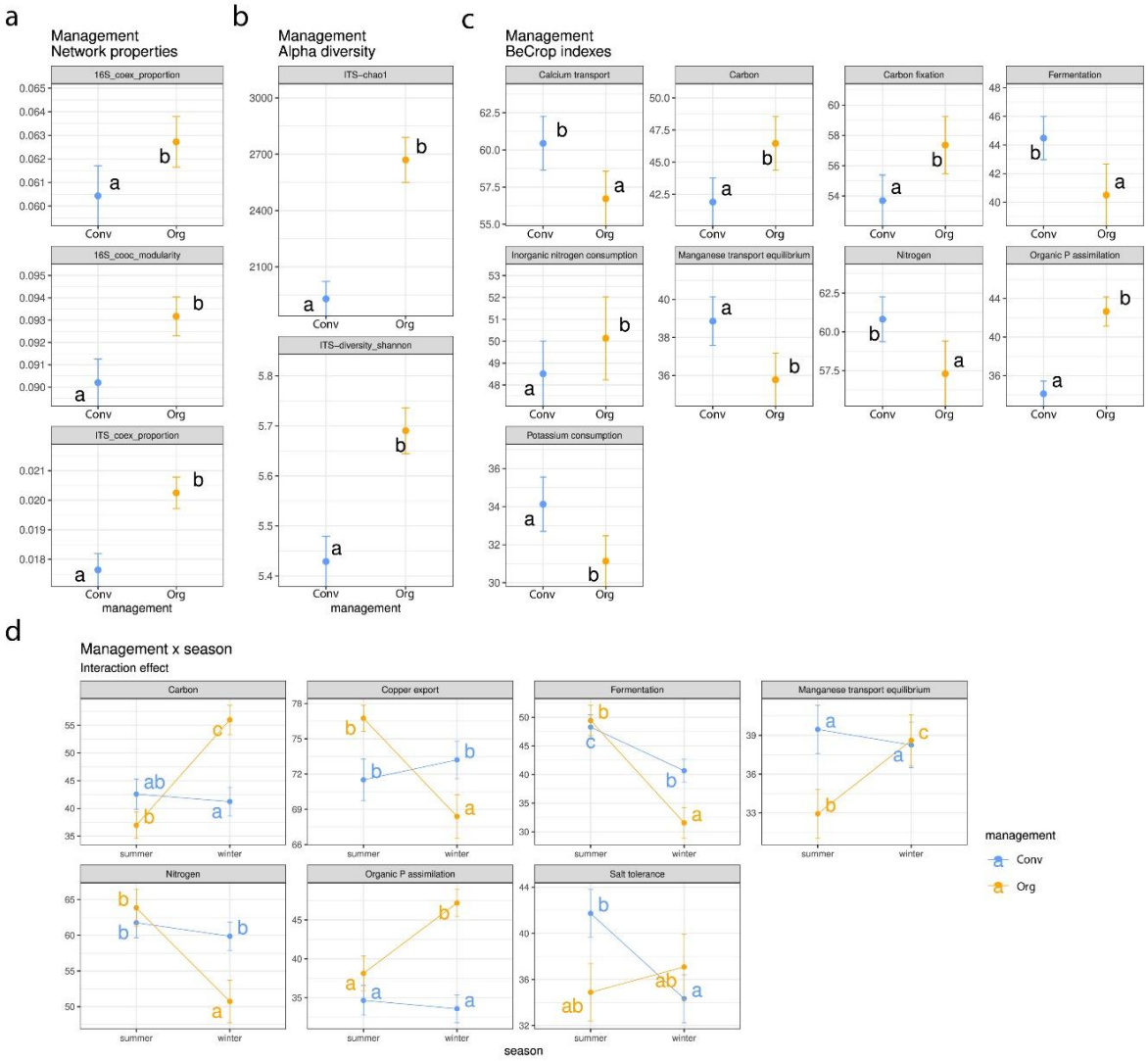

Figure 6 Network properties (panel a), alpha diversity (panel b) and microbiome BeCrop® indexes (panel c) factorial plots depending on management level. Microbiome BeCrop® indexes (panel d) interaction plots depending on management level by season. Superscript letters indicate statistically different groups (adj. p-value < 0.05).

5.4.3.3 BeCrop® indexes, with focus on management

Results presented in Figs. 6c show the variation of the indexes 'calcium transport', 'carbon', 'carbon fixation', 'fermentation', 'inorganic nitrogen consumption', 'manganese

transport equilibrium', 'nitrogen', 'organic P assimilation', and 'potassium consumption' in relation with the farming system of the orchards. Specifically, results indicated that the indexes 'carbon', 'carbon fixation', 'inorganic nitrogen consumption' and the 'organic P assimilation' were significantly higher in soils from organically managed orchards compared with those calculated for soils from conventionally managed orchards. All the other indexes showed the highest values in soils from conventionally managed orchards.

5.4.3.3 BeCrop® indexes with focus on management vs. seasonality

The results.presented in Fig. 6d show the variation of the following indexes, 'carbon', 'copper export', 'fermentation', 'manganese transport equilibrium', 'nitrogen', 'organic P assimilation', and 'salt tolerance', for orchards managed differently (organically vs. conventionally managed) in relation to seasonality (summer vs. win-ter). Specifically, in soils from organically managed orchards, significant higher values of the indexes 'carbon', 'manganese transport equilibrium', and 'organic P assimilation' were observed in winter. Conversely, 'copper export', 'fermentation', and 'nitrogen' showed a higher value in summer. Conversely, 'salt toler-ance' index did not show any significant seasonal pattern. In soils from conventionally managed orchards, a significant decrease in the indexes for 'carbon', 'fermentation' and 'salt tolerance' was observed. All oth-er indexes showed no significant seasonal variation.

5.4.4 Effects of environmental and management factors on microbial community array

The The analysis revealed significant differences in the structure of microbial communities, which were markedly influenced by both environmental variables, such as geographical location of the orchard (municipality) and soil type (textural class), and agronomic variables, including rootstock genotype (sour orange vs. 'Carrizo' citrange), tree age (young >40 years vs. old ≥40 years), farming system (conventional vs. organic), tillage frequency (no-tillage and 2, 3, 4 times per year) and depth (shallow <15 cm, deep >15 cm) and irrigation system (drip, T-shaped sprinklers, microsprinklers), soil sample ID. Specifically, the PERMANOVA analysis (Table 3) indicated that sampling site had the most significant influence on microbial community composition, accounting for 17.55% of the variance in prokaryotic communities ($p = 0.01$) and 9.45% in fungal communities ($p = 0.01$). Additionally, the cluster factor, had a significant impact, contributing for 5.65% of the variance as regards prokaryotes and 6.33% as regards fungi (both $p = 0.01$). Soil type accounted for 4.92% of the variance for prokaryotes and 2.73% for fungi ($p = 0.01$). Tillage number contributed with a proportion of 4.24% of the variance in prokaryotes and 2.91%

in fungi (p = 0.01). The influence of the irrigation system accounted for 3.40% of the variance in prokaryotes and 3.66% in fungi (p = 0.01). Agricultural management practices accounted for 3.19% of the variance in prokaryotes and 2.24% in fungi (p = 0.01). The rootstock genotype had a moderate impact, accounting for 2.35% of the variance in prokaryotes and 1.69% in fungi (p = 0.01). Factors such as tillage depth influenced prokaryotic variance by 1.75% and fungal variance by 1.12% (both p = 0.01). Tree age had a relatively low influence, accounting for 0.90% of the variance in prokaryotes and 1.77% in fungi (p = 0.01). Finally, the health status of trees as determined by visual observation did not have a significant impact on microbial communities.

Table 3. PERMANOVA analysis on microbiome data composition (16S marker for prokaryotes and ITS marker for fungi) for management, location, seasons, cluster and experimental factors. Terms in bold indicate statistically significant factors (p-value < 0.05).

Marker	16S		ITS	
Variable	p-value	R2	p-value	R2
sampling site	0.01	17.55	0.01	9.45
cluster	0.01	5.65	0.01	6.33
soil texture	0.01	4.92	0.01	2.73
tillage number per year	0.01	4.24	0.01	2.91
sampling season	0.01	3.52	0.01	2.41
irrigation system	0.01	3.40	0.01	3.66
farming system	0.01	3.19	0.01	2.24
rootstock genotype	0.01	2.35	0.01	1.69
tillage depth	0.01	1.75	0.01	1.12
tree age	0.01	0.90	0.01	1.77
tree health status	0.93	0.28	0.66	0.47

The principal coordinate analysis (PCoA) revealed that prokaryotic communities grouped primarily according to sampling site, while fungal communities were correlated with

seasonality (Fig. 7a). In addition, a deeper analysis evidenced that prokaryotic and fungal communities formed three microbiome groups, clustering primarily in relation to sampling site and, to a lesser extent, by management practices (Fig. 7b, Supplementary Table S4).

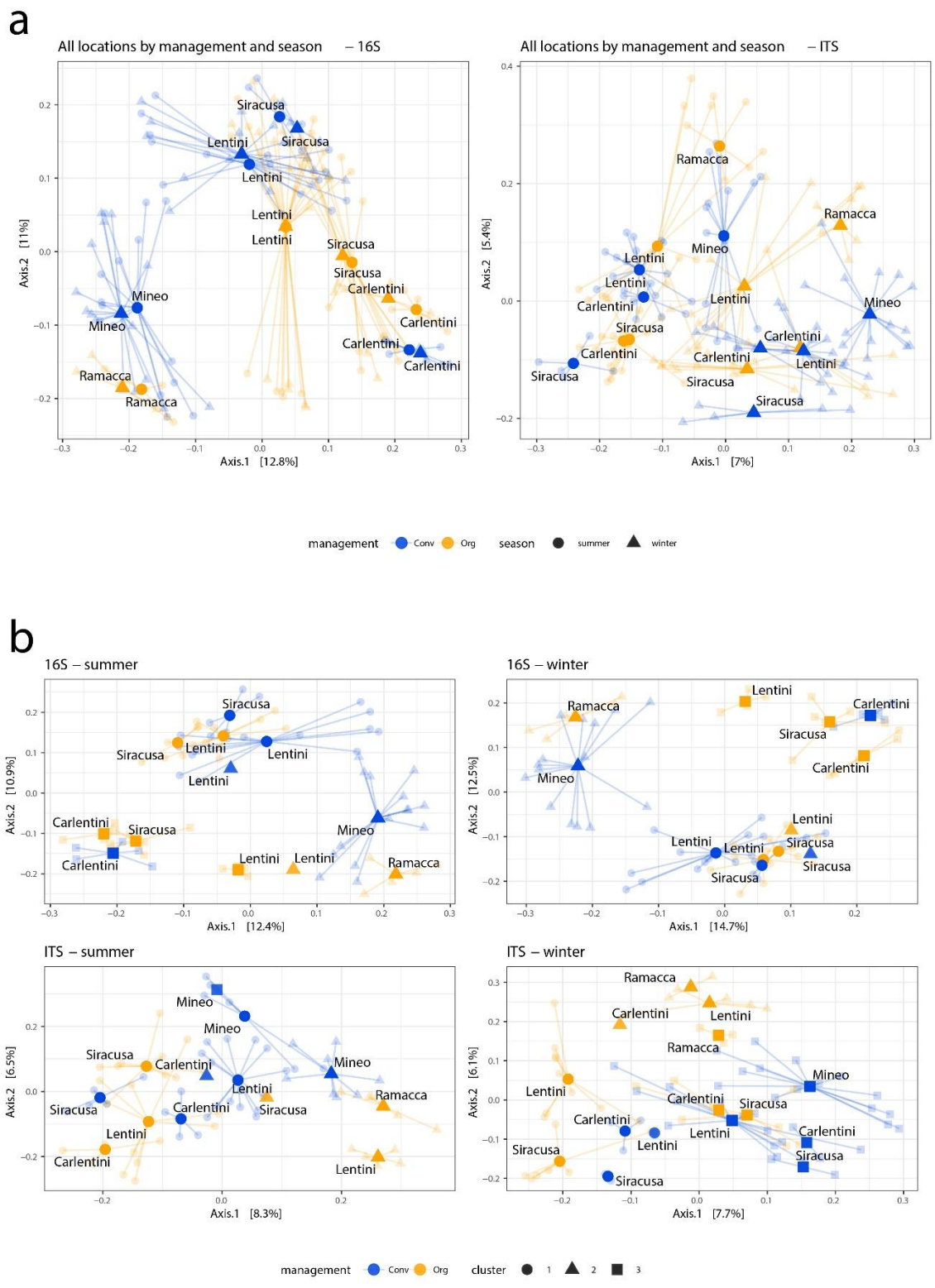

Figure 7. Principal Coordinate Analysis (PCoA) of the microbial community based on Bray-Curtis distances for 16S and ITS markers annotated farming system, sampling season and sampling site. Centroids are colored by management, shaped by sampling season and labeled by sampling site (panel a). PCoA split by season of panel a. Centroids are colored by farming system, shaped by cluster and labeled by sampling site (panel b).

The redundancy analysis (RDA) was conducted to assess the influence of various factors (see Table 4) on the assembly of microbial communities (Fig. 8). The analysis included models where the effect of sampling site was either included (unconstrained) or removed (constrained). When the sampling site effect was included, the composition of prokaryotic communities (Fig. 8 and Table 4) was significantly influenced by the frequency of soil tillage ($p = 0.043$), accounting for 3.60% of the variance. Other factors, such as rootstock genotype, irrigation system, soil type, tree age, tillage depth, management practices, and total nitrogen percentage were non-significant ($p > 0.05$), each explaining variance in the range of 1.12 to 3.25%. When the location effect was removed, the rootstock genotype became a significant factor ($p = 0.029$), accounting for 2.26% of the variance, while all the other factors, including the frequency of soil tillage, were non-significant accounting for a variance in the range of 0.98 to 3.57%.

For the fungal communities (Table 4), when the location effect was included, several factors showed significant effects. The irrigation system had the most substantial influence ($p = 0.014$), explaining 4.40% of the variance. The frequency of soil tillage was also significant ($p = 0.022$), explaining 4.04% of the variance. Farming systems ($p = 0.034$) and total nitrogen percentage ($p = 0.039$) were significant as well, explaining 2.18% and 2.17% of the variance, respectively. The rootstock genotype was significant ($p = 0.042$), explaining 2.11% of the variance. Other factors such as soil type, tillage depth, and tree age were not significant and explained variance in the range of 1.44 to 2.11%. When the sampling site effect was removed, none of the factors was statistically significant (all $p > 0.05$)

Table 4. Variance explained and ANOVA p-value of terms retrieved through forward model selection for redundancy analysis (RDA), either including (unconstrained) or removing (constrained) the sampling site effect for 16S and ITS microbial composition. Terms in bold indicate significant factors (p-value < 0.05)

	Sampling site effect	Included		Removed	
marker	Term	p-value	Explained variance (%)	p-value	Explained variance (%)
16S	**tillage number**	**0.043**	3.60	0.123	3.38
16S	irrigation system	0.096	3.25	0.077	3.57
16S	soil type	0.276	2.80	0.324	2.91

16S	**rootstock**	0.075	1.79	**0.029**	2.26
16S	tree age	0.252	1.45	0.227	1.58
16S	tillage depth	0.359	1.33	0.485	1.31
16S	farming sistem	0.454	1.26	0.211	1.60
16S	total N	0.730	1.12	0.931	0.98
ITS	**irrigation system**	**0.014**	4.40	0.056	4.03
ITS	**tillage number**	**0.022**	4.04	0.073	3.89
ITS	soil texture	0.246	2.76	0.393	2.74
ITS	**farming system**	**0.034**	2.18	0.196	1.60
ITS	**total N**	**0.039**	2.17	0.507	1.23
ITS	**Rootstock**	**0.042**	2.11	0.289	1.47
ITS	tillage depth	0.105	1.69	0.172	1.70
ITS	tree age	0.223	1.44	0.172	1.69

In particular, the effect of soil tillage number, which emerged as a key factor affecting the prokaryotic community assembly when the geographical origin was included, was observed in orchards subjected to tillage three to four times a year, such as organically managed orchards at Lentini and conventionally managed orchards at both Ramacca and Lentini (Fig. 8 and Table 4). Factors that significantly influenced the fungal component of soil microbiome included the irrigation system, the tillage number, the farming system and the soil TN. Notably, the soil TN influenced the assembly of fungal communities across all orchards in the Siracusa municipality (Fig. 8, Table 4). Moreover, soil tillage repeated three-times a year significantly affected the fungal communities in conventionally managed orchards at Mineo, while when repeated four-times affected the fungal communities in conventionally managed orchards at Lentini. Sprinklers (T-shaped) system influenced fungal communities in organically managed orchards at Mineo, while microsprinklers inter-row irrigation affected communities in conventional orchards from Syracuse. Lastly, organic farming system influenced the fungal communities in orchards at Lentini (Fig. 8, Table 4).

Finally, the rootstock 'sour orange' emerged as a key factor influencing prokaryotic communities, in conventionally managed orchards, after the exclusion of the geographical location effect (Fig. 8, Table 4).

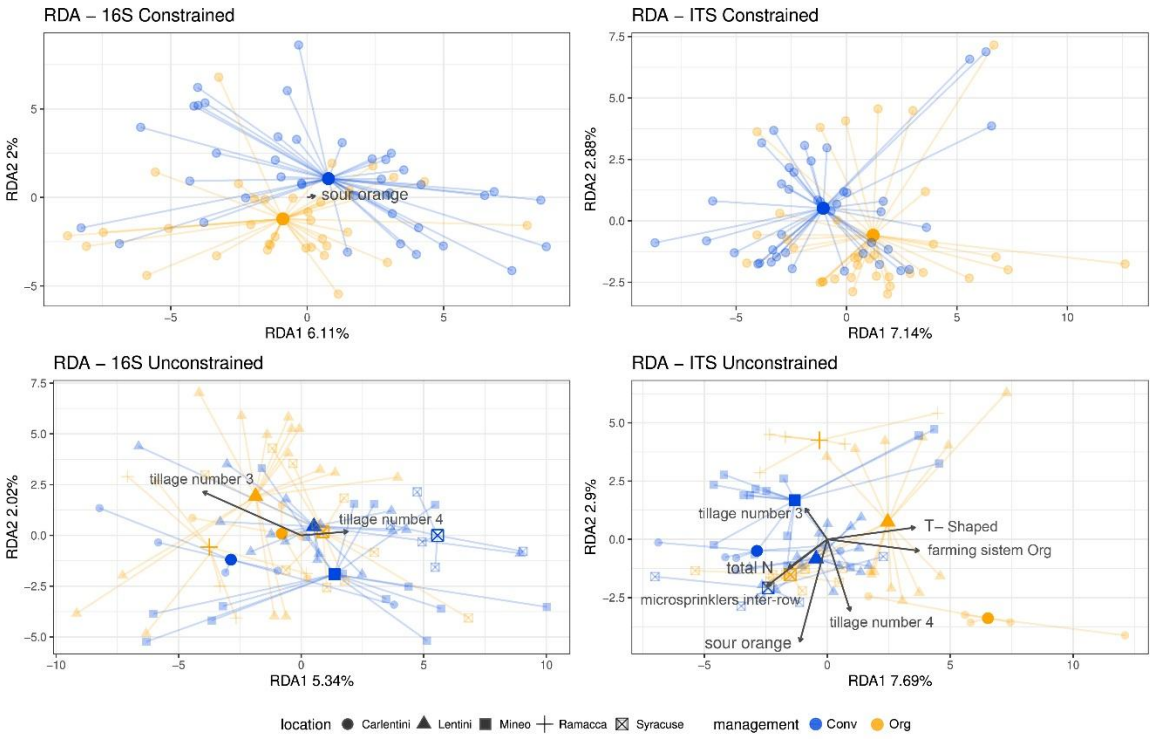

Figure 8. Redundancy analysis (RDA) for summer samples where sampling site effect was removed (top) and included (bottom) with forward model selection using physicochemical properties and experimental factors as linear predictors for 16S and ITS markers (panel c).

5.5 Discussion

Findings of this study showed the microbial communities associated with the soil explored by fine roots of citrus trees were influenced by diverse factors. According with the PERMANOVA analysis both bacterial and fungal communities grouped mostly according with the sampling site, which accounted for the largest proportion of variance. This result is consistent with a previous metagenomics study of tomato root microbiome which demonstrated that the sampling site impacted the bacterial communities more than root compartments (Anzalone et al., 2021). The classic microbiological approach in characterizing the soil microbiota of plants distinguishes diverse compartments of the interface between root and soil, i.e. rhizosphere, rhizoplane and bulk soil (Gregory, 2006; Barillot et al., 2013; Guo et al., 2024). In this study, the analysis of a large volume of soil from the horizon explored by fine roots was preferred to a fine resolution of microbial

communities of root-soil interface compartments, as the focus was on the effects of farming management on soil microbime associated with a perennial tree crop with an extended root system. Accordingly, soil sampling conformed to the protocol used by other authors in similar studies, who referred to soil samples containing fine roots as rhizosphere soil in a broader sense (Si et al., 2018; Lazcano et al., 2021). The effect of sampling site on soil microbiota is difficult to decipher as it is the result of complex interactions of several intrinsic and environmental factors. However, in this study the effects of some of these factors were separated and measured. Along with sampling site, other factors, such as sampling season (summer as opposed to winter), soil type, frequency and depth of soil tillage, irrigation system (drip, T- shaped sprinklers or microsprinkler) and rootstock genotype (sour orange as opposed to citrange) had a lower albeit significant impact on both prokaryotes and fungi, while the influence of tree age and health status was negligible. Interestingly, both prokaryotic and fungal communities of soil microbiome were influenced by the farming system (organic as opposed to conventional). In this respect, results confirmed the efficacy of BeCrop® indexes in fine tuning the analysis of the effects of management system on the structure and functionality of soil microbiome (Acedo et al., 2022). Organically managed orchards compared to those managed conventionally showed a higher microbial diversity as well as a unique composition of nutrient-cycling bacteria, which are crucial for enhancing soil fertility and plant health. Moreover, this study revealed that organic management promotes beneficial microbial functions, such as nitrogen fixation and phosphorus solubilisation. The significant influence of organic management on the enzymatic activity of rhizosphere soil microbiota observed in this study is consistent with the findings of Järvan et al., (2014), who reported noticeable effects of this farming system on the enzymatic activity of soil microbiota. Conversely, no significant difference was observed in most chemical soil properties between organically and conventionally managed citrus orchards, with the exception of TC carbon content which was significantly higher in organically managed orchards. As regards the effects of organic farming system on the physicochemical properties of soil, conflicting reports can be found in the literature. The prevailing opinion is that the transition to organic management improves key soil parameters such as pH, organic carbon, total nitrogen content, and the C:N ratio, with favourable effects on beneficial microbial activity (Canali et al., 2012; Montes-Borrego et al., 2013). However, other factors, such as the inherent soil nature depending mostly on its genesis, may prevail on management practices in conditioning and determining some soil physiochemical properties (Montes-Borrego et al., 2013; Blanco et al., 2024). As a

matter of fact, analysis revealed that the soil texture, exerted a significant effect in shaping both soil bacterial and fungal communities and influencing their functionality in surveyed citrus orchards of eastern Sicily. Silt and silt loam soils retain a higher amount of water and nutrients, supporting diverse microbial populations essential for nutrient cycling processes like carbon sequestration and nitrogen transformations. By contrast, sandy loam soils, which possess a lower water retention capacity, tend to support microbial communities more adapted to fluctuating moisture conditions, resulting in distinct nutrient cycling dynamics (Fierer and Jackson, 2006; Rillig et al., 2017). As for another soil property, soil organic C, it is known that it may be influenced more by other factors such as tree age than by management practices (Pardon et al., 2017; Mercado-Blanco et al., 2018; Zayani et al., 2023). Quite interestingly, in the present study the biochemical functions of rhizosphere soil microbioma as expressed by BeCrop® indices not only showed significant differences between organically and conventionally managed orange orchards but also a different seasonal pattern in the two farming systems. The indexes for C, Mn transport equilibrium and organic P assimilation of soils from organically managed orchards, in summer were higher than in conventionally managed orchards. By contrast, in winter indexes for Cu export, fermentation and N of soils from organically managed orchards were higher than in conventionally managed orchards. These results are in agreement with results of other authors indicating an enhancement of C and nutrient dynamics in organically managed systems (Canali et al., 2012; Berthrong et al., 2013; Roussos et al., 2019). Berthrong et al. (2013) highlighted the greater efficiency of respiration per unit of soil organic C in organically managed systems. According with these authors, the mulching of leaves in organic systems contributed to increase the litter biomass in the soil, enhancing microbial enzymatic activity. Moreover, Berthrong et al. (2013) reported that pesticides may have detrimental effects on certain groups of soil microrganisms. To confirm the complex relationships among management practices and biochemical functions of soil microbioma, BeCrop® indexes related to Mn, K, and N metabolism in conventionally managed orchards were significantly higher, whereas the index relative to inorganic C consumption was lower than in organically managed orchards. This is consistent with results of previous studies, reporting lower K and N availability in soil of organically managed systems, probably due to the lack of synthetic fertilizer supply (Stalenga, 2007; Canali et al., 2012). Berthrong et al. (2013) observed that microbial communities in soils of organically managed systems were more efficient at mineralizing N than soils of conventionally managed ones. It has been hypothesized the enhanced metabolism of organic C, P assimilation, and inorganic N

consumption in organic systems is linked to a greater microbial diversity (Mäder et al., 2002; Lori et al., 2017). Overall these findings suggest organic management may directly or indirectly influence the biochemical functions of soil microbioma, improving the capacity of soil to retain, metabolize and recycle organic matter, nutrients and even pollutants (Mauro et al., 2015; Rillig et al., 2017).

As for the effects of farming system on the diversity of soil microbiota in orange orchards results of this study indicate that there were no great differences between core microbiota of organically and conventionally managed orchards. However, there are differences in the seasonal pattern of microbial communities between the two farming systems. *Proteobacteria*, *Actinobacteriota*, and *Acidobacteriota*, were the predominant bacterial phyla across both systems, consistently with previous global mapping studies of soil microbial communities of the citrus rhizosphere (Xu et al., 2018). However, in winter *Chloroflexi* were detected exclusively in conventionally managed orchards, suggesting a possible effect of management system on bacterial community composition. *Proteobacteria*, *Actinobacteriota*, and *Acidobacteriota* remained dominant in both management systems across seasons, highlighting their fundamental role in citrus rhizosphere soils. Additionally, *Crenarchaeota* and *Firmicutes* were present in both management systems across all seasons. The fungal communities were predominantly composed of the phylum *Ascomycota*, regardless of management practices or season. During winter, the *Basidiomycota* was the second most prevalent phylum, particularly in conventionally managed orchards, while *Mortierellomycota* prevailed in summer, once again particularly in conventionally managed orchards. All three phyla were detected in both summer and winter. These findings are consistent with the results of Wu et al. (2021), who identified *Ascomycota* and *Mortierellomycota* as the most represented fungal phyla in soil microbiota. Similarly, Xi et al. (2023) reported *Ascomycota* as the predominant phylum in soil mycobiota, with higher relative abundance of *Basidiomycota* compared to *Mortierellomycota*. It is noteworthy that in winter, the bacterial genus *Nitrospira* was exclusively present in the core microbiome of soil from organically managed orchards. The presence of this bacterium, which has a crucial role in nitrification, might be related with a higher efficiency of the N cycle in organic systems during the winter. The genus *Nitrospira*, which is also involved in the nitrification process, exhibited a significantly greater abundance in organically managed orchards in winter. This taxon plays a pivotal role in the nitrification of ammonia (NH^{3+}) to nitrate ($NO3$-), a N form available to plants (Rice et al., 2016; Li et al., 2019). This would confirm a higher efficiency of the N cycle in

organic systems during the winter. Another relevant difference of the soil microbiota between organic and conventional farming systems is the richness in fungal taxa observed in organically managed orchards, particularly in winter. The number of fungal taxa detected in rhizosphere soil of organically managed orchards was 54, as opposed to 25 detected in soil of conventionally managed orchards. In particular, *Chaetomium convolutum*, a well-known biocontrol agent (BCA), exhibited differential abundance in organically managed orchards. This BCA has been demonstrated to be effective against a wide range of plant diseases, including root rot of citrus (Hung et al., 2015). Similarly, *Sphingobacterium*, which has been demonstrated to be a potential BCA of citrus diseases (Ezrari et al., 2021) and *Arthrobacter globiformis*, which has been reported to confer salt tolerance (Stassinos et al., 2022), were significantly more abundant in soil of organically managed orchards. Based on these findings, it can be speculated that organic management may improve the resilience of citrus trees to biotic and abiotic stresses. As for the effects of environmental factors on the structure of rhizosphere soil microbiota in citrus orchards, PCoA analysis showed that the prokaryotic component was predominantly influenced by geographical location and soil type, while the fungal component was influenced by the irrigation systems and exhibited significant seasonal variation. These findings are consistent with those of Mercado-Blanco et al. (2018), which reported that fungal communities were sensitive to seasonal changes and irrigation systems. Also bacterial communities fluctuate in response to seasons, which exert their influence more on α-diversity than β-diversity of these communities (Lauber et al., 2013). Results of this study indicated that both prokaryotic and fungal communities were significantly impacted by both the frequency and depth of tillage, confirming previous research indicating that microbial communities exhibit greater stability under reduced soil management regimes (Bevivino et al., 2014).

A general aspect highlighted by the analysis of the 16S (prokaryotes) and ITS (fungi) microbial networks is the significantly higher proportion of co-exclusion associated with organic management compared to those observed in conventionally managed orchards. Co-exclusion refers to the tendency of two species not to coexist in the same environment or ecological niche, often due to direct competition or antagonism. An increased level of co-exclusion might indicate that, in organically managed contexts, microorganisms may actively inhibit the presence or expansion of competitors, fostering a more competitive yet dynamically balanced microbial ecosystem. A study of other authors, focusing on the impact of organic versus conventional management on the diversity and community

structure of bacteria and fungi in tea plantations, demonstrated that under organic management soil micro-ecological networks are significantly more complex and stable (Huang et al., 2923). This would indicate that organic management fosters cooperative relationships among microbial species, enhancing soil resilience, while conventional management results in less complex microbial networks that are more susceptible to environmental stress (Huang et al., 2023). Overall, these findings suggest that organic management promotes a more resilient soil ecosystem. In the present study, the Shannon index for soil microbiome fungi was found to be significantly higher in organically managed orchards compared to those managed conventionally, consistently with previous studies that demonstrated an increase in soil microbial diversity under organic management (Montes Borrego et al., 2013; Shen et al., 2015; Schmidt et al., 2019; Ares et al., 2021; Suyal et al., 2021; Huang et al., 2023). Similarly, in the present study the Chao index indicated significantly higher richness in organically managed citrus orchards. Scotton et al., (2020) found that transitioning from conventional to organic management in citrus orchards in Brazil increased soil fungal diversity, as a consequence of a progressive reduction in the use of chemical substances. Similarly, Panelli et al. (2017) observed that organically managed and no-tillage crop soil hosted richer fungal consortia compared to those managed conventionally, with a predominance of *Ascomycota*.

As suggested by previous studies, higher microbial diversity can limit the invasion capacity of pathogenic species by saturating available ecological niches and increasing competition for resources (Van Elsas et al., 2012). Additionally, organic management appears to significantly influence the formation of more discrete and specialized prokaryotic networks, characterized by a significant increase in co-occurrence modularity. This implies that groups of microorganisms tend to form well-defined subcommunities, within specialized ecological niches (Wang et al., 2021). This type of organization reflects a complex and stratified microbial ecosystem, where intra-group interactions are more prevalent than those between different groups. For example, the modularization of microbial networks was observed in arid agricultural ecosystems, where the combined effect of irrigation and fertilization practices increased the modularity of bacterial networks and was positively correlated with soil fertility and crop productivity (Ye et al., 2021). The greater co-occurrence of microbial community members in organic agriculture would indicate a higher ecological balance and increased complexity, potentially making microbiomes of organically managed systems more resilient to environmental stress (Banerjee et al., 2019) .

The analysis of the structure and functionality of soil microbiome complements other methods such as Life Cycle Assessment (LCA) and Carbon Footprint (CF) in evaluating the sustainability of organic farming systems in citriculture (Ribal et al 2017 and 2019). Moreover, it paves the way toward the development of strategies based on engineered synthetic microbial consortia (McCarty et al., 2019, Duncker et al., 2021, Mahmud et al., 2021, Contreras-Salgado et al., 2024, Gómez-Lama Cabanás and Mercado-Blanco, 2025), which represent a promising breakthrough to manage plant diseases, enhance crop productivity and improve ecological sustainability in agriculture.

5.6 Conclusion

This study provides new insights into the effects of management practices and environmental variables on the structure and functionality of soil microbiome in commercial citrus orchards. Sampling site accounted for the highest proportion of variance observed in soil microbial communities associated with the roots of citrus trees underscoring the importance of spatial factor in interpreting the effects of cropping systems on the soil microbiome. Findings demonstrate that organic management fosters richer and more diverse soil microbial communities and enhances their functionality in terms of nutrient cycling and stress mitigation. In particular, organic farming system favoured beneficial processes, such as nitrogen fixation and organic phosphorus solubilization, which are critical for soil fertility. Bioinformatics processing of metagenomic data proved to be a powerful tool for elucidating the complex interactions among intrinsic soil and plant characteristics, environmental variables, management practices and root-associated microbial assemblages.

Overall, results confirm the rhizosphere microbiome is an indicator of both soil health status and ecological sustainability of management practices in citrus orchards. With the analysis of major factors shaping the soil microbiome, this study along with LCA and CF provides information for designing eco-friendly management strategies in citriculture.

CRediT author statement.

Sebastiano Conti Taguali: Conceptualization, Investigation, Methodology, Data Curation, Formal analysis, Validation, Writing - Original Draft, Writing - Review & Editing.

Rhea Pöter: Conceptualization , Investigation, Methodology, Data Curation, Validation, Writing - Original Draft, Writing - Review & Editing.

Francesco Aloi: Conceptualization, Investigation, Methodology, Data Curation, Formal analysis.

Clara Fernández-Trujillo: Methodology, Software, Data Curation, Formal analysis.

Alberto Acedo: Methodology, Software, Data Curation, Formal analysis.

Federico La Spada: Investigation, Methodology, Formal analysis, Writing - Original Draft, Writing - Review & Editing.

Maria Giulia Li Destri Nicosia: Writing - Review & Editing, Supervision, Funding acquisition.

Leonardo Schena: Writing - Review & Editing, Supervision, Funding acquisition.

Antonella Pane: Investigation, Writing - Review & Editing, Resources, Supervision.

Santa Olga Cacciola: Conceptualization, Investigation, Writing - Original Draft, Validation, Writing - Review & Editing, Resources, Supervision, Funding acquisition, Project administration.

FUNDS

This study was supported by the University of Catania, Italy, "Investigation of Phytopathological problems of the main Sicilian productive contexts and eco-sustainable defense strategies (MEDIT-ECO)"- PiaCeRi-PIAno di inCEntivi per la Ricerca di Ateneo 2020-22 linea 2" "5A722192155"; the project "Fields4ever" funded by the European Union's Horizon 2020 research and innovation programme under grant agreement No 947084; the project "Smart and innovative packaging, postharvest rot management, and shipping of organic citrus fruit (BiOrangePack)" under Partnership for Research and Innovation in the Mediterranean Area (PRIMA) – H2020 (E69C20000130001); the European Union (NextGeneration EU), through the MUR-PNRR project SAMOTHRACE (ECS00000022) and the project "PROMETEO", Strategic project ENI Italy-Tunisia 2014–2020.

Conflict of interest: Authors declare no conflict of interest. A.A. is a cofounder and C.F. are current employees of Biome Makers.

Declaration of availability of supplementary material

The raw bacterial (16S) and fungal (ITS) amplicon sequencing data have been deposited in the NCBI Se-quence Read Archive (SRA) under BioProject accession number PRJNA1242073.

The supplementary data of this study will be available to the evaluators upon request to the corresponding author.

Results of this study have been submitted as a scientific article to the Applied Soil Ecology – ScienceDirect (ELSEVIER)

5.7 References

Abdelfattah, A., Cacciola, S.O., Mosca, S., Zappia, R., Schena, L. (2017) Analysis of the fungal diversity in citrus leaves with greasy spot disease symptoms. Microbial Ecology 73, 739–749. doi: 10.1007/s00248-016-0874-x

Abdelfattah, A., Sanzani, S.M., Wisniewski, M., Berg, G., Cacciola, S.O., Schena, L. (2019) Revealing cues for fungal interplay in the plant–air interface in vineyards. Frontiers in Plant Science 10, 922. doi: 10.3389/fpls.2019.00922

Acedo, A., Ortega-Arranz, H. Almonacid, D., Ferrero, A. (2022) Methods and systems for generating and applying agronomic indices from microbiome-derived parameters (Patent No. US 2022/0268756 A1).

Acin-Albiac, M., García-Jiménez, B., Marín Garrido, C., Borda Casas, E., Velasco-Alvarez, J., Serra, N.S., Acedo, A. (2023) Lettuce soil microbiome modulated by an L-α-Amino Acid-based biostimulant. Agriculture 13, 344. doi:10.3390/agriculture13020344

Adamo, I., Acin-Albiac, M., Röttjers, S., de Prado, D.R., Benito, B.M., Zamora, J., Godara R, García-Jimènez, B., Jiang-Rempel, P., Cline L.C., Acedo, A. (2024) Short impact on soil microbiome of a *Bacillus amyloliquefaciens* QST713-based product that correlates with higher potato yield across the USA. Frontiers in Plant Science, 15, 1332840. doi: 10.3389/fpls.2024.1332840

Ali, S., Tyagi, A., Bae, H. (2023) Plant microbiome: An ocean of possibilities for improving disease resistance in plants. Microorganisms 11, 392. doi:10.3390/microorganisms11020392

Anzalone, A., Di Guardo, M., Bella, P., Ghadamgahi, F., Dimaria, G., Zago, R., Cirvilleri, G., Catara, V. (2021) Bioprospecting of beneficial bacteria traits associated with tomato root in greenhouse environment reveals that sampling sites impact more than the root compartment. Front.iers in Plant Sciences 12, 637582. doi: 10.3389/fpls.2021.637582

.

Ares, A., Costa, J., Joaquim, C., Pintado, D., Santos, D., Messmer, M.M., Mendes-Moreira, P.M. (2021) Effect of low-Input organic and conventional farming systems on maize rhizosphere in two portuguese open-pollinated varieties (OPV), "Pigarro" (improved landrace) and "SinPre" (a composite cross population). Frontiers in Microbiology 12, 636009. doi:10.3389/fmicb.2021.636009

Banerjee, S., Walder, F., Büchi, L., Meyer, M., Held, A.Y., Gattinger, A., Keller, T., Charles, R., van der Heijden, M.G.A. (2019) Agricultural intensification reduces microbial network complexity and the abundance of keystone taxa in roots. ISME Journal 13, 1722–1736. doi:10.1038/s41396-019-0383-2

Bansal, S., Gonzalez-Maldonado, N., Yao, E., Wong, C.T., Adamo, I., Acin-Albiac, M., García-Jiménez, B., Acedo, A., Lazcano, C. (2025) Regenerative soil management practices no-till and sheep grazing induce significant but contrasting short-term changes in the vineyard soil microbiome. Plants, People, Planet 7, 176-193. doi: 10.1002/ppp3.10575

Barillot, C.D.C., Sarde, CO., Bert, V., Tarnaud, E., Cochett, N. (2013) A standardized method for the sampling of rhizosphere and rhizoplan soil bacteria associated to a herbaceous root system. Annals of Microbiology 63, 471–476. doi:10.1007/s13213-012-0491-y

Berthrong, S.T., Buckley, D.H., Drinkwater, L.E. (2013) Agricultural Management and Labile Carbon Additions Affect Soil Microbial Community Structure and Interact with Carbon and Nitrogen Cycling. Microbial Ecology 66, 158–170. doi:10.1007/s00248-013-0225-0

Bevivino, A., Paganin, P., Bacci, G., Florio, A., Pellicer, M.S., Papaleo, M.C., Mengoni, A., Ledda, L., Fani, R., Benedetti, A., Dalmastri, C. (2014) Soil bacterial community response to differences in agricultural management along with seasonal changes in a Mediterranean region. PLoS ONE 9, e105515. doi:10.1371/journal.pone.0105515

Blanco, P., Rodríguez, I., Fernández-Fernández, V., Ramil, M., Castrillo, D., Acín-Albiac, M., Adamo, I., Fernández-Trujillo, C., García-Jiménez, B., Acedo, A., Calvo-Portela, N., Parente-Sendín, A., Acemel-Míguez, L., Alonso-Vega, F. (2024) Physicochemical properties and microbiome of vineyard soils from DOP Ribeiro (NW Spain) are influenced by agricultural management. Microorganisms 12, 1–26. doi:10.3390/microorganisms12030595

Bridges, E.M., 1978. World soils 2nd ed. Cambridge University Press. Cambridge, UK. ISBN 0521 29339 1

Canali, S., Roccuzzo, G., Tittarelli, F., Ciaccia, C., Stagno, F., Intrigliolo, F. (2012) Organic citrus: Soil fertility and plant nutrition management, in: Srivastava, A.K. (Ed.), Advances in Citrus Nutrition. Springer Science+Business. doi:10.1007/978-94-007-4171-3_24

Carrión, V.J., Perez-Jaramillo, J., Cordovez, V., Tracanna, V., De Hollander, M., Ruiz-Buck, D., Mendes, L.W., van Ijcken, W.F.J., Gomez-Exposito, R., Elsayed, S.S., Mohanraju, P., Arifah, A., van der Oost, J., Paulson, J.N., Mendes, R., van Wezel, G.P., Medema, M.H., Raaijmakers, J.M. (2019) Pathogen-induced activation of disease-suppressive functions in the endophytic root microbiome. Science 366, 606–612. doi:10.1126/science.aaw9285

Ciriminna, R., Angellotti, G., Luque R., Pagliaro M. (2024) The citrus economy in Sicily in the early bioeconomy era : a case study. Biofuels, Bioproducts and Biorefinings 18, 356–364. doi:10.1002/bbb.2588

Contreras-Salgado, E. A., Sánchez-Morán, A. G., Rodríguez-Preciado, S. Y., Sifuentes-Franco, S., Rodríguez-Rodríguez, R., Macías-Barragán, J., Díaz-Zaragoza, M. (2024) Multifaceted applications of synthetic microbial communities: Advances in biomedicine, bioremediation, and industry. Microbiology Research 15, 1709-1727. doi; 10.3390/microbiolres15030113

Costantini, E.A., Barbetti, R., Fantappiè, M., L'Abate, G., Lorenzetti, R., Magini, S. (2013) Pedodiversity, in: Costantini, E., Dazzi, C. (Ed.), The Soils of Italy. World Soils Book Series. Springer, Dordrecht. doi:https://doi.org/10.1007/978-94-007-5642-7_6

IUSS Working Group WRB. 2022. World Reference Base for Soil Resources. International soil classification system for naming soils and creating legends for soil maps. 4th edition. International Union of Soil Sciences (IUSS), Vienna, Austria

De Vries, F.T., Griffiths, R.I., Knight, C.G., Nicolitch, O., Williams, A. (2020) Harnessing rhizosphere microbiomes for drought-resilient crop production. Science 368, 270–274. doi:10.1126/science.aaz5192

Dewdney, M.M., Peres, N.A., 2018. Citrus Black Spot. EDIS. doi:10.32473/edis-pp274-2018

Duncker, K.E., Holmes, Z.A., You, L. (2021) Engineered microbial consortia: strategies and applications. Microbial Cell Factories 20, 211 doi:10.1186/s12934-021-01699-9

Edgar, R.C., Flyvbjerg, H. (2015) Error filtering, pair assembly and error correction for next-generation sequencing reads. Bioinformatics 31, 3476–3482. doi:10.1093/bioinformatics/btv401

Edgar, R.C., Haas, B.J., Clemente, J.C., Quince, C., Knight, R. (2011) UCHIME improves sensitivity and speed of chimera detection. Bioinformatics 27, 2194–2200.

doi:10.1093/bioinformatics/btr381

Ezrari, S., Mhidra, O., Radouane, N., Tahiri, A., Polizzi, G., Lazraq, A., Lahlali, R. (2021) Potential role of rhizobacteria isolated from citrus rhizosphere for biological control of citrus dry root rot. Plants 10. doi:10.3390/plants10050872

Ezrari, S., Radouane, N., Tahiri, A., El Housni, Z., Mokrini, F., Özer, G., Lazraq, A., Belabess, Z., Amiri, S., Lahlali, R. (2022) Dry root rot disease, an emerging threat to citrus industry worldwide under climate change: A review. Physiological and Molecular Plant Pathology 117, 101753. doi:10.1016/j.pmpp.2021.101753

Faddetta ,T., Abbate , L., Alibrandi, P., Arancio, W., Siino, D., Strati, F., De Filippo, C., Fatta Del Bosco, F., Carimi, F., Puglia ,A.M., Cardinale, M., Gallo, G., Mercati, F. (2021) The endophytic microbiota of *Citrus limon* is transmitted from seed to shoot highlighting differences of bacterial and fungal community structures. Scientific Reports 11, 7078. doi.org/10.1038/s41598-021-86399-5

FAO, 2021. Citrus Fruit Statistical Compendium. Rome, Italy. doi:https://openknowledge.fao.org/handle/20.500.14283/cb6492en

Fierer, N., Jackson, R.B. (2006) The diversity and biogeography of soil bacterial communities. Proceedings of the National Academy of Sciences of the United States of America 103, 631. doi:10.1073/pnas.0507535103

Fierotti, G., Dazzi, C., Raimondi, S. (1988). Commento alla carta dei suoli siciliani - Commentary on the map of Sicilian soils (In Italian). Palermo.

Glöckner, F.O., Yilmaz, P., Quast, C., Gerken, J., Beccati, A., Ciuprina, A., Bruns, G., Yarza, P., Peplies, J., Westram, R., Ludwig, W. (2017) 25 years of serving the community with ribosomal RNA gene reference databases and tools. Journal of Biotechnology 261, 169–176. doi:10.1016/j.jbiotec.2017.06.1198

Gobbi, A., Santini, R.G., Filippi, E., Ellegaard-Jensen, L., Jacobsen, C.S. & Hansen, L.H.(2019) Quantitative and qualitative evaluation of the impact of the G2 enhancer, bead sizes and lysing tubes on the bacterial community composition during DNA extraction from recalcitrant soil core samples based on community sequencing and qPCR. PLoS ONE, 14, e0200979. https://doi.org/10.1371/journal.pone.0200979

Gobbi, A., Acedo, A., Imam, N., Santini, R.G., Ortiz-Álvarez, R., Ellegaard-Jensen, L., Belda, I., Hansen, LH. (2022) A global microbiome survey of vineyard soils highlights the microbial dimension of viticultural *terroirs*. Communications Biology 5, 241. doi: 10.1038/s42003-022

Gómez-Lama Cabanás, C., Mercado-Blanco, J. (2025) Groundbreaking Technologies and the Biocontrol of Fungal Vascular Plant Pathogens. Journal of Fungi 11, 77.

https://doi.org/10.3390/jof11010077703202-5

Gregory, P.J. (2006) Roots, rhizosphere and soil: the route to a better understanding of soil science?European Journal of Soil Science, 57, 2–12. doi: 10.1111/j.1365-2389.2005.00778.x

Guo, T., Yao, X., Wu, K., Guo, A.,Yao, Y. (2024) Response of the rhizosphere soil microbial diversity to different nitrogen and phosphorus application rates in a hulless barley and pea mixed-cropping system. Applied Soil Ecology 195, 105262. doi.org/10.1016/j.apsoil.2023.105262

Huang, X., Zheng, Y., Li, P., Cui, J., Sui, P., Chen, Y., Gao, W. (2023) Organic management increases beneficial microorganisms and promotes the stability of microecological networks in tea plantation soil. Frontiers in Microbiology 19. doi:10.3389/fmicb.2023.12

Hung, P.M., Wattanachai, P., Kasem, S., Poeaim, S. (2015) Efficacy of *Chaetomium* species as biological control agents against *Phytophthora nicotianae* root rot in citrus. Mycobiology 43, 288–296. doi:10.5941/MYCO.2015.43.3.288

Imam, N., Belda, I., García-Jiménez, B., Duehl, A.J., Doroghazi, J.R., Almonacid, D.E., Varghese, P.T., Acedo, A. (2021) Local network properties of soil and rhizosphere microbial communities in potato plantations treated with a biological product are important predictors of crop yield. mSphere 6, e00130-21. doi: 10.1128/mSphere.00130-21.

Järvan, M., Edesi, L., Adamson, A., Võsa, T. (2014) Soil microbial communities and dehydrogenase activity depending on farming systems. Plant, Soil and Environment 60, 459–463. doi:10.17221/410/2014-pse

Lauber, C.L., Ramirez, K.S., Aanderud, Z., Lennon, J., Fierer, N. (2013) Temporal variability in soil microbial communities across land-use types. ISME Journal 7, 1641–1650. doi:10.1038/ismej.2013.50

Lazcano, C., Boyd, E., Holmes, G., Hewavitharana, S., Pasulka, A., Ivors, K. (2021) The rhizosphere microbiome plays a role in the resistance to soil-borne pathogens and nutrient uptake of strawberry cultivars under field conditions. Scientific Reports 11, 3188. doi: 10.1038/s41598-021-82768-2

Li, C., Hu, H.W., Chen, Q.L., Chen, D., He, J.Z. (2019) Comammox *Nitrospira* play an active role in nitrification of agricultural soils amended with nitrogen fertilizers. Soil Biology and Biochemistry 138, 107609. doi:10.1016/j.soilbio.2019.107609

Liao, J., Xu, Q., Xu, H. & Huang, D. (2019) Natural farming improves soil quality and alters microbial diversity in a cabbage field in Japan. *Sustainability (Switzerland)*, 11, 3131.

https://doi.org/10.3390/su11113131

Lima, H.S., Mancine, N., Peruchi, G.B., Francisco, C.S., Wang, N., de Souza ,R.S.C., Armanhi, J.S.L., Della Coletta-Filho, H. (2024) Microbial community of cultivated and uncultivated citrus rhizosphere microbiota in Brazil. Scientific Data. 11, 1294. doi: 10.1038/s41597-024-04141-y.

Lombardo, M.F., Zhang ,Y., Xu J., Trivedi, P., Zhang, P., Riera, N., Li, L., Wang, Y., Liu ,X., Fan, G., Tang, J., Coletta-Filho ,H.D., Cubero, J., Deng, X., Ancona, V., Lu Z., Zhong, B., Roper, M.C., Capote, N., Catara, V., Pietersen, G., Al-Sadi, A.M., Xu, X., Wang, J., Yang, H., Jin, T., Cirvilleri, G., Wang, N. (2024) Global citrus root microbiota unravels assembly cues and core members. Frontiers in Microbiology 15, 1405751. doi: 10.3389/fmicb.2024.1405751

Lori, M., Symnaczik, S., Mäder, P., De Deyn, G., Gattinger, A. (2017) Organic farming enhances soil microbial abundance and activity—A meta-analysis and meta-Regression. PLoS ONE 12, e0180442. doi:10.1371/journal.pone.0180442.

Luo, C., He, Y., Chen,Y. (2025). Rhizosphere microbiome regulation: Unlocking the potential for plant growth, Current Research in Microbial Sciences 8, 100322, doi:10.1016/j.crmicr.2024.100322.

Mäder, P., Fließbach, A., Dubois, D., Gunst, L., Fried, P., Niggli, U. (2002) Soil fertility and biodiversity in organic farming. Science 296, 1694–1697. doi:10.1126/science.1071148

Mahé, F., Czech, L., Stamatakis, A., Quince, C., De Vargas, C., Dunthorn, M., Rognes, T. (2022) Swarm v3: towards tera-scale amplicon clustering. Bioinformatics 38, 267–269. doi:10.1093/bioinformatics/btab493

Mahmud, K., Missaoui, A, Lee, K., Ghimire, B., Presley, H.W, Shiva Makaju, S. (2021) Rhizosphere microbiome manipulation for sustainable crop production, Current Plant Biology, 27, 100210, doi;10.1016/j.cpb.2021.100210.

Martin, F.M., Uroz, S., Barker, D.G. (2017) Ancestral alliances: Plant mutualistic symbioses with fungi and bacteria. Science 356. doi:10.1126/science.aad4501

Martin, M. (2011) Cutadapt removes adapter sequences from high-throughput sequencing reads. EMBnet.Journal 17, 10–12. doi:10.14806/ej.17.1.200

Mauro, R.P., Anastasi, U., Lombardo, S., Pandino, G., Pesce, R., Restuccia, A., Mauromicale, G. (2015) Cover crops for managing weeds, soil chemical fertility and nutritional status of organically grown orange orchard in Sicily. Italian Journal of Agronomy 10, 641. doi:10.4081/ija.2015.641

McCarty, M,S., Ledesma-Amaro, R. (2019) Synthetic biology tool to engineer microbial

communities for biotechnology. Trends in Biotechnology 37, 181-197. doi: 10.1016/j.tibtech.2018.11.002

McMurdie, P.J., Holmes, S. (2013) Phyloseq: An R Package for Reproducible Interactive Analysis and Graphics of Microbiome Census Data. PLoS ONE 8, e61217. doi:10.1371/journal.pone.0061217

Mendes, R., Kruijt, M., De Bruijn, I., Dekkers, E., Van Der Voort, M., Schneider, J.H.M., Piceno, Y.M., DeSantis, T.Z., Andersen, G.L., Bakker, P.A.H.M., Raaijmakers, J.M. (2011). Deciphering the rhizosphere microbiome for disease-suppressive bacteria. Science 332, 1097–1100. doi:10.1126/science.1203980

Mercado-Blanco, J., Abrantes, I., Caracciolo, A.B., Bevivino, A., Ciancio, A., Grenni, P., Hrynkiewicz, K., Kredics, L., Proença, D.N. (2018) Belowground microbiota and the health of tree crops. Frontiers in Microbiology 9. doi:10.3389/fmicb.2018.01006

Milke, F., Rodas-Gaitan, H., Meissner, G., Masson, V., Oltmanns, M., Möller, M., Wohlfahrt, Y., Kulig, B., Acedo, A., Athmann, M., Fritz, J. (2024) Enrichment of putative plant growth promoting microorganisms in biodynamic compared with organic agriculture soils. ISME Communications 4, ycae021. doi:10.1093/ismeco/ycae021

Mo, X., Huang, Q., Chen, C., Xia, H., Riaz, M., Liang, X., Li, J., Chen, Y., Tan, Q., Wu, S., Hu, C. (2024) Characteristics of rhizosphere microbiome, soil chemical properties, and plant biomass and nutrients in *Citrus reticulata* cv. Shatangju exposed to increasing soil Cu levels. Plants 13, 2344. doi.: 10.3390/plants13172344

Mondello, V., Lemaître-Guillier, C., Trotel-Aziz, P., Gougeon, R., Acedo, A., Schmitt-Kopplin, P., Adrian, M., Pinto, C., Fernandez, O., Fontaine, F. (2022) Assessment of a new copper-based formulation to control esca disease in field and study of its impact on the vine microbiome, vine physiology, and enological parameters of the juice. Journal of Fungi, 8, 151. doi: 10.3390/jof8020151

Montes-Borrego, M., Navas-Cortés, J.A., Landa, B.B. (2013) Linking microbial functional diversity of olive rhizosphere soil to management systems in commercial orchards in southern Spain. Agriculture, Ecosystems and Environment 181, 169–178. doi:10.1016/j.agee.2013.09.021

Mukhametzyanov, R.R., Brusenko, S.V., Khezhev, A.M., Kelemetov, E.M., Kirillova, S.S. (2024) Changing the Global Production and Trade of Citrus Fruits., in: Popkova, E.G., Bogoviz, A.V., Sergi, B.S., Kaurova, O.V., Maloletko, A.N. (Eds.), In: (Eds) Sustainable Development of the Agrarian Economy Based on Digital Technologies and Smart Innovations., Cham. Advances in Science, Technology & Innovation. Springer. doi:https://doi.org/10.1007/978-3-031-51272-8_4

Nilsson, R.H., Larsson, K.H., Taylor, A.F.S., Bengtsson-Palme, J., Jeppesen, T.S., Schigel, D., Kennedy, P., Picard, K., Glöckner, F.O., Tedersoo, L., Saar, I., Kõljalg, U., Abarenkov, K. (2019) The UNITE database for molecular identification of fungi: Handling dark taxa and parallel taxonomic classifications. Nucleic Acids Research 47, D259–D264. doi:10.1093/nar/gky1022

Oksanen, J., Simpson, G.L., Blanchet, F.G., Kindt, R., Legendre, P., Minchin, P.R., O'Hara, R.B., Solymos, P., Stevens, M.H.H., Szoecs, E., Wagner, H., Barbour, M., Bedward, M., Bolker, B., Borcard, D., Carvalho, G., Chirico, M., Caceres, M.D., Durand, S., ... Weedon, J. (2024) Vegan: Community Ecology Package. R package version 2.6-6.1. Community Ecology Package.

Ortiz-Álvarez, R., Ortega-Arranz, H., Ontiveros, V.J., de Celis, M., Ravarani, C., Acedo, A., Belda, I. (2021) Network Properties of Local Fungal Communities Reveal the Anthropogenic Disturbance Consequences of Farming Practices in Vineyard Soils. MSystems 6, 10. doi:10.1128/msystems.00344-21

Panelli, S., Capelli, E., Comandatore, F., Landinez-Torres, A., Granata, M.U., Tosi, S., Picco, A.M. (2017) A metagenomic-based, cross-seasonal picture of fungal consortia associated with Italian soils subjected to different agricultural managements. Fungal Ecology 30, 1–9. doi:10.1016/j.funeco.2017.07.005

Parasuraman, P., Pattnaik, S., Busi, S. (2019) Phyllosphere microbiome: Functional importance in sustainable agriculture, in: New and Future Developments in Microbial Biotechnology and Bioengineering: Microbial Biotechnology in Agro-Environmental Sustainability. pp. 135–148. doi:10.1016/B978-0-444-64191-5.00010-9

Pardon, P., Reubens, B., Reheul, D., Mertens, J., De Frenne, P., Coussement, T., Janssens, P., Verheyen, K. (2017) Trees increase soil organic carbon and nutrient availability in temperate agroforestry systems, Agriculture, Ecosystems and Environment. Agriculture, Ecosystems & Environment. doi:10.1016/j.agee.2017.06.018

Pieterse, C.M.J., Zamioudis, C., Berendsen, R.L., Weller, D.M., Van Wees, S.C.M., Bakker, P.A.H.M. (2014) Induced systemic resistance by beneficial microbes. Annual Review of Phytopathology 52, 347–375. doi:10.1146/annurev-phyto-082712-102340

Ribal, J., Ramírez-Sanz, C., Estruch, V., Clemente, G,. Sanjuán, N. (2017) Organic versus conventional citrus. Impact assessment and variability analysis in the Comunitat Valenciana (Spain). International Journal of Life Cycle Assessment 22, 571–586. doi.org/10.1007/s11367-016-1048-2

Ribal, J., Estruch, V., Clemente, G.. Fenollosa, M.L., Sanjuán, N. (2019) Assessing

variability in carbon footprint throughout the food supply chain: a case study of Valencian oranges. International Journal of Life Cycle Assessment 24, 1515–1532. doi.org/10.1007/s11367-018-01580-9

Rice, M.C., Norton, J.M., Valois, F., Bollmann, A., Bottomley, P.J., Klotz, M.G., Laanbroek, H.J., Suwa, Y., Stein, L.Y., Sayavedra-Soto, L., Woyke, T., Shapiro, N., Goodwin, L.A., Huntemann, M., Clum, A., Pillay, M., Kyrpides, N., Varghese, N., Mikhailova, N., Markowitz, V., Palaniappan, K., Ivanova, N., Stamatis, D., Reddy, T.B.K., Ngan, C.Y., Daum, C. (2016) Complete genome of Nitrosospira briensis C-128, an ammonia-oxidizing bacterium from agricultural soil. Standards in Genomic Sciences 11, 46. doi:10.1186/s40793-016-0168-4

Richardson, A.E., Simpson, R.J. (2011) Soil Microorganisms Mediating Phosphorus Availability Update on Microbial Phosphorus. Plant Physiology 156, 989–996. doi:10.1104/pp.111.175448

Rillig, M.C., Muller, L.A.H., Lehmann, A. (2017) Soil aggregates as massively concurrent evolutionary incubators. ISME Journal 11, 1943–1948. doi:10.1038/ismej.2017.56

Robinson Mark, D., McCarthy Davis, J., Smyth Gordon, K., 2010. edgeR: a Bioconductor package for differential expression analysis of digital gene expression data. Bioinformatics 26, 139–140. doi: 10.1093/bioinformatics/btp616

Rovetto, E.I., La Spada, F., Aloi, F., Riolo, M., Pane, A., Garbelotto, M., Cacciola, S.O. (2024) Green solutions and new technologies for sustainable management of fungus and oomycete diseases in the citrus fruit supply chain. Journal of Plant Pathology 106, 411–437. doi:10.1007/s42161-023-01543-6

Roussos, P.A., Flessoura, I., Petropoulos, F., Massas, I., Tsafouros, A., Ntanos, E., Denaxa, N.K. (2019) Soil physicochemical properties, tree nutrient status, physical, organoleptic and phytochemical characteristics and antioxidant capacity of clementine mandarin (Citrus clementine cv. SRA63) juice under integrated and organic farming. Scientia Horticulturae 250, 414–420. doi:10.1016/j.scienta.2019.02.082

Schmidt, J.E., Vannette, R.L., Igwe, A., Blundell, R., Casteel, C.L., Gaudin, A.C.M. (2019) Effects of agricultural management on rhizosphere microbial structure and function in processing tomato plants. Applied and Environmental Microbiology 85. doi:10.1128/AEM.01064-19

Scotton, J.C., Homma, S.K., Costa, W.L.F., Pinto, D.F.P., Govone, J.S., Attili-Angelis, D. (2020) Transition management for organic agriculture under citrus cultivation favors fungal diversity in soil. Renewable Agriculture and Food Systems 35, 120–127.

doi:10.1017/S1742170518000352

Shen, Z., Ruan, Y., Chao, X., Zhang, J., Li, R., Shen, Q. (2015) Rhizosphere microbial community manipulated by two years of consecutive biofertilizer application associated with banana Fusarium wilt disease suppression. Biology and Fertility of Soils 51, 553–562. doi:10.1007/s00374-015-1002-7

Si, P., Shao, W., Yu, H., Yang, X., Gao, D., Qiao, X., Wang, Z., Wu, G. (2018) Rhizosphere microenvironments of eight common deciduous fruit trees were shaped by microbes in northern China. Frontiers in Microbiology 9, 3147. doi: 10.3389/fmicb.2018.03147

SINAB (2020) Areas, crops, operators and livestock. Figures on organic farming. Facts and Figures on organic farming in Italy 2020. Vol. 6. Rome, Italy. www.sinab.it

Spreen, T.H., Gao, Z., Fernandes, W., Zansler, M.L. (2020) Global economics and marketing of citrus products. The Genus Citrus 471–493. doi:10.1016/B978-0-12-812163-4.00023-1

Stalenga, J. (2007) Applicability of different indices to evaluate nutrient status of winter wheat in the organic system. Journal of Plant Nutrition 30, 351–365. doi:10.1080/01904160601171207

Stassinos, P.M., Rossi, M., Borromeo, I., Capo, C., Beninati, S., Forni, C. (2022) Amelioration of salt stress tolerance in rapeseed (Brassica napus) cultivars by seed inoculation with *Arthrobacter globiformis*. Plant Biosystems 156, 370–386. doi:10.1080/11263504.2020.1857872

Suyal, D.C., Soni, R., Singh, D.K., Goel, R. (2021) Microbiome change of agricultural soil under organic farming practices. Biologia 76, 1315–1325. doi:10.2478/s11756-021-00680-6

Trivedi, P., Leach, J.E., Tringe, S.G., Sa, T., Singh, B.K. (2020) Plant–microbiome interactions: from community assembly to plant health. Nature Reviews Microbiology 18, 607–621. doi:10.1038/s41579-020-0412-1

Trivedi, P., Trivedi, C., Grinyer, J., Anderson, I.C., Singh, B.K. (2016) Harnessing host-vector microbiome for sustainable plant disease management of phloem-limited bacteria. Frontiers in Plant Science 7, 1423. doi:10.3389/fpls.2016.01423

Turner, T.R., James, E.K., Poole, P.S. (2013) The plant microbiome. Genome Biology 14, 1–10. doi:10.1186/gb-2013-14-6-209

Utermann, J., Gorny, A., Hauenstein, M., Malessa, V., Müller, U., & Schefer, B. (2000) Geologisches Jahrbuch Reihe G, Band G 8 (Basenneutralisationskapazität). Stuttgart: Schweizerbart´sche Verlagsbuchhandlung.

van der Voort, M., Kempenaar, M., van Driel, M., Raaijmakers, J.M., Mendes, R. (2016) Impact of soil heat on reassembly of bacterial communities in the rhizosphere microbiome and plant disease suppression. Ecology Letters 19, 375–382. doi:10.1111/ele.12567

Van Elsas, J.D., Chiurazzi, M., Mallon, C.A., Elhottova, D., Krištůfek, V., Salles, J.F. (2012) Microbial diversity determines the invasion of soil by a bacterial pathogen. Proceedings of the National Academy of Sciences of the United States of America 109, 1159–1164. doi:10.1073/pnas.1109326109

Veech, J.A. (2013) A probabilistic model for analysing species co-occurrence. Global Ecology and Biogeography 22, 252–260. doi:10.1111/j.1466-8238.2012.00789.x

Wang, W., de Silva, D.D., Moslemi, A., Edwards, J., Ades, P.K., Crous, P.W., Taylor, P.W.J. (2021) *Colletotrichum* species causing anthracnose of citrus in australia. Journal of Fungi 7, 1–24. doi:10.3390/jof7010047

Willer, H., Trávníček, J., Schlatter, Eds, B. (2024) The world of organic agriculture. Statistics and emerging trends 2024. Research Institute of Organic Agriculture FiBL and IFOAM - Organics International, Frick (Switzerland) and Bonn (Germany). doi: https://orgprints.org/52272. available on line at: http://www.organic-world.net/yearbook/yearbook-2024.html

Wu, B., Wang, P., Devlin, A.T., Xiao, S., Shu, W., Zhang, H., Ding, M. (2021) Influence of soil and water conservation measures on soil microbial communities in a citrus orchard of Southeast China. Microorganisms 9, 319. doi:10.3390/microorganisms9020319

Xi, M.Y., Deyett, E., Stajich, J.E., El-Kereamy, A., Roper, M.C., Rolshausen, P.E. (2023) Microbiome diversity, composition and assembly in a California citrus orchard. Frontiers in Microbiology 14, 1100590. doi:10.3389/fmicb.2023.1100590

Xiong, W., Zhao, Q., Zhao, J., Xun, W., Li, R., Zhang, R., Wu, H., Shen, Q. (2015) Different continuous cropping spans significantly affect microbial community membership and structure in a vanilla-grown soil as revealed by deep pyrosequencing. Microbial Ecology 70, 209–218. doi:10.1007/s00248-014-0516-0

Xu, J., Zhang, Y., Zhang, P., Trivedi, P., Riera, N., Wang, Y., Liu, X., Fan, G., Tang, J., Coletta-Filho, H.D., Cubero, J., Deng, X., Ancona, V., Lu, Z., Zhong, B., Roper, M.C., Capote, N., Catara, V., Pietersen, G., Vernière, C., Al-Sadi, A.M., Li, L., Yang, F., Xu, X., Wang, J., Yang, H., Jin, T., Wang, N. (2018) The structure and function of the global citrus rhizosphere microbiome. Nature Communications 9, 4894. doi:10.1038/s41467-018-07343-2

Ye, Z., Li, J., Wang, J., Zhang, C., Liu, G., Dong, Q. (2021) Diversity and co-occurrence

network modularization of bacterial communities determine soil fertility and crop yields in arid fertigation agroecosystems. Biology and Fertility of Soils 57, 809–824. doi:10.1007/s00374-021-01571-3

Yin, C., Hulbert, S.H., Schroeder, K.L., Mavrodi, O., Mavrodi, D., Dhingra, A., Schillinger, W.F., Paulitz, T.C. (2013) Role of bacterial communities in the natural suppression of *Rhizoctonia solani* bare patch disease of wheat (*Triticum aestivum* L.). Applied and Environmental Microbiology 79, 7428–7438. doi:10.1128/AEM.01610-13

Zayani, I., Ammari, M., Ben Allal, L., Bouhafa, K. (2023) Agroforestry olive orchards for soil organic carbon storage: Case of Saiss, Morocco, in: Heliyon. p. e22910. doi:10.1016/j.heliyon.2023.e22910

Zhang, Y., Trivedi, P., Xu, J., M. Roper, C., Wang, N. (2021) The citrus microbiome: From structure and function to microbiome engineering and beyond . Phytobiomes Journal 2021 5:3, 249-262

.

6. Is climate change impacting *Phytophthora* diversity in organically and conventionally managed citrus orchards in Sicily? Insights from metabarcoding and baiting

Sebastiano Conti Taguali[1,2], Federico La Spada[1], Peter J. A. Cock[3], Beatrix Keillor[3], David E. L. Cooke[3*], Santa Olga Cacciola[1*]

[1] University of Catania, Department of Agriculture, Food and Environment (UniCT, Di3A), Via Santa Sofia 100, 95123 Catania (Italy).

[2] Mediterranea University of Reggio Calabria, Department of Agricultural Science, Località Feo di Vito, 89122 Reggio di Calabria (Italy).

[3] The James Hutton Institute, Invergowrie, Dundee DD2 5DA, UK

* Corresponding authors: olga.cacciola@unict.it; david.cooke@hutton.ac.uk

6.1 Abstract

Phytophthora species pose a significant threat to citrus production in the Mediterranean, particularly in Sicily, a major citrus-producing region. This study explores the diversity and distribution of *Phytophthora* taxa in Sicilian citrus orchards, addressing the urgent need to tackle increasing agricultural challenges, such as climate change. Specifically, it aimed to evaluate how environmental factors, specifically the type of management (organic vs. conventional) and geographical area, influence the composition of *Phytophthora* communities in Sicilian citrus orchards, and whether these communities correlate with tree health. An additional objective was to compare the effectiveness of traditional baiting and high-throughput metabarcoding techniques (targeting the ITS1 region and rps10 gene) in capturing this diversity, as well as to assess potential shifts in community structure resulting from climate change by comparing current data with historical records.

Soil samples were collected from multiple citrus-producing areas (Siracusa, Lentini, Mineo, and Ramacca) under various agronomic practices and tree health conditions. Traditional baiting recovered 556 isolates of well-known species, while ITS1 metabarcoding identified additional taxa, demonstrating higher specificity (99.5% of ITS1 reads classified as Phytophthora compared to 82.5% for rps10). Our findings indicate that

geographical location is a key driver of community composition. Although statistical analyses did not reveal significant differences in *Phytophthora* diversity between organic and conventional management systems, these results provide valuable insights into the factors shaping pathogen communities. These insights are crucial for developing targeted disease management strategies and for understanding how environmental stressors, including climate change, impact pathogen dynamics in Mediterranean citrus orchards.

Keys word: Metabarcoding, DNA sequencing, citrus orchards, illumina, ITS1, rps10 gene leaf baiting

6.2. Introduction

Citrus, one of the leading cash fruit crops in the world, includes plant species from *Citrus* and other genera, such as *Eremocitrus*, *Fortunella*, *Microcitrus*, and *Poncirus* (Rovetto *et al.*, 2024). Citrus are cultivated in more than 140 countries worldwide, with international production primarily focused on sweet oranges and, to a lesser extent, mandarins, lemons, limes, pomelo, citron and grapefruits (FAO, 2021). Among the citrus-producing regions in the Mediterranean, Sicily (Italy), particularly the provinces of Catania and Siracusa, is notable for its production of oranges and lemons as well as for distinctive local varieties of blood oranges (Rovetto et al., 2023). As an intensively cultivated crop, citrus is subject to several abiotic and biotic stresses. Of the latter, diseases caused by *Phytophthora* species are among the major limiting factors for citrus cultivation worldwide (Gams, 2000; Naqvi, 2006; Cacciola & Magnano di San Lio, 2008; Liu et al., 2013; Talibi et al., 2014; Puglisi et al., 2017; Rovetto et al., 2024). The genus *Phytophthora* comprises over 250 plant pathogenic species well-known for their ability to cause severe diseases in a broad range of plants from both natural environments and agro-ecosystems (Erwin & Ribeiro, 1996; Cacciola & Magnano di San Lio, 2008; Jung et al., 2016; Riolo et al., 2022; Abad et al., 2023; Aloi et al., 2023; Conti Taguali et al., 2024; Bačová et al., 2024) . The life cycle of *Phytophthora* is predominantly associated with roots, soil, and aquatic environments. *Phytophthora* species may infect roots often without showing evident symptoms in host plants until advanced stages of disease occur (Erwin & Ribeiro, 1996). Within the framework of citrus crops, *Phytophthora* spp. are known to cause root and collar rots, gummosis, and brown rot of fruit (Cacciola & Magnano di San Lio, 2008). The major species associated with these diseases worldwide are *P. nicotianae*, *P. citrophthora*,

and *P. palmivora.* Other species isolated less frequently include *P. cactorum*, *P. cinnamomi*, *P. citricola*, *P. cryptogea*, P. *hibernalis*, *P. syringae*, *P. humicola, P. insolita P. inundata, P. palmivora, P. prodigiosa*, and *P. mekongensis* (Ko & Ann, 1985; Naqvi, 2006; Vial et al., 2006; Cacciola & Magnano di San Lio, 2008; Das et al., 2012; Faedda et al., 2013; Crous et al., 2017; Khanchouch et al., 2017; Puglisi et al., 2017; Chi et al., 2020; Gai et al., 2021).

In Sicily, the predominant *Phytophthora* species associated with diseases of citrus are *P. citrophthora* and *P. nicotianae*, two highly polyphagous species (Cacciola & Magnano di San Lio, 2008). In citrus orchards, the primary inoculum for *Phytophthora* species consists of long-lasting structures like chlamydospores and oospores, primarily found in the plant's rhizosphere as well as mycelium associated with plant debris. When environmental conditions become favorable, these dormant propagules reactivate, leading to the infection of rootlets and fruit. Infected parts then act as sources of secondary inoculum, mainly as sporangia forming on their surfaces. The main inoculum reservoir of these species is the rhizosphere soil, where they persist as mycelium within the roots or associated plant debris, as well as long-lasting structures, such as chlamydospores and oospores. Infected rootlets and fruit with brown rot serve as sources of secondary inoculum, with sporangia forming on their surfaces. Sporangia are produced in contact with air in the most superficial soil layers and are dispersed by rain, irrigation water, and wind. Their germination occurs in water and is influenced by temperature and soil water potential (Cacciola & Magnano di San Lio, 2008). The incidence of either *P. citrophthora* or *P. nicotianae* in citrus orchards is reported to depend on the temperature. *Phytophthora nicotianae* has an optimum temperature for mycelium growth of 28-30°C, while *P. citrophthora* of 25-28°C. These features make *P. citrophthora* more active than *P. nicotianae* during cooler months. Conversely, the activity of *P. citrophthora* is significantly reduced during the summer months (Cacciola & Magnano di San Lio, 2008). Apart from *P. citrophthora*, *P. nicotianae*, and the other less frequent *Phytophthora* spp. associated with citrus crops, interesting new records of additional *Phytophthora* taxa have recently emerged in citrus orchards. A recent study by La Spada et al. (2022), using an ITS1 Illumina metabarcoding protocol, for example, recorded the presence of DNA from *P. occultans* and of two unknown *Phytophthora* taxa belonging to ITS clade 8b in a Sicilian citrus orchard. In the Mediterranean basin, *P. occultans* had previously been reported exclusively in a declining *Buxus sempervirens* forest located in the Black Sea region (Akıllı Şimşek *et al.*, 2019) . The findings from the study by La Spada et al. (2022) suggest that Mediterranean citrus orchards may be favorable for the establishment of *Phytophthora* species uncommon in these environments and that they

could also host still unknown *Phytophthora* taxa, whose presence warrants further investigation. Moreover, recent studies have significantly increased the number of described *Phytophthora* species, thereby highlighting the diversity and complexity of this genus (Abad et al., 2023; Jung et al., 2024). Before 2009, only 90 species had been formally recognized, with global estimates of species ranging from 200 to 600 (Brasier, 2009). Scott et al. (2019) refined this estimate to a range of approximately 274–378 species. The most recent study by Jung et al. (2024) reported 43 new species in *Phytophthora* major Clade 2, bringing the total number of known *Phytophthora* species to approximately 260. Due to the climatic change that has occurred globally in recent years, the Mediterranean climate is undergoing significant changes characterized by unusually warm and dry winters (Toreti et al., 2024). These changes are having a severe effect on Sicily, and in February 2024 the regional government was forced to declare a state of natural disaster due to severe drought that has affected the entire region (Resolution of the Council of Ministers dated May 6, 2024 - Declaration of a state of emergency in relation to the ongoing severe water deficit in the territory of the Sicilian Region). The potential impact of Mediterranean climate change on the diversity of *Phytophthora* communities and level of root disease in citrus orchards should not be underestimated, as it could have significant phytopathological implications. These changes may create conditions that favor certain species over others, leading to potentially harmful consequences for Sicilian citrus orchards. This risk is particularly concerning in organically managed orchards, where the absence of scheduled chemical treatments may intensify the effects of *Phytophthora* infections. Given these factors, a comprehensive investigation into the presence and distribution of *Phytophthora* species in Sicilian citrus orchards is warranted. In recent years, advanced environmental monitoring techniques, such as metabarcoding combined with traditional isolation methods, like baiting, have emerged as the most effective approach for reliable and accurate monitoring of *Phytophthora* communities in environmental samples (La Spada et al., 2022; Sarker et al., 2023). Baiting, which uses plant baits to isolate living propagules of pathogens from the soil, is a crucial tool not only for detecting the presence of active *Phytophthora* species, but also for conducting in-depth studies on the biology and pathogenicity of newly isolated taxa (Jung et al., 2019; Riolo et al., 2022). Concurrently, metabarcoding technologies, which employ high-throughput DNA sequencing of amplified barcodes, identify known and unknown microbial species in an environmental sample and can also be used to examine the genetic diversity within a specific taxonomic group (Català et al., 2015; Riddell et al., 2019; Van der Heyden et al., 2024). Currently, two barcode regions are

emerging as the best tools for recording the diversity of *Phytophthora* taxa within an environmental sample: (i) the Internal Transcribed Spacer 1 (ITS1) region of the nuclear ribosomal DNA (rDNA gene) (Scibetta et al., 2012) and (ii) the mitochondrial 40S ribosomal protein S10 (*rps10*) gene, encoding the 40S ribosomal protein (Foster *et al.*, 2022). Although the ITS1 barcode has been the most widely used so far, it is unable to resolve some closely related taxa (Redekar et al., 2019). Conversely, the assay based on the *rps10* gene (Foster et al., 2022) offers amplification of a wider taxonomic range and has demonstrated higher taxonomic resolution than ITS1, allowing for greater discrimination of closely related species. The amplification of both barcodes in simplified ecosystems, such as citrus orchards, where a limited number of *Phytophthora* taxa is expected, should provide a valuable comparison of their specificity and accuracy.

This study aimed to evaluate how environmental factors such as the type of management (organic versus conventional) and the geographical area, influence the diversity of *Phytophthora* communities in citrus orchards in Sicily. Moreover, this study investigated whether the structure of *Phytophthora* communities these samples is correlated with the health status of trees. An additional specific objective of this study was to compare the effectiveness of two methods, i.e., baiting and metabarcoding based on ITS1 and *rps10* as barcodes, in revealing the diversity of these communities. Finally, the hypothesis that in the last years the structure of *Phytophthora* communities in citrus orchards of Sicily has changed as a consequence of climate change was considered. To this aim, results of this study were compared with historical data of previous investigations in the same geographical area.

6.3 Material and methods

6.3.1 Citrus orchards

The field research for this study was conducted in March 2024, at the start of the spring season and in the citrus-producing areas in the Sicilian municipalities of Siracusa, Lentini, Mineo, and Ramacca (Table 1). These areas differ in climatic conditions as shown in Table 1 which details temperature and rainfall figures for October 2023 to March 2024. Within these citrus-producing areas, ten citrus orchards were selected as sampling sites (Table 1). These orchards consisted of orange (*Citrus* × *sinensis* (L.) Osbeck) and lemon (*Citrus* × *limon* (L.) Osbeck) plantations, from different varieties, with all plants nested on sour orange (*Citrus* × *aurantium* L.) as rootstock. Among the selected orchards, five were managed conventionally and five organically (Table 1). Orchards under conventional agronomic management used glyphosate, 2,4-dichlorophenoxyacetic acid, and

oxyfluorfen as herbicides, along with various synthetic insecticides and copper-based fungicides. Organic orchards used paraffinic oils, primarily against scales, and copper-based fungicides to control fungal and oomycete pathogens, such as *Colletotrichum* spp., *Alternaria* spp., and *Phytophthora* spp. Additionally, inputs in conventional orchards included complex NPK fertilizers, while animal manure and organic commercial fertilizers were applied in organically managed orchards. Both organic and conventional orchards incorporated pruning material into the soil. Orchards were also categorized on the basis of overall plant health status as 'healthy,' with vigorous plants, or 'unhealthy,' with plants showing generalized poor vigor. In all the selected orchards, the irrigation regime per plant during the seasons preceding the field sampling (namely, autumn and winter – from October 2023 to March 2024) consisted of 1.0 m^3 of water, delivered through drip irrigation every 20 days. This regime was far below the desired water amount (300 mm/m^2) and, therefore, served as emergency irrigation to compensate for the water shortage caused by the scarcity of precipitation during the autumn and winter of 2023/2024.

.

Table 1. Sampling sites selected in this study along with the citrus producing area and related climatic conditions, type of plantation, agronomical management, overall health of plants, collected rhizosphere soil samples, *Phytophthora* taxa isolated by baiting, suitability of the sample to *Phytophthora*-Metabarcoding processing, *Phytophthora* taxa identified by DNA metabarcoding through ITS1 region and *rps10* gene amplification.

Sampling Site – ID, company name; geographic coordinates[a] of the orchard	Citrus-producing area – Municipality	Climatic conditions[b] – min/mean/max temperatures (°C) and total rainfall (mm)	Type of Plantation	Agronomic management (conventional/organic)	Overall Health of Plants (healthy/unhealthy)	Rhizosphere Soil Sample ID	Baited *Phytophthora* Taxa[c]	Eligibility of sample to *Phytophthora*-Metabarcoding processing (Yes/No)[c]	ITS1-metabarcoding detected *Phytophthora* Taxa[c]	*rps10*-metabarcoding detected *Phytophthora* Taxa[c]
CO_1 – Tenuta Grimaldi; 37°32'78.02'' N; 14°83'27.58'' E	Lentini (Siracusa, Italy)	min. = 4.68°C mean = 15.33°C max. = 28.17°C rain = 101.2 mm	*Citrus* × *sinensis* (L.) Osbeck	Organic	Healthy	CO_1_P1	NIC	No	-	-
						CO_1_P2	-	No	-	-
						CO_1_P3	NIC	Yes	NIC; OLE; ITS1 UNK1; ITS1 UNK2; ITS1 UNK3	NIC
						CO_1_P4	NIC	No	-	-
						CO_1_P5	NIC	Yes	NIC	-
CO_2 - Tenuta Grimaldi; 37°34'21.66'' N; 14°83'46.02'' E			*Citrus* × *limon* (L.) Osbeck	Conventional	Healthy	CO_2_P1	CIT; NIC	Yes	CRA/MEG; NIC; ITS1 UNK1	NIC; *rps10* UNK1; *rps10* UNK2
						CO_2_P2	NIC	Yes	CITR; CRA/MEG; NIC; ITS1 UNK1	NIC
						CO_2_P3	CIT;	No	-	-
						CO_2_P4	CIT; NIC	No	-	-
						CO_2_P5	CIT; NIC	No	-	-

CO_08 - Tenuta Biviere; 37°30'91.51'' N; 14°95'63.29'' E			*C.* × *limon* (L.) Osbeck	Organic	Healthy	CO_8_P1	-	No	-	-
						CO_8_P2	-	No	-	-
						CO_8_P3	-	No	-	-
						CO_8_P4	-	No	-	-
						CO_8_P5	-	No	-	-
CO_09 - Tenuta Guastella; 37°31'08.24'' N; 15°01'13.15'' E			*C.* × *sinensis* (L.) Osbeck	Conventional	Healthy	CO_9_P1	NIC	No	-	-
						CO_9_P2	NIC	No	-	-
						CO_9_P3	-	No	-	-
						CO_9_P4	NIC	No	-	-
						CO_9_P5	NIC	No	-	-
CO_05 - Tenuta Giardina Scammacca; 37°05'30.96'' N; 15°17'64.03'' E	Siracusa (Italy)	min. = 4.07°C mean = 14.65°C max. = 28.33°C rain = 179 mm	*C.* × *sinensis* (L.) Osbeck	Organic	Unhealthy	CO_5_P1	CIT	Yes	CIT; OCC	CIT
						CO_5_P2	CIT	Yes	CIT; NIC; OCC	CIT
						CO_5_P3	CIT; NIC	Yes	CIT; NIC; OCC	CIT; NIC
						CO_5_P4	CIT	Yes	CIT; OCC	CIT
						CO_5_P5	CIT; NIC	Yes	CIT; NIC; OCC	CIT; *rps10* UNK1

CO_06 - Tenuta Giardina Pantanelli; 37°06'33.82'' N; 15°25'61.79'' E			*C.* × *limon* (L.) Osbeck	Organic	Unhealthy	CO_6_P1	CITR; CIT; NIC	Yes	CITR; CIT; NIC; OCC; PAC	CITR; NIC; *rps10* UNK3
						CO_6_P2	CITR; CIT; NIC	Yes	CITR; CIT; NIC; OCC; PAC	CITR; CIT; NIC; *rps10* UNK3; *rps10* UNK4; *rps10* UNK7
						CO_6_P3	CIT; NIC	Yes	CITR; CIT; NIC; OCC	CIT; NIC; *rps10* UNK1
						CO_6_P4	CIT; NIC	Yes	CITR; CIT; NIC; OCC; ITS1 UNK4	CITR; CIT; NIC
						CO_6_P5	CITR; NIC	Yes	CITR; NIC; PAC	CITR; NIC; *rps10* UNK3
CO_04 - Tenuta Borzì; 37°48'58.15'' N; 14°78'58.73'' E	Ramacca (Catania, Italy)	min. = 5.23°C mean = 14.33°C max. = 25.98°C rain = 149 mm	*C.* × *sinensis* (L.) Osbeck	Organic	Healthy	CO_4_P1	NIC	No	-	-
						CO_4_P2	NIC	Yes	NIC	NIC
						CO_4_P3	NIC	Yes	CITR; NIC	NIC
						CO_4_P4	-	No	-	-
						CO_4_P5	NIC	No	-	-

CO_03 - Tenuta Serravalle; 37°33'78.82'' N; 14°69'24.23'' E			*C.* × *sinensis* (L.) Osbeck	Conventional	Healthy	CO_3_P1	CIT; NIC	Yes	CIT; NIC; OCC	CIT; *rps10* UNK1
						CO_3_P2	CIT; NIC	Yes	CIT; NIC; OCC	CIT; NIC; *rps10* UNK5; *rps10* UNK6
						CO_3_P3	NIC	No	-	-
						CO_3_P4	NIC	Yes	CIT; NIC; OCC	CIT; NIC
						CO_3_P5	NIC	Yes	CIT; NIC; OCC	CIT
CO_07 - Tenuta Leonardo; 37°35'17.99'' N; 14°70'09.70'' E	Mineo (Catania, Italy)	min. = 5.37°C mean = 14.58°C max. = 26.80°C rain = 146.6 mm	*C.* × *limon* (L.) Osbeck	Conventional	Unhealthy	CO_7_P1	CIT	Yes	CIT; NIC; OCC	CIT
						CO_7_P2	CIT	Yes	CIT; NIC; OCC	CIT
						CO_7_P3	CIT	Yes	CIT; NIC; OCC	CIT
						CO_7_P4	CIT	Yes	CIT; OCC	CIT
						CO_7_P5	CIT	Yes	CIT; NIC; OCC; ITS1 UNK5; ITS1 UNK6	CIT; NIC
CO_10 - Tenuta Salinella; 37°19'22.5'' N; 14°40'59.5'' E			*C.* × *sinensis* (L.) Osbeck	Conventional	Healthy	CO_10_P1	CIT, NIC	No	-	-
						CO_10_P2	NIC	No	-	-
						CO_10_P3	NIC	No	-	-
						CO_10_P4	-	No	-	-
						CO_10_P5	-	No	-	-

[a] DATUM WGS84;

[b] data are referred to the period October 2023 – March 2024 and they have been provided by the Sicilian Agrometeorological Information Service (SIAS);

[c] CITR = *P. citricola*; CIT = *P. citrophthora;* CRA/MEG = *P. crassamura / P. megasperma*; NIC = *P. nicotianae*; OCC = *P. occultans*; OLE = *P. oleae*; PAC = *P. pachypleura*; ITS1 UNK1-6 = *Phytophthora* ITS1 UNK1-6; *rps10* UNK1-7 = *Phytophthora rps10* UNK1-7.

[c] Samples that produced amplicons confirmed their eligibility to subsequent metabarcoding processing (see M&M).

6.3.2 Collection of rhizosphere soil samples and establishment of sub-samples for metabarcoding and baiting processing

A total of 50 composite rhizosphere soil samples were collected from 10 citrus orchards in this study (Table 1). For each citrus orchard, soil was sampled from beneath five trees located in representative positions. Specifically, to ensure the representativeness of the soil samples in the rhizosphere and minimize within-plot variability, the trees were selected for a uniform distribution across the citrus grove, adequately representing the prevailing agronomic and microclimatic conditions in the studied area. The procedures for the collection of rhizosphere soil samples from each tree are detailed: the top 5 cm layer of litter was removed; four soil cores (at a depth of approximately 20–30 cm), including secondary roots, were collected at four cardinal points located approximately 50–100 cm from the trunk; the four soil cores were combined and mixed to form a single composite soil sample of approximately 1 L. Back in the laboratory an aliquot of 50.0 mL from each composite sample containing fine roots and soil was taken and immediately frozen in liquid nitrogen and transported to the Molecular Plant Pathology Laboratory (MPPL) of the Department of Agriculture, Food and Environment (Di3A) of the University of Catania (Catania, Italy) and stored at –80°C until use for metabarcoding analyses. The remaining rhizosphere soil (soil associated with fine roots) was placed in sterile bags and stored until bait testing.

6.3.3 Baiting processing, isolation procedure and molecular identification

For each composite rhizosphere soil sample, the baiting process was carried out in a walk-in growth chamber, with 12 hours of natural daylight and at a temperature of 20°C. Baiting procedures were in accordance with Jung et al. (2019): each sample was placed in a plastic container and flooded with distilled water. After approximately 30 minutes any organic debris floating on the water surface was removed and then, young and tender leaves of carob (*Ceratonia siliqua*) were floated on the water surface of the flooded soil. Following an incubation period of 24-48 hours, leaves showing necrotic spots were examined under a stereo-microscope at 80x magnification to detect any emerging hypha. Each necrotic spot was excised and plated on selective PARPNH agar Petri dishes and incubated at 20°C in the dark. After incubation, isolates were obtained by transferring outgrowing hyphae into clarified V8 agar (V8A). All isolates were maintained on V8A at 15°C in the MPPL Culture Collection of Di3A at the University of Catania (Catania, Italy).

For each composite rhizosphere soil sample, the isolates were grouped in morphotypes; then, one isolate per morphotype was selected for the subsequent molecular identification. For each isolate selected for molecular identification, total DNA was extracted from a seven-day-old culture grown on V8A at 20 °C using the DNeasy® Plant Mini Kit (QIAGEN, Hilden, Germany) following the manufacturer's instructions. Identification was carried out by amplification, sequencing and analysis of the internal transcribed spacer (ITS) regions of ribosomal DNA (rDNA). In detail, PCR amplifications were conducted using the Taq DNA polymerase recombinant kit (Invitrogen™, Waltham, MA, USA). Each amplification was carried out in a 25 µL reaction mixture containing PCR buffer (1X), dNTP mix (0.2 mM), $MgCl_2$ (1.5 mM), forward and reverse primers (ITS6 and ITS_4; Cooke et al., 2000; 0.5 µM each), Taq DNA polymerase (1 U), and 100 ng of DNA. The thermocycler conditions were as follows: 94 °C for 3 minutes, followed by 35 cycles of 94 °C for 30 s, 55 °C for 30 s, and 72 °C for 30 s, and followed by 72 °C for 10 minutes. Amplicons were detected on 1% agarose gels and sequenced in both directions by an external service (Macrogen, Seoul, South Korea). Obtained sequences were analyzed using FinchTV v.1.4.0 and MEGA11. Consensus sequences were compared with those of species ex-types deposited in the NCBI nucleotide database (https://www.ncbi.nlm.nih.gov/nucleotide/). Isolates were assigned to a species when their sequences had at least 99% identity to a reference isolate. The ITS sequences of representative isolates from this study have been deposited in GenBank (accession numbers provided in Table S1).

6.3.4. Sample processing for metabarcoding analyses

6.3.4.1 Environmental DNA (eDNA). Extraction from rhizosphere soil samples and PCR amplification

For each 50 mL rhizosphere soil sub-sample, eDNA was extracted from three replicates using the DNeasy PowerSoil® kit (Qiagen, Hilden, Germany) and following the manufacturer's instructions. .

6.3.4.2 Screening for the eligibility of eDNA samples to *Phytophthora*-metabarcoding processing

All eDNA samples obtained in the previous step were subjected to a preliminary PCR screening step to assess their suitability for the subsequent metabarcoding protocols. For this purpose, all eDNA samples were subjected to nested PCR as reported in Scibetta et al. (2012). In detail, the primer pair 18Ph2F (5′-GGATAGACTGTTGCAATTTTCAGT-3′) and 5.8S-1R (5′GCARRGACTTTCGTCCCYRC-3′) (Scibetta *et al.*, 2012) was used in the first

round; primer pairs ITS6 (5′GAAGGTGAAGTCGTAACAAGG-3′) (Cooke et al., 2000) and 5.8S-1R were used in the second round. After the PCR run, all PCR products were subjected to electrophoresis in 1% agarose gel. Samples that produced amplicons were subject to metabarcoding.

6.3.4.3 PCR amplifications

6.3.4.3.1 ITS-1 region barcode

The internal transcribed spacer 1 (ITS1) region of the nuclear ribosomal DNA (rRNA gene) was amplified through a nested PCR assay conducted in accordance with the protocol of Riddell et al. (2019). In detail, the primer pair 18Ph2F (5′-GGATAGACTGTTGCAATTTTCAGT-3′) and 5.8S-1R (5′GCARRGACTTTCGTCCCYRC-3′) (Scibetta *et al.*, 2012) was used in the first round; primer pairs ITS6 (5′GAAGGTGAAGTCGTAACAAGG-3′) (Cooke et al., 2000) and 5.8S-1R were used in the second round. Primers employed in the second round were modified with overhang adapters to ensure compatibility with the Illumina indexing and sequencing adapters. These were: forward overhang; 5′ TCGTCGGCAGCGTCAGATGTGTATAAGAGACAG-[ITS6] and reverse overhang; 5′ GTCTCGTGGGCTCGGAGATGTGTATAAGAGACAG-[5.8S-1R] (Illumina, 2013). PCRs were performed using the KAPA HiFi HotStart ReadyMix kit (KAPA Biosystems, Wilmington, MA, USA) following the manufacturer's instructions and the amplicons were checked on a 1.5% agarose gel.

6.3.4.3.2 *Rps10* gene barcode

The *rps10* gene was amplified using the metabarcoding method described in Foster et al. (2022). This method involves the use of a multiplex PCR with two forward primers, rps10_F1 (5′-TCGTCGGCAGCGTCAGATGTGTATAAGAGACAGGTTGGTTAGAGYAAAAGACT-3′) and rps10_F2 (5′-TCGTCGGCAGCGTCAGATGTGTATAAGAGACAGGTTGGTTAGAGTAGAAGACT-3′), and a pool of seven reverse primers, rps10_R1 (5′-GTCTCGTGGGCTCGGAGATGTGTATAAGAGACAG ATGCTTAGAAAGATTTGAACT-3′), rps10_R2 (5′-GTCTCGTGGGCTCGGAGATGTGTATAAGAGACAGATACTTAGAAAGATTTGAACT-3′), rps10_R3 (5′-GTCTCGTGGGCTCGGAGATGTGTATAAGAGACAGATGCTTAGAAAGACTTGAACT-3′), rps10_R4 (5′-GTCTCGTGGGCTCGGAGATGTGTATAAGAGACAGATGCTTAGAAAGACTCGAACT-3′),

rps10_R5 (5′-GTCTCGTGGGCTCGGAGATGTGTATAAGAGACAG ATGCCTAGAAAGACTCGAACT-3′), rps10_R6 (5′-GTCTCGTGGGCTCGGAGATGTGTATAAGAGACAGATGTTTAGAAAGATTCGAACT-3′) and rps10_R7 (5′- GTCTCGTGGGCTCGGAGATGTGTATAAGAGACAG-3′).

PCR amplifications were carried out using the QIAGEN Type-it Mutation Detect PCR Kit (Qiagen) following the manufacturer's instructions. The obtained amplicons were checked on a 1.5% agarose gel.

6.3.4.4 Illumina sequencing library preparation and sequencing

For the preparation of libraries intended for metagenomic sequencing, the Nextera XT Index Kit (Epicentre, Madison, WI, USA) was used, in accordance with the instructions provided in the Illumina 16S Metagenomic Sequencing Library protocol. As first step, all PCR products were purified using the Agencourt® AMpure® XP kit (Agencourt Bioscience, Beverly, MA, USA). Subsequently, an indexing PCR was performed to add dual indices and Illumina-specific sequencing adapters to each sample, thus ensuring their unique identification during sequencing. Following this, a second PCR purification was conducted, after which the DNA from each sample was visualised on a 1.5% agarose gel and quantified via fluorometry using the Quant-iT™ PicoGreen™ dsDNA kit (Invitrogen™, Waltham, MA, USA). The final concentration was adjusted to 5 nM. Subsequently, the samples were subjected to sequencing at the James Hutton Institute (Dundee, United Kingdom) using the Illumina NextSeq2000 reagent kit (P1 Reagents (600cycles, 20075294) Illumina, San Diego, CA, USA) for a paired-end sequencing run (2 × 300 bp). Subsequently, the resulting FASTQ files, comprising reads from each sample, were exported for bioinformatic analysis. This process ensured quality control and accurate de-multiplexing.

6.3.4.5 Bioinformatics analyses

For each sequenced sample, sequence data were processed and reduced down to unique barcode sequences termed amplicon sequence variants (ASVs) using v1.0.14 of the sequence-based diagnostic/profiling Tree Health and Plant Biosecurity Initiative (THAPBI) *Phytophthora* ITS1 Classifier Tool (PICT) (Cock et al., 2023). Species identification was based on the curated THAPBI PICT v1.0.14 *Phytophthora* ITS1 database and on BLAST searches on a local database containing sequences of ex-type or key isolates from published studies (Cooke et al., 2000; Aghighi et al., 2012; Scanu et al., 2014; Safaiefarahani et al., 2015; Jung et al., 2019, 2024; Riolo et al., 2020; Abad et al., 2023). For the *rps10* gene, the reference database was downloaded from OomyceteDB (Foster

et al., 2022) and consisted of 351 oomycete sequences, primarily *Phytophthora* (144 species) and *Pythium* (133 species). For both ITS1 and *rps10* gene sequences, ASVs were assigned to a species when they were identical or only differed at a single base pair from the sequences of a reference isolate. ASVs that were not assigned to a species following the above procedures were compared to those deposited on the NCBI nt database by using BLASTN+ (Altschul et al., 1990) to find the closest match (100% identity). Finally, ASVs that were not assigned to any species but were closely related to *Phytophthora* taxa were subjected to phylogenetic analysis to determine their position within *Phytophthora* clades. To this aim, sequences were aligned using MUSCLE and the phylogenetic reconstruction was conducted by using the maximum likelihood method with the Tamura-Nei model with a bootstrap of 1000 replicates (the software MEGA11 was used)..

6.3.4.6 Statistical analyses

To evaluate the effects of explanatory variables associated with each orchard (i.e., 'overall health of plants' – healthy/unhealthy, 'agronomic management' – conventional/organic, and 'citrus producing area' – Siracusa/Lentini/Mineo/Ramacca) on the distribution of *Phytophthora* taxa detected by the combined approach of baiting, ITS1 metabarcoding, and *rps10* gene sequencing, multivariate statistical analyses were performed using R software (version 4.3.1). For each *Phytophthora* taxon, presence/absence data was recorded for each rhizosphere sample. To analyze differences in species composition among groups, a distance matrix was calculated based on the Jaccard index using the vegan package (version 2.6-6.1), which is appropriate for binary (presence/absence) data. Subsequently, a PERMANOVA (Permutational Multivariate Analysis of Variance) was conducted using the adonis2 function from the *vegan* package, with 999 permutations to test for statistical significance. This analysis was performed separately for each independent variable ('overall health of plants', 'agronomic management', and 'citrus producing area') to determine whether significant differences in species composition were associated with each variable. Non-Metric Multidimensional Scaling (NMDS) based on the Jaccard index was employed to visualize any multivariate relationships among samples. The NMDS analysis was performed using the metaMDS function from the *vegan* package, specifying two dimensions (k = 2) and a maximum of 100 iterations to achieve convergence. The stress value obtained from the NMDS was assessed to ensure a reliable representation of the data; a stress value below 0.2 was considered acceptable. The NMDS results were visualized through plots generated using the *ggplot2* package. NMDS component scores were extracted and integrated with environmental variables, and two-

dimensional graphs were produced in which samples were represented as points in NMDS space, colored according to the variables 'overall health of plants', 'agronomic management', and 'citrus producing area'. Additionally, confidence ellipses were added using the stat_ellipse function to highlight trends within groups. To identify species contributing most to the observed patterns, the envfit function from the *vegan* package was utilized to fit species vectors onto the NMDS ordination. These vectors represent the direction and strength of the association between species presence and the NMDS axes. The inclusion of species vectors allowed for the visualization of how individual taxa are associated with the multivariate gradients represented in the NMDS plots.

6.4 Results

6.4.1 *Phytophthora* species isolated by baiting

A total of 556 *Phytophthora* isolates were recovered from 40 of the 50 rhizosphere soil samples processed by baiting. *Phytophthora* was recovered from all citrus orchards except at the sampling site CO_08 - Tenuta Biviere – Lentini (Catania, Italy) (Table 1). Sequencing of the ITS regions identified three *Phytophthora* species: *P. nicotianae*, *P. citrophthora*, and *P. citricola*. The dominant species was *P. nicotianae,* found in 31 of 50 rhizosphere soil samples and 8 of the 10 sampling sites (Table 1). Additionally, *P. nicotianae* was isolated from both organic and conventionally managed orchards, as well as from orchards with both healthy and unhealthy plants (Table 1). The other common species, *P. citrophthora*, was isolated from 21 of 50 samples from 6 of 10 sampling sites, distributed across all production areas except Ramacca (Table 1); this species occurred in both organically and conventionally managed orchards and from those presenting both healthy and unhealthy plants. Finally, isolates of *P. citricola* were recovered from only three rhizosphere soil samples, all collected in an organically managed orchard presenting unhealthy plants (CO_06 - Tenuta Giardina Pantanelli in the citrus-producing area of Siracusa) (Table 1).

6.4.2 *Phytophthora* taxa identified by metabarcoding

6.4.2.1 Preliminary screening for checking suitability of eDNA samples to *Phytophthora*-metabarcoding processing

The preliminary screening of the 150 replicated eDNA samples obtained in this study resulted in 75 suitable for *Phytophthora*-metabarcoding processing. These 75 samples represented 25 of the 50 rhizosphere soil samples collected from 7 of the 10 sampled citrus orchards (Table 1). Rhizosphere soil samples from the orchards CO_08 - Tenuta Biviere, CO_09 - Tenuta Guastella, and CO_10 - Tenuta Salinella tested PCR negative and

thus not used for metabarcoding. Nevertheless, all orchards that passed this preliminary screening were distributed across all the citrus-producing areas selected in this study.

6.4.2.2 *Phytophthora* taxa identified by metabarcoding of the ITS-1 region

The Illumina sequencing of the ITS1 PCR products generated 14,291,223 ITS1 sequence reads that passed the quality threshold and had an abundance of 1000 or more reads per sample. Their bioinformatic processing revealed that sequences belonging to the genus *Phytophthora* constituted 99.52% of the reads and 87.18% of the ASVs, while those from other oomycetes represented only 0.48% of the reads and 12.82% of the ASVs (Figure 1). Oomycetes other than *Phytophthora* were assigned to the genera *Phytopythium* and *Peronospora*. Specifically, 5 ASVs of *Phytopythium* and *Peronospora* were identified, including 3 unknown *Phytopythium* taxa and 2 unknown *Peronospora* taxa (Figure 1).

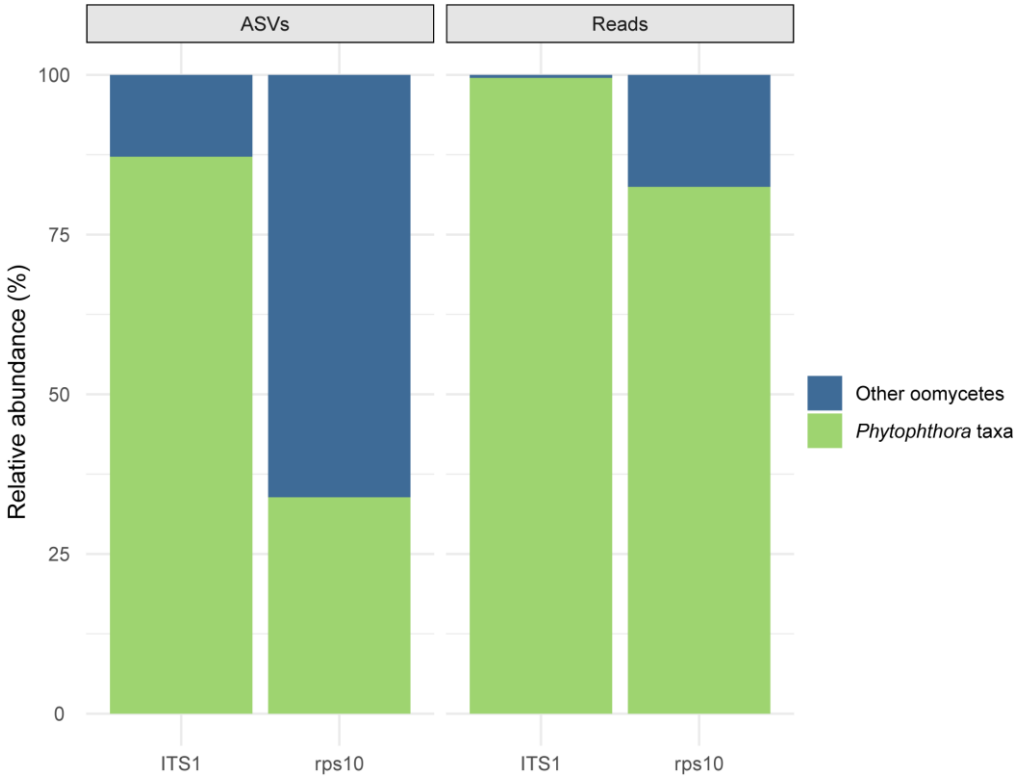

Figure 1. Relative abundance (%) of amplicon sequence variants (ASVs) and number of reads assigned to *Phytophthora* species and other Oomycetes though internal transcribed spacer 1 (ITS1) and 40S ribosomal protein S10 (*rps10*) protocols.

Bioinformatic and phylogenetic analyses of ITS1 data resulted in 13,867,259 *Phytophthora* reads across 39 *Phytophthora* ASVs in 13 categories with almost identical variants within 1 to 2 bp. These comprised: (i) six clearly distinguishable known species, *P. nicotianae*, *P. oleae*, *P. citricola*, *citrophthora*, *P. occultans*, and *P. pachypleura*; (ii) an ASV matching a pair

of closely related species, *P. crassamura* and *P. megasperma*, that could not be differentiated using ITS1 barcodes; and (iii) six unknown *Phytophthora* taxa (Table 1).

The proportion of ITS1 reads assigned to known *Phytophthora* taxa indicated that the most recorded species were *P. citrophthora* (35.53%), *P. nicotianae* (35.08%), *P. occultans* (16.59%), and *P. citricola* (10.37%) (Figure 2). Less abundant ITS1 reads were those assigned to *P. oleae* (0.01%), *P. pachypleura* (0.08%) and to *P. crassamura*/*P. megasperma* (1.69%) (Figure 2).

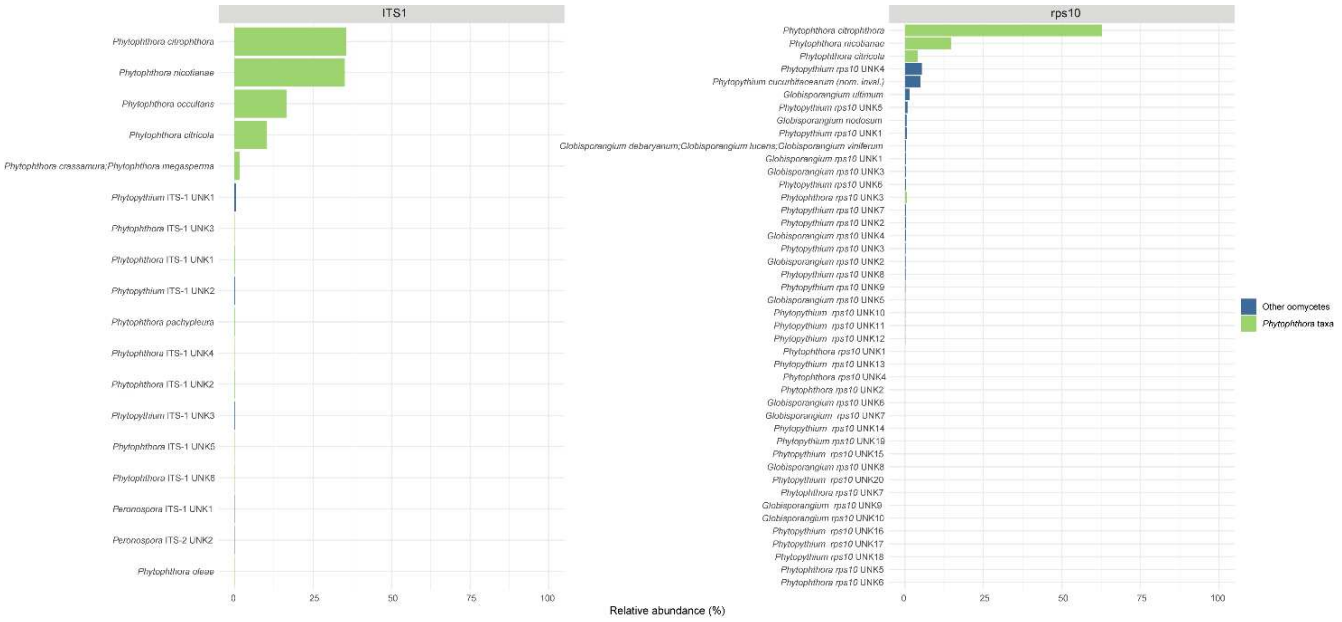

Figure 2. Relative abundance of reads assigned to *Phytophthora* taxa and other oomycete genera though internal transcribed spacer 1 (ITS-1) (left) and 40S ribosomal protein S10 (*rps10*) (right) protocols.

The two species most commonly detected across the sampling sites were *P. citrophthora* and *P. nicotianae*. The former was detected in 18 of 25 *Phytophthora* ITS1 metabarcoding-positive samples collected from four citrus orchards distributed across the citrus-producing areas of Siracusa and Mineo (Table 1). Notably, *P. citrophthora* was not recorded in any orchard from the citrus-producing areas of Lentini and Ramacca (Table 1). ITS1 reads of *P. citrophthora* were recorded in orchards defined as both healthy and unhealthy, as well as in those managed conventionally and organically (Table 1). Reads of *P. nicotianae* were detected in 22 out of 25 *Phytophthora* ITS1 metabarcoding-positive samples collected from seven citrus orchards distributed across all the citrus-producing areas analyzed in this study. *P. nicotianae* was also recorded without distinction between

organically and conventionally managed orchards, as well as in orchards with trees defined as both healthy and unhealthy.

Reads of *P. occultans* were detected in 18 out of 25 *Phytophthora* ITS1 metabarcoding-positive samples collected from four citrus orchards distributed only across the citrus-producing areas of Siracusa and Mineo (Table 1). As with *P. citrophthora* and *P. nicotianae*, *P. occultans* was found in both organically and conventionally managed citrus orchards, as well as in those characterized by either healthy or unhealthy plants.

P. citricola reads were recorded in seven out of 25 *Phytophthora* ITS1 metabarcoding-positive samples collected from three citrus orchards located in the citrus-producing areas of Lentini, Siracusa and Ramacca (Table 1). Notably, *P. citricola* was not recorded in orchards from the citrus-producing area of Mineo. Additionally, *P. citricola* was only recorded in organically managed citrus orchards and almost exclusively on trees defined as unhealthy (Table 1).

P. oleae was recorded in only one rhizosphere soil sample collected from an organically managed citrus orchard (CO_1 - Tenuta Grimaldi), with healthy plants and in the citrus-producing area of Lentini.

P. pachypleura was recorded in three out of 25 *Phytophthora* ITS1 metabarcoding-positive samples collected from the citrus orchard CO_06 - Tenuta Giardina Pantanelli, which was organically managed, characterized by unhealthy plants, and located in the citrus-producing area of Siracusa.

Finally, reads assigned to the *P. crassamura*/*P. megasperma* ITS1 barcode were found in two rhizosphere soil samples collected from healthy plants in the conventionally managed citrus orchard CO_2 - Tenuta Grimaldi, in the citrus-producing area of Lentini.

Unknown ITS1 *Phytophthora* ASVs, designated here as "*Phytophthora* ITS1 unknown taxon" (*Phytophthora* ITS1 unk1 to unk6) were found very low numbers; 0.08%, 0.06%, 0.02%, 0.02%, 0.01%, 0.01% of the reads respectively. Phylogenetic analyses placed *Phytophthora* ITS1 unk 1-3 in the *Phytophthora* ITS clade 1d, *Phytophthora* ITS1 unk 5-6 in the *Phytophthora* ITS clade 2a and *Phytophthora* ITS1 unk 4 in the *Phytophthora* ITS clade 2c (Figure 3).

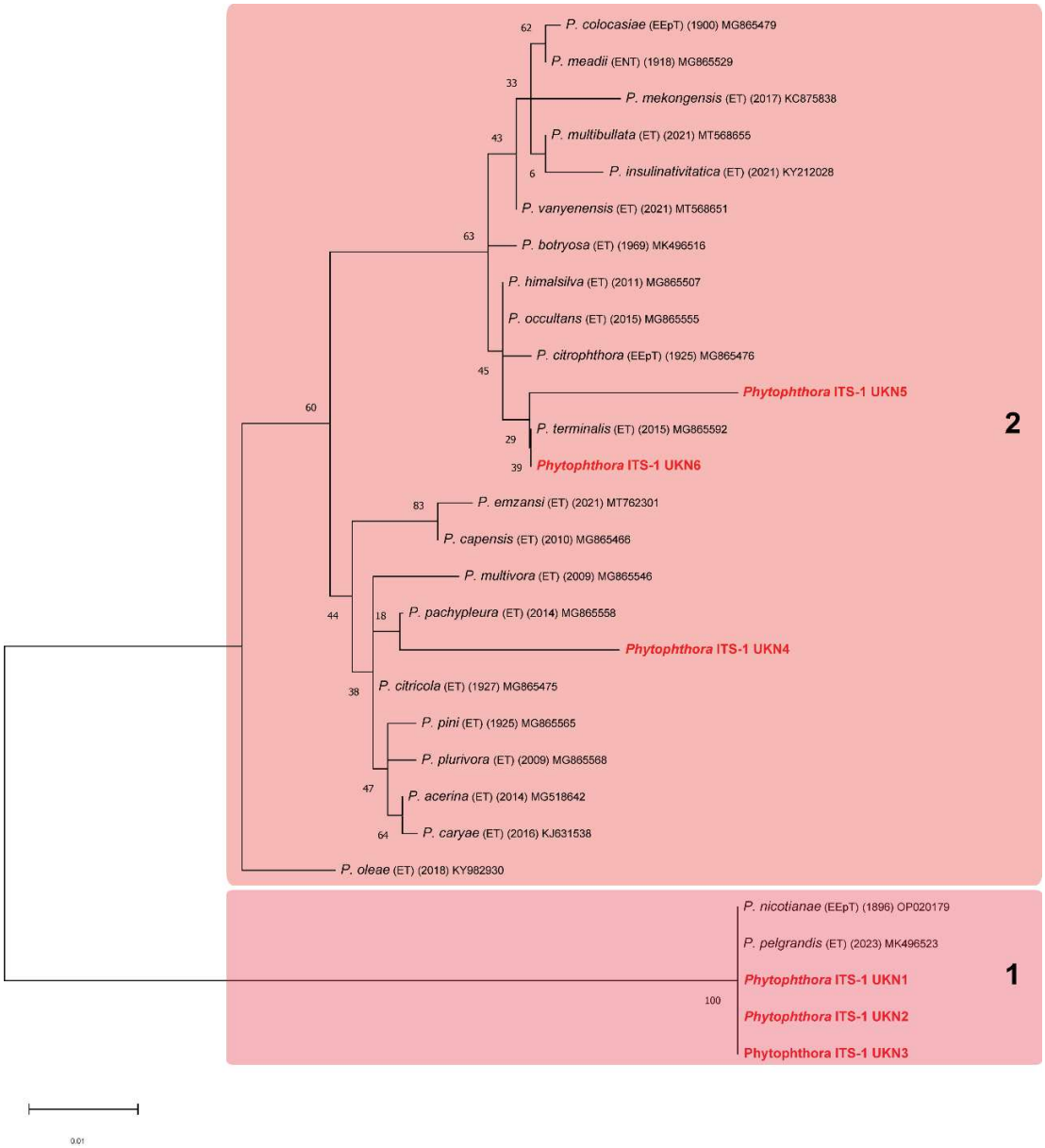

Figure 3. Sections from the phylogenetic tree of the *Phytophthora* ITS-1 showing the position of *Phytophthora* ITS-1 unk 1-6 ASVs recorded in this study (highlighted in red). The tree was generated by the Maximum Likelihood method, based on the Tamura-Nei model. The percentage of trees in which the associated taxa clustered together is shown next to the branches. The tree is drawn to scale, with branch lengths measured in the number of substitutions per site. The bootstrap consensus tree inferred from 1000 replicate.

Overall, these unknown *Phytophthora* taxa occurred rarely across the sampling sites. Specifically, *Phytophthora* ITS1 unk 1 was recorded in 3 out of 25 *Phytophthora* ITS1 metabarcoding-positive samples collected from two healthy citrus orchards, one conventionally and one organically managed, located in Lentini (Table 1). *Phytophthora*

ITS1 unk 2 and unk 3 were recorded in only one rhizosphere soil sample from healthy plants collected in the organically managed orchard CO_1 - Tenuta Grimaldi in Lentini (Table 1). *Phytophthora* ITS1 unk 4 was recorded in one rhizosphere soil sample from organically managed and unhealthy plants collected in the orchard CO_6 - Tenuta Giardina Pantanelli in the Siracusa area (Table 1). Finally, reads of the taxa designated as *Phytophthora* ITS1 unk 5 and unk 6 were recorded in only one rhizosphere soil sample collected from healthy plants in the conventionally managed orchard CO_10 - Tenuta Salinellain the Mineo area (Table 1).

6.4.2.3 *Phytophthora* taxa identified by metabarcoding of the *rps10* gene

The Illumina sequencing of the *rps10* gene produced 4,949,494 high-quality reads. *Phytophthora* constituted 82.5% of the reads and 33.9% of the ASVs, while other oomycetes accounted for the remaining 17.5% of the reads and 66.1% of the ASVs (Figure 1). Oomycetes other than *Phytophthora* were assigned to the genera *Globisporangium* and *Phytopythium*. Specifically, 62 ASVs of *Globisporangium* and *Phytopythium*, grouped into 34 categories with nearly identical variants differing by only 1 to 2 bp, were identified, including (i) three clearly distinguishable known species, *Globisporangium nodosum*, *Globisporangium ultimum*, and *Phytopythium cucurbifacearum*; (ii) one ASV matching a group of closely related species *Globisporangium dabaryanum*, *Globisporangium lucens*, and *Globisporangium viniferum* that could not be differentiated using rps10 barcodes; (iii) 10 unknown *Globisporangium* taxa and 20 unknown *Phytopythium* taxa (Figure 2).

The bioinformatic and phylogenetic analyses of the *rps10* data enabled the discrimination of 4,080,517 *Phytophthora* reads, organized into 21 *Phytophthora* ASVs, comprising (i) three clearly distinguishable known species, *P. nicotianae*, *P. citrophthora* and *P. citricola*, and (ii) seven unknown *Phytophthora* taxa (Table 1). Amongst the known taxa, *P. citrophthora* was the most prevalent taxon with an abundance of reads at 62.8%; followed by *P. nicotianae* (14.7%) and *P. citricola* (4.1%). These three species were distributed across all the sampling sites; *P. citrophthora* in 17 of 24 *Phytophthora rps10* metabarcoding-positive samples collected from four citrus orchards distributed across the citrus-producing areas of Siracusa and Mineo (Table 1). Noteworthy is that *P. citrophthora* was not recorded in any orchard from the citrus-producing areas of Lentini and Ramacca (Table 1). Moreover, *rps10* reads of *P. citrophthora* were recorded in both healthy and unhealthy orchards, as well as in those managed either conventionally or organically (Table 1). Reads of *P. nicotianae* were recorded in 11 out of 24 *Phytophthora rps10* metabarcoding-positive samples collected from seven citrus orchards distributed across

all the areas analyzed in this study. The species *P. nicotianae* was also recorded in both organically and conventionally managed orchards, as well as in orchards with both healthy and unhealthy plants (Table 1). Finally, *P. citricola* was recorded in four out of 24 *Phytophthora rps10* metabarcoding-positive samples, all of them collected in an organically managed citrus orchard, which was characterized by the presence of unhealthy plants and within Siracusa area (Table 1).

The unknown *rps10 Phytophthora* ASVs, designated here as "*Phytophthora rps10* unknown taxon" 1 (*Phytophthora rps10* unk1) through to 7 (*Phytophthora rps10* unk7) were found at relative abundances of 0.09%, 0.05%, 0.57%, 0.09%, 0.03%, 0.03% and 0.02%, respectively. Phylogenetic analyses placed *Phytophthora rps10* unk 5 in *Phytophthora* clade 1, *Phytophthora rps10* unk 1,3,4,6,7, in clade 2 and *Phytophthora rps10* unk 2 in clade 6 (Figure 4).

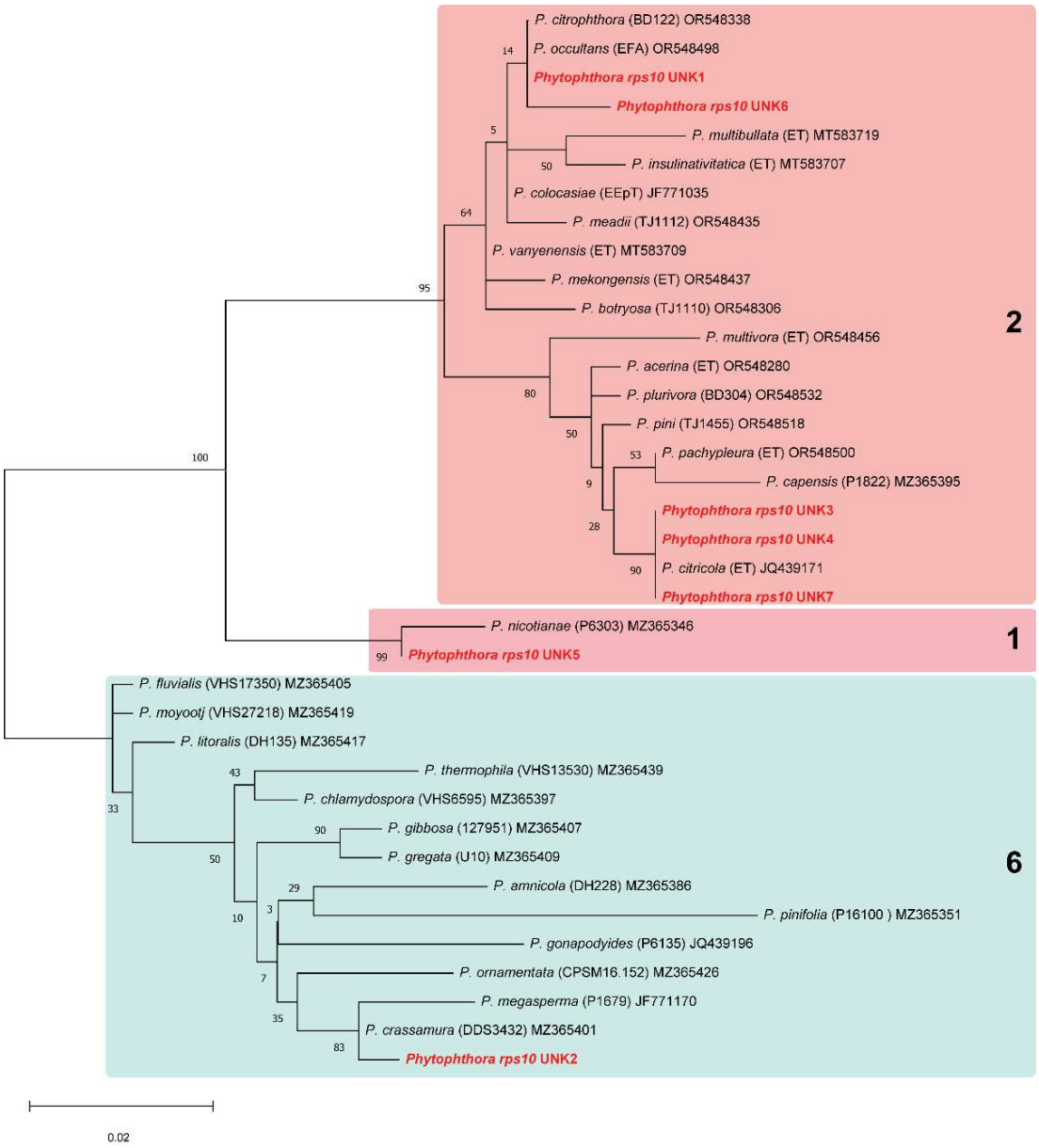

Figure 4. Sections from the phylogenetic tree of the *Phytophthora rps10* showing the position of *Phytophthora rps10* unk 1-7 ASVs recorded in this study (highlighted in red). The tree was generated by the Maximum Likelihood method, based on the Tamura-Nei model. The percentage of trees in which the associated taxa clustered together is shown next to the branches. The tree is drawn to scale, with branch lengths measured in the number of substitutions per site. The bootstrap consensus tree inferred from 1000 replicate.

Regarding the distribution of these unknown *Phytophthora* taxa across the sampling sites, *Phytophthora rps10* unk 1 was recorded in four rhizosphere soil samples collected from as many citrus orchards in the citrus-producing areas of Lentini, Siracusa, and Mineo (Table 1). The occurrence of *Phytophthora rps10* unk 1 was recorded in orchards managed both organically and conventionally, as well as in those with either healthy or unhealthy plants.

Reads of *Phytophthora rps10* unk 2 were recorded in only one rhizosphere soil sample collected in the conventionally managed citrus orchard CO_2 - Tenuta Grimaldi, which was characterized by healthy plants and was located in the citrus-producing area of Lentini (Table 1). *Phytophthora rps10* unk3 was recorded was recorded in three rhizosphere soil samples, all of them collected in the organically managed citrus orchard CO_06 - Tenuta Giardina Pantanelli, which was characterized by unhealthy and was located in the citrus-producing area of Siracusa (Table 1). The orchard CO_06 - Tenuta Giardina Pantanelli was also the only location in which reads of *Phytophthora rps10* unk4 and unk7 were recorded. Finally, *Phytophthora rps10* unk5 and unk6 were recorded in only one rhizosphere soil sample collected in the conventionally managed citrus orchard CO_03 - Tenuta Serravalle, which was characterized by healthy plants and was located in the citrus-producing area of Mineo (Table 1).

6.4.3 *Phytophthora*-positive rhizosphere soil samples recorded - comparison of outcomes from baiting and metabarcoding of ITS-1 and *rps10* gene

The combined use of baiting and metabarcoding of the ITS1 region and *rps10* gene enabled the detection of *Phytophthora* taxa in 40 out of 50 rhizosphere soil samples collected from all the citrus orchards studied (Table 1). Baiting identified 40 *Phytophthora*-positive rhizosphere soil samples (Figure 5). All samples that tested positive through metabarcoding of either the ITS1 region or the *rps10* gene were among the *Phytophthora*-positive rhizosphere soil samples detected by baiting (Figure 5). Specifically, metabarcoding of the ITS1 region detected 25 *Phytophthora*-positive rhizosphere soil samples, while that of the *rps10* gene identified 24 *Phytophthora*-positive samples (Figure 5). Additionally, all samples that were *Phytophthora*-positive through metabarcoding of the *rps10* gene were also identified as *Phytophthora*-positive by metabarcoding of the ITS1 region (Figure 5).

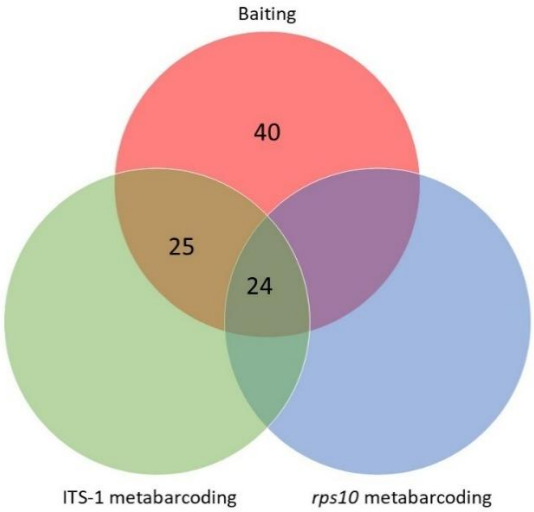

Figure 5. Comparison among the number of *Phytophthora*-positive rhizosphere soil samples obtained by baiting, and the metabarcoding of the ITS-1 and *rps10* gene.

The *Phytophthora* taxa identified through the combined use of baiting and metabarcoding of the ITS1 region and *rps10* gene included several known species, such as *P. nicotianae*, *P. citrophthora*, *P. citricola*, *P. occultans*, *P. oleae* and *P. pachypleura*, as well as one pair of taxa that could not be distinguished from each other, *P. crassamura/P. megasperma*, along with 13 unknown *Phytophthora* taxa (Table 1). Six of these unknown taxa were detected by metabarcoding of the ITS1 region (i.e., *Phytophthora* ITS1 unk 1-6), and seven were identified through the *rps10* gene (*i.e.*, *Phytophthora rps10* unk 1-7) (Table 1). Both ITS1 and *rps10* metabarcoding protocols detected all three taxa isolated by baiting. In addition to identifying six unknown *Phytophthora* taxa (*Phytophthora* ITS1 unk 1-6), metabarcoding of the ITS1 region also detected additional known species such as *P. occultans*, *P. oleae*, *P. pachypleura*, and the indistinguishable taxon *P. crassamura/P. megasperma*. Finally, apart from the known species *P. nicotianae*, *P. citrophthora*, and *P. citricola*, which were detected by both baiting and ITS1 metabarcoding, the *rps10* gene exclusively identified unknown *Phytophthora* taxa (*i.e.*, *Phytophthora* rps10 *unk* 1-7) (Figure 6).

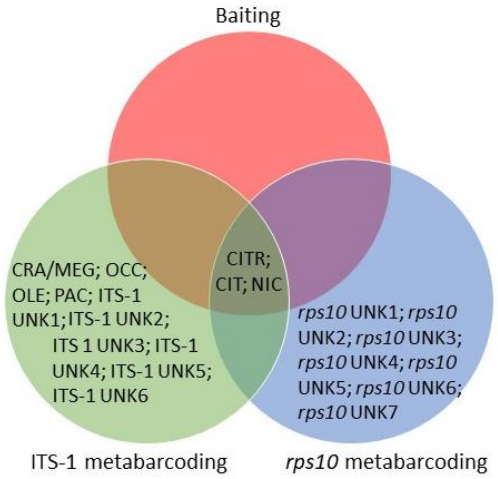

Figure 6. Comparison among the different *Phytophthora* taxa (CITR = *P. citricola*; CIT = *P. citrophthora;* CRA/MEG = *P. crassamura / P. megasperma*; NIC = *P. nicotianae*; OCC = *P. occultans*; OLE = *P. oleae*; PAC = *P. pachypleura*); ITS-1 UNK1-6 = *Phytophthora* ITS-1 UNK1-6; *rps10* UNK1-7 = *Phytophthora rps10* UNK1-7) recorded by baiting, and the metabarcoding of the ITS-1 and *rps10* gene.

6.4.5 . Known *Phytophthora* taxa recorded per citrus-producing area - comparison of outcomes from baiting, metabarcoding of ITS-1 region and *rps10* gene

Data on the presence/absence of the known *Phytophthora* taxa recorded by each technique were combined to assess the individual performance of baiting, metabarcoding of the ITS1 region, and the *rps10* gene (Figure 7). In detail, in Lentini (Figure 7a), *P. nicotianae* was the only species recorded by all three techniques. *P. citrophthora* was exclusively recorded by baiting, while *P. crassamura*/*P. megasperma*, *P. oleae*, and *P. citrophthora* were recorded only through metabarcoding of the ITS1 region. The metabarcoding of the *rps10* gene did not record any exclusive species (Figure 7a). In Siracusa (Figure 7b), *P. nicotianae*, *P. citrophthora*, and *P. citricola* were recorded by all three techniques. *P. pachypleura* was exclusively recorded through metabarcoding of the ITS1 region, while neither baiting nor the metabarcoding of the *rps10* gene provided any exclusive records (Figure 7b). In Ramacca (Figure 7c), *P. nicotianae* was the only species recorded by all three techniques. *P. citricola* was exclusively recorded through metabarcoding of the ITS1 region, and no exclusive records were provided by either baiting or *rps10* metabarcoding (Figure 7c). Finally, in Mineo (Figure 7d), *P. nicotianae* and *P. citrophthora* were recorded by all three techniques. *P. occultans* was exclusively

recorded through metabarcoding of the ITS1 region, and no exclusive records were provided by either baiting or *rps10* metabarcoding (Figure 7d).

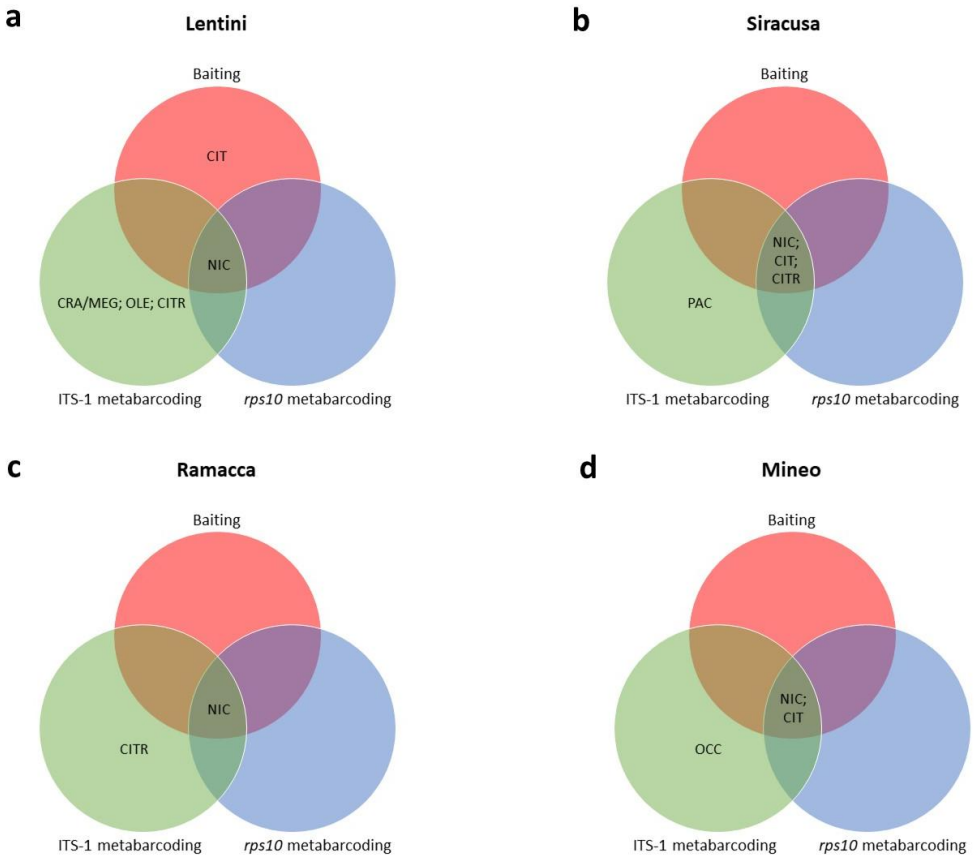

Figure 7. Known *Phytophthora* taxa (CITR = *P. citricola*; CIT = *P. citrophthora;* CRA/MEG = *P. crassamura / P. megasperma*; NIC = *P. nicotianae*; OCC = *P. occultans*; OLE = *P. oleae*; PAC = *P. pachypleura*) recorded by baiting, metabarcoding of ITS-1 region or *rps10* gene in the citrus-producing areas of Lentini (a), Siracusa (b), Ramacca (c) and Mineo (d).

6.4.6 Influence of environmental factors on the overall occurrence of *Phytophthora* taxa

The combined approach of baiting and metabarcoding of ITS1 and *rps10* revealed an unexpected diversity of *Phytophthora* taxa in citrus orchards. Figure 8 shows the grouping of recorded *Phytophthora* taxa related to the environmental variables, including 'overall healthy status of trees' in the orchard (healthy versus unhealthy), 'type of agronomic management' (organic versus conventional) and 'citrus-producing area' (Siracusa/Lentini/Mineo/Ramacca).

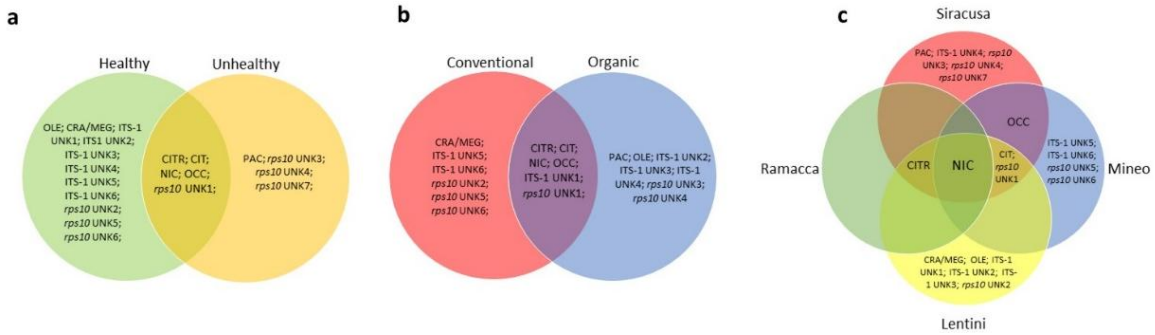

Figure 8. Grouping of *Phytophthora* taxa (CITR = *P. citricola*; CIT = *P. citrophthora;* CRA/MEG = *P. crassamura / P. megasperma*; NIC = *P. nicotianae*; OCC = *P. occultans*; OLE = *P. oleae*; PAC = *P. pachypleura*); ITS-1 UNK1-6 = *Phytophthora* ITS-1 UNK1-6; *rps10* UNK1-7 = *Phytophthora rps10* UNK1-7) recorded through the combined approach of baiting and metabarcoding of the ITS-1 region and rps10 gene, based on the environmental variables: (a) 'overall health of plants' (healthy/unhealthy), (b) 'agronomical management' (organic/conventional), and (c) 'citrus-producing area' (Siracusa/Lentini/Mineo/Ramacca).

To investigate the statistical significance of the occurrence of *Phytophthora* taxa across these environmental variables, records on their presence/absence, in relation to 'overall health of trees' (healthy/unhealthy), 'type of agronomic management' (organic/conventional) and 'citrus-producing area' (Siracusa/Lentini/Mineo/Ramacca), were subjected to PERMANOVA analysis. The results of this analysis showed a significant impact of the variables 'overall health of trees' and 'citrus-producing area' on the presence/absence of *Phytophthora* taxa, while 'agronomic management' had no significant impact (Table 2).

Table 2. PERMANOVA analysis of the impact of the variables 'overall health of plants', 'agronomical management' and 'citrus-producing area' in determining the recorded composition in *Phytophthora* taxa.

Name of the variable	R2	p-value	Variance explained (%)	Significance
Overall Health of Plants (healthy/unhealthy)	0.26903	0.001	26.90%	***
Agronomical Management (conventional/organic)	0.03152	0.253	3.15%	
Citrus-producing Area (Syracuse/Lentini/Mineo/Ramacca)	0.31655	0.001	31.66%	***

In detail, the 'overall health of trees', which took into account wether the orchard was characterized by large prevalence of either healthy or unhealthy trees, explained 26.90% of the variance in determining the presence/absence of recorded *Phytophthora* taxa (R^2 = 0.26903, p = 0.001). The 'citrus-producing area', Siracusa, Lentini, Mineo or Ramacca, accounted for 31.66% of the variance (R^2 = 0.31655, p = 0.001) in determining the composition of *Phytophthora* communities. Finally, the 'agronomic management', organic or conventional, did not have a significant effect in determining the recorded *Phytophthora* taxa (R^2 = 0.03152, p = 0.253).

To further describe the impact of the three variables in determining the probability of presence/absence of *Phytophthora* taxa, a Non-metric Multidimensional Scaling (NMDS) ordination was conducted based on the Jaccard index. The NMDS ordination produced a two-dimensional solution with a stress (Stress NMDS: 0.09783) value below 0.2, indicating an acceptable representation of the data, whose results are visualized in Figure 9. The NMDS ordination provides a graphical representation of the community structure across the sampled orchards, showing clear patterns associated with the health status of the trees (Figure 9a), agronomic management practices (Figure 9b), and citrus-producing area (Figure 9c). In the NMDS ordination, species vectors that are longer in the NMDS plot (e.g. *P. crassamura/P. megasperma* and *P. oleae*) indicate taxa that are more constrained to fewer sites or variables. In contrast, shorter vectors (e.g. *P. citrophthora* and *P. nicotianae*) reflect taxa that are more widespread across multiple samples, indicating a broader distribution across the conditions examined.

.

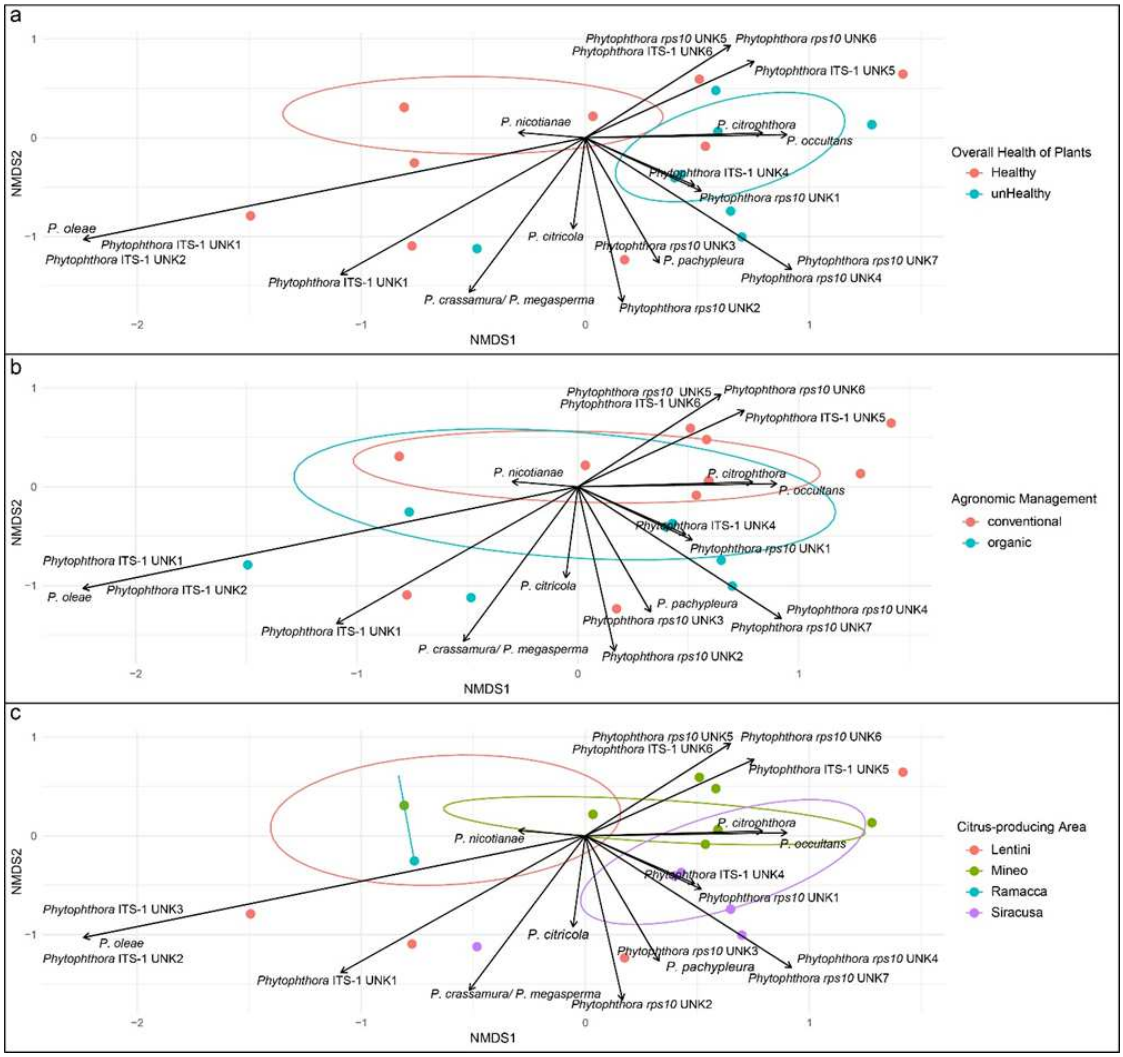

Figure 9. Non-metric Multidimensional Scaling (NMDS) of *Phytophthora* taxa presence/absence data in relation to: (a) tree health status (healthy/unhealthy); (b) agronomical management (conventional/organic) and (c) citrus-producing area (Syracuse, Lentini, Mineo, Ramacca). Vectors represent the association of individual *Phytophthora* taxa with the different explanatory variables. Longer vectors indicate species that are more restricted to certain conditions, while shorter vectors represent species that are more widespread across condition. The ellipses represent the confidence intervals for the centroids of each grouping.

Unhealthy trees were associated with *Phytophthora* taxa, such as *P. citrophthora* and *P. occultans*, as evidenced by their proximity to the unhealthy tree category and their longer species vectors (Figure 9a). Conversely, taxa such as *P. nicotianae* were more strictly associated with healthy plants. Although the agronomic management practice was not shown as significant in PERMANOVA the NMDS plot suggests a tendency for certain species, like *P. pachypleura*, *Phytophthora* ITS1 unk5, *Phytophthora* ITS1 unk6 to be more frequent in conventionally managed orchards, though this pattern is not as pronounced

as with the other explanatory variables (Figure 9b). In terms of the region, orchards from Siracusa, Lentini, Mineo, and Ramacca show distinct clusters in the ordination space (Figure 9c). For example, taxa such as *P. pachypleura*, *P. citricola*, *Phytophthora* ITS1 unk4, *Phytophthora rps10* unk1 and *Phytophthora* ITS1 unk4 appear prevalent in the area of Siracusa. Other taxa, such as *P. oleae*, *Phytophthora* ITS1 unk1, *Phytophthora* ITS1 unk3 are more common in Lentini, while *P. citrophthora*, *P. occultans*, *Phytophthora* ITS1 unk5, *Phytophthora* ITS1 unk6, *Phytophthora rps10* unk5, *Phytophthora rps10* unk6 are more common in Mineo. Finally, *P. nicotianae* was associated with the area of Ramacca.

6.5 Discussion

This is the first study to investigate the diversity of *Phytophthora* communities in citrus orchards of Eastern Sicily using the complementary methods of leaf-baiting and metabarcoding, the latter based on both the ITS1 region and the rps10 gene. Baiting detected three *Phytophthora* species: *P. citrophthora*, *P. nicotianae*, and *P. citricola*. In contrast, metabarcoding identified a total of 20 taxa, including those detected by bairing and additional ones like *P. oleae*, *P. pachypleura*, and P. *occultans*, along with 13 unidentified taxa. This discrepancy underscores the greater sensitivity of the metabarcoding approach. While baiting effectively isolates actively sporulating species, metabarcoding is capable of detecting species that may not sporulate as readily, are present at a lower frequency or more difficult to grown on agar media. These findings are consistent with previous studies that reported a higher number of species detected through metabarcoding compared to traditional isolation techniques (Burgess et al., 2021; La Spada et al., 2022; Sarker et al., 2023). The analysis of metabarcoding results, utilizing both PERMANOVA and non-metric multidimensional scaling (NMDS), revealed a significant correlation between the presence of certain *Phytophthora* taxa and both the health status of trees and the geographical areas of the orchards. This suggests that these factors are significant influences shaping the communities of these oomycetes in the rhizosphere soil of citrus trees in investigated citrus orchards. Conversely, no significant correlation was found between the diversity and distribution of *Phytophthora* species and the type of orchard management, i.e. organic versus conventional. Expanding the sampling effort in subsequent studies will be essential to better capture the dynamics of these communities across a broader range of orchards and to confirm the observed pattern throughout Eastern Sicily.

Moreover, although in this study the sampling campaign was carried out after a prolonged period of drought, perhaps related to the desertification process impacting

some areas of the Mediterranean macroregion including Sicily (Toreti *et al.*, 2024), no evidence supported the hypothesis that in recent years substantial modifications have occurred in *Phytophthora* communities of the rhizosphere soil of citrus orchards. According to Toreti et al. (2024), the Mediterranean region, including Sicily, has experienced a significant increase in drought events over the last decade, leading to prolonged periods of soil moisture deficit. These extreme conditions may influence both pathogen survival and plant susceptibility, emphasizing the role of climate change as a key factor in future pathogen dynamics. However, the lack of observable shifts in *Phytophthora* diversity in this study may be attributed to increased irrigation practices used to counteract drought stress, which could buffer the immediate effects of reduced rainfall. Long-term projections suggest that without mitigation strategies, the cumulative impact of drought on soil microbial communities and pathogen dynamics could become more pronounced (Loiko and Islam, 2024). As a matter of fact, in this study *P. citrophthora* and *P. nicotianae* were by far the most prevalent species identified by both leaf baiting and metabarcoding. These two species were also the most frequently isolated species in citrus orchards of Eastern Sicily during surveys carried out decades ago using less precise and sensitive detection methods such as fruit baitings or direct isolation from tissues and soil using selective media (Cacciola and Magnano di San Lio, 2008; Favaloro and Sammarco, 1973, Magnano di San Lio et al., 1988). Although drought is known to influence and alter microbial community structures, its effects are expected to be mitigated in irrigated crops. On the other hand, it is known that drought may increase host susceptibility to infections by pathogens due to reduced water and nutrient availability (Pautasso et al., 2012; Ruiz-Gómez et al., 2019; Ulrich et al., 2019). This has particular relevance in the case of waterborne pathogens, like oomycetes, which are favoured by irrigation. Previous studies have shown that drought conditions do not significantly impair the infectivity of *Phytophthora* species (Serrano et al., 2021; Contreras-Cornejo et al., 2023). However, drought may exert a selective pressure on *Phytophthora* communities by favoring species more resistant to water stress conditions. For instance, it has been hypothesized that the thick oospore wall of *P. multivora*, a homothallic species segregated from the *P. citricola* complex, is an ecological adaptation to extreme seasonally dry soil conditions (Scott et al., 2009).

In this study, 50 rhizosphere soil samples were collected from a total of 10 sampling sites, corresponding to an equal number of citrus orchards across four major citrus-producing areas of Eastern Sicily, i.e. Siracusa, Lentini, Mineo and Ramacca. The sampling design

included orchards either organically or conventionally managed, as well as orchards with predominantly either healthy-looking or unhealthy-looking trees. Overall 40 out of 50 rhizospheric soil samples tested positive for *Phytophthora* using baiting. This detection technique enabled the isolation and identification of the three most common *Phytophthora* species pathogenic to citrus, confirming its robustness as a routine diagnostic method. In fact, baiting can be regarded as more effective than metabarcoding given that 25 out of 50 soil eDNA samples collected in this study did not produce PCR amplicons and may be considered false negatives. Specifically, 25 samples tested positive with ITS1 region metabarcoding assay, compared to 24 with the *rps10* gene metabarcoding assay. Several factors may explain why some samples were unsuitable for molecular analysis. An important consideration is the volume of soil employed in different techniques. Molecular analyses typically utilize much smaller sample volumes compared to baiting methods, which may account for the higher number of *Phytophthora*-positive samples obtained through baiting (La Spada et al., 2022). Additionally, drought conditions not only reduce *Phytophthora* activity, but may also compromise the representativeness of the soil sample by reducing the overall microbial biomass (Qu et al., 2023) and DNA concentration, further diminishing the likelihood of detecting *Phytophthora* using molecular techniques. Finally, the use of rps10 oomycete primers may preferentially amplify oomycetes other than *Phytophthora*, as reported in previous studies using the rps10 gene (Foster et al., 2022).

This suggests that baiting could be more sensitive in conditions where the presence of Phytophthora is diminished, such as during drought periods. Conversely, molecular analyses may be more affected by variables related to the quality of DNA extracted from soil samples collected under suboptimal climatic conditions.

It is noteworthy that all samples that tested positive using metabarcoding were also positive via baiting, further confirming the efficacy of the classical method for detecting *Phytophthora* inoculum in rhizosphere soil of citrus trees. However, metabarcoding showed greater resolving power in revealing a higher diversity of *Phytophthora* communities in almost all examined rhizosphere soil samples. Besides the three *Phytophthora* species identified with baiting, i.e. *P. nicotianae*, *P. citrophthora*, and *P. citricola*, ASVs consistent with 20 known species and new unknown taxa were detected with barcoding (Table 1). Among the unknowns, those designated as *Phytophthora* ITS1 unk1, unk2, and unk3 in the phylogenetic analysis clustered closely with both *P. nicotianae* and *P.* × *pelgrandis*. This result suggests that these unknown taxa could be variants of

either *P. nicotianae* or *P.* × *pelgrandis*. However, the close phylogenetic alignment between *P. nicotianae* and *P.* × *pelgrandis* can be explained by the fact that *P.* × *pelgrandis* is a hybrid of *P. nicotianae* and *P. cactorum*, as previously described by Nirenberg et al. (2008). Despite minor sequence differences, the hybrid nature of *P.* × *pelgrandis* contributes to its strong similarity with *P. nicotianae* in the ITS region. Given that *P.* × *pelgrandis* has not previously been recorded either by isolation or through metabarcoding of eDNA in association with rhizosphere soil of citrus orchards, and that the occurrence of *P. nicotianae* in citrus orchards is well-documented worldwide, it is therefore more likely that the unknown taxa represent minor ITS variants of *P. nicotianae* that need to be added to the reference database. Similarly, the phylogenetic analysis based on the ribosomal rps10 gene revealed a high genetic similarity among the sequences attributed to *P. citricola* and the unidentified taxa *Phytophthora* rps10 unk3, unk4, and unk7, as well as between *P. citrophthora*, *P. occultans*, and *Phytophthora rps10* unk1. In both cases, the detection of a single nucleotide substitution within a highly conserved gene suggests that these ASVs are intraspecific variants of the respective reference species rather than distinct taxa. Indeed, metabarcoding, which examines pooled environmental DNA rather than individual pure isolates, is more more likely to amplify and identify such minor variants which may limit its ability to distinguish closely related taxa and/or intraspecific variants. Furthermore such minor variants may be PCR errors or Illumina sequencing artefacts.

Phytophthora occultans is a homothallic species in the ITS phylogenetic clade 2a (Man in't Veld *et al.*, 2015), the same subclade as *P. citrophthora*, a well known aggressive pathogen of citrus (Puglisi et al., 2017), while *P. pachypleura* is a homothallic species in subclade 2c (Henricot et al., 2014), the same subclade as *P. citricola*, also an aggressive pathogen of citrus (Thomidis et al., 2005). *Phytophthora oleae* is also in clade 2, but in a distinct subclade (2d) (Ruano-Rosa et al., 2018). The range of known hosts and the geographical distribution of this species are relatively restricted (Ruano-Rosa *et al.*, 2018; González *et al.*, 2019; Riolo *et al.*, 2020; Linaldeddu *et al.*, 2023) . As reported by Abad et al. (2023), all clade 2 species occur in terrestrial habitats, and most are aggressive plant pathogens. In humid environments, some can temporarily adapt to an aerial lifestyle and infect the above-ground organs of the plant, including fruit and leaves. In citrus, aerial infections on fruit and leaves cause the diseases known as brown rot and blight, respectively (Rovetto et al., 2024). After the recent description of 43 new species clade 2 has become the largest clade of *Phytophthora* (Jung et al., 2024). The prevalence of reads of *P. citrophthora* and *P. nicotianae*, identified as the most abundant species by both ITS1 and

rps10 gene, supports the established role of these two species as key citrus pathogens in Mediterranean areas and major species responsible for Phytophthora diseases of citrus worldwide (Gams 2000; Cacciola and Magnano di San Lio, 2008; Rovetto et al., 2024). *Phytophthora citrophthora* was the most abundant species in both metabarcoding analyses, with a prevalence of 35.5% in ITS reads and 62.8% in *rps10* reads. This species is well-documented as one of the main causative agent of trunk rot in citrus (Ippolito et al., 2002; Dirac et al., 2003; Alvarez et al., 2009). The dominance of its reads in both ITS1 and *rps10* metabarcoding confirms is significance under Sicilian agroecological conditions. Similarly, *P. nicotianae*, with 35.1% of ITS1 reads and 14.7% in *rps10* reads, has been reported as an important pathogen in citrus orchards, being more active under warm conditions and primarily attacking fine roots (Timmer et al., 1998; Ippolito et al., 2002; Dirac et al., 2003; Alvarez et al., 2009). Interestingly, a series of previous studies aimed at characterizing the genetic varibility of a global collection of isolates of this species from a wide range of hosts using both mitochondrial and nuclear molecular markers, demonstrated that isolates of *P. nicotianae* from citrus grouped separately from isolates recovered from other hosts, suggesting either a host-specific subgroup or a founder effect in citrus propagation stocks (Mammella et al., 2011, 2013; Biasi et al., 2016). The identification of *Phytophthora occultans* (16.6% of ITS reads) and *P. citricola* (10.4% of ITS reads; 4.1% of *rps10* reads) adds complexity to the *Phytophthora* communities in Sicilian citrus orchards. Initially isolated from *Buxus* (Man in't Veld et al., 2015) and now other horticultural crops (Gitto et al., 2018; Ghaderi et al., 2023) this pathogen has not been reported as a pathogen of Citrus. In a previous survey, however, it was detected in association with citrus trees in Eastern Sicily using ITS1 region metabarcoding (La Spada et al., 2022). Consequently, *P. occultans* appears to be a widespread albeit less damaging occupant of the citrus tree rhizosphere in this production area. To assess the potential threat that *P. occultans* and sporadically occurring *Phytophthora* species, such as *P. oleae* and *P. pachypleura*, along with the 13 unidentified *Phytophthora* taxa, pose to citrus orchards, a more detailed understanding of their ecology and tests of their pathogenicity are required. Unfortunately, living isolates of these species and unidentified taxa are not available, as they were detected exclusively through metabarcoding. The detection of *Phytopythium* and *Globisporangium* species in the rhizosphere soil of *citrus* trees using metabarcoding based on amplification of the *rps10* gene would support a possible involvement of these oomycetes in the etiology of trunk gummosis and crown rot of citrus as reported by Benfradj et al. (2017).

As expected, the ITS1 marker assay was significantly more specific and sensitive at detecting *Phytophthora* species than that based on the *rps10* gene; 99.5% of the ITS1 reads and 87.2% of the amplified sequence variants (ASVs) were detected as *Phytophthora*, compared to 82.5% of the reads and 33.9% of the ASVs for rps10. These results are consistent with previous studies that demonstrated the greater discriminative power of the ITS1 region assay based on the Scibetta *et al*. (2012) primers in detecting *Phytophthora* species compared to other genetic markers (Burgess et al., 2022; Migliorini et al., 2023). However, in this study the *rps10* gene metabarcoding amplified genera other than *Phytophthora*, confirming the assay's value in obtaining a wider overview of the oomycete community in soil (Foster et al., 2022). This result is supported by previous studies indicating that *rps10* can be a useful marker for large-scale investigations of oomycete communities (Burgess et al., 2022; Migliorini et al., 2023).

Overall, these results confirm the potential of metabarcoding in revealing the complexity of *Phytophthora* communities in natural, agricultural and horticultural ecosystems, as demonstrated in several recent studies (Prigigallo et al., 2015, 2016; Català et al., 2017; Khaliq et al., 2018; Ruiz Gómez et al., 2019; Burgess et al., 2021; La Spada et al., 2022; Green et al., 2025). The metabarcoding findings in this study reported *P. oleae*, and *P. pachypleura* in association with citrus rhizosphere soil for the first time worldwide. Similarly, for the identical *P. crassamura* or *P. megasperma* ITS1 barcode, this is the first report in association with citrus worldwide if the ASV is considered as *P. crassamura*, whereas it is the first report in association with citrus in Italy if the ASV is considered as *P. megasperma*. Recent studies compared baiting and metabarcoding and, in agreement with the present study, observed the number of *Phytophthora* species detected with baiting was lower than the number of species identified with metabarcoding (Burgess et al., 2021; La Spada et al., 2022; Sarker et al., 2023). To explain the selectivity of baiting, it has been hypothesized that baiting conditions favor parasitic species that sporulate early, are able to infect baits with relatively few zoospores and grow more rapidly than others on selective agar media.

The correlation seen in PERMANOVA and NMDS analysis between the unhealthy status of orchards and the presence of *P. citrophthora* and *P. occultans* confirms the pathogenicity of the former species on citrus and suggests the latter can be regarded as a potential citrus pathogen. Conversely, the significant correlation between the presence of *P. nicotianae* and the absence of symptoms on trees can be explained assuming that citrus trees infected by this pathogen, which typically infects roots, show symptoms in the

canopy only if a high proportion of roots are infected. Only quantitative studies can shed light on this aspect. Finally, there is no single explanation as regards the relationship between the distribution of diverse *Phytophthora* taxa and the geographical area where the orchards were located. This may depend on either a founder effect, i.e. the dominant *Phytophthora* taxa in the nuseries which originally supplied the plants, or local ecological conditions. The latter hypothesis aligns with other studies that emphasized the effect of both environment and climate change on *Phytophthora* diversity in natural ecosystems (Burgess et al., 2019; Riddell et al., 2019). Further in-depth sampling would be required to resolve these questions.

6.6 Conclusions

This study confirmed the complementarity between the traditional baiting and metabarcoding to identify the diversity and distribution of oomycete communities associated with the rhizosphere of citrus trees. Baiting proved to be a robust diagnostic method to detect the most dominant and aggressive species, such as *P. citrophthora*, *P. nicotianae* and *P. citricola*. Metabarcoding was more effective in revealing the diversity and complexity of oomycete communities in these Sicilian citrus tree rhizosphere samples. The number of *Phytophthora* taxa identified with this molecular diagnostic method was greater than the number detected with baiting; 20 versus three. Beside the seven described species, metabarcoding detected numerous still unknown taxa. Some of the *Phytophthora* species identified with metabarcoding are new reports on citrus. The sensitivity of this molecular diagnostic technique makes it a powerful tool to study the impact of environmental factors, such as climate change, on oomycete soil populations. An interesting novelty of this study is that the analysis of metabarcoding data using PERMANOVA and NMDS identified a correlation between the composition of *Phytophthora* communities in rhizosphere soil of citrus trees and both the health status of the trees and the geographic area of the citrus orchard. Conversely no substantive differences were observed in *Phytophthora* communities between organically and conventionally managed citrus orchards. In generally, this type metabarcoding study appears very promising to identify major environmental factors shaping the diversity of oomycete communities associated with the rhizosphere of crop plants.

CRediT author statement.

Sebastiano Conti Taguali: Conceptualization, Investigation, Methodology, Software, Data Curation, Formal analysis, Validation, Writing - Original Draft, Writing - Review & Editing.

Federico La Spada: Investigation, Methodology, Formal analysis, Writing - Original Draft, Writing - Review & Editing.

Peter Cock: Methodology, Software, Data Curation, Formal analysis.

Beatrix Keillor: Methodology, Data Curation, Formal analysis.

David E.L Cooke: Conceptualization, Investigation, Methodology, Formal analysis, Writing - Review & Editing, Resources, Supervision.

Santa Olga Cacciola: Conceptualization, Investigation, Writing - Original Draft, Validation, Writing - Review & Editing, Resources, Supervision, Funding acquisition, Project administration.

FUNDS

This study was supported by the University of Catania, Italy, "Investigation of Phytopathological problems of the main Sicilian productive contexts and eco-sustainable defense strategies (MEDIT-ECO)"- PiaCeRi-PIAno di inCEntivi per la Ricerca di Ateneo 2020-22 linea 2" "5A722192155"; the project "Smart and innovative packaging, postharvest rot management, and shipping of organic citrus fruit (BiOrangePack)" under Partnership for Research and Innovation in the Mediterranean Area (PRIMA) – H2020 (E69C20000130001); the European Union (NextGeneration EU), through the MUR-PNRR project SAMOTHRACE (ECS00000022) and the project "PROMETEO", Strategic project ENI Italy-Tunisia 2014–2020.

Conflict of interest: Authors declare no conflict of interest.

Declaration of availability of supplementary material

The supplementary data of this study will be available to the evaluators upon request to the corresponding authors.

Results of this study have been submitted as a scientific article to the Mycological Progress -Springer

6.7 References

Abad, Z.G., Burgess, T.I., Bourret, T., Bensch, K., Cacciola, S.O., Scanu, B., et al. (2023) *Phytophthora*: taxonomic and phylogenetic revision of the genus. *Studies in Mycology*, 106, 259–348. https://doi.org/10.3114/sim.2022.106.05.

Aghighi, S., Hardy, G.E.S.J., Scott, J.K. & Burgess, T.I. (2012) *Phytophthora bilorbang* sp. nov., a new species associated with the decline of *Rubus anglocandicans* (European blackberry) in Western Australia. *European Journal of Plant Pathology*, 133, 841–855. https://doi.org/10.1007/s10658-012-0006-5.

Akıllı Şimşek, S., Katırcıoğlu, Y.Z., Çakar, D., Rigling, D. & Maden, S. (2019) Impact of fungal diseases on common box (*Buxus sempervirens* L.) vegetation in Turkey. *European Journal of Plant Pathology*, 153, 1203–1220. https://doi.org/10.1007/s10658-018-01636-4.

Aloi, F., Parlascino, R., Conti Taguali, S., Faedda, R., Pane, A. & Cacciola, S.O. (2023) *Phytophthora pseudocryptogea*, *P. nicotianae* and *P. multivora* Associated to *Cycas revoluta*: First Report Worldwide. *Plants*. https://doi.org/10.3390/plants12051197.

Altschul, S.F., Gish, W., Miller, W., Myers, E.W. & Lipman, D.J. (1990) Basic local alignment search tool. *Journal of Molecular Biology*, 215, 403–410. https://doi.org/10.1016/S0022-2836(05)80360-2.

Alvarez, L.A., Gramaje, D., Abad-Campos, P. & García-Jiménez, J. (2009) Seasonal susceptibility of citrus scions to *Phytophthora citrophthora* and *P. nicotianae* and the influence of environmental and host-linked factors on infection development. *European Journal of Plant Pathology*, 124, 621–365. https://doi.org/10.1007/s10658-009-9449-8.

Bačová, A., Cooke, D.E.L., Milenković, I., Májek, T., Nagy, Z.Á., Corcobado, T., et al. (2024) Hidden *Phytophthora* diversity unveiled in tree nurseries of the Czech Republic with traditional and metabarcoding techniques. *European Journal of Plant Pathology*, 170, 131–156. https://doi.org/10.1007/s10658-024-02886-1.

Benfradj, N., Migliorini, D., Luchi, N., Santini, A. & Boughalleb-M'Hamdi, N. (2017) Occurrence of *Pythium* and *Phytopythium* species isolated from citrus trees infected with gummosis disease in tunisia. *Archives of Phytopathology and Plant Protection*, 50, 286–302. https://doi.org/10.1080/03235408.2017.1305479.

Biasi, A., Martin, F.N., Cacciola, S.O., Magnano Di San Lio, G., Grünwald, N.J. & Schena, L. (2016) Genetic analysis of *Phytophthora nicotianae* populations from different hosts using microsatellite markers. *Phytopathology*, 106, 1006–1014. https://doi.org/10.1094/PHYTO-11-15-0299-R.

Boughalleb-M'hamdi, N., Benfradj, N., Migliorini, D., Luchi, N., Santini, A. (2018) *Phytophthora nicotianae* and *P. cryptogea* causing gummosis of citrus crops in Tunisia. *Tropical plant pathology*, 43, 36–48. https://doi.org/10.1007/s40858-017-0180-2

Brasier, C. (2009) *Phytophthora* biodiversity: How many *Phytophthora* species are there? *Proceedings of the Fourth Meeting of the International Union of Forest Research Organizations (IUFRO) Working Party S07.02.09: Phytophthoras in forest and natural ecosystems*, 101–115.

Burgess, T.I., López-Villamor, A., Paap, T., Williams, B., Belhaj, R., Crone, M., et al. (2021) Towards a best practice methodology for the detection of *Phytophthora* species in soils. *Plant Pathology*, 70, 604–614. https://doi.org/10.1111/ppa.13312.

Burgess, T.I., McDougall, K.L., Scott, P.M., Hardy, G.E.S.J. & Garnas, J. (2019) Predictors of *Phytophthora* diversity and community composition in natural areas across diverse Australian ecoregions. *Ecography*, 42, 401–620. https://doi.org/10.1111/ecog.03904.

Burgess, T.I., White, D. & Sapsford, S.J. (2022) Comparison of primers for the detection of *Phytophthora* (and Other Oomycetes) from Environmental Samples. *Journal of Fungi*, 8, 980. https://doi.org/10.3390/jof8090980.

Cacciola, S.O. & Magnano di San Lio, G. (2008) Management Of Citrus Diseases Caused By *Phytophthora* Spp. Integrated Management of Diseases Caused by Fungi, Phytoplasma and Bacteria. Springer, pp. 61–82.

Català, S., Berbegal, M., Pérez-Sierra, A. & Abad-Campos, P. (2017) Metabarcoding and development of new real-time specific assays reveal *Phytophthora* species diversity in holm oak forests in eastern Spain. *Plant Pathology*, 66, 115–123. https://doi.org/10.1111/ppa.12541.

Català, S., Pérez-Sierra, A. & Abad-Campos, P. (2015) The use of genus-specific amplicon pyrosequencing to assess *Phytophthora* species diversity using eDNA from soil and water in northern spain. *PLoS ONE*, 10. https://doi.org/10.1371/journal.pone.0119311.

Chi, N.M., Thu, P.Q., Nam, H.B., Quang, D.Q., Phong, L. V., Van, N.D., et al. (2020) Management of *Phytophthora palmivora* disease in Citrus reticulata with chemical fungicides. *Journal of General Plant Pathology*, 86, 494–502. https://doi.org/10.1007/s10327-020-00953-z.

Cock, P.J.A., Cooke, D.E.L., Thorpe, P. & Pritchard, L. (2023) THAPBI PICT—a fast, cautious, and accurate metabarcoding analysis pipeline. *PeerJ*, 11. https://doi.org/10.7717/peerj.15648.

Conti Taguali, S., Bua, C., Rovetto, E.I., Pane, A., Spada, F. La & Cacciola, S.O. (2024) Bleeding stem cankers and root rot caused by *Phytophthora multivora* in *Morus alba*, *Pistacia atlantica* and *Sterculia diversifolia* trees in eastern Sicily. *Journal of Plant Pathology*, 106, 291. https://doi.org/10.1007/s42161-023-01547-2.

Contreras-Cornejo, H.A., Larsen, J., Fernández-Pavía, S.P. & Oyama, K. (2023) Climate change, a booster of disease outbreaks by the plant pathogen *Phytophthora* in oak forests. *Rhizosphere*, 27, 100719. https://doi.org/10.1016/j.rhisph.2023.100719.

Cooke, D.E.L., Drenth, A., Duncan, J.M., Wagels, G. & Brasier, C.M. (2000) A molecular phylogeny of *Phytophthora* and related oomycetes. *Fungal Genetics and Biology*, 30, 17–32. https://doi.org/10.1006/fgbi.2000.1202.

Crous, P.W., Wingfield, M.J., Burgess, T.I., J. Hardy, G.E. St., Barber, P.A., Alvarado, P., et al. (2017) Fungal planet description sheets: 558-624. *Persoonia: Molecular Phylogeny and Evolution of Fungi*, 38. https://doi.org/10.3767/003158517X698941.

Das, A.K., Kumar, A., Nerkar, S. & Bawage, S. (2012) First report of *Phytophthora insolita* in India. *Australasian Plant Disease Notes*, 7, 131–132. https://doi.org/10.1007/s13314-012-0066-6.

Dirac, M.F., Menge, J.A. & Madore, M.A. (2003) Comparison of seasonal infection of citrus roots by *Phytophthora citrophthora* and *P. nicotianae* var. *parasitica*. *Plant Disease*, 87, 493–501. https://doi.org/10.1094/PDIS.2003.87.5.493.

Erwin, D.C. & Ribeiro, O.K. (1996) *Phytophthora* Diseases Worldwide. *American Phytopathological Society (APS)*, St Paul, M. https://doi.org/10.2307/3761286.

FAO (2021) *Citrus Fruit Statistical Compendium.* Rome, Italy.

Favaloro, M., Sammarco, G. (1973) Ricerche sul marciume radicale e del colletto degli agrumi. Specie di Phytophthora presenti negli agrumeti della Sicilia Orientale. Investigations on collar and root rot of Citrus orchards of eastern Sicily. *Phytopathologia Mediterranea*, 105–107.

Foster, Z.S.L., Albornoz, F.E., Fieland, V.J., Larsen, M.M., Jones, F.A., Tyler, B.M., et al. (2022) A New Oomycete Metabarcoding Method Using the *rps10* Gene. *Phytobiomes Journal*, 6, 214–226. https://doi.org/10.1094/PBIOMES-02-22-0009-R.

Gai, Y., Ma, H., Chen, Y., Li, L., Cao, Y., Wang, M., et al. (2021) Chromosome-scale genome sequence of *Alternaria alternata* causing alternaria brown spot of citrus. *Molecular Plant-Microbe Interactions*, 34, 726–732. https://doi.org/10.1094/MPMI-10-20-0278-SC.

Gams, W. (2000) Citrus Health Management. In: Timmer, L.W. and Duncan, L.W. (Ed.) European Journal of Plant Pathology. pp. 399–400.

Ghaderi, F. (2023) New report of *Phytophthora occultans* associated with root and crown rot on Sansevieria. *Mycologia Iranica*, 10, 45–54. https://doi.org/10.22043/MI.2023.361284.1250.

Gitto, A.J., Jeffers, S.N., Graney, L.S., Loyd, A.L. & Bechtel, C.N. (2018) First report of *Phytophthora occultans* causing root rot on American boxwood planted in residential landscapes in the Eastern United States. *Plant Disease*, 102, 2384–2384. https://doi.org/10.1094/PDIS-04-18-0684-PDN.

González, M., Pérez-Sierra, A. & Sánchez, M.E. (2019) *Phytophthora oleae*, a new root pathogen of wild olives. *Plant Pathology*, 68, 901–907. https://doi.org/10.1111/ppa.13024.

Green, S., Cooke, D.E.L., Barwell, L., Purse, B.V., Cock, P., Frederickson-Matika, D., Randall, E., Keillor, B., Pritchard, L., Thorpe, P., Pettitt, T., Schlenzig, A., Barbrook, J., (2025) The prevalence of *Phytophthora* in British plant nurseries; high-risk hosts and substrates and opportunities to implement best practice. Plant Pathology, 00, 1–22.

Henricot, B., Pérez Sierra, A. & Jung, T. (2014) *Phytophthora pachypleura* sp. nov., a new species causing root rot of Aucuba japonica and other ornamentals in the United Kingdom. *Plant Pathology*, 63, 1095–1109. https://doi.org/10.1111/ppa.12194.

Illumina (2013) 16S Metagenomic sequencing library preparation. San Diego: Illumina. 28. *San Diego: Illumina. 28*.

Ippolito, A., Schena, L. & Nigro, F. (2002) Detection of *Phytophthora nicotianae* and *P. citrophthora* in citrus roots and soils by nested PCR. *European Journal of Plant Pathology*, 108, 855–868. https://doi.org/10.1023/A:1021208106857.

Jung, T., Milenković, I., Balci, Y., Janoušek, J., Kudláček, T., Nagy, Z., et al. (2024) Worldwide forest surveys reveal forty-three new species in *Phytophthora* major Clade 2 with fundamental implications for the evolution and biogeography of the genus and global plant biosecurity. *Studies in Mycology*, 107, 251–388. https://doi.org/10.3114/sim.2024.107.04.

Jung, T., Orlikowski, L., Henricot, B., Abad-Campos, P., Aday, A.G., Aguín Casal, O., et al. (2016) Widespread *Phytophthora infestations* in European nurseries put forest, semi-natural and horticultural ecosystems at high risk of *Phytophthora* diseases. *Forest Pathology*, 46. https://doi.org/10.1111/efp.12239.

Jung, T., Spada, F. La, Pane, A., Aloi, F., Evoli, M., Jung, M.H., et al. (2019) Diversity and distribution of *Phytophthora* species in protected natural areas in Sicily. *Forests*, 10, 259. https://doi.org/10.3390/f10030259.

Khaliq, I., Hardy, G.E.J. St., White, D. & Burgess, T.I. (2018) eDNA from roots: A robust tool for determining *Phytophthora communities* in natural ecosystems. *FEMS Microbiology Ecology*, 94, 1–11. https://doi.org/10.1093/femsec/fiy048.

Khanchouch, K., Pane, A., Chriki, A. & Cacciola, S.O. (2017) Major and Emerging Fungal Diseases of Citrus in the Mediterranean Region. *Citrus Pathology*. https://doi.org/10.5772/66943.

Ko, W.H. & Ann, P.J. (1985) *Phytophthora humicola*, a New Species from Soil of a Citrus Orchard in Taiwan. *Mycologia*, 77, 631–636. https://doi.org/10.2307/3793361.

La Spada, F., Cock, P.J.A., Randall, E., Pane, A., Cooke, D.E.L, Cacciola, S.O. 2022. DNA Metabarcoding and Isolation by Baiting Complement Each Other in Revealing *Phytophthora* Diversity in Anthropized and Natural Ecosystems. *Journal of Fungi* 8: 330.

Linaldeddu, B.T., Rossetto, G., Maddau, L., Vatrano, T. & Bregant, C. (2023) Diversity and pathogenicity of *Botryosphaeriaceae* and *Phytophthora* species associated with emerging olive diseases in Italy. *Agriculture (Switzerland)*, 13, 1575. https://doi.org/10.3390/agriculture13081575.

Liu, J., Sui, Y., Wisniewski, M., Droby, S. & Liu, Y. (2013) Review: Utilization of antagonistic yeasts to manage postharvest fungal diseases of fruit. *International Journal of Food Microbiology*, 167, 153–160. https://doi.org/10.1016/j.ijfoodmicro.2013.09.004.

Loiko, N., Islam, M.N. (2024) Plant–Soil Microbial Interaction: Differential Adaptations of Beneficial vs. Pathogenic Bacterial and Fungal Communities to Climate-Induced Drought. *Agronomy* **14**: 1949.

Mammella, M.A., Cacciola, S.O., Martin, F. & Schena, L. (2011) Genetic characterization of *Phytophthora nicotianae* by the analysis of polymorphic regions of the mitochondrial DNA. *Fungal Biology*, 115, 4–5. https://doi.org/10.1016/j.funbio.2011.02.018.

Mammella, M.A., Martin, F.N., Cacciola, S.O., Coffey, M.D., Faedda, R. & Schena, L. (2013) Analyses of the population structure in a global collection of *Phytophthora nicotianae* isolates inferred from mitochondrial and nuclear DNA sequences. *Phytopathology*, 103, 610–622. https://doi.org/10.1094/PHYTO-10-12-0263-R.

Man in't Veld, W.A., Rosendahl, K.C.H.M., Rijswick, P.C.J. Van, Meffert, J.P., Westenberg, M., Vossenberg, B.T.L.H. Van De, et al. (2015) *Phytophthora terminalis* sp. nov. and *Phytophthora occultons* sp. nov., two invasive pathogens of ornamental plants in Europe. *Mycologia*, 107, 54–65. https://doi.org/10.3852/12-371.

Migliorini, D., Vivas, M., Wingfield, M.J., Shaw, C. & Burgess, T.I. (2023) Oomycete

composition in Proteaceae orchards and natural stands on three continents. *Mycological Progress*, 22, 75. https://doi.org/10.1007/s11557-023-01925-1.

Naqvi, S.A.M.H. (2006) Diagnosis and Management of Pre and Post-harvest Diseases of Citrus fruit. *Diseases of Fruits and Vegetables Volume I*, 1, 339–359. https://doi.org/10.1007/1-4020-2606-4_8.

Pautasso, M., Döring, T.F., Garbelotto, M., Pellis, L. & Jeger, M.J. (2012) Impacts of climate change on plant diseases-opinions and trends. *European Journal of Plant Pathology*, 133, 295–313. https://doi.org/10.1007/s10658-012-9936-1.

Prigigallo, M.I., Abdelfattah, A., Cacciola, S.O., Faedda, R., Sanzani, S.M., Cooke, D.E.L., et al. (2016) Metabarcoding analysis of *Phytophthora* diversity using genus-specific primers and 454 pyrosequencing. *Phytopathology*, 106, 305–313. https://doi.org/10.1094/PHYTO-07-15-0167-R.

Prigigallo, M.I., Mosca, S., Cacciola, S.O., Cooke, D.E.L. & Schena, L. (2015) Molecular analysis of *Phytophthora* diversity in nursery-grown ornamental and fruit plants. *Plant Pathology*, 64, 1308–1319. https://doi.org/10.1111/ppa.12362.

Puglisi, I., Patrizio, A. De, Schena, L., Jung, T., Evoli, M., Pane, A., et al. (2017) Two previously unknown *Phytophthora* species associated with brown rot of Pomelo (*Citrus grandis*) fruits in Vietnam. *PLoS ONE*, 12. https://doi.org/10.1371/journal.pone.0172085.

Qu, Q., Wang, Z., Gan, Q., Liu, R., Xu, H. (2023) Impact of drought on soil microbial biomass and extracellular enzyme activity. Frontiers in Plant Science, 14, 1221288.

Redekar, N.R., Eberhart, J.L. & Parke, J.L. (2019) Diversity of *Phytophthora*, *Pythium*, and *Phytopythium* species in recycled irrigation water in a container nursery. *Phytobiomes Journal*, 3, 31–45. https://doi.org/10.1094/PBIOMES-10-18-0043-R.

Riddell, C.E., Frederickson-Matika, D., Armstrong, A.C., Elliot, M., Forster, J., Hedley, P.E., et al. (2019) Metabarcoding reveals a high diversity of woody host-associated *Phytophthora* spp. In soils at public gardens and amenity woodlands in Britain. *PeerJ*, 7. https://doi.org/10.7717/PEERJ.6931.

Riolo, M., Aloi, F., Conti Taguali, S., Pane, A., Franco, M. & Cacciola, S.O. (2022) *Phytophthora* × *cambivora* as a Major Factor Inciting the Decline of European Beech in a Stand within the Southernmost Limit of Its Natural Range in Europe. *Journal of Fungi*, 8, 973. https://doi.org/10.3390/jof8090973.

Riolo, M., Aloi, F., Spada, F. La, Sciandrello, S., Moricca, S., Santilli, E., et al. (2020) Diversity of *Phytophthora communities* across different types of mediterranean vegetation in a nature reserve area. *Forests*, 11, 853.

https://doi.org/10.3390/F11080853.

Rovetto, E.I., Luz, C., Spada, F. La, Meca, G., Riolo, M. & Cacciola, S.O. (2023) Diversity of Mycotoxins and Other Secondary Metabolites Recovered from Blood Oranges Infected by *Colletotrichum*, *Alternaria*, and *Penicillium* Species. *Toxins*, 15, 407. https://doi.org/10.3390/toxins15070407.

Rovetto, E.I., Spada, F. La, Aloi, F., Riolo, M., Pane, A., Garbelotto, M., Cacciola S.O. (2024) Green solutions and new technologies for sustainable management of fungus and oomycete diseases in the citrus fruit supply chain. *Journal of Plant Pathology*, 106, 411–437. https://doi.org/10.1007/s42161-023-01543-6.

Ruano-Rosa, D., Schena, L., Agosteo, G.E., Magnano di San Lio, G. & Cacciola, S.O. (2018) *Phytophthora oleae* sp. nov. causing fruit rot of olive in southern Italy. *Plant Pathology*, 67, 1362–1373. https://doi.org/10.1111/ppa.12836.

Ruiz-Gómez, F.J., Pérez-de-Luque, A. & Navarro-Cerrillo, R.M. (2019) The Involvement of Phytophthora Root Rot and Drought Stress in Holm Oak Decline: from Ecophysiology to Microbiome Influence. *Current Forestry Reports*, 5, 251–266. https://doi.org/10.1007/s40725-019-00105-3.

Ruiz Gómez, F.J., Navarro-Cerrillo, R.M., Pérez-de-Luque, A., Oβwald, W., Vannini, A. & Morales-Rodríguez, C. (2019) Assessment of functional and structural changes of soil fungal and oomycete communities in holm oak declined dehesas through metabarcoding analysis. *Scientific Reports*, 9, 5315. https://doi.org/10.1038/s41598-019-41804-y.

Safaiefarahani, B., Mostowfizadeh-Ghalamfarsa, R., Hardy, G.E.S.J. & Burgess, T.I. (2015) Re-evaluation of the *Phytophthora cryptogea* species complex and the description of a new species, *Phytophthora pseudocryptogea* sp. nov. *Mycological Progress*, 14, 108. https://doi.org/10.1007/s11557-015-1129-9.

Sarker, S.R., Burgess, T.I., Hardy, G.E.S.J. & McComb, J. (2023) Closing the gap between the number of *Phytophthora* species isolated through baiting a soil sample and the number revealed through metabarcoding. *Mycological Progress*, 22, 39. https://doi.org/10.1007/s11557-023-01892-7.

Scanu, B., Hunter, G.C., Linaldeddu, B.T., Franceschini, A., Maddau, L., Jung, T., et al. (2014) A taxonomic re-evaluation reveals that *Phytophthora cinnamomi* and *P. cinnamomi* var. *parvispora* are separate species. *Forest Pathology*, 44, 1–20. https://doi.org/10.1111/efp.12064.

Scibetta, S., Schena, L., Chimento, A., Cacciola, S.O. & Cooke, D.E.L. (2012) A molecular method to assess *Phytophthora* diversity in environmental samples. *Journal of*

Microbiological Methods, 88, 356–368. https://doi.org/10.1016/j.mimet.2011.12.012.

Scott, P.M., Burgess, T.I., Barber, P.A., Shearer, B.L., Stukely, M.J.C., Hardy, G.E.S.J., et al. (2009) *Phytophthora multivora* sp. nov., a new species recovered from declining Eucalyptus, Banksia, Agonis and other plant species in Western Australia. *Persoonia: Molecular Phylogeny and Evolution of Fungi*, 22, 1–13. https://doi.org/10.3767/003158509X415450.

Serrano, M.S., Pérez, F.J. & Gómez-Aparicio, L. (2021) Disentangling the interactive effects of climate change and *Phytophthora cinnamomi* on coexisting Mediterranean tree species. *Agricultural and Forest Meteorology*, 298–299, 108295. https://doi.org/10.1016/J.AGRFORMET.2020.108295.

Talibi, I., Boubaker, H., Boudyach, E.H. & Ait Ben Aoumar, A. (2014) Alternative methods for the control of postharvest citrus diseases. *Journal of Applied Microbiology*, 117, 1–17. https://doi.org/10.1111/jam.12495.

Thomidis, T., Exadaktylou, E. & Sotiropoulos, T. (2005) Susceptibility of three citrus rootstocks towards *Phytophthora cactorum*, *P. citrophthora*, *P. parasitica* and *P. citricola*. *Zeitschrift fur Pflanzenkrankheiten und Pflanzenschutz*, 204–207.

Timmer, L.W., Graham, J.H. & Zitko, S.E. (1998) Metalaxyl-resistant isolate of *Phytophthora nicotianae*: Occurrence, sensitivity, and competitive parasitic ability on citrus. *Plant Disease*, 82, 254–261. https://doi.org/10.1094/PDIS.1998.82.2.254.

Toreti, A., Bavera, D., Acosta Navarro, J., Acquafresca, L., Arias-Muñoz, C., Avanzi, F., et al. (2024) Drought in the Mediterranean Region - January 2024. *Publications Office of the European Union, Luxembourg*. https://doi.org/10.2760/384093.

Ulrich, D.E.M., Sevanto, S., Ryan, M., Albright, M.B.N., Johansen, R.B. & Dunbar, J.M. (2019) Plant-microbe interactions before drought influence plant physiological responses to subsequent severe drought. *Scientific Reports*, 9, 249. https://doi.org/10.1038/s41598-018-36971-3.

Van der Heyden, H., Duceppe, M.O., Charron, G., Tanguay, P. & Bilodeau, G.J. (2024) Oomycete communities are influenced by land use and disease status in Christmas tree production in Southern Québec, Canada. *Environmental DNA*, 6, 1–17. https://doi.org/10.1002/edn3.529.

Vial, A., Latorre, B.A. & Ortúzar, J. (2006) Characterization of *Phytophthora citrophthora* and *P. inundata* associated to foot and root rot of citrus trees in Chile. *Ciencia e Investigación Agraria*, 33, 173–184. https://doi.org/10.7764/rcia.v33i3.347.

7. Conclusions and Future Perspectives

This thesis explored and confirmed the potential of omics sciences to address challenges posed by emerging and re-emerging citrus and olive diseases caused by fungi and oomycetes in the Mediterranean region (Cacciola and Gullino, 2019), in a scenario of climate change and pursuing the objective of improving sustainability in agriculture. In particular, genomics, transcriptomics, metabolomics and metagenomics were applied to tackle specific aspects of important diseases of these two typical Mediterranean tree crops, such as Phytophthora rot and anthracnose of olive fruit and Phytophthora root rot of citrus. The findings provided interesting insights into the plant-pathogen interaction in these pathosystems, the pathogenicity and virulence determinants of pathogens such as *P. oleae* and *Colletotrichum* spp., the capability of biocontrol agents to modulate gene expression in olive drupes infected by *P. oleae*, the metabolic response of olive fruit to the infection by *Colletotrichum* spp. and putative biochemical markers of resistance, the effects of environmental conditions and cropping systems on both the structure and dynamics of soil-borne *Phytophthora* communities and rhizosphere soil microbioma. Overall this information can be leveraged to develop more effective strategies of eco-friendly disease management and breeding for disease resistance, as well as to evaluate and counteract the effects of climate change on crop diseases.

Key findings of the diverse research lines were as follows:

i. Genome sequencing. The genome sequencing and assembly of *Phytophthora oleae* , an emerging pathogen of olive (Ruano-Rosa et al., 2018), provided essential information on its pathogenicity mechanisms and genes involved in pathogenesis, aligning with previous studies that emphasize the need for genomic data in understanding virulence factors in plant pathogens (Lahlali et al., 2024; Singh et al., 2023). This knowledge is fundamental for developing targeted control strategies.

ii. Biocontrol Agents and Transcriptomics. RNA sequencing revealed how biocontrol agents, such as *Candida oleophila* and *Trichoderma atroviride*, modulate gene expression in olive drupes infected by anthracnose incited by *Colletotrichum* spp., suggesting effective mechanisms through which these biotechnologies can be optimized (Contreras-Cornejo et al., 2023). This supports findings from other studies that advocate for biocontrol as a viable alternative to chemical treatments (Zhou et al., 2024).

iii. Metabolomic Profiles of Olive Cultivars Differing in Susceptibility to Fruit Anthracnose. The analysis of metabolomic responses of diverse olive cultivars to the infection of *Colletotrichum* species differing in virulence identified key metabolites, such as photosynthetis pigments (chlorophylls and carotenoids), malondialdehyde and hydrogen peroxide, that served as stress markers for decifering the physiological and biochemical response of olive drupes to the anthracnose infection and could also be markers of disease resistance or susceptibility. This emphasizes the importance of utilizing metabolomics in understanding olive cultivar responses to the infection, as highlighted by recent research on the role of phenolic compounds in plant defense (Miho et al., 2024).

iv. Soil Microbial Communities in Rhizosphere of Citrus Trees. The analysis of microbial diversity in citrus orchards using metagenomics demonstrated the profound impact of organic and conventional cropping systems on soil microbiome composition. These findings align with studies showing that sustainable management enhances microbial biodiversity, which is crucial for maintaining plant health and resilience (Karpouzas et al., 2014; Stanley and Preetha, 2016). Interestingly, the analysis proved to be very sensitive in revealing the effects of environmental conditions, in shaping the structure of core rhizosphere micorbiome, indicating it can be an effective tool to evaluate in the long term the effects of climate change on soil microbioma and communities of soil-borne pathogens (Singh et al., 2023).

v. Diversity of *Phytophthora* Communities in Sicilian Citrus Orchards. The results of metagenomic analysis were compared with those of the conventional baiting technique revealing the two methods wer complementary. However metagenomic was more effective in revealing the diversity of *Phytophthora* communities associated to the citrus rhizosphere and identified taxa that were new or unreported on this host, further confirming it is crucial to evaluate the effects of climate change on soil microbioma and communities of soil-borne pathogens.

Overall these findings contribute to a more profound understanding of the complex molecular interactions among plants, pathogens, biocontrol agents and microbial communities. Moreover they confirm the complementarity of omic sciences and their enormous potential in shedding light on still unexplored or unresolved aspects of plant pathology. The integration of omics technologies into crop protection offers actionable

insights for developing resilient agricultural systems, reducing dependence on chemical inputs, and fostering long-term sustainability od agriculture in the Mediterranean region (Zhou et al., 2024).

Despite the progress made, challenges remain in fully integrating these findings into practical agricultural systems and in particular to demonstrate that stress markers detected in this study are linked to disease resistance. The complexity of plant-pathogen-microbiome interactions necessitates further research to develop consistent biocontrol treatments and translate metabolomic markers into field-ready diagnostic tools or apply them either to develop disease management strategies based on resistance induction or in breeding programs aimed at improving genetic resistance of crops. Moreover long-term studies are needed to assess and demonstrate the effects of climate change on pathogen and whole microbial communities (Lahlali et al., 2024).

Future Directions:

i. Optimization of Biocontrol Agents: Future studies should focus on enhancing the efficacy of biocontrol agents through improved formulations and their application as part of integrated pest management strategies (Contreras-Cornejo et al., 2023).
ii. Soil Microbiome and Plant Health: A deeper exploration of soil microbiome interactions with plant health, particularly under varying environmental conditions, will refine sustainable practices that maintain biodiversity while suppressing pathogens (Karpouzas et al., 2014).
iii. Early Disease Detection: Developing early diagnostic tools based on metabolomic markers or gene expression profiles will facilitate faster, more accurate detection of infections before symptoms become visible (Zhou et al., 2024).
iv. Targeting genes involved in disease resistance. The expansion of metabolomic and transcriptomic studies, including additional metabolic functions and biochemical markers as well as a greater number of olive cultvars susceptible or resistant to anthracnose, might help identify genes involved in resistance to this disease (Li et al., 2024; Zhang et al., 2022).
v. Adaptation to Climate Change: Predictive models linking climate change to pathogen dynamics will be crucial for forecasting outbreaks and preparing adaptive strategies to mitigate risks in olive and citrus production (Singh et al., 2023).

By integrating these approaches, future research can continue to advance eco-friendly disease management strategies, ensuring the sustainability and resilience of Mediterranean agriculture in the face of evolving phytopathological and environmental threats.

7.1 References

Ahouangninou, C., Martin, T., Edorh, P., Bio-Bangana, S., Samuel, O., St-Laurent, L., et al. (2012) Characterization of health and environmental risks of pesticide use in market-gardening in the rural city of Tori-Bossito in Benin, West Africa. *Journal of Environmental Protection*, 03, 241–248. https://doi.org/10.4236/jep.2012.33030.

Cacciola, S.O. & Gullino, M.L. (2019) Emerging and re-emerging fungus and oomycete soil-borne plant diseases in Italy. *Phytopathologia Mediterranea*, 58, 451–472. https://doi.org/10.14601/Phyto-10756.

Contreras-Cornejo, H.A., Larsen, J., Fernández-Pavía, S.P. & Oyama, K. (2023) Climate change, a booster of disease outbreaks by the plant pathogen *Phytophthora* in oak forests. *Rhizosphere*, 27, 100719. https://doi.org/10.1016/j.rhisph.2023.100719.

Karpouzas, D.G., Kandeler, E., Bru, D., Friedel, I., Auer, Y., Kramer, S., et al. (2014) A tiered assessment approach based on standardized methods to estimate the impact of nicosulfuron on the abundance and function of the soil microbial community. *Soil Biology and Biochemistry*, 75, 282–291. https://doi.org/10.1016/j.soilbio.2014.04.022.

Lahlali, R., Taoussi, M., Laasli, S.E., Gachara, G., Ezzouggari, R., Belabess, Z., et al. (2024) Effects of climate change on plant pathogens and host-pathogen interactions. *Crop and Environment*, 3, 159–170. https://doi.org/10.1016/J.CROPE.2024.05.003.

Li, F.H., Lu ,D.X., Meng, F.L., Tian, C.M..(2024) Transcription factor CgSte12 regulates pathogenicity by affecting appressorium structural 501 development in the anthracnose-causing fungus *Colletotrichum gloeosporioides*. *Phytopathology* 114, 1832-1842. https://doi.org/10.1094/PHYTO-12-23-0484-R.

Singh, B.K., Delgado-Baquerizo, M., Egidi, E., Guirado, E., Leach, J.E., Liu, H., et al. (2023) Microbiology nature reviews microbiology Climate change impacts on plant pathogens, food security and paths forward. *Nature Reviews Microbiology*, 21, 640–656.

Stanley, J. & Preetha, G. (2016) Pesticide Toxicity to Microorganisms: Exposure, Toxicity

and Risk Assessment Methodologies. Pesticide Toxicity to Non-target Organisms. pp. 351–410.

Syafrudin, M., Kristanti, R.A., Yuniarto, A., Hadibarata, T., Rhee, J., Al-Onazi, W.A., et al. (2021) Pesticides in drinking water-a review. *International Journal of Environmental Research and Public Health*, 18, 468. https://doi.org/10.3390/ijerph18020468.

Zhang, Y., An, B., Wang, W., et al. (2022)Actin-bundling protein fimbrin regulates pathogenicity via organizing F - actin dynamics during 491 appressorium development in *Colletotrichum gloeosporioides*. *Molecular Plant Pathology*, 23, 1472-1486. https://doi.org/10.1111/mpp.13242

Zhou, W., Li, M. & Achal, V. (2024) A comprehensive review on environmental and human health impacts of chemical pesticide usage. *Emerging Contaminants*, 11, 100410. https://doi.org/10.1016/J.EMCON.2024.100410.